Beaches in McMurdo Sound, Antarctica.

by

Edward R. T. Butler

A thesis

submitted to the Victoria University of Wellington

in fulfilment of the

requirements for the degree of

Doctor of Philosophy

in Geology

Victoria University of Wellington

2001

Frontispiece. Waves at Cape Bird during a southerly storm, 7th February 1998.

Abstract

Modern beaches in McMurdo Sound can be divided into 3 process regimes. Beaches on Ross Island (eastern McMurdo Sound) are characterised by marine processes with little ice modification. On ice-bound western McMurdo Sound, coastal orientation is of paramount importance. Ice thrust features are prominent on south facing beaches, which are open to the predominant wind direction and receive relatively small waves from the fetch restricted south. A greater degree of marine dominance is exhibited by beaches on north facing coasts where sea ice is blown offshore and the beaches are open to the larger storm waves from the eastern Ross Sea. The single most useful indicator of the relative importance of marine and ice processes on the beaches is the roundness of the beach material.

Unlike the modern beaches, raised beach ridges at all sites comprise poorly sorted cobbles in a mixed sand and gravel matrix. These are inferred to be storm ridges. In contrast with the raised beaches, the modern beaches on the western side of the Sound have evidence of ice processes on them. This suggests that the modern beach has not experienced the same magnitude storms that produced the raised beaches. The size and frequency of the ridges is a product of the local wave climate. The number of raised beaches at any site is a useful indicator of the paleo-wave climate. More ridges occur in sheltered south facing locations, because they are more protected from open marine conditions, than on beaches in ice-free or north facing locations.

When determining the marine limit of a site the most useful features are, low energy marine bedding features (such as flaser bedding) and boulder pavements. Based on inferred process information at the time of deposition, revised estimates of marine limits in McMurdo Sound and a new marine limit at Cape Barne are presented. Because the nature of the raised beaches has not been fully considered by previous authors sea level curves are inaccurate.

The reconstruction of the retreat of the Ross Ice Shelf from marine limits in McMurdo Sound shows a three stage stepwise southward retreat of the Ross Ice Shelf. A breakout from somewhere north of Cape Roberts and south of Cape Ross back to Marble Point (on the western side of the Sound) while remaining north of Cape Bird (on the eastern side of the Sound), occurred sometime around 8,000 years ago. Another breakout cleared ice from Cape Bird to somewhere south of Cape Barne and south of Cape Bernacchi around 5,000 years ago. This differs with other authors work (Hall and Denton, 1999, Kellogg et al., 1996, Stuiver et al., 1981) by suggesting a considerably older date for the Ross Ice Sheet retreating from McMurdo Sound.

The data presented here suggests that much of McMurdo Sound was ice free about 1,500 years before earlier estimates at about 6,500 years. The effect of the change in deglaciation timing is to reduce isostatic rebound rates. This suggests that there was less ice in McMurdo Sound during the Last Glacial Maximum.

Acknowledgments

Well, what can you say after 4 years of beavering away on a thesis? It has been a wonderful experience, challenging, frustrating and awe-inspiring. There are many people who made this thesis possible and considerably more enjoyable! I sincerely hope I remember to thank all the people who helped along the way and if I managed to forget someone, I apologise.

Firstly to my supervisors, Dr Jamie Shulmeister and Prof Bob Kirk. Bob told me of the possibility of this project and helped pull together a scholarship application on very short notice that managed to appease the Ross Dependency Research Committee. He also read and provided great feedback on my draft chapters AND he taught me a thing or two about rabbits. Jamie joined me in the field for a month in Antarctica and managed to show me what was what when I really needed to know!! He introduced me to fine wine and managed to read draft after draft of thesis and paper stuff and get me motivated when I needed to really get things done. He has been a real inspiration and a good friend without which this would never have been a reality. Thanks heaps guys.

Antarctica New Zealand and the Ross Dependency Research Committee managed to persuade New Zealand Post to fund me for 2 years. Without the support (both financial and logistical) the project would not have been possible. The Victoria University of Wellington internal grants committee also provided some funding for equipment. Many of the people in Antarcitca New Zealand helped me along the way with good advice and special thanks should go to Paul Fitzgerald who helped me fight a battle or two. All of the people at Scott Base made the stay in Antarctica even more enjoyable.

I had plenty of help in the field from Julie Quinn, Peter Webb, Alexis Lambeck and Jon Allen. All of those games of 500 have honed my card shark skills! The guys at Victoria University of Wellington were crazy enough to keep me sane (does that make sense?). My hacky sac skills were never quite up to it but it was good fun all the same. Maybe now that I've gone Cliff Atkins, Phil Holme, Nancy Bertler, Ursula Cocran, Dr Vanessa Thorn and the rest of the crew can do some work!! Alex Pyne gave me advice on almost everything Antarctic and helped me get things together. Prof Peter Barrett supported this project from the start and read drafts of papers and encouraged me in many ways! Over the last year of the thesis my colleagues at the Foundation for Research Science and Technology provided support and another crazy set of skills to my repertoire. Damian Diack did a marathon proof read of the entire thesis in the 11th hour. Many thanks!

Last but certainly not least was the support and encouragement I got from my family and friends. Butch and Bridget, Tanya and Graeme and John and Jackie have had to put up with constant barrage of thesis since they've known me. Thanks for putting up with it and I look forward to times when I can think about something other than what I should be doing on my thesis. My family has been a source of fun and encouragement over the years and a place I can always count on. You've all been a big part of this thesis!! I guess I can attribute my fascination of the Antarctic to Dad...thanks. Lastly, Anita has been extremely supportive and understanding and been a great friend and someone who has managed to put up with having me buried in my thesis since I've known her. Thank you for your ongoing support.

I hope that I've managed to thank everyone who has contributed to this thesis if not thank you very much.

Table of Contents

List of Figures

List of Tables

List of Appendices

Chapter 1

Introduction

1.1 Introduction

Beaches and beach processes are relatively well understood in temperate regions but high latitude coasts have received much less attention. Beaches in McMurdo Sound Antarctica offer a unique opportunity to examine coastal systems that have had almost no human interference and a combination of high energy marine and extreme cryogenic processes operating on them. Only a handful of studies have investigated them as morphological features (Nichols, 1953; 1961; 1966; Kirk, 1972; Gregory *et al.* 1984; Gregory and Kirk, 1990) and there has been no stratigraphical or sedimentological work on the beaches. The previous work that has been undertaken seems to be contradictory with Nichols (1961; 1966; 1968) explaining the beaches in McMurdo Sound in terms of ice processes while Kirk (1966; 1972; 1991) showed clear evidence of marine processes. These studies have never been reconciled. The overall lack of work is unsurprising as these high latitude beaches have different process controls than temperate beaches. In addition, the flights of raised beaches in McMurdo Sound are extensively invoked in debates in the timing of Antarctica deglaciation and for inferring ice thickness of West Antarctic Ice Sheet thickness during the Last Glacial Maximum from rebound patterns.

This thesis addresses two fundamental questions. How do Antarctic beaches respond to the interaction between the marine and cryogenic processes acting on them? What do raised beaches in McMurdo Sound tell us about the Holocene and/or the Last

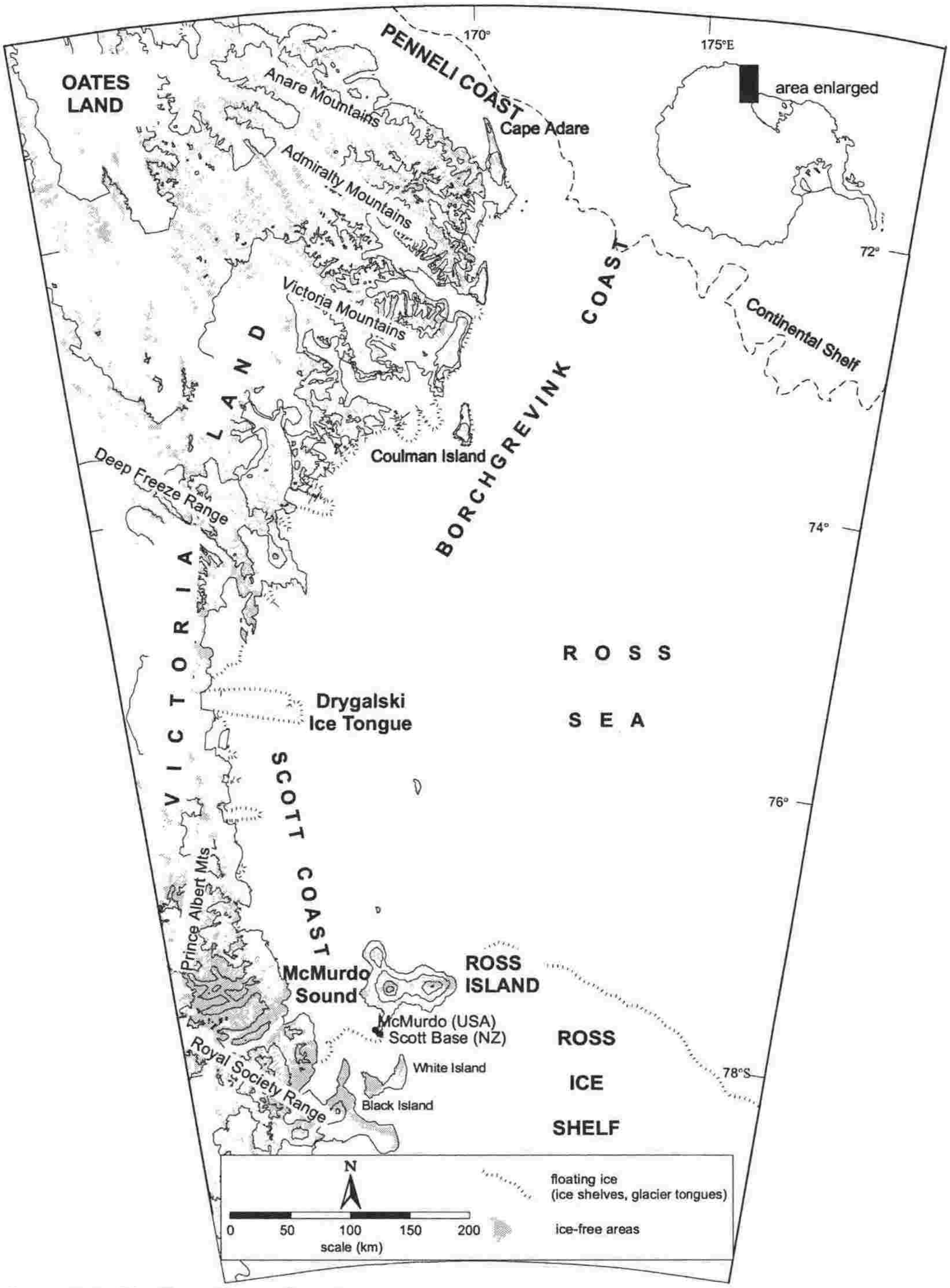

Figure 1.1. The Ross Sea and environs.

Glacial Maximum history of McMurdo Sound? In the context of this thesis a beach is an unconsolidated accumulation of sediment that has been modified by marine action, which, in McMurdo Sound, includes the action of sea ice. To do this, the thesis examines the beaches in McMurdo Sound using morphological, stratigraphic and sedimentological techniques and undertakes optically stimulated luminescence dating of some raised beaches ridges.

1.2 Regional physiognomy

McMurdo Sound (Figure 1.1 and Figure 1.2) lies at the south-western end of the Ross Sea. It is bordered on its western shores by the Prince Albert Mountains and the Royal Society Range, and to the east by Ross Island. To the south of Ross Island the Ross Ice shelf extends a further 450km south to the Shakleton Coast at the base of the Churchill Mountains and the Queen Alexandra Range. To the south west of Ross Island the McMurdo Ice Shelf reaches south to White Island.

On the western side of McMurdo Sound the Prince Albert Mountains and Royal Society Ranges rise to an elevation of 2,410m (Round Mountain) and 4,045m (Mt Lister) respectively. The Wilson Piedmont Glacier, a local piedmont cap extends from the end of the Dry Valleys and terminates along the coast from Cape Roberts in the north to just south of Cape Bernacchi. At locations where the glacier has receded, there are ice free areas along the coast, which are examined in this thesis. They comprise Cape Bernacchi, Marble Point, Kolich Point, Spike Cape and Dunlop Island.

Ross Island sits on the eastern side of the Sound and the Ross Ice Shelf buts onto the southern flank of the Island. Ross Island is of volcanic origin and Mt Erebus, which rises to an elevation of 3,794m, is an active volcano. There are sizeable penguin rookeries at Cape Bird, Cape Crozier and at Cape Royds. Apart from small areas at Cape Bird, Cape Royds, Cape Barne Cape Crozier and Cape Armitage, and the tops of the peaks, Ross Island is covered by glaciers and permanent ice. The first three of these ice free pockets are considered in this study.

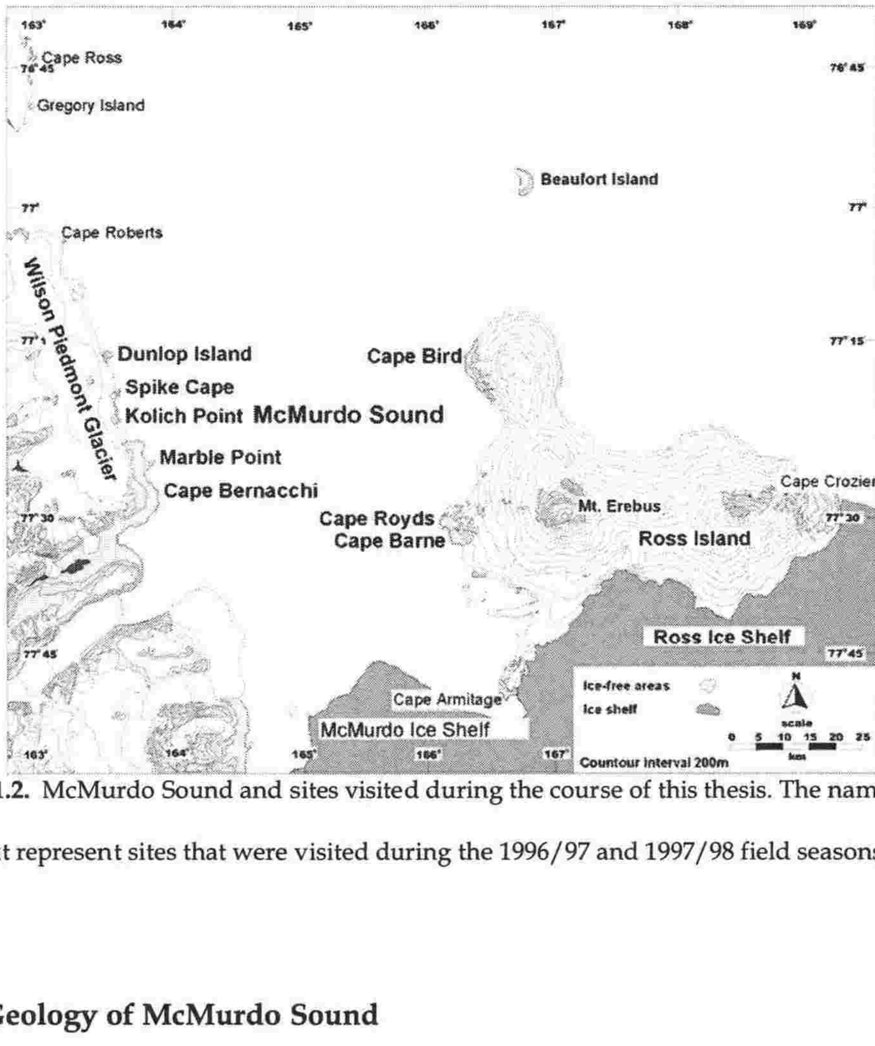

Figure 1.2. McMurdo Sound and sites visited during the course of this thesis. The names in bold text represent sites that were visited during the 1996/97 and 1997/98 field seasons.

1.2.1 Geology of McMurdo Sound

The field sites visited in McMurdo Sound can be broadly spilt into two major geological areas; eastern McMurdo Sound (Cape Bird, Cape Royds and Cape Barne) dominated by basaltic material (Kyle, 1976); western McMurdo Sound dominated by granodiorite, gneiss and marble (Gunn and Warren, 1962) which outcrop at Gneiss

Point, Marble Point, Kolich Point, Spike Cape and Dunlop Island. Thin veneers of glacial sediments, occasionally of distal provenance are widespread.

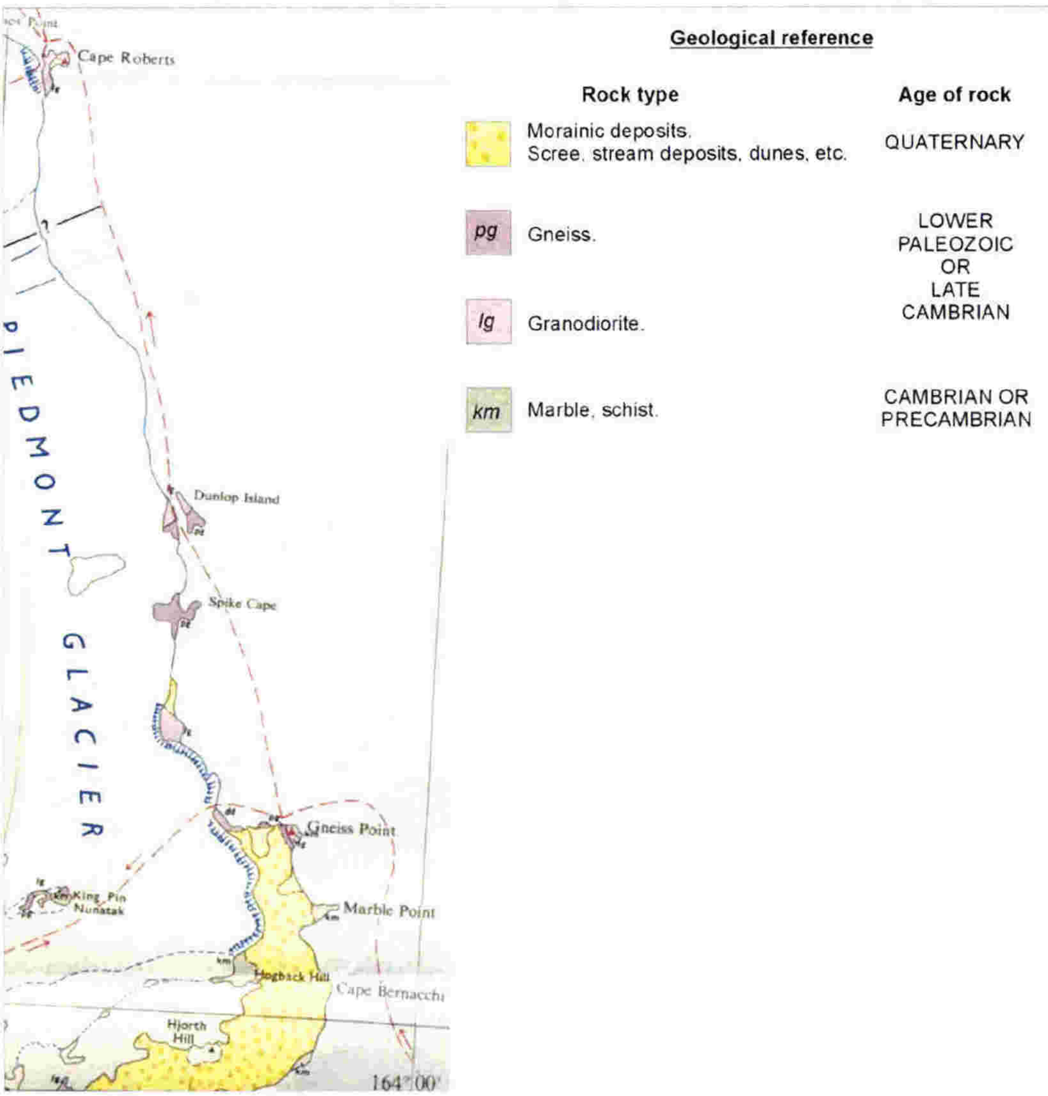

Figure 1.3. Geological map of area from Cape Roberts to Cape Bernacchi (Gunn and Warren, 1962).

Figure 1.3 shows the geology from Cape Roberts to Cape Bernacchi. At all locations from Cape Bernacchi to Cape Roberts, the underlying bedrock (which is exposed at points along the coast) is described by Gunn and Warren (1962). However, the ice free areas are overlain by glacial sediments.

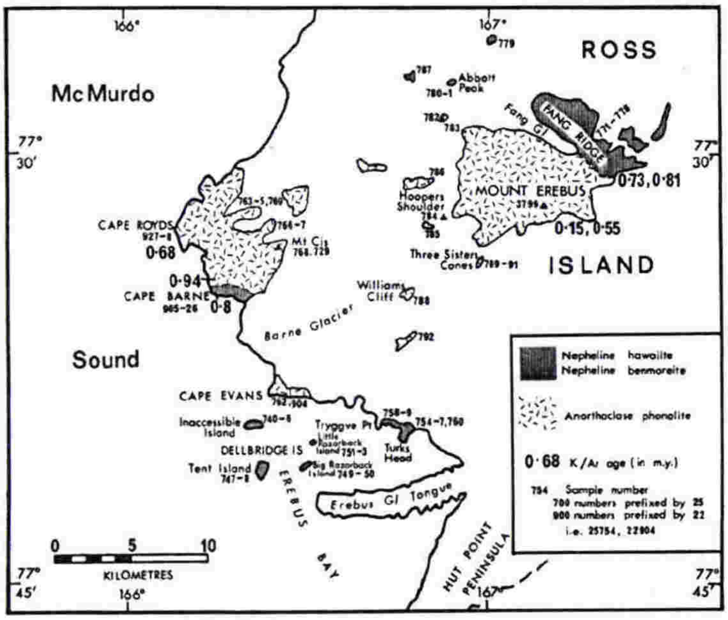

Figure 1.4. Geological map of the Cape Royds and Cape Barnes area (Kyle, 1976).

Figure 1.4 shows the geology around the Cape Royds area. Note the age difference between the rocks at Cape Royds (680k from K/Ar dating) and Cape Barne (940k from K/Ar dating).

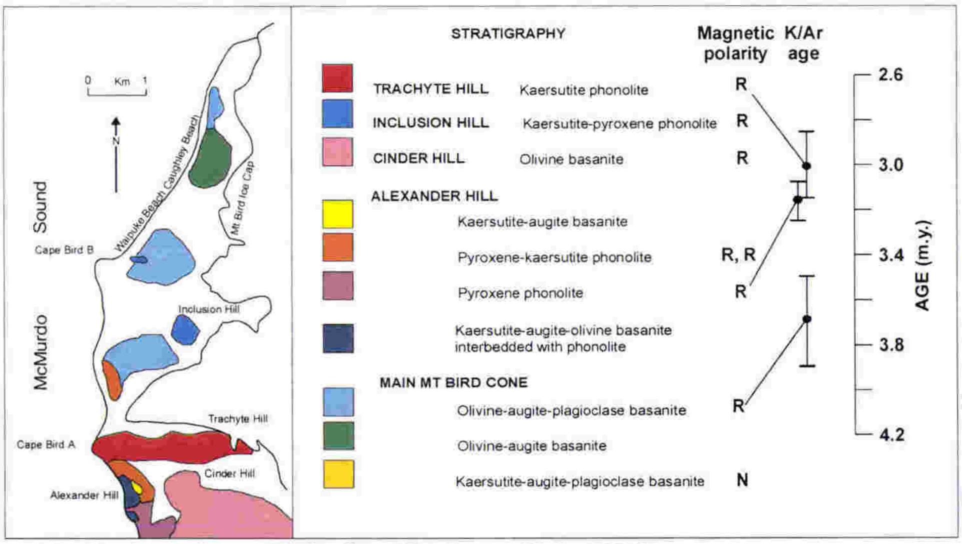

Figure 1.5. Geological map of the Cape Bird area (Kyle, 1976).

Figure 1.5 shows the geology at Cape Bird (Kyle, 1976). The area at Cape Bird B (a focus of this study) is overlain by locally derived glacial sediments.

1.2.2 Climate of the McMurdo Sound area

1.2.2.1 Wind

Windroses for Cape Roberts and Marble Point in 1995, 1996, 1997 and 1998 (for Cape Roberts only) are shown in Figure 1.6. The windroses for Marble Point were constructed from 10 minute averaged data from the University of Wisconsin automatic weather station at Marble Point. The Cape Roberts wind data was collected by the Victoria University of Wellington automatic weather station located at Cape Roberts. Wind data were averaged every hour.

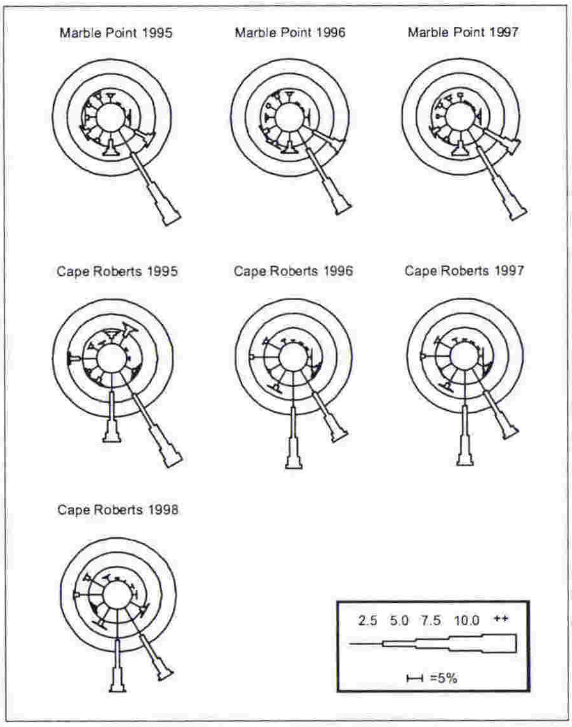

Figure 1.6. Windroses for Marble Point weather station between 1995 and 1997 and Cape Roberts weather station between 1995 and 1998. The Marble Point weather station is situated 120m above mean sea level (AMSL) with the wind instruments at an elevation of 3m above the

ground. The tower at Cape Roberts is located approximately 14m AMSL with the instruments at an elevation of 4m above the ground.

Both of the sites show a dominantly southerly wind direction with a slightly more south-easterly component at Marble Point. This difference is due to local topographic effects.

1.2.2.2 Temperature

Figure 1.7 shows the monthly mean maximum and minimum air temperature for Marble Point in 1995 and part of 1996. The temperature seldom rises above zero, even in the summer months and the range can be as great as 30 ^{0}C in a particular month.

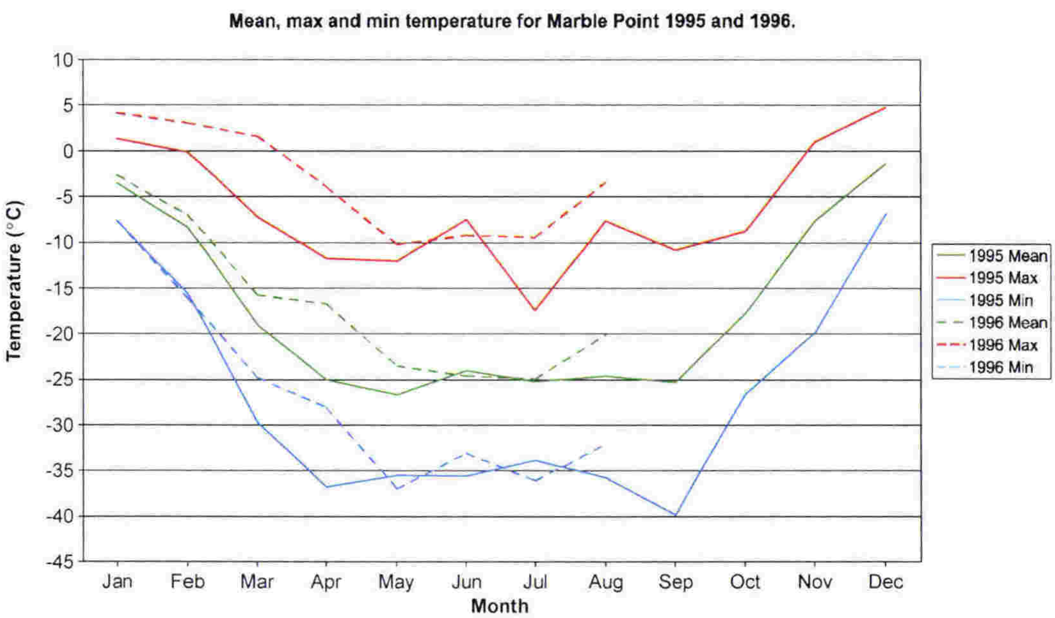

Figure 1.7. Monthly mean, maximum and minimum air temperatures at Marble Point 1995 and 1996. The data are from the University of Wisconsin automatic weather station at Marble Point. The weather station is located 120m AMSL with the temperature sensor located at 3m above the ground.

Although there is little diurnal change in the radiation budget for much of the year (none in the winter months and only small changes for much of the summer), diurnal temperature changes are apparent during some of the summer months. Figure 1.8 shows a chart of 10 minute data for January and July (each day represents 144, 10 minute averages). The July chart shows no diurnal change, which contrasts with the strong diurnal variation in the January chart.

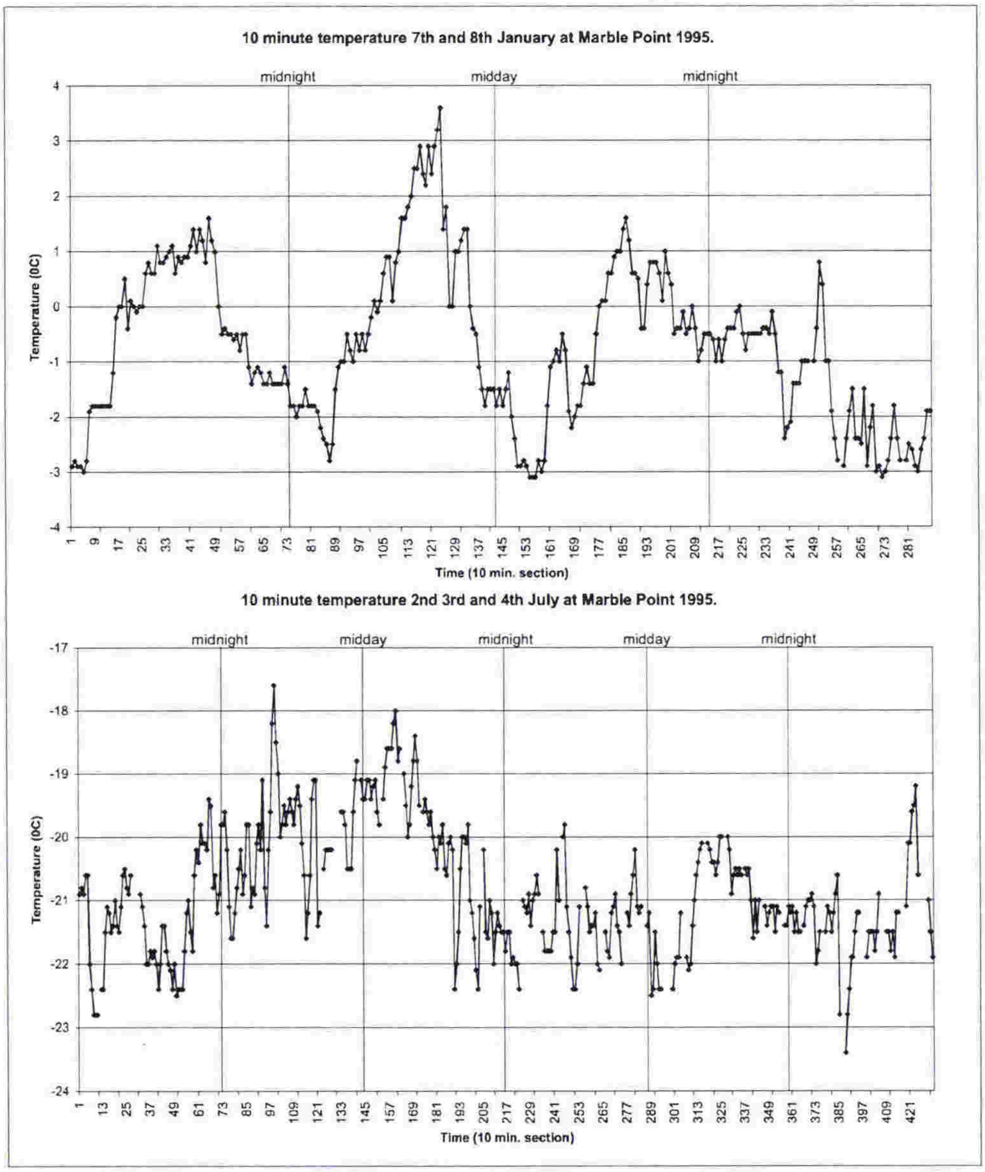

Figure 1.8. 10 minute average temperature data for Marble Point in July and January 1995.

1.2.3 Sea ice in McMurdo Sound

The different extent of sea-ice for the Ross Sea is shown in Figure 1.9. This shows weekly total coverage and extent of sea-ice in hundreds of thousands of square kilometres from January 1973 to December 1982 (NOCD, 1985). As can clearly be seen, the extent of sea-ice at any given time varies dramatically from one season to the next. Long-term trends of sea-ice extent are not clear due to the relatively short collection period (satellite data since January 1973). However, de la Mare studied ship-based records and suggested that the Antarctic sea-ice extent may have declined over the past 100 years (de la Mare, 1997).

Winter satellite images of McMurdo Sound sometimes show large ice-free areas in the Sound. These ice free areas are usually the result of large storms which break up the sea-ice and push it out of the sound. Examination of satellite images from McMurdo Sound show that the Scott Coast has a very short ice free period and is rarely ice free in the winter. This is due to the relatively sheltered nature of the Scott Coast compared with parts of the coast on Ross Island. Table 1.1 shows numbers of images from 1987 to 1997 that revealed ice free areas at Cape Bird or along the Scott Coast. The number in the 'Total Images' column refers to the number of images that were available for analysis that particular year. (The availability of images for analysis was dependent on the weather conditions at the time the satellite was over McMurdo Sound so the number of images in any particular month was not consistent from one year to the next. Most of the images examined were from May, June, July August and September). The '% ice free' columns refer to the % of the images that were ice free. The resolution of the images made it impossible to determine the presence or absence of an ice foot. In contrast with the Scott Coast, which is usually surrounded by pack ice, Cape Bird is largely sea-ice free. It appears likely that these ice free areas extend as far as the coast and depending on the development of the icefoot, the beaches at Cape Bird may experience periods in winter where marine processes act on them.

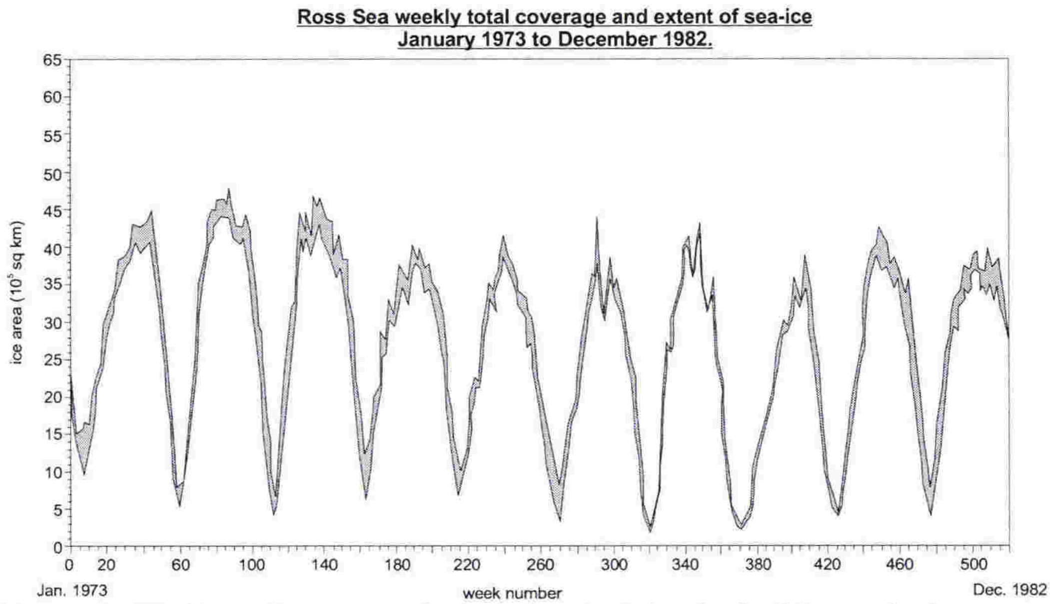

Figure 1.9. Weekly total coverage and extent of sea-ice in hundreds of thousands of square kilometres from January 1973 to December 1982 (NOCD, 1985). The range between the maximum and minimum ice extents has been shaded.

Year	Total images	Eastern % ice free	Western % ice free
1987	13	7.7	84.6
1988	17	0.0	41.2
1989	5	0.0	40.0
1990	23	0.0	21.7
1991	21	0.0	14.3
1992	33	3.0	42.4
1993	19	5.3	36.8
1994	40	0.0	30.0
1995	26	0.0	57.7
1996	44	0.0	70.5
1997	66	3.0	75.8
TOTALS	**307**	**1.6**	**51.1**

Table 1.1. Presence/absence data from satellite images of sea-ice cover at Cape Bird and Cape Royds (eastern McMurdo Sound) and Cape Bernacchi to Dunlop Island (western McMurdo Sound).

Image of McMurdo Sound 17/10/1996. Image of McMurdo Sound 30/1/1997.

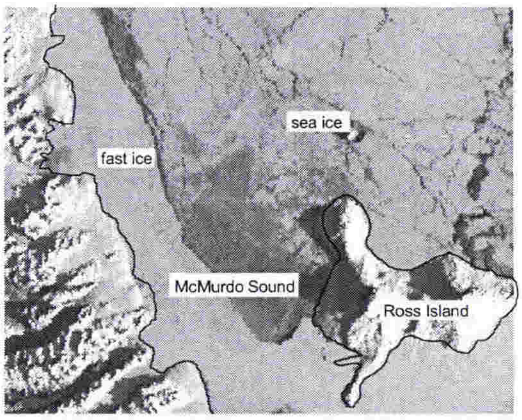

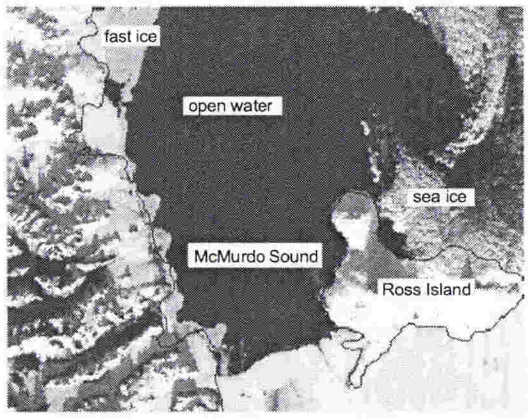

Figure 1.10. Visible images of McMurdo Sound showing heavy pack ice conditions along the Scott Coast and Cape Bird (photo to the left, October, 1996) and ice free areas along the Scott Coast and Cape Bird (photo to the right, January, 1997). (The dark areas indicate ice free land or open water, the lighter colours indicate ice). The images used in this analysis were thermal infra red and visible images from the DMSP and AVHRR satellites. The resolution of the AVHRR images is 1.1km/pixel and the resolution of the DMSP images is 0.55km/pixel.

Figure 1.10 shows visible images of McMurdo Sound on October 17 1996 and January 30 1997. The January 30 image shows both Cape Bird and the Scott Coast relatively ice-free. In contrast, the winter image from October 23 1996 shows Cape Bird and the Scott Coast surrounded by dense pack ice. An investigation of the 1998 images shows a similar trend to that revealed in Table 1.1. Of 28 images covering April and May, all of the images showed the Scott Coast surrounded by dense pack ice. In contrast, 53% of the images showed Cape Bird as ice free.

1.2.4 Wave climate in McMurdo Sound

McMurdo Sound offers a number of problems when attempting to determine the local wave climate. The size of waves depends chiefly on wind-speed, wind duration and fetch length. Under ice-free conditions, McMurdo Sound is both fetch restricted (to the south) and fetch unlimited (to the north-east). However, sea ice may restrict the fetch in the generation area, the direction of travel or at the area of interest making wave predictions based on wind-speed and direction alone often ineffective.

The direction of the dominant locally generated waves will match the dominant wind direction in the area. Consequently, most of the local waves will come from a south/south-easterly direction.

Deep ocean swell waves from the north were calculated by Richard Gorman at the National Institute of Water and Atmospheric Research Limited (Laing and Gorman, 2000). The model is driven by archived windfield data, a combination of meteorological measurements and atmospheric modeling, from the European Centre for Medium Range Weather Forecasting that were synthesised with 15 years of wave data.

Figure 1.11 shows the 2^0 x 2^0 grid used to calculate the hind-cast data. Three points were sampled which are highlighted by white crosses. The middle of Site 1 is 166^0 east 78^0 south, the middle of Site 2 is 168^0 east 78^0 south and the middle of Site 3 is 172^0 east 76^0 south. The program ignores the absence or presence of sea ice, taking the permanent ice and rocky shoreline as the shoreline at all times. Two years of data were calculated. The wave roses that were constructed from these data are the yearly summed roses. Seasonal changes over the two years were minimal. Figure 1.9 shows wave roses that were constructed from this data. The roses show wave direction and significant wave height in m. As can be seen the deep-water swell wave direction has a strong south easterly component but site 1 and 2 are dominated by easterly, north-easterly and south-easterly waves.

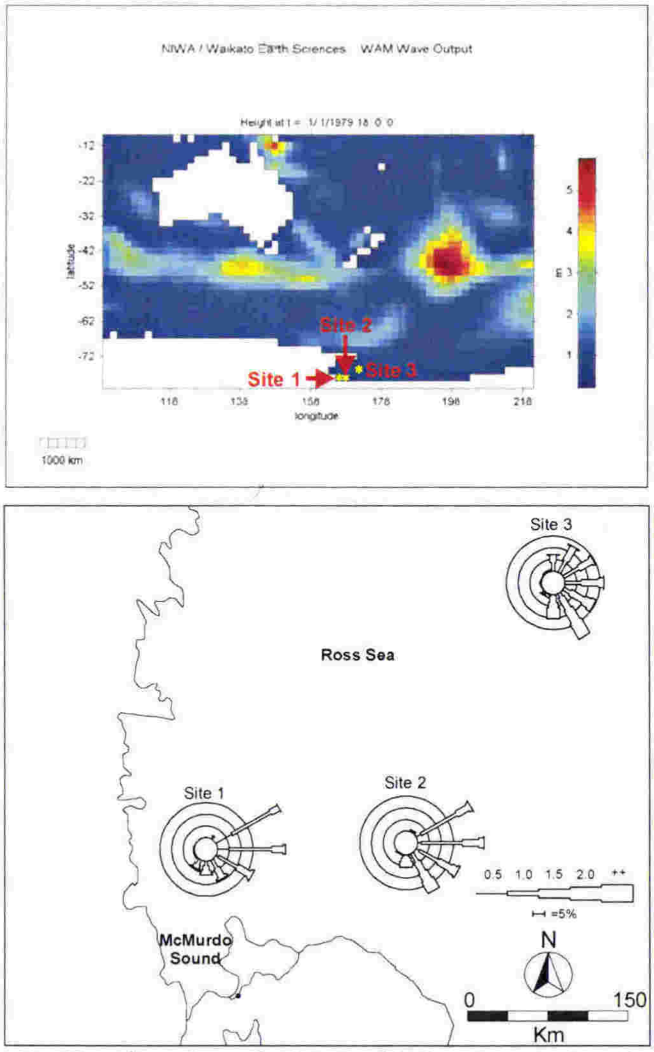

Figure 1.11. The $2^0 \times 2^0$ grid used to calculate the hind-cast wave data (Laing and Gorman, 2000) (top) and wave roses showing direction of dominant swell waves in McMurdo Sound (bottom).

1.3 This study

In order to determine the processes operating on beaches at various time scales in McMurdo Sound, both modern process information and stratigraphic and sedimentological information from modern and raised beach ridges is examined. The thesis layout is as follows; Chapter 2 reviews the literature on both Arctic and Antarctic beaches to frame the rest of the study. Chapter 3 outlines the methods used to collect the survey, sedimentological and stratigraphic data and the luminescence data. Chapter 4 presents the data on the morphology, stratigraphy and sedimentology and the luminescence ages from the beaches. These data are discussed with respect to other literature on polar and temperate beaches, which highlight typical characteristics of the beaches in McMurdo Sound. The luminescence ages provide comparisons with other work that has dated the raised beaches in the Sound.

Chapter 2

Polar beaches: the story so far.

2.1 Introduction

The primary aim of this chapter is to summarise current understanding of polar coastlines. Comparatively little is known about process environments on polar coasts. Much of the research on polar coastlines has been undertaken on Arctic beaches or lake beaches in North America, while most of the studies investigating Antarctic beaches have focussed on the raised beaches. There is a dearth of information on beach processes in the Antarctic.

The Antarctic coastline is 30,000km long but Dubrovin (1979) estimates that only 3-5% of the Antarctic coastline is ice free with the larger part of the coast terminating in ice cliffs. In the Ross Sea area this figure increases to 28% ice free (Gregory et al., 1984). Even here only 5% of the coastline is comprised of beaches.

Two distinct sets of processes operate on high latitude beaches. Marine processes, which are ubiquitous on all marine beaches and ice processes, which are limited to seasonally frozen conditions. Ice can affect polar beaches in a number of different ways. Early work by Nichols (1961) noted the occurrence of several different types of ice processes on beaches and suggested 13 features that were characteristic of polar beaches. These are:

(1) They rest on ice,

(2) they are pitted,

(3) they have ridges or mounds formed because of ice-push and / or deposition from stranded ice. Those formed by ice-push are commonly associated with beach scars,

(4) they have beach ridges that terminate abruptly because ice was present when they were formed,

(5) ice rafted fragments are found on them,

(6) they have poorly rounded beach stones,

(7) frost cracks and mounds, stone circles and polygons, and solifluction deposits are found on them,

(8) they are associated with striations formed by sea-ice and icebergs,

(9) the beach ridges may have short erosional gaps that were formed by meltwater streams,

(10) the beaches are associated with ice-contact features (proglacial deltas, eskerlike features) and glaciomarine deposits,

(11) ventifacts are present,

(12) they contain cold-water fossils,

(13) they may contain the soft parts of marine organisms.

These thirteen features Nichols (1961) describes are products of marine processes, ice processes (including sea ice and glacier ice) and fluvial action. Some of the features are common on temperate shores as well as polar coastlines. The distinction between the different processes that produced the features is not made clear by Nichols (1961).

Ice type	Coastal processes and products
Glacial ice Including ice shelves	***Tidewater calving and ice-contact deposition*** Ice cliffs Moraines and other ice-contact deposits ***Iceberg drifting and grounding*** Scour pits and troughs Wallow depressions Ice-rafted deposits
Permafrost and ground ice	***Erosion by mechanical and thaw failure*** Ice-wedge polygons and block failures Massive and retrogressive-thaw flows Active-layer detachment failures
Snow and ice on beaches	***Codeposition of sediments and snow or ice*** Icefoot development Interstratified sediment and snow or ice Snow- and ice-melt collapse structures
Surface ice cover on Lakes and seas, pressure ridges, ice floes and fragments	***Ice as a barrier to surface wave motion*** Negligible or limited beach development Finger deltas in ice-protected settings ***Enhanced hydrodynamic scour*** Strudel scour pits in prodelta settings Seaward offset of breaking wave zone Scour depressions around ice blocks ***Ice scour*** Wallow pits Grooved scour marks Ice-pushed ridges and levees Cobble pavements Boulder ramparts ***Ice ride-up and pile-up*** Beach deposits on bluffs Anomalously high barriers Shore ridges (sediment or ice) Shoreface profile adjustment ***Ice rafting*** Boulder-strewn tidal flats and platforms Boulder barricades and garlands
Frazil-, slush- and anchor-ice	***Sediment entrained by ice*** Shoreface profile adjustment

Table 2.1. Some forms of coastal ice occurrence and a selection of processes and products associated with each type (Forbes and Taylor, 1994).

2.2 Ice effects on polar beaches

In contrast with the 13 features Nichols (1961) describes, Forbes and Taylor's (1994) list lists the feature and a selection of processes and products associated with each type. This is useful as it allows identification of a related process in conjunction with the product and helps distinguish between an ice dominated and marine dominated environments.

Recent work by Forbes and Taylor (1994) highlighted forms of coastal ice occurrence and a selection of processes and products associated with each type. This is shown in Table 2.1. Although not an exhaustive list, it draws attention to the dominant types of ice at work in polar coastlines and some of the morphological products. The size of the features produced on the beaches by these different types of ice processes can range from cm scale melt pits on beaches to entire ice-push ridge systems that are several hundred metres long.

2.2.1 The icefoot

The degree to which ice processes affect beaches depends on a number of factors including the offshore slope, the orientation of the beach to the dominant wave and wind directions and the presence of an icefoot (see Appendix 1 for a glossary of some of the terms related to ice processes used in this thesis). The icefoot is arguably one of the most important features in polar beach morphology and has been widely studied (David and Priestly, 1909, Wright and Priestly, 1922, Kirk, 1966, 1972, Evenson, 1973, Hansom and Kirk, 1989, Miner and Powell, 1991, Barnes et al. 1994).

The icefoot has been defined as *"a narrow fringe of ice attached to the coast which may remain long after the fast ice has broken free"* (Armstrong et al., 1973). The icefoot forms due to the shallow water close to the shore freezing to the sea floor and onto the shore itself. Because it is frozen to the shore and the sea floor, the icefoot usually persists longer than the sea ice in the same area. David and Priestly (1909) briefly described the icefoot and Wright and Priestly (1922) described the formation and disappearance of the icefoot at Cape Adare in 1911.

Later work by Kirk (1966, 1972, Hansom and Kirk, 1989) investigated the geomorphological significance of the icefoot. Kirk (1966) examined the development of Blacksand Beach at Cape Royds from before breakout of the icefoot (19th November 1965) until 14th February 1966. While previous work on the icefoot identified it as a barrier to processes and essentially a "beach protector", Kirk (1966) saw the icefoot as an important agent in beach development.

Figure 2.1 shows shore normal profiles of icefoot breakout at different stages of the summer. Not only does the icefoot influence the offshore profile but its influence is apparent on the foreshore and backshore. On the backshore, meltwater from snowdrifts or piles of sea-ice may form ponds behind the icefoot or cut channels through it. This may saturate unfrozen beach material, which can cause accelerated erosion during storm events, or refreeze, thereby cementing the sediment.

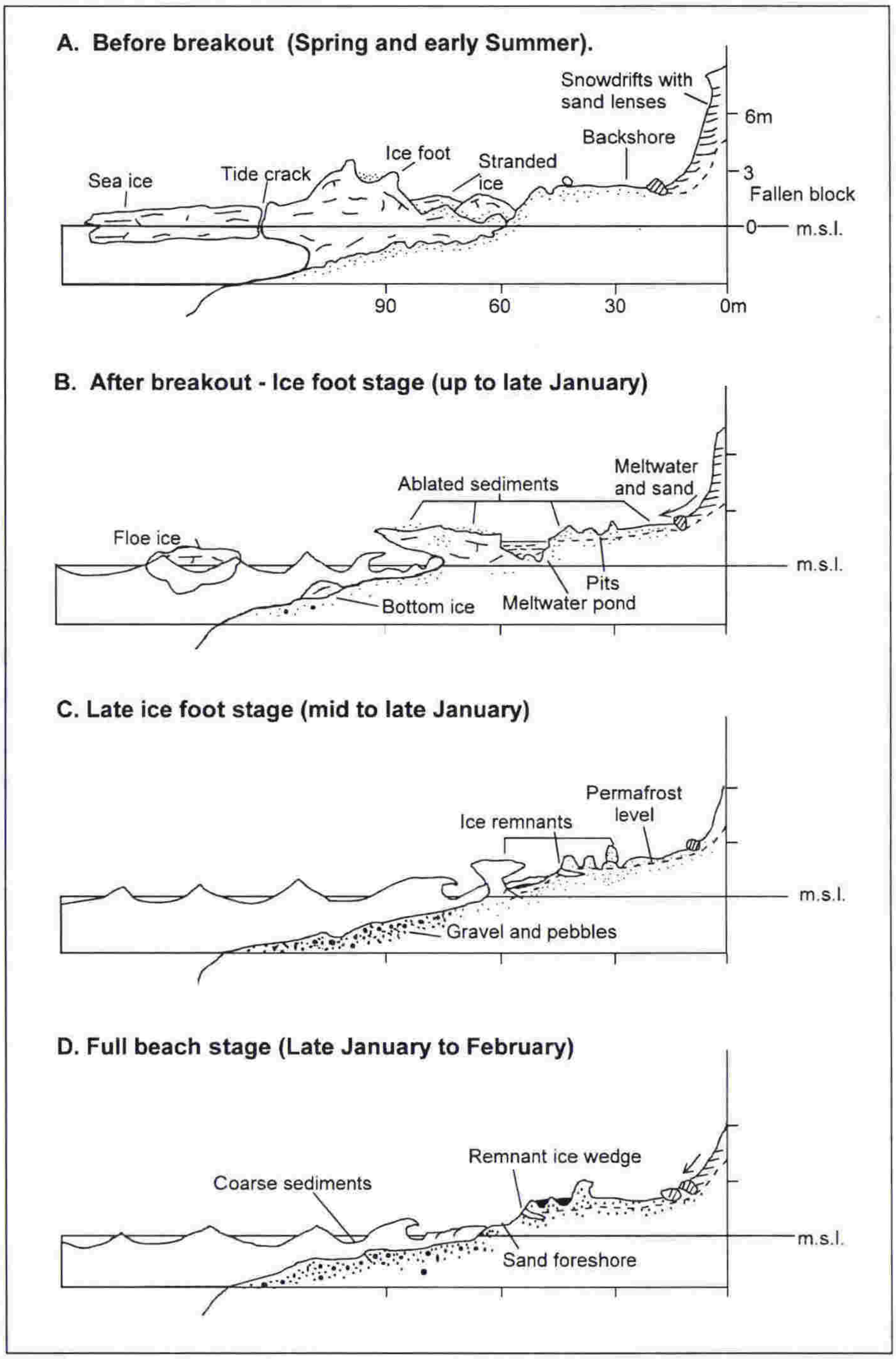

Figure 2.1. Representative profiles normal to the shore at different times during the summer (vertical exaggeration 15 times) (Kirk, 1966).

The conditions that are conducive to icefoot development are site specific. For example, local conditions that influence the type of icefoot that develops could include the offshore slope, the aspect of the coast and the presence of rivers. However, a number of authors have investigated fundamental factors that are important to beach freezeup (Marsh et al., 1973, Evenson, 1973, McCann and Taylor, 1975, Short and Wiseman, 1974). Marsh et al. (1973) observed the freezeup sequence at locations around the Great Lakes and suggested that four conditions must be met before an icefoot begins to form:

1 sub-freezing air temperatures

2 open water

3 storm waves

4 a supply of ice fragments.

This study was undertaken on the Great Lakes, which are fresh water and not affected significantly by tides.

McCann and Taylor (1975) documented the development of the icefoot at Radstock Bay in Arctic Canada from 1968 to 1973. They concluded that temperature, wind and wave and pack ice conditions were the main variables influencing beach freezeup and the type of icefoot that formed. Although the rate of temperature decrease is the most important variable, beach freezeup may be delayed by periods of wave action. If there is heavy pack ice offshore waves are unlikely to exert a major influence on the shore unless it is blown onto the beach where it may become part of the icefoot. Short and Wiseman (1974) arrived at the same conclusions regarding Arctic beach freezeup.

The most obvious effect the icefoot has is to obstruct movement of sediment on the foreshore. Marsh et al. (1973) estimated that the net sediment transport along the Eastern Shore of Lake Superior was 11 times greater than that at Point Barrow Alaska due to the shorter ice-free season at Point Barrow. The initial effect of the icefoot is to prevent wave activity between its seaward edge and the shore and provide a protective barrier for the beach from sea-ice. If there are strong currents in an area or the icefoot is in shallow water sediment can become mobile and may pile-up under the water on the icefoot itself. As the icefoot continues to break up, more sediment is thrown onto the icefoot and in places where the icefoot is several seasons old it is often possible to see several layers of sand and gravel incorporated into the ice from successive seasons. Marsh et al. (1973) suggest that this layering in the Lake Superior icefoot is due to a "two part" formation. The first or lower part of the icefoot forms from a mass of sea-ice fragments or ball-ice and is likely to be comparatively "clean ice". The second part is formed from ice added by the turbid overwash and spray from waves, creating a layer of sediment-rich ice.

Sediment is entrained in lake icefoot complexes by four primary mechanisms (Barnes et al., 1994);

1 anchor ice formation

Anchor ice is formed on the sea floor and sometimes can be part of an icefoot that has been protected by sediment. When the anchor ice becomes buoyant, it can dislodge sediment from the sea floor.

2 wave splash and overwash

As waves break on the face of the icefoot the water becomes turbid and sediment is washed up onto the icefoot. In shallow water, waves can deposit sediment onto the bottom of the icefoot or throw sediment on top of it during storms.

3 frazil and ball ice formation

Frazil ice consists of ice crystals 1-4mm in diameter that is formed in supercooled water. During periods of supercooling the frazil ice is sticky and may adhere to bottom sediment either removing it or forming anchor ice (Reimnitz et al., 1987). If the sediment is removed it may become part of an icefoot or sea-ice.

4 aeolian action

The amount of sediment entrained in the icefoot by aeolian action will depend on, the availability of sand-sized material on the beach and how frozen the beach material is. Evenson (1973) and Marsh et al. (1973) acknowledge aeolian action as a contributor to the sediment budget of the icefoot. Marsh et al. (1973) reported that a thin layer (less than 2cm thick) of sediment covered most of the icefoot on Lake Superior during spring as the icefoot was breaking up and attributed this to aeolian activity. Miner and Powell (1991) quantified aeolian addition of sediment to the ice foot on the shores of Lake Michigan during the winter of 1988/1989 and estimated that 1.5 tonnes of sediment per metre of coast was due to aeolian action.

The relative importance of each of the mechanisms for entraining sediment into the icefoot will undoubtedly depend on a variety of site specific factors. For example Barnes et al. (1994) suggest that frazil ice formation leading to anchor ice is the most important process for sediment entrainment in the icefoot. Reimnitz et al. (1987) and Kempema et al. (1989) showed that anchor ice was an important process in shallow Arctic seas and could lead to sediment loss due to rafting of material. In contrast, Miner and Powell (1991) indicated that the most influential mechanism of sediment entrainment in Lake Michigan was wave action. The differences between these studies are most likely due to site specific factors.

Although differences exist between lake and marine freezeup processes, the only quantitative measurements of sediment concentrations in icefoot complexes are from lakes. These measurements may not be comparable with marine sites but they provide a guide to sediment concentrations in icefoot complexes. Barnes et al. (1993) measured sediment concentrations of 0.28 t/m to 0.18 t/m of coast in an icefoot complex on Lake

Michigan. In contrast, Miner and Powell (1991) determined that the total amount of sediment in the icefoot during an entire winter season was as high as 5.9 t/m of coast. They calculated that 4.1 tonnes of sediment per metre of coast was added by wave action alone. Other studies have found $3cm^3$ per 1 litre of melted ice (Marsh et al. 1973). Similarly, the differences between these studies are most likely due to site specific factors.

The type of icefoot that forms is site specific. Wright and Priestly (1922) suggested that the type of icefoot that formed depended on the weather at the time of formation and the local environment. They identified 5 different types of icefoot. Three main types, (1) the tidal platform icefoot, (2) the storm icefoot, (3) the drift icefoot, and two less common types, (4) the pressure icefoot, (5) the stranded floe icefoot. These are discussed below. (The terminology and icefoot types presented by Wright and Priestly (1922) have been adopted in preference to other terminologies due to their direct applicability to the McMurdo Sound coast). A number of other forms have been described in the literature, "gravel-sand-icefoot" reported at Barrow Alaska by Rex (1964), the "kaimoo" found in the Cape Thompson region (Moore, 1966), or the "false icefoot" and the "wash and strain icefoot" found in Graham Land, Antarctica (Joyce, 1950).

2.2.1.1 The tidal platform icefoot

The tidal platform icefoot is the most common of all forms of icefoot. It forms in the colder months of the year when sea-water freezes to the shore as the tides rise and fall. As the icefoot develops, sea-water will freeze onto the ice edge that is frozen to the land. For this to occur, the air temperature must be well below the freezing point of sea-water and the sea-water must be slightly above freezing point. This type of icefoot will reflect the range of the tides in the region.

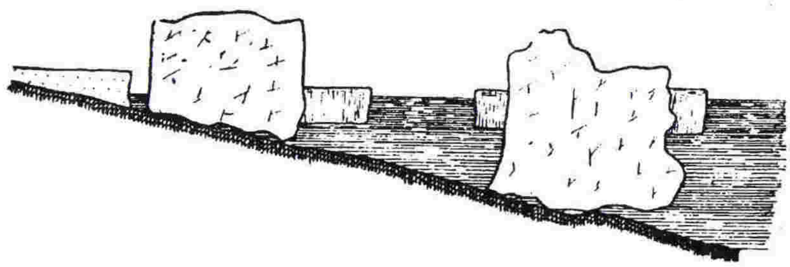

Figure 2.2. Tidal platform icefoot at Cape Adare (reproduced from Wright and Priestly, 1922).

Figure 2.2 shows an idealised section through the tidal platform icefoot at Cape Adare. As can be seen, a type of icefoot has formed on the grounded icebergs as well as the land. This occurs due to the same process that builds the icefoot on the land. There are a number of variations to the basic form shown in Figure 1, including tidal platforms with a prow or jutting edge, and platforms with extra ice on the seaward extent of the beach.

The width of the icefoot is variable and depends on the physical nature of the part of the coast on which it is forming. If the coastline is an open one and the icefoot is not fast-bound to the shore, then in extreme cases the tidal platform icefoot may reach up to one hundred metres from shore (Wright and Priestly, 1922). On the other hand, if the icefoot forms on a shore that drops off steeply, the icefoot may only be a few metres wide. The icefoot will continue to grow provided the air temperature is below the freezing point of seawater and the sea-ice has not formed. As soon as the sea-ice forms, it will scrape off any additional ice that freezes on the icefoot preventing the icefoot from extending seaward (Wright and Priestly, 1922).

2.2.1.2 The storm icefoot

High winds or a heavy swell breaking on an exposed coast creates the storm icefoot. Usually the effect of heavy seas is to remove any icefoot that has formed. However, if the heavy seas continue, spray from the breaking waves may be frozen onto the beach face. This ice is usually a cloudy-looking ice due to the presence of air and brine in the ice. The icefoot will be prevented from extending seaward due to the heavy seas but it will extend landward as spray is frozen higher up the beach than would normally occur.

Figure 2.3 shows a storm icefoot at Cape Adare with spray ice on the top of the beach extending landward. The ice can build up to thickness' of as much as 2 metres as occurred at Cape Royds during a single 3 day blizzard in 1908 (Wright and Priestly, 1922). The presence of a spray icefoot is most common, and they are best developed on the windward sides of projecting points. At Cape Adare, a spray deposit was observed to contain fragments of shells, seaweed and small pebbles. Wright and Priestly (1922) suggested that if dissected, such a deposit could be used to estimate the number and severity of storms on that part of the coast during open water conditions.

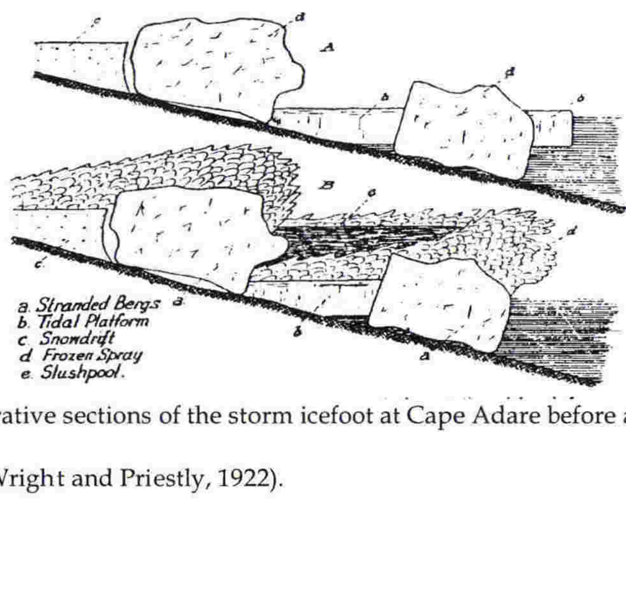

Figure 2.3. Comparative sections of the storm icefoot at Cape Adare before and after a gale (reproduced from Wright and Priestly, 1922).

2.2.1.3 The drift icefoot

This type of icefoot was first described by David and Priestly (1909) and again by Wright and Priestly (1922). It forms as snowdrifts accumulate on sea-ice. This accumulation can increase the perceived height of the sea-ice and create a ramp-like appearance to the sea-ice. Figure 2.4 shows a section through a typical drift icefoot. As can be seen, sea-ice cracks will propagate through the snowdrift. This will cause the sea-ice to sink slightly due to the weight of the snow.

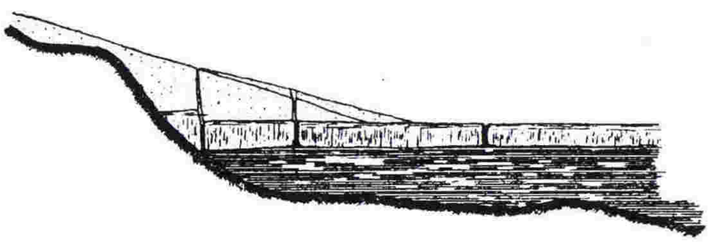

Figure 2.4. Section through a typical drift icefoot (reproduced from Wright and Priestly, 1922).

2.2.1.4 The pressure icefoot

The pressure icefoot occurs most frequently in deep bays or areas of the coast that are exposed to severe pressure from pack-ice. In some situations, the pack may push the inner line of pressure blocks onto the shore or tidal platform of the icefoot. Figure 2.5 shows a pressure icefoot that has been bound together by a cement of frozen spray. This may occur if the sea-ice is blown out following the deposition of ice on the shore and a storm blows spray onto the ice.

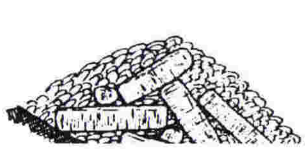

Figure 2.5. Pressure icefoot (reproduced from Wright and Priestly, 1922).

2.2.1.5 The stranded floe icefoot

This type of icefoot occurs due a tidal platform-type icefoot developing around stranded ice on the foreshore. This is shown diagrammatically in Figure 2.6. These types of icefoot usually occur on shallow gently sloping foreshores. A similar type of icefoot occurs if an iceberg becomes stranded. When this type of icefoot forms it is an indication that the water the berg is sitting in is quite shallow.

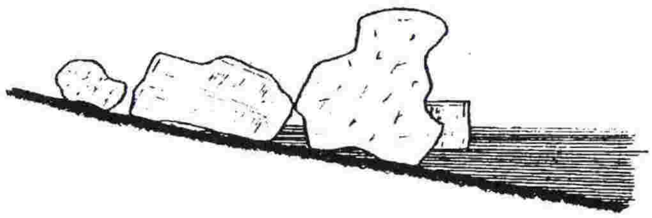

Figure 2.6. Stranded floe icefoot (reproduced from Wright and Priestly, 1922).

2.2.1.6 The breakup of the icefoot

Following the winter, as the sea-ice begins to break out, the icefoot will begin to break down. This can occur in a number of ways. The primary way that it is removed is by melting. Melting will occur from the bottom, as warmer water is circulated below the icefoot and from the top by the sun. In this way the icefoot can become weak at the edge due to undercutting by the warmer water. If gravel was incorporated in the formation of the icefoot, then the surface of the icefoot will appear to be honeycombed. Kirk (1966) suggested six primary ways the icefoot is destroyed. These are;

1. *direct melting;*
2. *melting beneath the water's surface owing to the difference in the salinity between the seawater and the sea-ice, even though the water temperature is 1.9°C below zero;* (fresh water and sea water freeze at different temperatures so if fresh water ice begins to become saline as a result

of contact with the surrounding sea water, it will melt in sea water that is warmer then -1.9^{0}C)

3. *the grinding action of floe ice along the seaward face;*
4. *localised melting caused by heat transmitted from sediments in and on the ice;*
5. *melting by ponded meltwater from the backshore;*
6. *the hydraulic action of waves which run under the seaward face of the icefoot and break in confined spaces.*

Miner and Powell (1991) studied an icefoot on Lake Michigan and concluded that wave action was the dominant process that caused break-up of the icefoot. The differences in dominant processes for icefoot break-up further highlight the differences that exist due to site specific variables.

As the icefoot breaks up it is rafted offshore in pieces. Any sediment that is entrained in the icefoot at this time may be rafted alongshore or offshore and then dumped into deeper water as the ice melts. This method of erosion has been reported to cause relatively high rates of erosion in some areas. Barnes et al. (1993) and Barnes et al. (1994) reported that between 350 and 2,750 t/day of sediment could be transported alongshore and around obstacles such as groynes. Assuming a density of about 3.5 g/cm^3 for the material being transported, this represents between 100 m^3 and 780 m^3 of material being transported daily. Sites in McMurdo Sound are likely to have considerably less erosion due to the break up of the icefoot than the beaches in that Barnes et al. (1993) and Barnes et al. (1994) studied. This is due to the nature of the break up of the icefoot in McMurdo Sound, which is predominantly melting.

2.2.2 Sea-ice

The degree to which sea-ice will affect an area will depend on both the presence of an icefoot, the extent of sea-ice in that area and the duration the sea-ice remains at that location (Taylor and McCann, 1976). Although sea ice creates distinctive coastal morphologies Forbes and Taylor (1994) have shown that the primary effect of sea ice cover is as a barrier to wave action.

Sea-ice affects polar coasts in two primary ways. Firstly, wave energy is reduced as the waves travel through pack ice. Secondly, sea-ice can be pushed up the beach face and create a number of features such as melt out pits or ice-push ridges. Direct observations and mathematical modelling of waves in sea-ice has shown that the attenuation of wave energy is dependent on the wave period (Squire and Moore, 1980, Meylan and Squire, 1994).

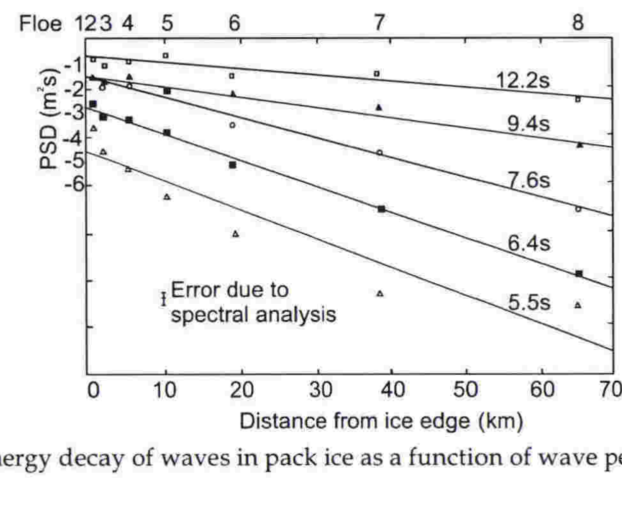

Figure 2.7. Energy decay of waves in pack ice as a function of wave period (Squire and Moore, 1980).

Figure 2.7 shows the energy decay of waves in pack ice as a function of wave period. As can be seen, the longer the wave period the less energy is lost as the waves travel through the pack ice. Squire and Moore (1980) also showed that the pack ice responds to wave period by breaking into different size floes. The sea-ice close to the ice edge breaks into smaller floes as the shorter period waves act on it. The shorter period waves are rapidly attenuated by the sea-ice so the size of the ice floes increases with distance from the ice edge. The longer period waves can propagate through pack ice and act on the shore. Pack ice will also limit the fetch of an area. The magnitude of this effect will depend entirely on the extent of the pack ice.

Where sea-ice extends up to the shore, a number of characteristic features can be formed. In extreme circumstances sea-ice can bulldoze sediment up the beach face into ridges of sediment at least 80m long and 7m high (Owens and McCann, 1970) or build piles of sea-ice up to 12m high (Boyd, 1981). Sea-ice pushed onto the beach may become stranded and can result in the formation of melt pits. In intertidal areas ice has been known to cut grooves into tidal flat sediment measuring up to 0.8m wide 0.35m deep and 2,000m long (Dionne, 1969). The relative importance of ice features on the profile of a beach is dependent on the length of time sea-ice is present in an area, the tidal range in the area and whether an icefoot is present.

Ice-push features are well-documented both in the Arctic and the Antarctic (Hume and Schalk, 1964, Hume and Schalk, 1967, Owens and McCann, 1970, Taylor and McCann, 1976, Nichols 1953, 1961, 1968, Boyd, 1981). They occur when sea-ice is pushed onto the beach by currents or wind. There are two distinct types of ice-push features, those produced by ice pile-up and those produced by ice ride-up.

1 *"Ice ride-up is a process in which a sheet of ice slides smoothly landward across a low relief beach and steeper relief areas beyond for distances as great as 800m, but generally much shorter"* (Reimnitz et al., 1990).

2 *"Ice pile-up is accompanied by buckling and crumbling of an advancing sheet of ice"* (Reimnitz et al., 1990).

Boyd (1981) recorded an ice piling event on Lake St. Clair in Canada. He documented two types of ice piling on the shore:

1 *ice slides progressively on top of the preceding floe forming a pile, with smaller blocks dropping off the leeward side forming an ice talus slope*

2 *incoming ice buckles the fast ice and/or slides under the preceding floe, seemingly forming a pile from the bottom* (Boyd, 1981, page 10).

Gilbert (1990) makes a further distinction between ice-pushed and ice-lifted landforms. He studied the shoreline around a small lake in Maine and suggested that ice-lifting could occur during the rise and fall of tides on tidal coastlines or the thermal expansion of the floating ice, whereas ice-push could be attributed to wind and current action on sea-ice. Because of the presence of the icefoot in polar regions, ice-lifting is probably a fairly insignificant process.

Hume and Schalk (1964) reported an ice ride up event at Point Barrow, Alaska where a 130 metre wide tongue of sea-ice advanced over 40 metres up a low sandy beach. The ice planed and striated the beach and created an almost continuous line of low mounds along the beach where it terminated. Taylor (1978) reported ice-push features as far as 185 metres inland along the northern coast of Somerset Island, North West Territory. Sometimes ice-push ridges will be ice-cored as ice pushes directly into the beach alternatively ice can becomes stranded on the beach and become buried by sediment thus creating an ice cored ridge.

Similar to the icefoot rafting sediment offshore, sea-ice has been reported to raft sediment both offshore and onshore (Hume and Schalk, 1964, Kempema et al. 1989, Reimnitz et al. 1990). Hume and Schalk (1964) investigated ice-push mounds on Cooper Island and found that they comprised 10% of the sediments above sea level. The beaches at Point Barrow Alaska were reported to comprise 11-22% of rafted material. From profiles measured in 1982 Reimnitz et al. (1990), determined that at least 700m^3 of coarse sediment was supplied by ice encroachment to a 350m long stretch of Spy Island. Reimnitz et al. (1990) calculated in 1978 the seasonal ice cover in Northern Alaska, carried 16 times as much sediment as the total annual suspended sediment input from adjacent coastal rivers. Sea-ice pile-up (as opposed to sea-ice ride-up) is reported to be the more significant mechanism for transporting sediment onto the beach (Reimnitz et al., 1990).

Although ice-push ridges and ice piles appear impressive, only 1-2% of local beach material is involved in producing these features (Hume and Schalk, 1964). Further, Taylor and McCann (1976) and Owens and McCann (1970) suggested that ice-push features do not affect the overall shape of the beach. McCann and Owens (1970) surveyed beaches in the Cape Ricketts area in the Canadian Arctic and also found that the effect of ice-push on the profile of the beach was not significant.

After ice pile-up events or ice ride-up events small pieces of ice stranded on the beach often form melt pits that can persist for several seasons. Melt pits about 6,000 years old can be found at Marble Point up to 15m AMSL (Nichols, 1968). These features form as large pieces of sea-ice melt on the beach or small pieces of buried ice melt forming hollow depressions up to 3 m in diameter and 0.6 m deep (Taylor and McCann, 1976).

Two closely linked features characteristic of ice-rafting are boulder pavements and shore platforms. Boulder pavements occur as flat tightly packed areas of boulders and may result from either ice-pushed or ice-rafted boulders being forced into the substrate by grounded ice or by wave winnowing of glacial till at sea level that is subsequently modified by grounded ice (Hansom, 1983a). Boulder pavements will only form if three conditions are met;

1 *a boulder supply exists;*

2 *there is frequent onshore movement of floating ice; and,*

3 *a low-gradient intertidal zone* (Hansom, 1983a).

Although all of these criteria must be met for a boulder pavement to form, Hansom (1983a) suggests that boulder pavement development is best where there is a high frequency of onshore ice movement. Dating of these features in sub-Antarctic locations indicates that well-developed boulder pavements will form within 300 years.

McCann et al., (1981) reported two different types of boulder barricades along the Baffin Island coast. They suggested the two different features required different transport mechanisms but were unable to reach any conclusions as to what these might be. Drake and McCann (1982) calculated the ability of ice floes to move isolated boulders on tidal flats by floatation and by pushing and/or rolling them along the bed. They suggested that floatation was sufficient to carry most of the boulders they had seen but rolling was probably the most likely form of boulder transport. Dionne (1981) investigated boulder accumulation in the St. Lawrence estuary. The presence of accumulations of boulders in a relatively temperate estuarine environment highlights the effectiveness of sea-ice in transporting them. Dionne (1981) measured boulders up to 6m across and weighing up to 170 tonnes. Some of the features these boulders created while being dragged or rolled across the estuary include; *ice-push ridges*, which are semi-continuous ridges that have been bulldozed into place by the ice rafted boulders, *circular depressions*, which are shallow depressions where a boulder was removed by ice; and *gouges or furrows* which are associated with frontal and lateral ridges made by the boulders as they were pushed along the bottom by ice floes (Dionne, 1981). Philip (1990) reported scars from ice-pushed boulders that were visible after several years despite being filled with new sediment. Dionne (1998) found well-preserved 200 to 600 year old sedimentary structures in recently emerged tidal deposits in the St. Lawrence estuary. Two distinct types of structures were distinguished; bowl shaped circular and elongate structures which are former scoured depressions subsequently filled with mud, fine sands and organic debris; and ice-block pressure deformations a few centimetres to a few metres long which occur as a result of large blocks of ice deforming the soft estuarine sediments (Dionne, 1998). In contrast, Gordon and Desplanque (1981) measured shallow ice-gouges in the Bay of Fundy and suggested that they were fairly short-lived, lasting only until spring when tidal currents redistribute the sediments.

Shore platforms in polar regions are formed by ice freezing-on and quarrying by impact and abrasion (Hansom, 1983b). Their morphology is generally characterised by wide (up to 800m) platforms that are broken by abrupt changes at or just below low and high water marks. Shore platforms are best developed in areas where shore or fast ice persists longest (Hansom, 1983b). Figure 2.8 shows shore platforms at Byers Peninsula, Livingston Island. The wider and flatter platforms (profile A and B) are generally located in sheltered bays where fast ice remains for long periods. In contrast, the shorter platforms (profiles C and D) are located in headland situations where fast ice only remains for relatively short periods of time (Hansom, 1983b).

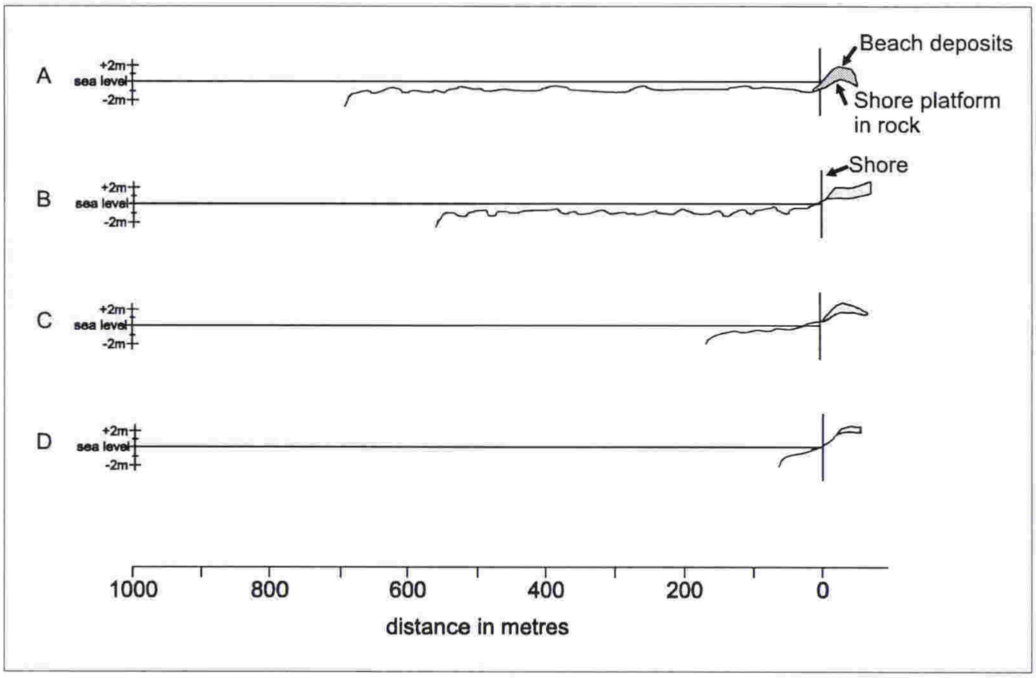

Figure 2.8. Profiles of shore platforms at sea level, Byers Penninsula, Livingston Island. The wider and flatter platforms (profiles A and B) are generally located in sheltered bays in contrast to the shorter platforms (profiles C and D) that are located in headland situations (modified from Hansom, 1983b).

2.2.3 The effects of icebergs on polar beaches

The effects of icebergs on polar beaches and offshore areas have been widely studied (Dionne, 1968, Dionne, 1969, Reimnitz et al.,197 2, Dionne, 1981, Dredge, 1982, Lien et al., 1989, Dionne, 1998,). They can affect beach morphology directly by pushing into the beaches, and scouring the offshore bed, or indirectly by sheltering the beaches from wave action and providing pinning points for sea-ice thereby shortening the ice-free season. Icebergs may be pushed onto polar beaches in the same way sea-ice is pushed onto the beaches. Reimnitz et al. (1972) documented the nearshore influence of grounding ice in the Beaufort Sea. They attributed the irregular bottom topography to the action of grounded ice.

Figure 2.9 shows bottom profiles of the Beaufort Sea traced from echosounder records. Reimnitz et al. (1972) called this type of sea-bed topography ice-gouging and showed that it occurred from the beach to at least 75m deep. Lien et al. (1989) used side scan sonar and shallow seismic profiles to examine the sea-bed topography in the Weddell Sea, Antarctica. They found that iceberg plough marks were the dominant feature and reported iceberg gouges at depths up to 400m with an average depth of scouring 300 to 320m. Reimnitz et al. (1977) resurveyed several profiles in the Beaufort Sea at 6 to 14 metres depth and calculated that the bottom sediments were completely reworked to a depth of 20cm every 50 years.

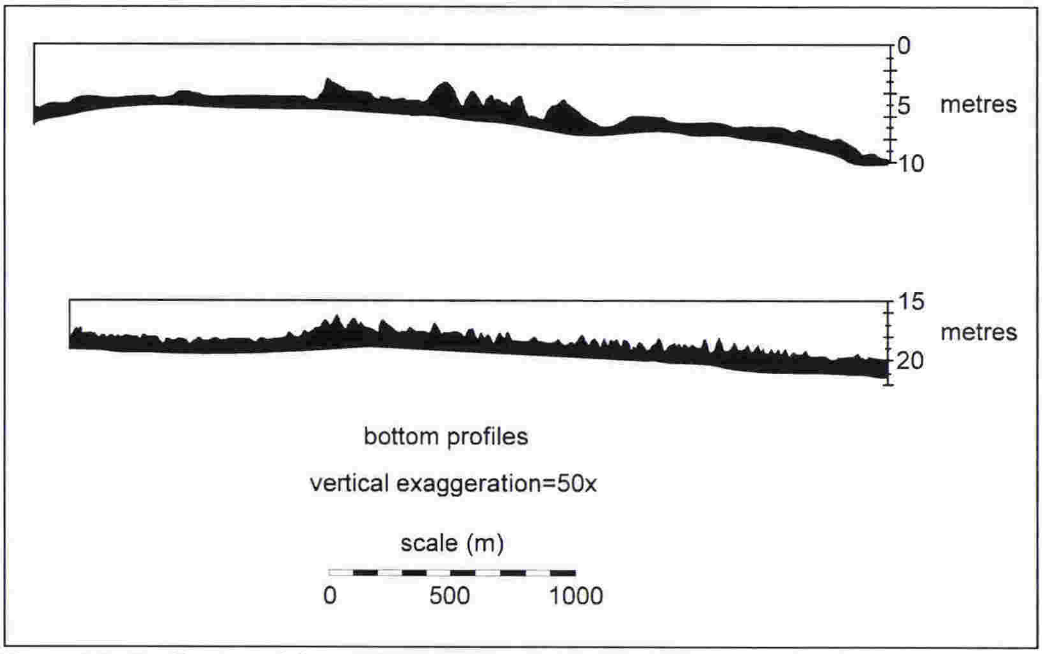

Figure 2.9. Profiles traced from echosounder records illustrating microrelief of the Beaufort Sea (modified from Reimnitz et al., 1972).

Reimnitz and Kempema (1982) studied the effects of icebergs on nearshore profiles in the Beaufort Sea and identified large potholes and mounds with 2 to 3 metres of relief in many nearshore areas. These mounds and potholes were found to be the result of small icebergs grounding in the nearshore. After grounding the icebergs would cause pulsating currents due to rocking motions or vertical oscillations, and intensified currents where the iceberg was grounded would cause a complex pattern of erosion and deposition. The potholes and mounds were called ice-wallow features.

Another way in which icebergs can affect the morphology of a beach is by sheltering the beaches from wave action. This has not been reported in the literature but large tabular icebergs grounding close to shore can remain in place for several seasons crating a complex pattern of waves at the shore. At Cape Royds on the 25th January 1998 a small iceberg (20 metres by 10 metres) became grounded about 45 metres offshore. This caused wave heights to be reduced almost by half at the point that was sheltered by the iceberg. If a larger iceberg was grounded offshore it could shelter an entire bay for several seasons considerably reducing the wave activity. If icebergs became grounded they can also provide pinning points for sea-ice effectively shortening the ice-free season in the immediate area.

2.2.4 Permafrost on polar beaches

There have been no published studies of the effect of permafrost on Antarctic beaches. However, permafrost can play a major part in the formation of polar beaches. If beach material is frozen, waves and wind can not move the sediment. During a storm at Cape Royds on the 25 January 1998, waves were up to 0.6 m high and had a period of about 4 to 5 seconds. Usually waves of such short period are erosional. However very little change was recorded because the beach and large areas in the nearshore were frozen. Rather than erode any material under these storm conditions (windspeeds up to 15 m/s and temperatures approximately $-5^{0}C$) the beach merely became armoured with a layer of ice from swash and spray from the waves.

In addition to preventing movement of sediment, permafrost forms an impenetrable layer within the beach, which inhibits the downward percolation of water. This will have a number of effects on the beach. Firstly, the beach material that is not frozen will become saturated and more prone to erosion by waves. Secondly, melt pits will begin to form as small depressions fill with water, which melts the underlying ice. If larger depressions such as swales fill with water, subsequent freezing can lead to total isolation of the sediment in the swale. On older beach deposits constant freeze thaw cycles can lead to the development of patterned ground. This can modify the stratigraphy within the beach thereby erasing the record that would otherwise be preserved. Patterned ground is present at a number of locations in McMurdo Sound on both the raised and active beaches. The best-developed patterned ground can be found on Dunlop Island on raised beaches. At Cape Bernacchi frost wedges have advanced to the waters edge.

2.3 Polar beach morphology

The morphology of polar beaches has been widely studied both qualitatively (Dubrovin, 1979, Araya-Vergara, 1982, Gregory et al., 1984, Hansom and Kirk, 1989, Gregory and Kirk, 1990, Kirk, 1991) and quantitatively (McCarthy, 1953, Hume and Schalk, 1964, Rex, 1964, Greene, 1970, McCann and Owens, 1970, Reimnitz et al., 1978, Rosen, 1978, Taylor, 1980,Harper, 1990). Komar (1998) suggests that the overall morphology of a beach reflects a combination of the composition of its sediments and the physical processes of waves and currents. Therefore, large changes in beach morphology might be expected from season to season due to the periodical derangement and rearrangement of sediments by ice in the winter months and by waves in the summer months in much the same manner as "summer" and "winter" profiles on lower latitude coasts.

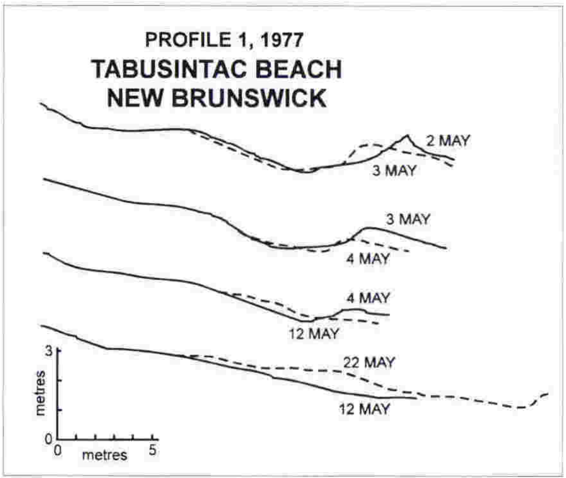

Figure 2.10. Profile changes on an ice-push ridge New Brunswick, 2 May to the 22 May 1977 (Rosen, 1978).

The presence of ice adds another dimension to beach profile development. For example, Rosen (1978) investigated ice-push ridges and kaimoos in New Brunswick and found that these depositional features protect the beach from storms for a short period but profiles can be altered significantly by storms when the ice is removed. These rapid changes in morphology following the removal of ice are shown in Figure 2.10. McLaren (1980) investigated the sensitivity of the Labrador coastline to oil spills and showed that beach slope increased linearly with an increase in the grain size on the beach. He measured beach slopes ranging from 8.9^0 to 1.9^0 which corresponded with material size from -0.22ϕ to 6.85ϕ respectively (McLaren, 1980). These studies suggest that these coastlines were dominated by wave activity.

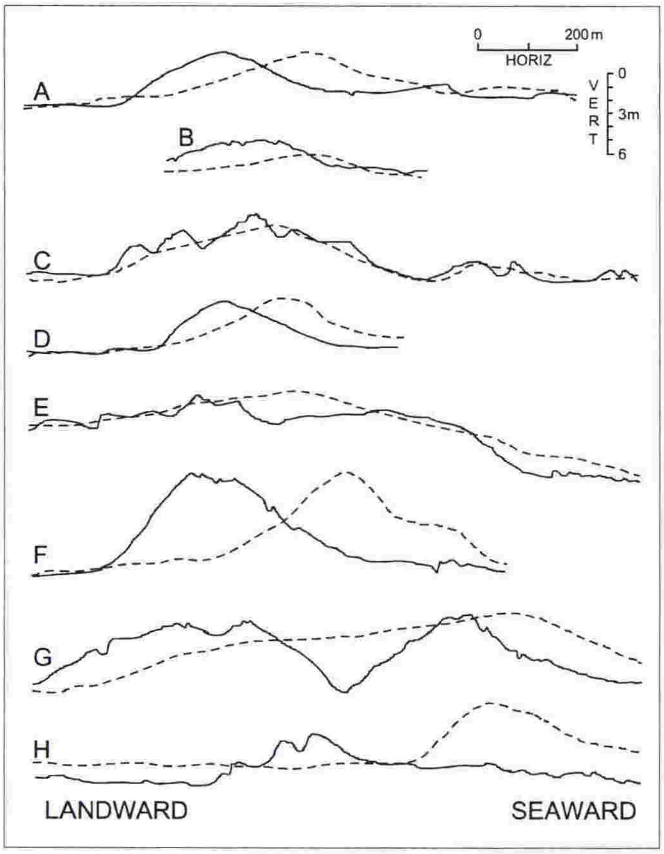

Figure 2.11. Cross sectional profiles of shoals in the Beaufort Sea as surveyed 1949-51 (dashed line) and 1975 (solid line). All but one of the shoals has migrated landward through distances of 100-400 m of the 25 years (Reimnitz, et al., 1978).

In contrast to the modification by wave action, Reimnitz et al. (1978) showed large profile variations of shoals in the Beaufort Sea that have been linked to ice processes. They suggested that the shoals migrated as much as 100-400m in 25 years as a result of ice-bottom interaction. These changes are shown diagrammatically in Figure 2.11. Hequette and Barnes (1990) studied coastal changes in the Canadian Beaufort Sea. They suggested that rapid erosion of the nearshore zone was also attributable to ice processes. In this case they proposed that the erosion was primarily driven by sea-ice gouging of offshore sediments. As material was removed from offshore by sea-ice gouging the profile attempted to return to a dynamic equilibrium by eroding the nearshore slope.

These conflicting ideas about what processes are dominant on polar coasts show that large changes in beaches can be expected over short distances depending on whether ice processes or waves and currents are the dominant process. Shaw et al. (1990) described a number of barriers in eastern Canada that occur in different environments. They show that sediment supply and the physical setting of a particular coast will determine the resultant morphology of the beaches even though ice processes are active on this coast. For example, two barriers with limited sediment supply were shown to display strikingly different characteristics with one of them being stable for the past 20 years while the other has been retreating at 8m/a since 1954 (Shaw et al., 1990). Although both of the barriers have a limited supply of sediment the differences in their stability were attributed to the diversity of the physical setting. Shaw et al. (1990) suggest that differences in barrier morphology, stability and evolution are governed primarily by:

a) the physical setting in which the barrier has formed

b) the type and size of the glacial sediment source from which the barrier is derived and the way in which that sediment has been dispersed; and,

c) the rate of relative sea-level change (Shaw, et al., 1990).

Taylor (1980) studied the coastal environments along the northern shore of Somerset Island in the Canadian Arctic. He characterised the coastline into six shore types. These were;

1. High rock cliffs

2. Low rock shores with pocket beaches

3. Sand and gravel plain

4. Gravel beaches (a) beaches with sloping backshores

   (b) beach accumulation forms

5. Deltas

6. Estuary (Taylor, 1980).

Taylor (1980) also presented characteristic beach profiles of (a) sand and gravel plain, (b) gravel beach with sloping backshore and (c) gravel beach barrier systems on Somerset Island. These are shown in Figure 2.12.

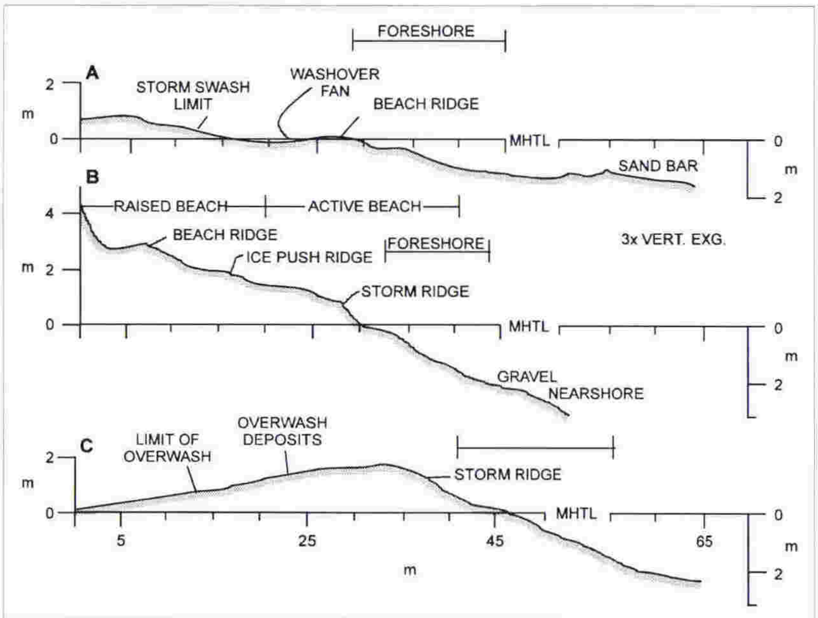

Figure 2.12. Characteristic beach profiles of (a) sand and gravel plain, (b) gravel beach with sloping backshore, (c) gravel barrier beach (Taylor, 1980).

The profiles shown in Figure 2.12 seem to display characteristics of temperate beaches. The gravel beaches are considerably steeper than the sandy beach and storm ridges can be identified on the profiles. This implies that they may be dominated by marine processes rather than ice processes.

Several authors have described the major types of shorelines found in the Antarctic (Dubrovin, 1979, Araya-Vergara, 1982, Gregory et al., 1984, Hansom and Kirk, 1989, Gregory and Kirk, 1990, Kirk, 1991). Dubrovin (1979) and Araya-Vergara (1982) present broad continental-wide shoreline classifications. In contrast, Gregory et al. (1984), Gregory and Kirk (1990), and Kirk (1991) present a classification system for the Victoria Land coast. They identified five different types of shoreline and described their distribution in the Ross Sea. The five types of shoreline in order of significance are:

1. high ice cliffs
2. high rocky cliffs
3. low rocky coasts
4. beaches
5. landfast sea-ice.

Landfast sea-ice varies a great deal spatially and temporally so the order does not necessarily indicate that it is the least common shore type in the Ross Sea. The percentages of the different types of shoreline are shown in Figure 2.13. This clearly shows that non-ice shores are regionally common features in the Ross Sea but on a continental scale they are relatively rare. In McMurdo Sound from Gregory Island to Cape Bird the amount of shoreline that is ice-free is 36.5% with only 1.5% of the shoreline comprising beaches (Taylor, 1922).

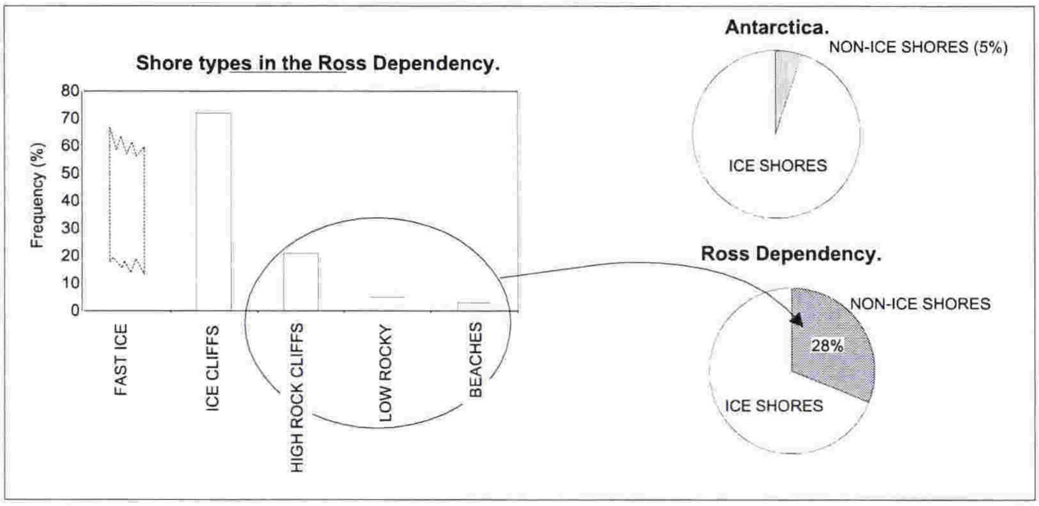

Figure 2.13. The extent of shore types in the Ross Dependency mapped by Gregory et al. (1984). The bar graph shows percentages of a particular shore type and the pie chart represents the percentage of ice-free shore line (high rock cliffs, low rocky shorelines and beaches) (after, Gregory et al., 1984).

Hansom and Kirk (1989) make a further distinction between the beaches in the Ross Sea. They describe strandlines and cuspate forelands and spits. Strandlines are accumulations of beach sediments formed by marine reworking of in situ glacial debris. Cuspate forelands and spits form at the downdrift ends of eroding cliffs or at the leeward ends of islands. Apart from a cuspate foreland at Cape Bird, all of the beaches in McMurdo Sound are strandlines.

2.4 Polar beach sedimentary and stratigraphic characteristics

Only a handful of studies have investigated the sedimentary and stratigraphic characteristics of polar coastlines (Nichols, 1961, 1968, McCann and Owens, 1969, McLaren, 1980, Shaw et al., 1990, Reinson and Rosen, 1982, King and Buckley, 1968, Dionne, 1998). Most of these have only presented qualitative descriptions of sediments found on polar beaches and have very little quantitative data of clast size, shape or bedding characteristics.

Nichols' (1961, 1968) descriptions of the beaches in McMurdo Sound include poorly rounded and poorly sorted beach stones. Based on work in Devon Island, McCann and Owens (1969) also showed that beach stones in an Arctic environment are less well rounded than beach stones on temperate beaches. McCann and Owens (1969) found that larger material was found at the top of beach ridges and material appeared to be better rounded further from the source indicating a strong influence from marine processes. King and Buckley (1968) noted that beach material in West-central Baffin Island became more rounded and better sorted further from the source areas. In addition, they showed that material was smaller and better sorted on beaches than in deltaic deposits (King and Buckley, 1968). These differences are almost certainly due to the highly selective nature of marine processes.

Reinson and Rosen (1982) described some stratigraphic sequences on beaches in Labrador. The sequences they described represented a change from summer to winter conditions on a sub-Arctic beach. Figure 2.14 shows the sedimentary sequence at the mouth of the Michael River in Labrador. Reinson and Rosen (1982) interpreted this as a yearly cycle of beachface accretion. Although they acknowledge that some of the units in the sequence (see Figure 2.14) may be missing, the likelihood of any units being preserved in many environments is probably quite rare. Large magnitude storm events would almost certainly obliterate these sequences. Dionne (1998) also investigated ice-made sedimentary structures in the St. Lawrence estuary Quebec. He described numerous ice-made erosional and deformational structures that were between 200 and 600 years old. Erosional structures include former scour circular depressions (30 to 100 cm across and 20 to 40 cm deep) and elongated shallow depressions 20 to 40 cm wide and a few metres long) (Dionne, 1998). Both Reinson and Rosen (1982) and Dionne (1998) suggest that identification of these structures in the sedimentary record could be a useful tool for interpreting former climatic conditions in an area.

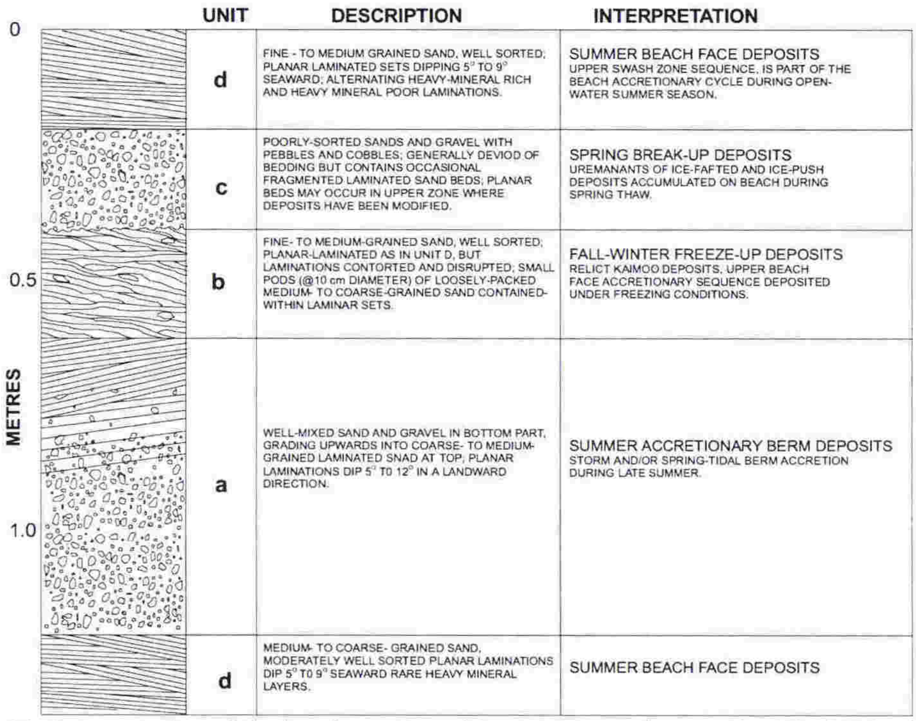

Figure 2.14. Interpretation of the beach stratigraphic sequence at the mouth of the Michael River, Southern Labrador. The sequence is described in terms of a yearly cycle of beachface accretion (Reinson and Rosen, 1982).

Similar to the morphology of coastlines in polar climates, it is apparent that the dominance of either ice processes or waves and currents will play a major role in the sedimentary characteristics and stratigraphic structures that are preserved on the beaches.

2.5 Summary

There have been a limited number of studies concerning aspects of polar beaches. Most of these studies have given qualitative descriptions of the beaches with only a handful providing quantitative data on the beaches. Polar beaches are subject to both waves, currents and other temperate coastal processes, and ice-type processes. Ice processes that act on polar beaches include:

1. **the icefoot** which; (a) acts to protect the beach from waves in the winter; (b) removes sediment from the beach as it breaks up; (c) creates features such as melt pits; (d) creates ponds on the shoreward side of the icefoot.
2. **sea-ice** affects the beaches in three fundamental ways; (a) it can severely restrict wave fetch and attenuate waves; (b) push sediment or sea-ice up beaches and form ice-push ridges or striate the beaches; (c) gouge offshore sediments.
3. **icebergs** can affect polar beaches by; (a) gouging offshore sediments; (b) acting as a nearshore buffer to waves.
4. **permafrost** will act to cement beach sediment thereby reducing the effectiveness of waves in resorting the sediment.

Polar beach morphology reflects the combination of ice and coastal processes. Depending on the dominant process in a particular area the beaches may be chaotic and hummocky in appearance (reflecting an ice-dominated environment) or have well formed shore normal beach ridges (reflecting a wave and current dominated environment). The sedimentary and stratigraphic characteristics of polar beaches will also depend on the dominance of one process over another. Well-rounded and sorted sediments and strong bedding will reflect a wave-dominated environment in contrast to poorly rounded and sorted sediments and no bedding present reflecting an ice-dominated environment.

Chapter 3

Methodology

3.1 Introduction

Two major groups of techniques were used in this project, topographical surveying and sedimentological investigations. In addition some beach process investigations were undertaken and ages were calculated for sediment samples using optically stimulated luminescence (OSL). This chapter outlines all the techniques used.

3.2 Field Logistics

All field sites in McMurdo Sound were accessed by helicopter from Scott Base. Preparations for field seasons were undertaken with help from Antarctica New Zealand. Tent camps were made at Cape Bernacchi, Marble Point, Kolich Point, Spike Cape, Dunlop Island, Cape Bird and Cape Royds. Table 3.1 shows the locations of field camps and the dates these sites were visited. As can be seen the field seasons were relatively short with all of the field seasons about 1 month in duration.

1996/1997 Season	1997/1998 Season	1998/1999 Season
Marble Point 1 January-16 January	**Cape Bernacchi** 15 January-21 January	**Cape Bird** 30 December 1998-7 January 1999
Kolich Point 17 January-20 January	**Cape Royds** 22 January-3 February	**Cape Royds** 8 January-11 January
Spike Cape 21 January-25 January	**Cape Bird** 5 February-13 February	**Dunlop Island** 12 January-14 January
Dunlop Island 26 January-1 February		**Spike Cape** 15 January-18 January
		Marble Point 19 January-23 January
		Cape Bernacchi 24 January-28 January

Table 3.1. Locations and duration of field camps in McMurdo Sound.

3.2 Morphology

3.2.1 Surveying

Surveys of the beaches were undertaken using either a Sokkia C3-A survey level or a Sokkisha model C3-E survey level. Profile locations were chosen to represent the widest possible range of energy environments on beaches in McMurdo Sound. Where possible, profiles were surveyed to benchmarks established by the New Zealand Department of Survey and Land Information (DoSLI), which have errors of ±2m. The location and heights of these benchmarks is shown in Figure 3.1. Most of the profiles were also surveyed to still water level and the surveys were timed so that they could be tied to the tide gauge at Cape Roberts. The Cape Roberts tide gauge (shown in Figure 3.1) provided a better sea-level control than the benchmarks.

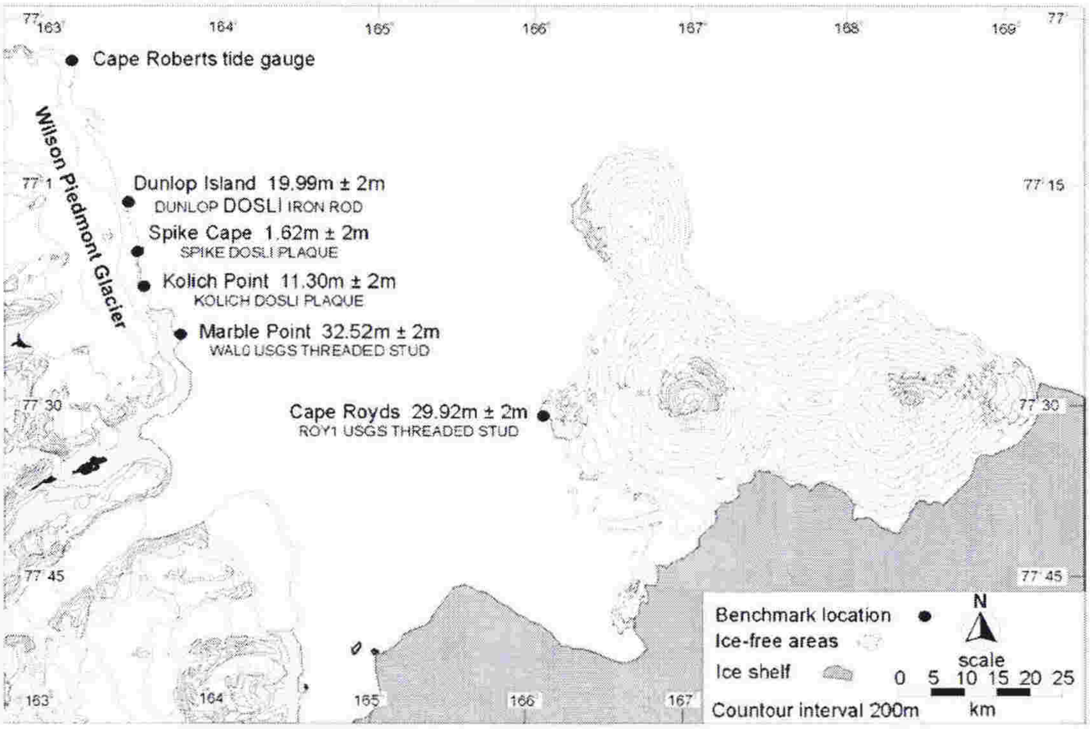

Figure 3.1. Location of survey benchmarks in McMurdo Sound used in the 1996/97, 1997/98 and 1998/99 field seasons. Heights of benchmarks are in metres above mean sea level.

3.2.2 Tidal surveys

To resolve the surveys for mean sea level, lag times from Cape Roberts to various locations along the coast were calculated from tidal measurements taken at Cape Bernacchi between 1735 hrs on 26 January 1999 to 0100 hrs on 28 January 1999. Errors in reading the staff during the Cape Bernacchi tidal survey were visually estimated to be ±0.1m due to small waves propagating through the pack ice surrounding the shore. These caused small variations in the water level during measurements. The tidal curve constructed from these data was compared with the observed tidal data for Cape Roberts. Figure 3.2 shows the two tidal charts. (The Cape Bernacchi polynomial line represents a 6th order polynomial that was calculated to resolve the tidal cycle at Cape Bernacchi). The tidal cycles at Cape Bernacchi and Cape Roberts exhibit a very strong correlation, with the tidal maximums for both sites corresponding. At high tide on 28 January the polynomial line shows that Cape Bernacchi advances Cape Roberts by 1 hour however, note that the difference in water depth between the low point and 1 hour before is only 0.03m — well within the error measurement of 0.1m.

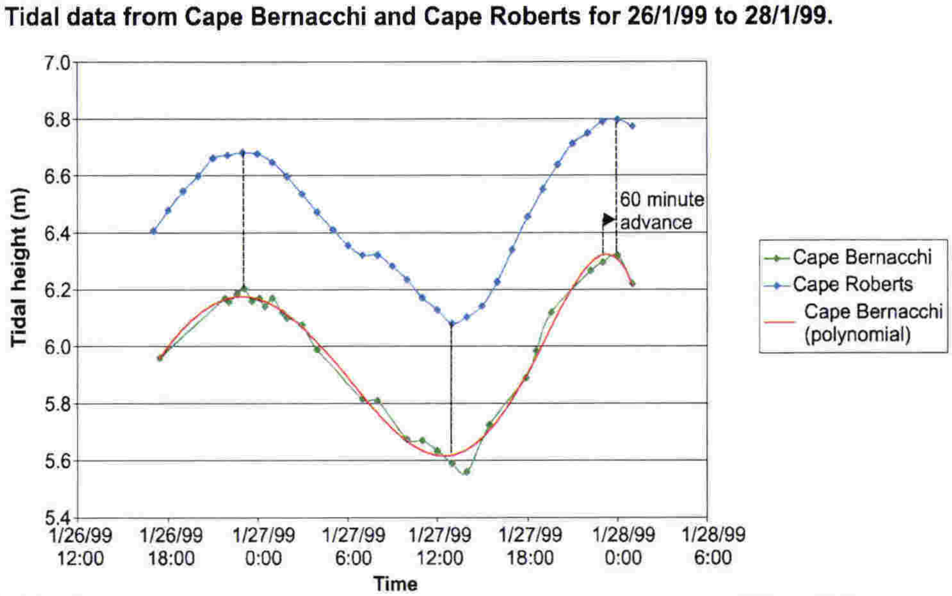

Figure 3.2. Tidal curves for Cape Bernacchi and Cape Roberts 26 January 1999 to 28 January 1999. The trend line fitted to the Cape Bernacchi data is a 6 order polynomial.

In addition to the calculation of a lag time for Cape Roberts to Cape Bernacchi, the time lag from Cape Roberts to Cape Bird was also calculated. The lag was calculated using 13 hours of water level data that was surveyed from 27 December 1983 to 28 December 1983 (Antarctic Field Book 144, p. 5) and comparing these data with Cape Roberts information. 1983 tidal records were not available for Cape Roberts so the tides were hind-cast from data collected between 1 January 1990 and 1 January 1991 (the data for Cape Roberts was the earliest collected). These data were entered into the University of Hawaii Sea Level Centre Tidal Analysis program to hind-cast the tide for 27 December 1983 to 28 December 1983. The resultant comparison chart is shown in

Figure 3.3. Using the 6th order polynomial the lead from Cape Roberts to Cape Bird is about 90 minutes for high and low tides. The lead is difficult to determine from these data because the dates predicted for (27 December 1983 to the 28 December 1983) were part of a neap tide. Due to the low amplitude of the wave at this time, peaks and troughs are less obvious and more difficult to correlate.

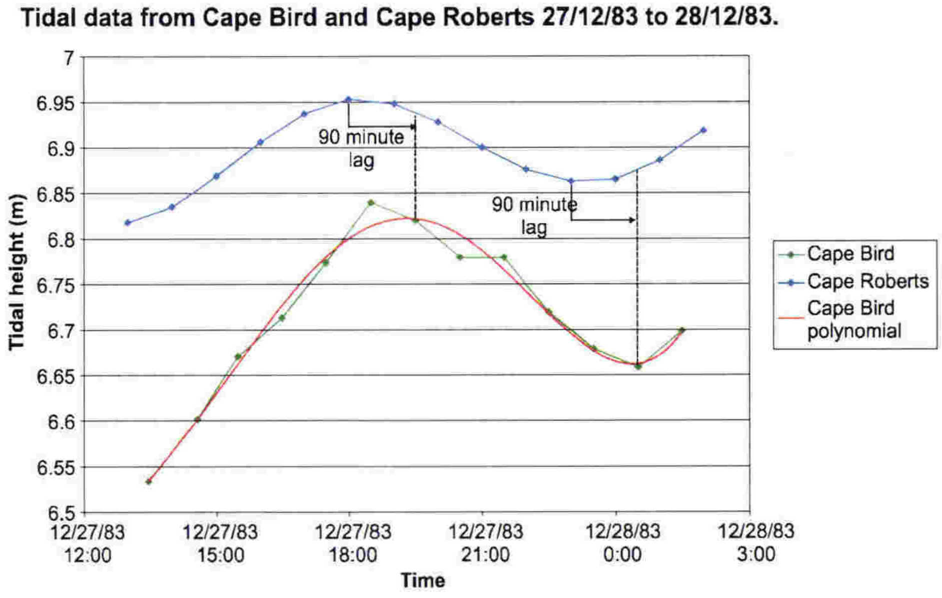

Figure 3.3. Tidal curves for Cape Bird and Cape Roberts 27 December 1983 to 28 December 1999. The trend line fitted to the Cape Bird data is a 6 order polynomial.

The predicted leads and lags determined from the Cape Roberts data and the data collected at Cape Bernacchi and Cape Bird present a complex tidal pattern in McMurdo Sound. Figure 3.4 shows the leads and lags that have been measured around McMurdo Sound (Rowe, 1990). Rowe (1990) used data collected from McMurdo Station and Scott Base to calculate an advance of 90, 30 and 12 minutes depending on which data he used. Hindcast data for Cape Bird showed a possible 60 minute lag from Cape Bird to Cape Roberts. Simultaneous measurements at Cape Roberts and Cape Bernacchi showed good correlation so all of the surveys were corrected using the difference between the Cape Roberts tidal value and mean sea level at the time the survey was undertaken. For example, Marble 1 was surveyed at 1052 hrs 11 January 1997 and a 0.02m correction was applied (Table 3.2). At this time the water level was 0.02m higher than mean sea level (MSL) as calculated from tide data at Cape Roberts between 27 November 1994 to 20 February 1997 (the most recent continuous run of data available). This is illustrated in Figure 3.5.

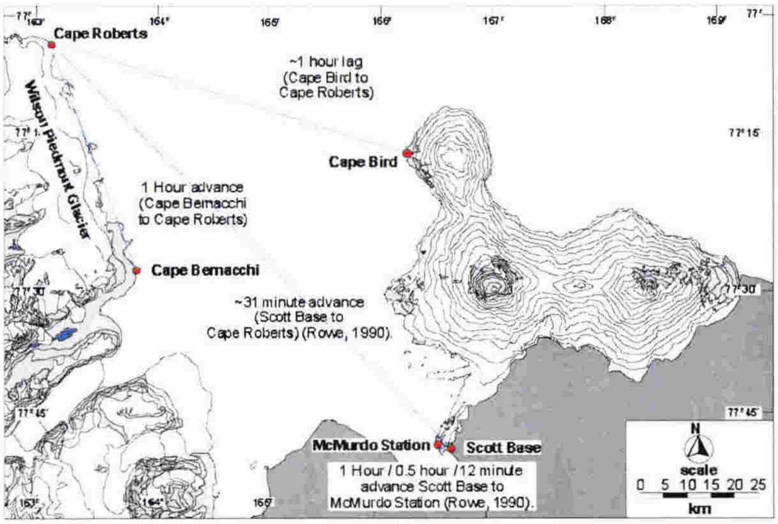

Figure 3.4. Tidal lags and advances at locations around McMurdo Sound.

Table 3.2 shows how much survey elevations were corrected for tidal effects. Figures 3.5 and 3.6 show the relationships of the surveys in the 1996/97 and 1997/98 seasons to the tides in McMurdo Sound calculated from the Cape Roberts tide data.

Survey name	Time at still water level	Relationship to tide (correction used) (m)
Marble 1	11/1/97 10:52	-0.02
Kolich 1	18/1/97 12:11	0.05
Kolich 2	17/1/97 16:10	0.21
Kolich 3	19/1/97 10:25	0.21
Spike 1	21/1/97 12:17	0.22
Dunlop 1	26/1/97 12:00	0.03
Dunlop 2	27/1/97 11:38	0.04 ▲ 1997
Marble 1	18/1/98 15:07	0.18 ▼ 1998
Bernacchi 1	17/1/98 17:05	0.18
Bernacchi 2	17/1/98 09:14	0.15
Bernacchi 3	21/1/98 9:59	0.00
Bernacchi 4	21/1/98 8:50	0.01
Barne 1	31/1/98 13:22	0.14
Barne 2	31/1/98 16:41	0.31
Barne 3	31/1/98 17:40	0.35
Barne 4	31/1/98 18:30	0.36
Barne 5	31/1/98 19:19	0.36
Barne 6	31/1/98 20:25	0.34
Royds 1	29/1/98 15:30	0.42
Royds 2	29/1/98 15:42	0.43
Royds 3	23/1/98 19:00	-0.02
Royds 4	23/1/98 19:00	-0.02
Royds 5	23/1/98 18:30	0.02
Royds 6	23/1/98 17:40	0.08
Royds 7	23/1/98 14:23	0.19
Royds 8	23/1/98 13:35	0.18
Bird 1	11/2/98 18:40	0.13
Bird 2	8/2/98 15:01	0.26
Bird 3	11/2/98 12:21	-0.15

Table 3.2. List of profiles surveyed to still water level and the time of the survey. Corrections are calculated from the relationship to the Cape Roberts tide at the time of survey (see Figures 3.5 and 3.6).

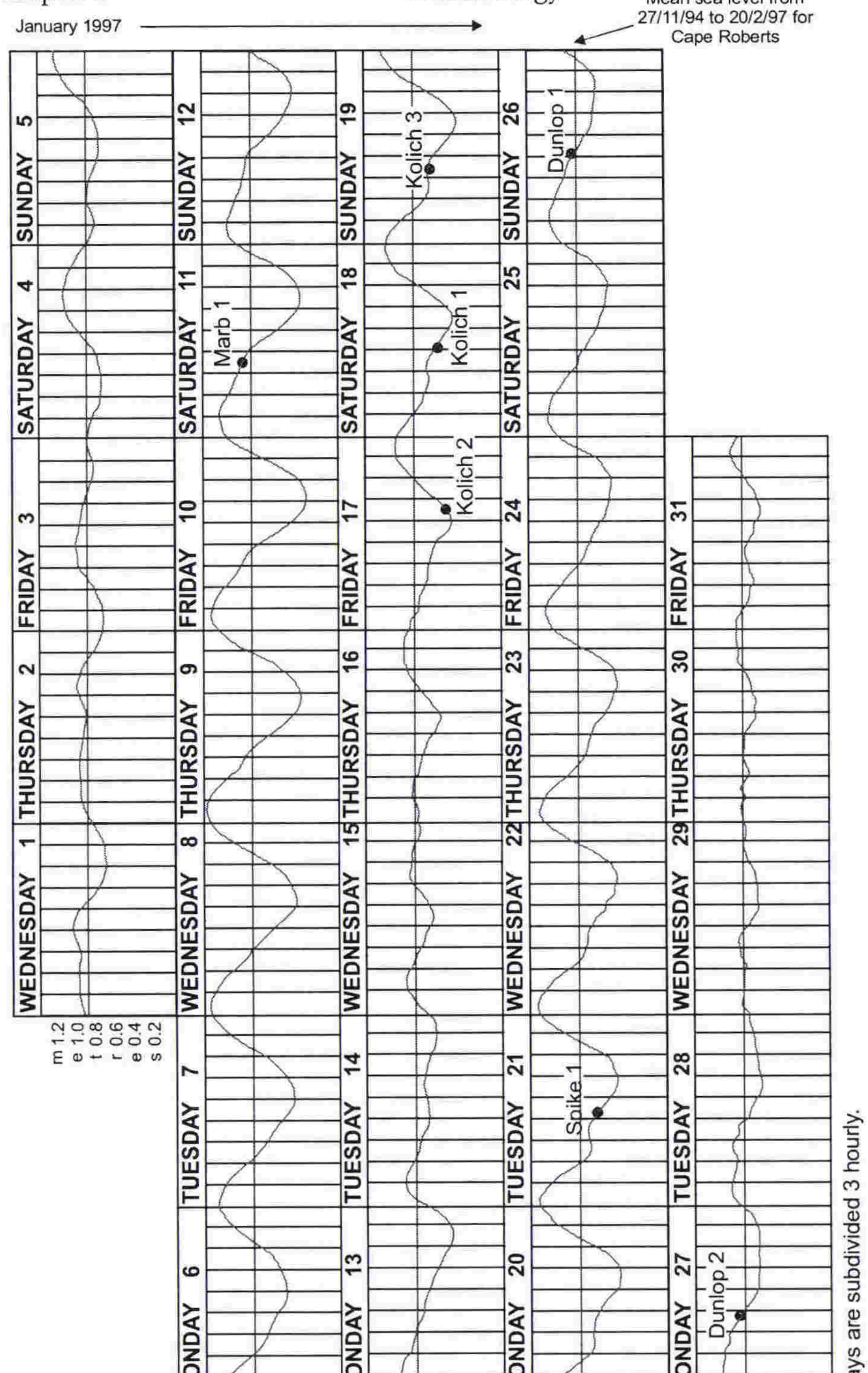

Figure 3.5. Actual tidal data for Cape Roberts from 1/1/1997 to 31/1/1997. The surveys undertaken during this season are also shown on the chart.

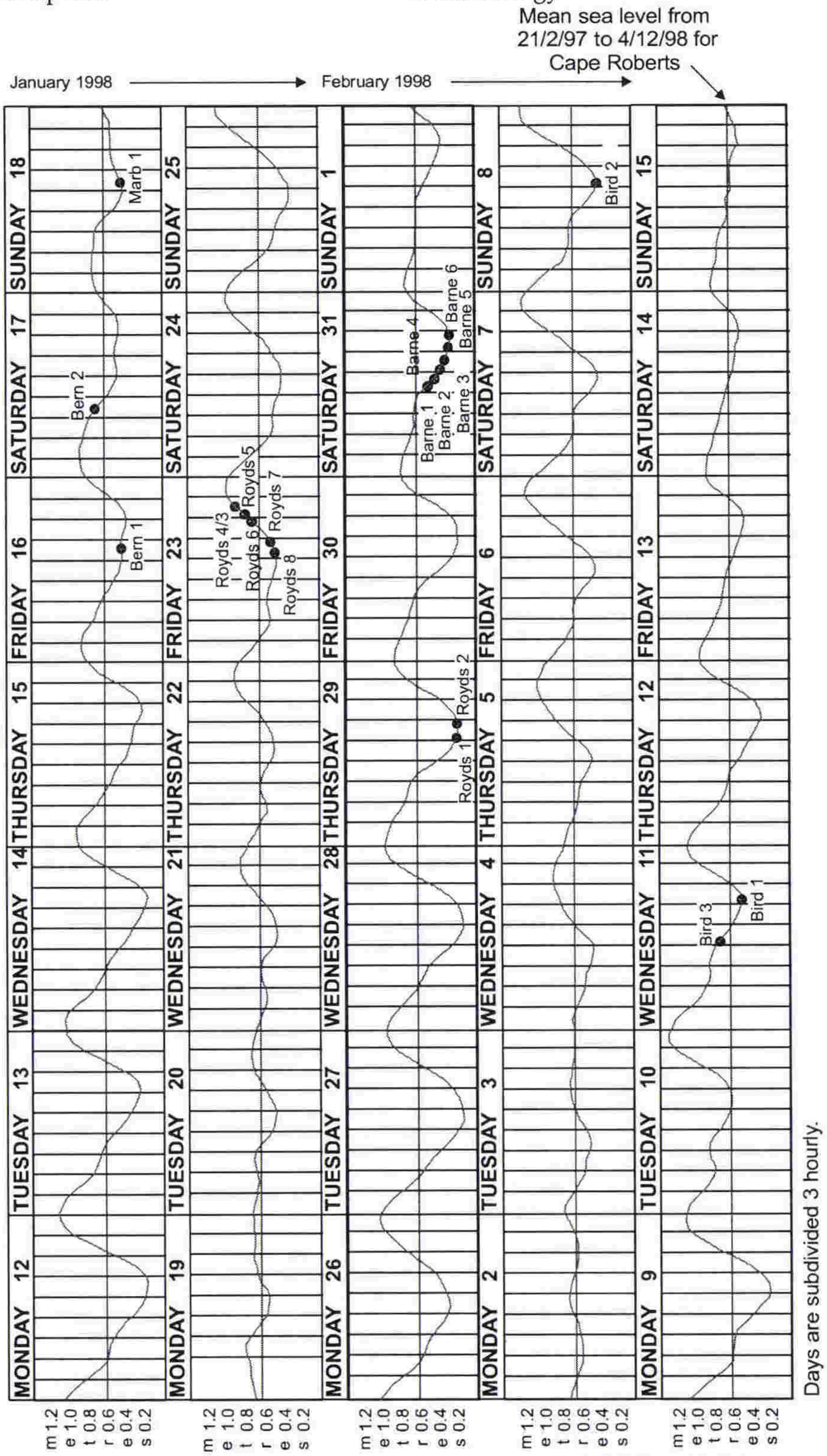

Figure 3.6. Actual tidal data for Cape Roberts from 12/1/1998 to 15/2/1998. The surveys undertaken during this season are also shown on the chart.

3.2.3 Offshore surveys

Surveys were extended offshore at Marble Point, Cape Royds and Cape Bird. Two methods were used to measure offshore profiles. Offshore profiles at Marble Point were measured using standard surveying techniques using the sea-ice as a platform. Water depth was measured at cracks in the sea-ice either with a drop-tape or the survey staff. Where there were no cracks present a screw auger was used to create a hole and a drop tape was lowered to measure water depth.

Offshore profiles at Cape Royds and Cape Bird were measured using a kite deployment system developed for this project (Butler, submitted, see Appendix 2). This system allowed for depth determinations up to about 30m offshore using a 40m cable with a pressure transducer at its end. The 40m cable was pulled ashore at 1m intervals, which were marked on the cable. At each meter interval a depth reading was taken for 30 seconds and a value recorded every 1 second.

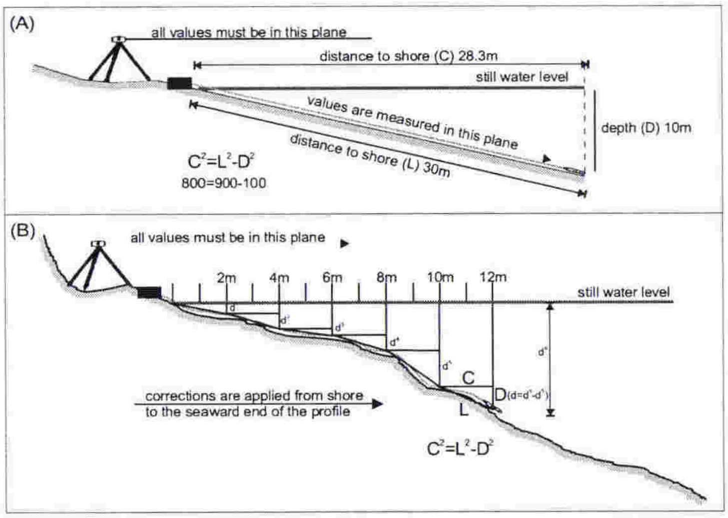

Figure 3.7. **Diagram showing how the measured values were corrected for slope.**

The method only measures points at 1m intervals so the profile that is surveyed assumes that the sea-bed between points is flat. The profile that can be constructed from this data does not represent the actual profile in the field because the depths that were being measured are measured at an angle to the plane that has been surveyed (see Figure 3.7). In Figure 3.7 (A) the pressure transducer is 30m from shore as measured from the cable. The distance from shore in the same plane the surveying was undertaken on, is 28.3m ($C^2=L^2-D^2$ so 800=900-100). This correction was applied successively at each 1m distance value from the shore.

3.2.4 Summary of survey errors

The survey errors can be divided into 3 groups, those errors that can be attributed to surveying a single profile, errors that occur when comparing one survey with another (e.g. tidal errors) and non-standard errors attributed to offshore surveys.

3.2.4.1 Survey errors

Due to time restrictions at each site only some of the surveys were closed. The errors of the surveys that were closed and the acceptable errors (for ordinance surveys) for those surveys are shown in Table 3.3. The "acceptable errors" column was calculated assuming a single staff reading to have a ±1mm error (Bannister et al., 1992). The error in the difference in height between two staff positions measured from the same instrument position is ± 2mm. Assuming an average sight distance of 60 metres then there will be about 8 change points per kilometre of levelling. Thus the standard error per km is ± 8/2 = 4mm. However, it is generally accepted that the maximum discrepancy should not exceed three times the standard error. Therefore, the limits of acceptability should be $\pm 12\sqrt{K}$mm (where K is the length of the profile in km). In rough terrain where more change points are necessary, the limits of acceptability are doubled to $\pm 24\sqrt{K}$mm (Bannister et al., 1992).

Location	Difference at closure (mm)	Acceptable error ($\pm 24\sqrt{K}$ mm)	Difference between acceptable and actual error (mm)
Marble Point (Pocket Beach)	40	16	+24
Marble Point (Nth Sth profiles)	20	24	-4
Kolich Point (KBT1)	20	15	+5
Kolich Point (KBT2)	10	15	-5
Kolich Point (KBT3)	10	18	-8
Spike Cape (SCBT1)	40	16	+24

Table 3.3. List of survey profiles and their respective errors. (The acceptable error is calulated by the square root of the ditance of the survey in km, (*K*) multiplied by 24mm, (the acceptable survey error over rough terrain) (Bannister et al., 1992)).

As can be seen from Table 3.3 not all of the errors fall within acceptable limits for standard ordinance surveys. Marble Point and Spike Cape both have misclosure errors of 40mm where 16mm is acceptable for ordinance surveys. For surveys at other locations that have not been closed an error of ±40mm, the maximum measured survey error (see Table 3.3) has been adopted. The maximum measured error of ±40mm is not significant for any purpose that these surveys will be used for. ±40mm in most cases, is the difference between placing the staff on a rock in a survey or on the beach next to it. The elevations of surveys along the western side of McMurdo Sound were between 9m and 21m.

3.2.4.2 Tidal correction errors

There are two main groups of error associated with tidal corrections; errors due to surveying to still water level and errors identifying a suitable lag or lead time from a particular site to Cape Roberts. The error surveying to still water level is estimated from the maximum change in water level while taking tidal measurements at Cape Bernacchi between 26 January 1999 to 28 January 1999. (Waves propagating through the pack ice caused small current-induced water level changes as readings were being taken). This error was visually estimated to be 0.1m. One of the problems with estimating still water level on an ice-bound coast was the lack of open water. In most cases, a tidal crack or small patches of open water were used to determine this.

Quantifying the error for differences in the lag time from a specific site to Cape Roberts is difficult due to the complex nature of the tides in McMurdo Sound. The only long-term simultaneous tidal measurements taken in McMurdo Sound were taken at Scott Base and Cape Roberts in 1988. These show a lead of 31±5 minutes from Scott Base to Cape Roberts. If the tidal advance from Scott Base to Cape Roberts is only 31±5 minutes it is reasonable to expect that tidal differences between Cape Roberts and any of the other surveyed sites in McMurdo Sound would be the same as or less than 31±5 minutes. The maximum water level difference over 30 minutes at Cape Roberts (during the time surveys were being undertaken) was 0.09m. Root mean square of these errors is ±0.13m (total error = $\sqrt{0.09^2 + 0.1^2}$). This error is only applicable when surveys are compared to each other.

3.2.4.3 Offshore survey errors

The errors involved in the offshore survey are difficult to quantify but include the actual measurement of water depth, the distance from shore, and the correction for the offshore slope. The accuracy of the Unidata model 6508 D pressure transducer is ±1% of full scale. (This means that when the maximum depth for that instrument is reached (10m) the errors will be within 1%). This equates to a maximum ±0.1m water depth. The effects of waves altering the water depth during measuring were calculated by taking the difference between the maximum and minimum values for 20 seconds. Although the measurement time for each depth was actually 30 seconds, 5 seconds either side of the 30 second mark were deleted because of possible errors due to moving the cable. The largest recorded difference between recorded values (probably due to waves), over the 20 second measurement time was 0.2m. Root mean square of these errors is ±0.22m (total error = $\sqrt{0.1^2 + 0.2^2}$).

3.3 Stratigraphy and sedimentology

In addition to surveying profiles, pits were excavated so that the structure of the beach could be examined. Pits were located on survey profiles so that they could be related to each other. In order to provide some means of inter-site comparison, pits were located at the top and the bottom of beach ridges. It was also hoped that by siting the pits at these locations, surface sediment zones for gravel beaches as described by Bluck, (1967) could be identified. If the pits displayed bedding it was described following Jopling and Walker (1968), Brookfield (1992) and Dalrymple (1992), and measured and samples were removed for size analysis.

Size analyses was carried out in the Sedimentology Laboratory at Victoria University of Wellington. Samples were sieved at 0.5ϕ intervals from –4.0ϕ to 5ϕ. The shaking time was 18 minutes. This consisted of 3 sets of 6 minutes shakings at intensity 6.5, two on interval and one on micro sieving. The sieve fractions were weighed.

At Cape Bird and Cape Royds the dominant material size on the modern beaches was sand and gravel. Composite samples such as those described by Shih and Komar (1994) were collected from the modern beaches. Sub-samples were collected from the base of the active berm or scarp, the low tide point and halfway between the base of the active berm or scarp and the low tide point. Shih and Komar (1994) suggest that composite samples eliminate the effects of cross-shore sorting and obtain a more representative sediment sample.

Where the pits contained pebble sized material the dip directions and orientations of these were measured from each bedding unit using a Silva compass and a clinometer. The error associated with the compass and clinometer readings is estimated at no more than ±2°. Thirty clasts were measured from each stratigraphic unit. Where imbrication was measured for clasts on the surface of the beach, clasts were chosen at the top and the bottom of beach ridges. Triaxial measurements were undertaken on each of the clasts using vernier callipers. Where clasts with A axes larger than 150mm were encountered they were measured using a measuring tape.

The number of clasts required to provide a representative sample of mean grain size depends on the sample itself. If the sample comprises wide range of particle sizes and shapes, more clasts must be measured to approximate the population mean. Several theories exist that describe the number of clasts required for a representative sample. The ideal sample size can be expressed as:

$$n = \left(\frac{zs}{d} \right)^2$$

where n is the required size of the sample, s is the standard deviation of the sample (this can be calculated from a pilot sample), d is the tolerable margin of error at a specified level of confidence, and z is obtained from Z tables (Griffith and Amrhein, 1991). Mosley and Tindale (1985) estimated that to estimate the mean grain size of river gravels in New Zealand to ±10% confidence, 228 samples were required. Other authors such as Gale and Hoare (1992), use the size of particles to suggest a mass for a representative sample rather than an actual number of measurements. They suggest that for an average clast size of 50mm, 100kg of sample is required.

It was impractical to process data in the field to obtain a representative sample size for every site sampled at using the method described by Griffith and Amrhein (1985). It was also impractical to select sample sizes as large as those suggested by Mosley and Tindale (1985) or Gale and Hoare (1992). Due to time constraints and because many parametric tests rely on a sample size of at least n=30 it was decided that 30 clasts would be measured in each identified unit from numerous sites rather than >30 clasts being collected at fewer locations. This allowed greater inter-site comparison.

If re-measurement of clasts is undertaken, measurements obtained for individual clasts can be compared and errors associated with triaxial measurements can be quantified. In the laboratory, 50 clasts of various size and roundness were measured three times and the values compared, to quantify operator error. The clasts had b axes of between 30mm and 140mm. The maximum difference of three measurements on a single axis was 10mm and the error at 2σ was 3.8mm. Errors were most likely due to differences in interpretation of the axes.

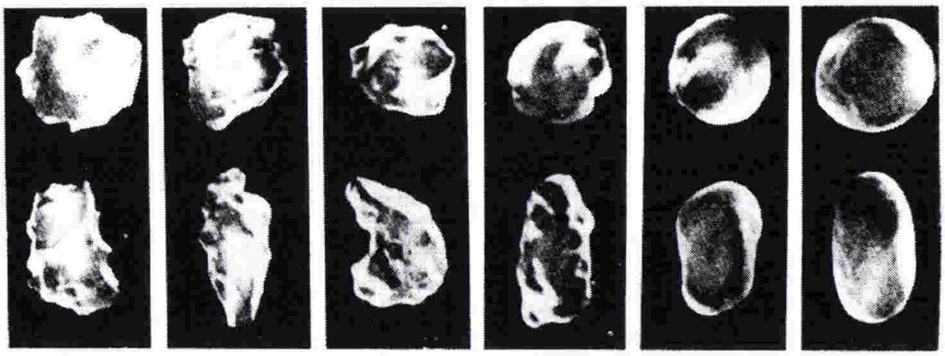

Figure 3.8. Powers roundness scale (Powers, 1953).

There are a number of different scales for determining the roundness of a clast (see Barrett, 1980 for a review). For the purposes of this study the Powers (Powers, 1953) roundness scale was adopted as it offered a quick and relatively easy method for quantifying roundness. This is a six-point visual scale that grades clasts from very angular to well-rounded. The Powers visual scale is shown in Figure 3.8. The accuracy of this method relies in part on a single operator measuring all of the clasts. In this study all of the clast measurements were undertaken by the author.

Statistical analysis was undertaken on the roundness data using a computer-based statistical analysis programme called SPSS.

3.4 Optically stimulated luminescence (OSL) dating

3.4.1 Sample collection techniques for luminescence dating

Optically stimulated luminescence samples were collected at Cape Bernacchi, Marble Point, Kolich Point, Spike Cape and Cape Barne. All samples were collected from at least 160mm below the surface and from homogeneous beds of sand at least 150mm thick. The homogeneity of the sample is important because dose rates can be variable in heterogeneous sediment and field gamma spectrometry was not available. The samples were collected in 150mm long aluminium tubes pushed into the face of the pits. Once the samples were collected, the ends were capped and then sealed using plastic caps and packing tape. This ensured that the samples maintained their field moisture capacity and were only exposed to the light at each end. When the samples were unpacked in the laboratory the 'end' of the sample was removed and discarded, leaving only the unexposed section in the tube to be dated.

In an ideal situation, sample sites would be chosen on the basis of the likely environmental conditions at the time of deposition. This is primarily because shallow-water environments are more likely to be well exposed to sunlight during deposition. In addition, low-energy conditions are important because a close approximation to sea level is required to reconstruct an accurate history of uplift. The beaches in McMurdo Sound had a paucity of suitable sample sites. Therefore, the first order control on the location of a sample was the availability of material. Once suitable material was located, an effort was made to sample from the unit in a pit most likely to represent an intertidal bed. Only a select number of dates could be processed so a further reduction on the number of sample sites was made. The final choice of sites was based on the likelihood of samples yielding good dates in key locations with a strong correlation to sea level at the time of deposition.

Samples were returned to New Zealand and prepared at the Victoria University of Wellington (VUW) luminescence laboratory by the author under the supervision of Dr Olav Lian, the VUW luminescence scientist. Detailed sample preparation techniques are provided in Appendix 3.

3.4.2 Luminescence dating procedure

Luminescence dating is a measurement of when a sediment was last exposed to sunlight or heat. α, β and γ radiation energy from the decay of potassium (^{40}K), uranium, thorium and rubidium from surrounding sediment, and from cosmic rays is accumulated in feldspar and quartz grains in the form of tempoary storage of electorns in high energy 'traps'. The energy is released as photons of light when the sample is heated (thermoluminescence) or exposed to light (optically stimulated luminescence). The longer the sample remains buried the more energy is stored and hence the more photons are released when it is heated or exposed to light. The age of the sample is calculated from:

$$\text{Age} = \frac{\text{Equivalent dose}}{\text{Paleodose}}$$

For a full review of luminescence dating techniques see Huntley and Lian (1999) and Aitken, (1994).

A fundamental precondition for luminescence dating is that the target material has no residual luminescence signal at the time of burial. Consequently the technique is useful for materials which have been well exposed to light or heat during transport (eg. wind blown sand, loess, beach sand, some river sediments, tephras).

The central problem with luminescence dating is determining the laboratory dose that produces the same luminescence signal, as the environmental radiation dose. Laboratory techniques vary but the additive dose method is the most widely used. In this case the additive dose method with thermal correction was used for all samples.

Samples are given different laboratory doses, heated, stored and then measured. The samples are heated because the laboratory dose produces some additional luminescence that would not have been produced with the environmental radiation dose. However, heating the samples also produces some additional luminescence. To correct for this, samples are given a radiation dose, bleached (to remove the luminescence that we want to measure from the non-bleached samples), heated, stored and then measured. This is called the thermal correction curve and it is subtracted from the additive dose curve to provide a corrected equivalent dose. It should be noted that the thermal correction approach was developed by Dr Dave Huntley at Simon Frazer University in Canada and is not often applied by other laboratories.

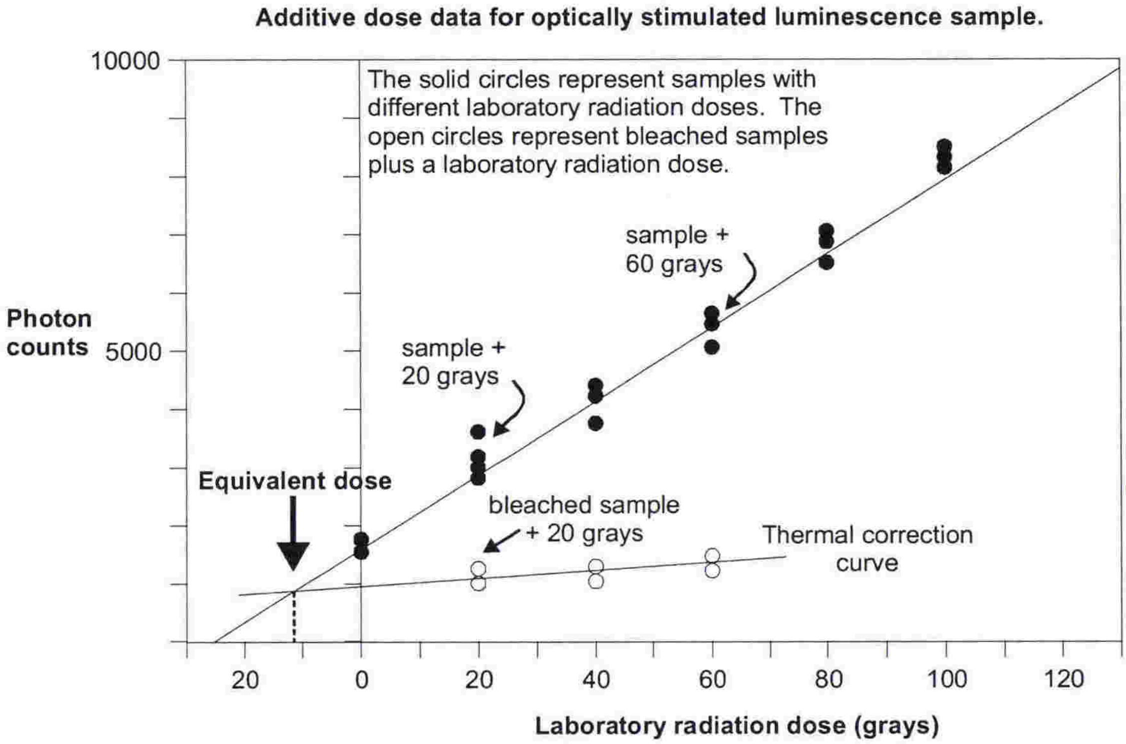

Figure 3.9. Additive dose technique with thermal correction for optically stimulated luminescence dating (modified from Huntley and Lian, 1999).

Fine fraction samples (4-11μm) were dated concentrating on the luminescence signal of K feldspars. This was achieved by infra-red stimulation of the samples (IRSL). The dose rate can be calculated from the contribution of cosmic radiation, the water content of the collected sample (water surrounding the sediments absorbs radiation and reduces the dose received) and the relative contribution of potassium, uranium and thorium within the sample itself. In this case cosmic radiation refers to neutrons (β radiation) which are absorbed primarily in the top 0.5m of the ground. Cosmic radiation increases with elevation and latitude and is calculated empirically. A sub-sample of all samples was collected, powdered and sent to SRC Analytical Saskatoon in Canada to be analysed for potassium, thorium and uranium by atomic absorption spectroscopy, neutron activation analysis and delayed neutron analysis respectively. Age calculations were undertaken by Dr Olav Lian.

Chapter 4

Results

4.1 Introduction

This chapter presents morphology, sedimentology, stratigraphy results and luminescence ages of the beaches at locations around McMurdo Sound.

4.2 Profiles of beaches in McMurdo Sound

Survey profiles of the beaches in McMurdo were undertaken for two primary reasons. Firstly, the surveys provided an accurate measure of the features on the beaches so that they could be compared with other beaches in the Sound and given some sense of scale. Secondly, the surveys allow accurate measures of marine limits (the highest level of marine action at a site) to be determined.

Thirty three surveys were undertaken in McMurdo Sound, 16 on the western side of the Sound, 14 from Cape Royds to Cape Barne and 3 at Cape Bird (see Figures 4.1 to 4.3). Figures 4.4 to 4.9 present profile information on a site basis. The upper limit of all of the surveys (except Spike 2 where the marine limit is identified) represents the marine limit, which was defined on morphological and sedimentological characteristics (shown on the air photographs by the yellow line).In most cases, the marine limit was easy to identify because the shore normal ridges terminated abruptly and the sediments became poorly sorted.

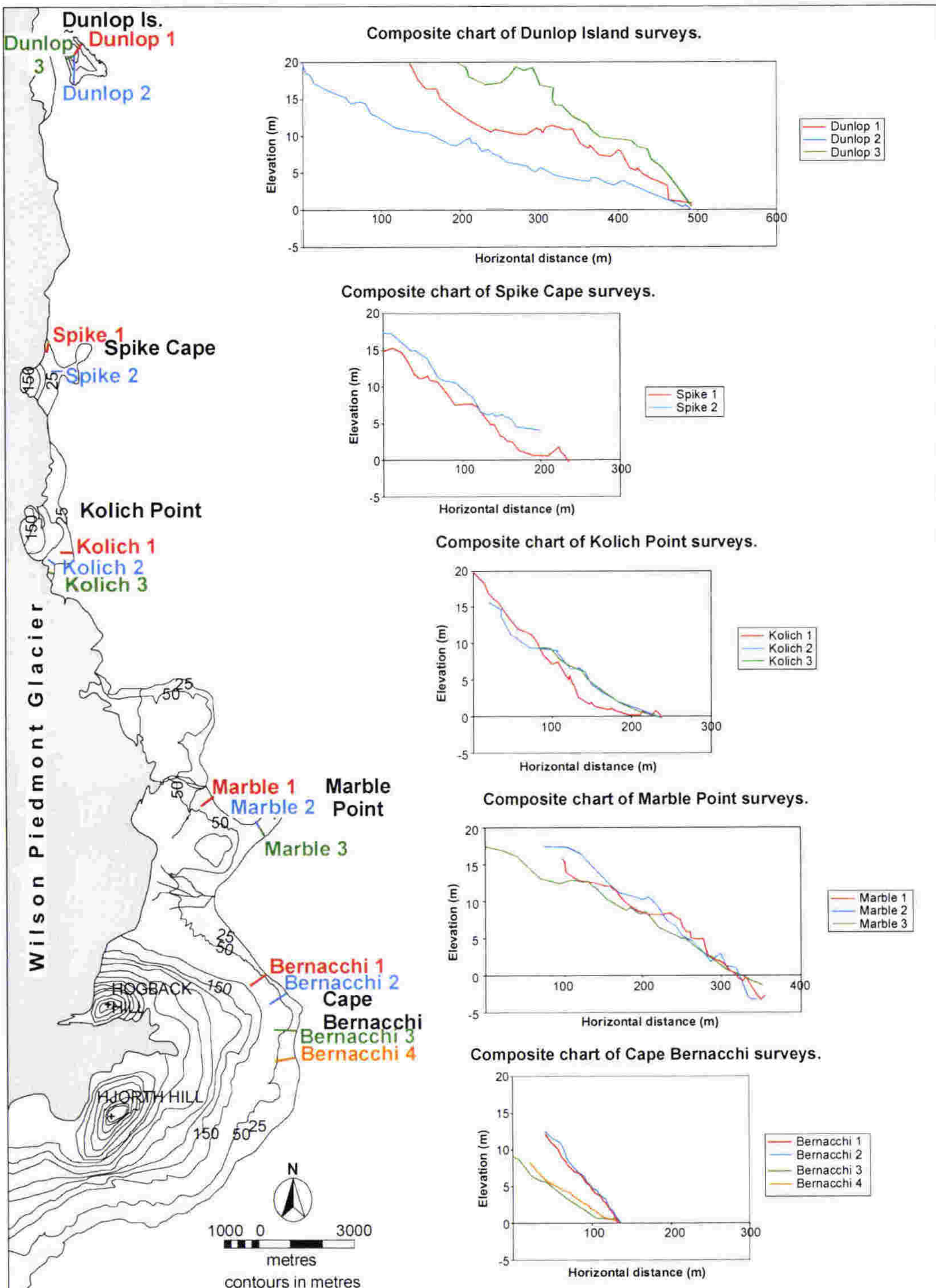

Figure 4.1. Survey lines (western McMurdo Sound) from Cape Bernacchi to Dunlop Island (note vertical exaggeration of 11.25x on all surveys).

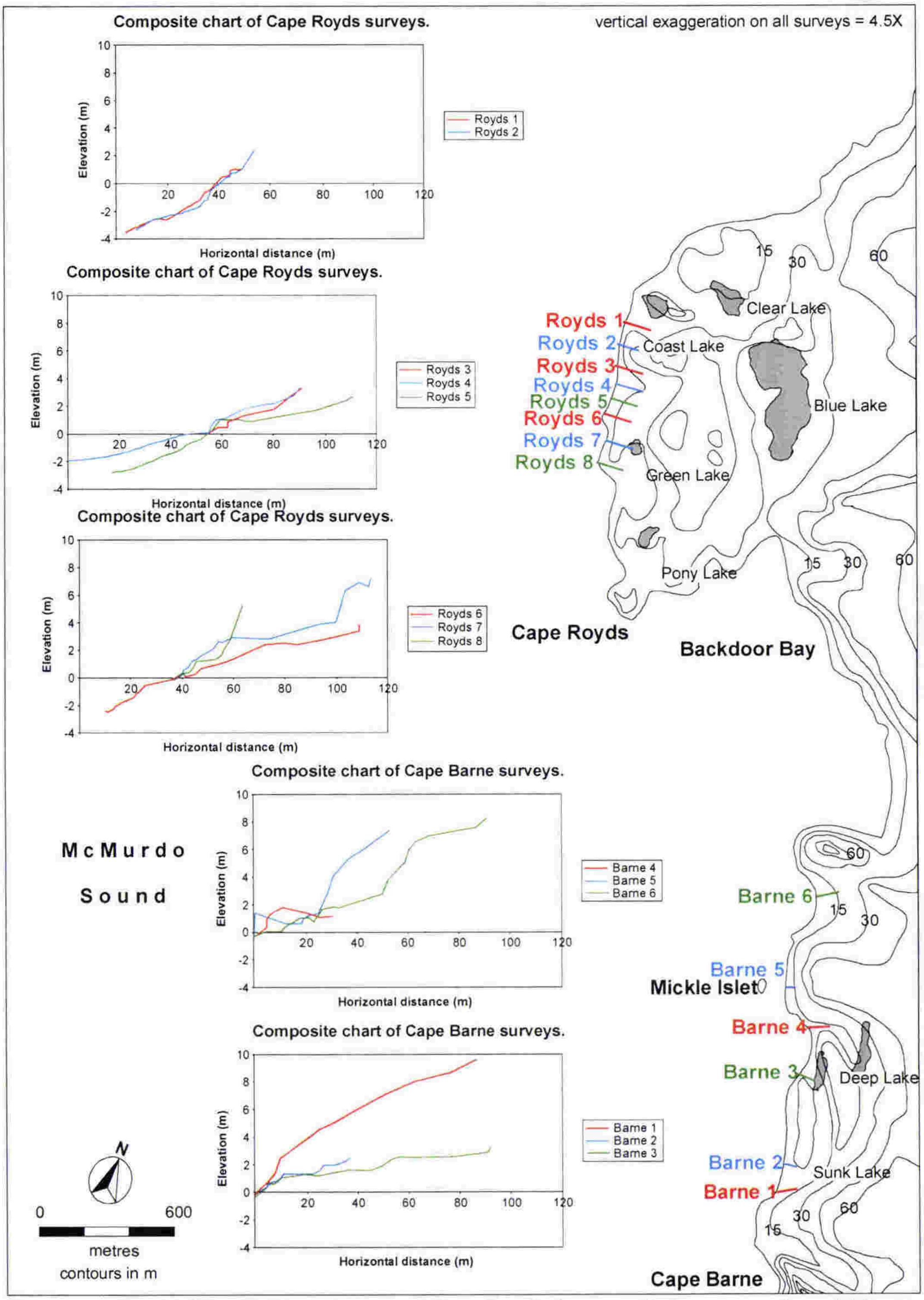

Figure 4.2. Survey lines at Cape Barne and Cape Royds (note vertical exaggeration of 4.5x on all surveys).

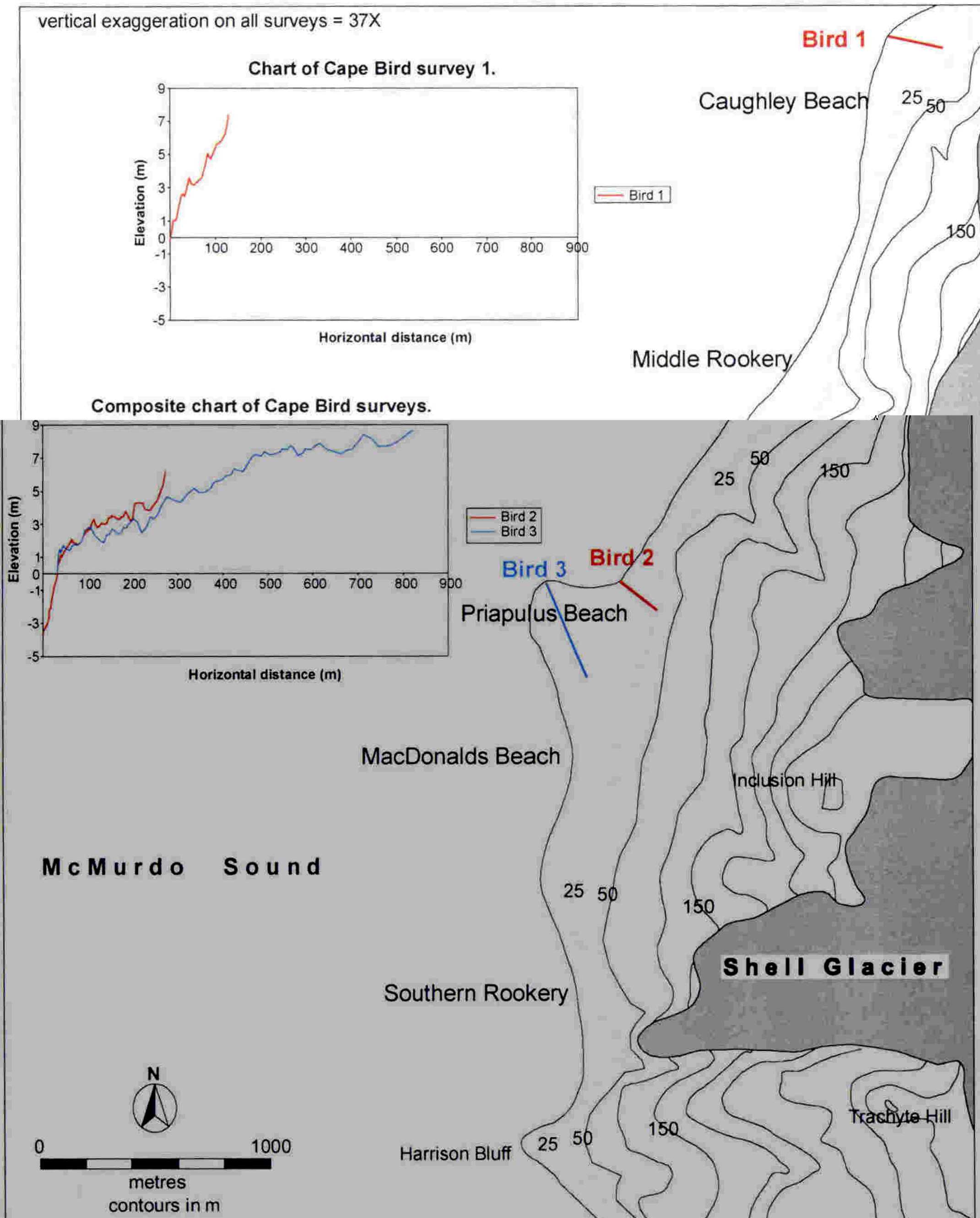

Figure 4.3. Survey lines at Cape Bird (note vertical exaggeration of 37x on all surveys).

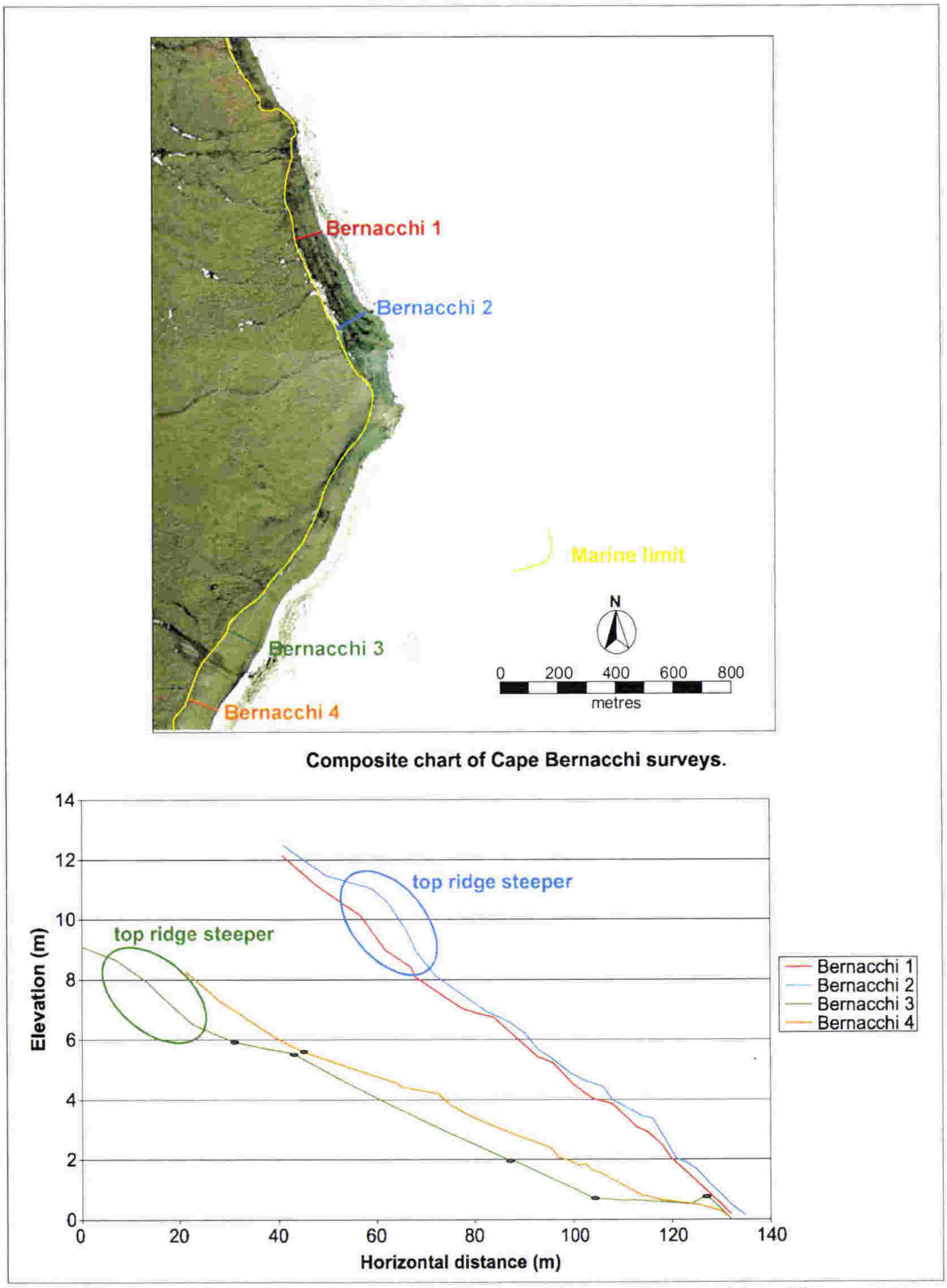

Figure 4.4. Survey lines at Cape Bernacchi. The top ridges on Bernacchi 2 and Bernacchi 3 (circled) are steeper than the average for that profile. The coloured circles on Bernacchi 3 and Bernacchi 4 represent pits excavated at these locations.

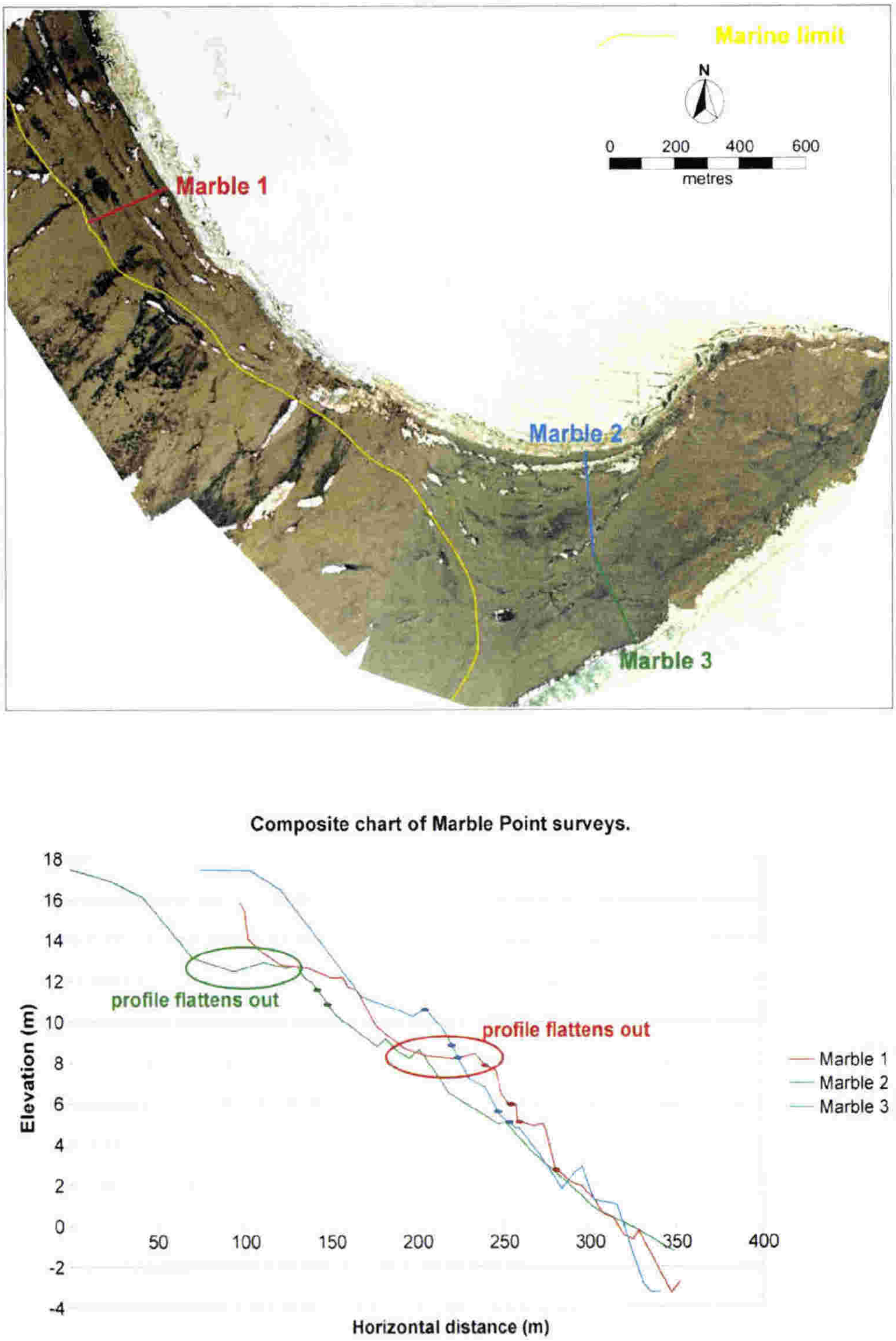

Figure 4.5. Survey lines at Marble Point. The large open circles on Marble 1 and Marble 3 show where these profiles flatten out. The coloured circles on the profiles represent the locations of pits excavated along the profile.

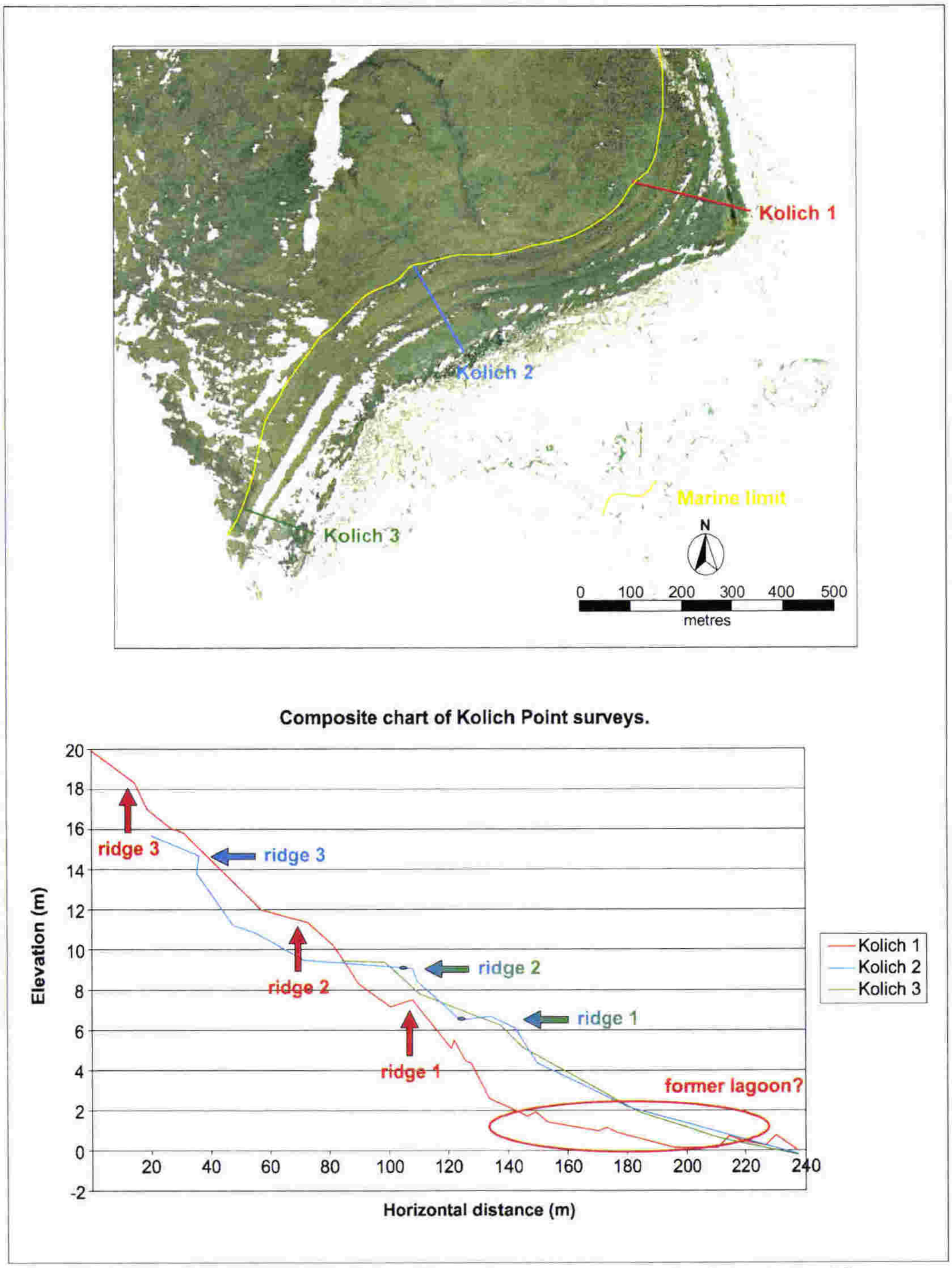

Figure 4.6. Survey lines at Kolich Point. The red arrows indicate the three major ridges identifiable on the air photo at Kolich survey 1, the blue arrows indicate the same three ridges on Kolich 2 (note the difference in elevation). The coloured circles on Kolich 2 represent locations of pits excavated along the profile. At the base of Kolich 1 there is what appears to be a relict lagoon indicated by an open circle.

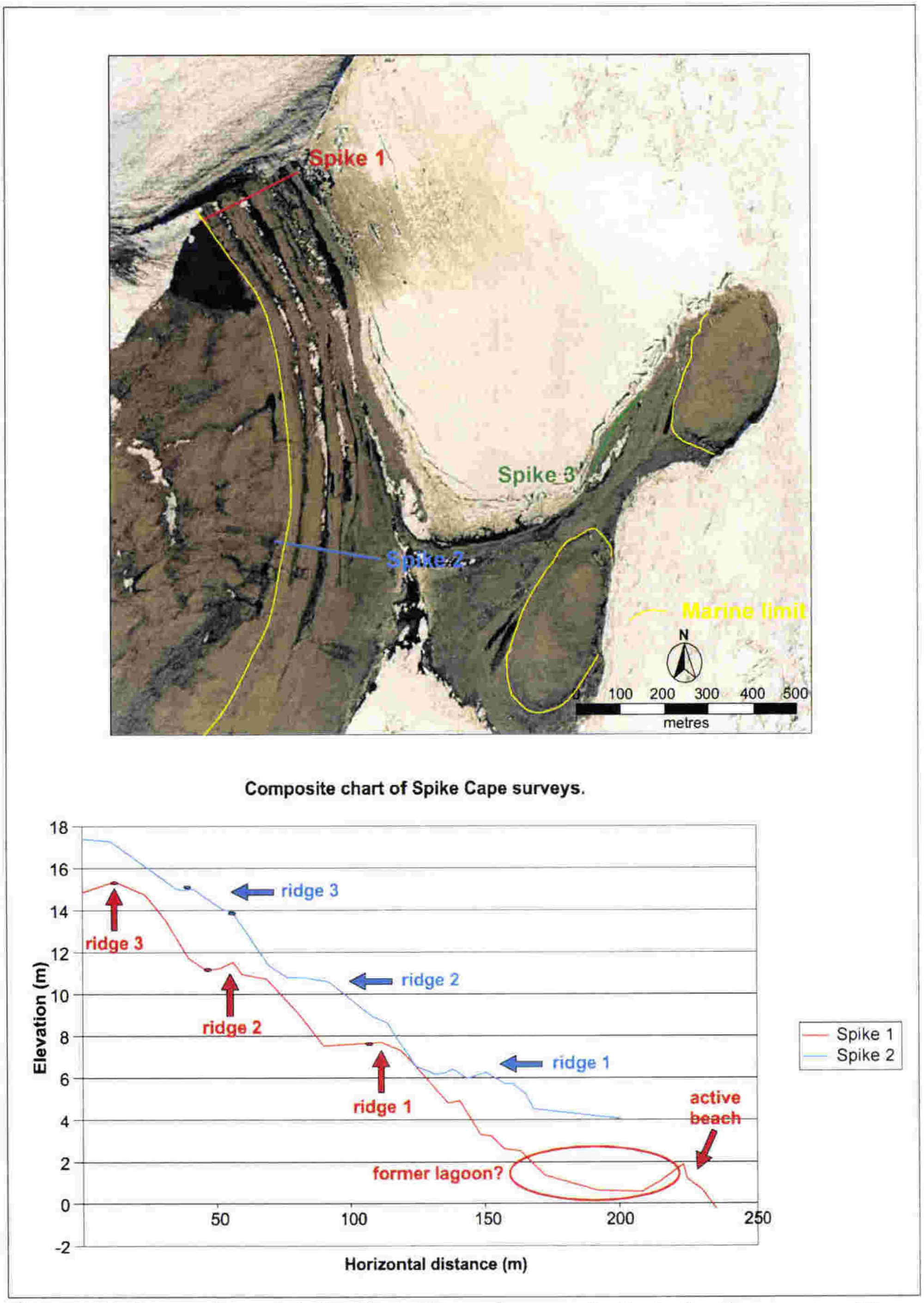

Figure 4.7. Survey lines at Spike Cape. The red arrows indicate the three major ridges identifiable on the air photo on Spike survey 1, the blue arrows indicate the same three ridges on Spike 2. The coloured circles on the profiles represent locations of pits excavated along the profile. At the base of Spike 1 there is what appears to be a relict lagoon indicated by an open circle.

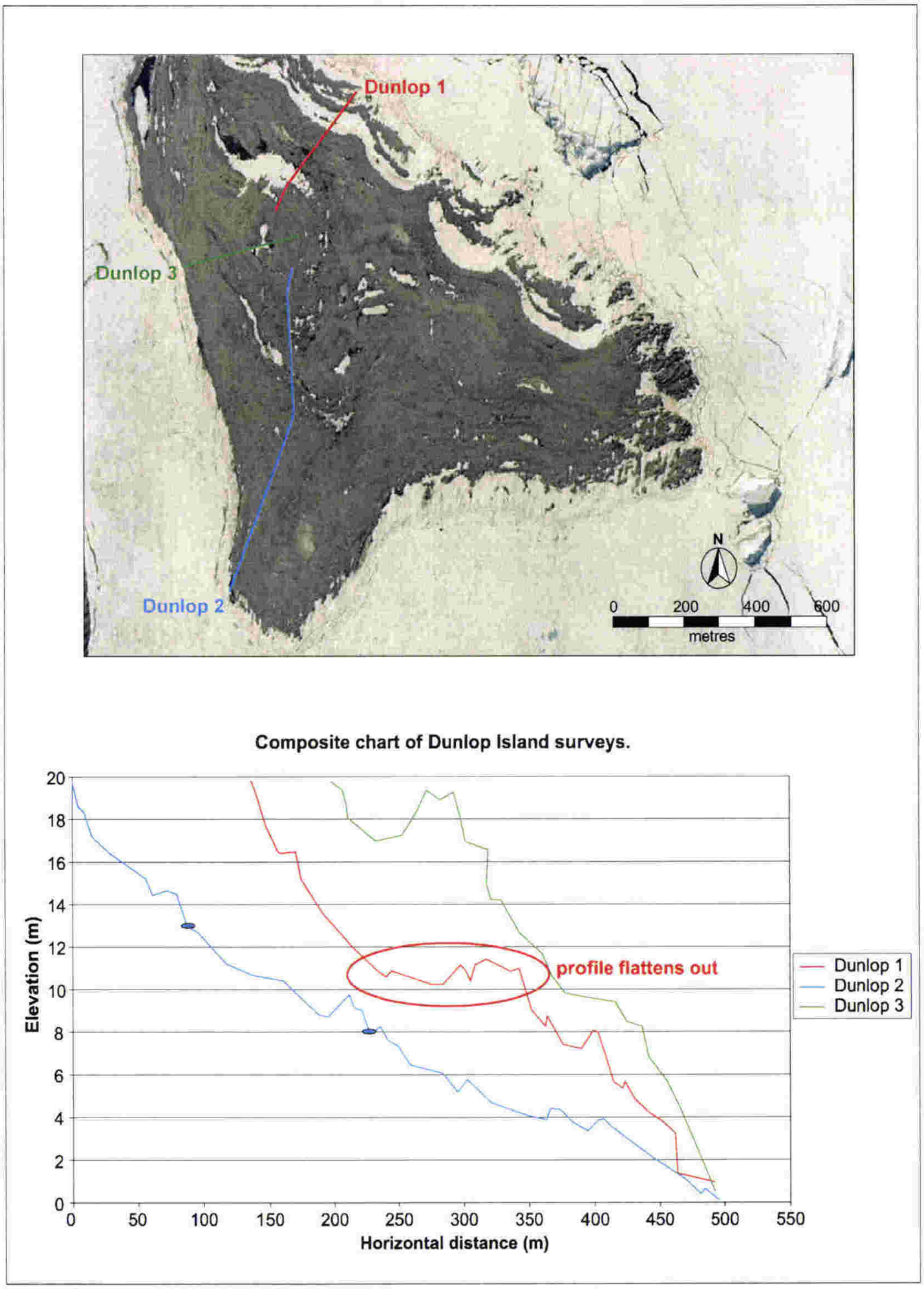

Figure 4.8. Survey lines at Dunlop Island. The coloured circles on Dunlop 2 represent locations of pits excavated along the profile. The large open circle on Dunlop 1 represents an area where the average slope of the profile flattens considerably compared with the rest of the profile.

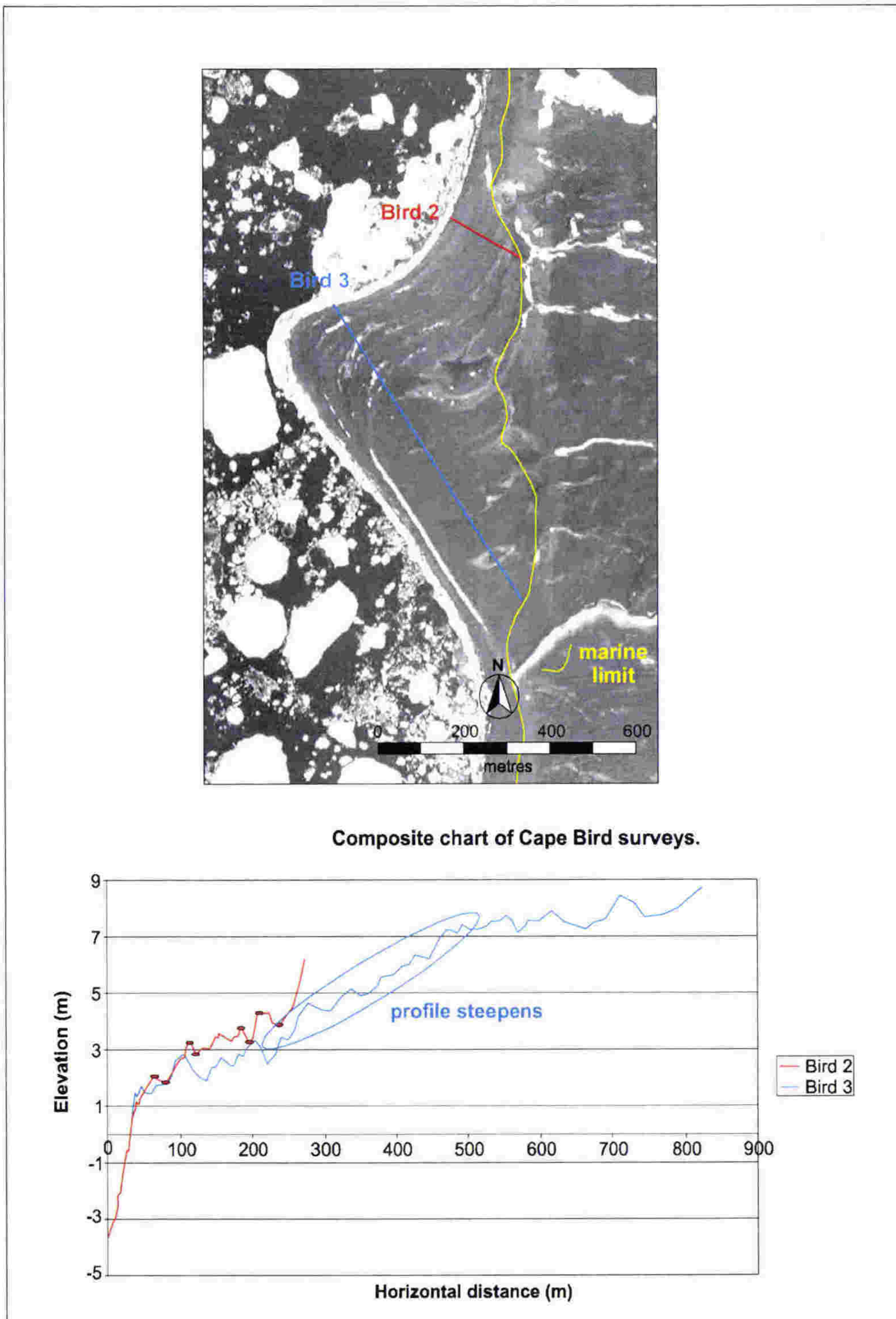

Figure 4.9. Survey lines at Cape Bird. The coloured circles on Bird 2 represent pits excavated at these locations. The large open circle on Bird 3 represents an area where the average slope of the profile is 1^0 which is between 0.6^0 and 0.8^0 more than the rest of the profile.

For example, the air photographs in Figures 4.4, 4.6, 4.7 and 4.9 clearly show the delineation between shore normal beach ridges and sediments that are not organised into shore normal ridges. Above the marine limit sediments were generally poorly sorted and angular and the ground surface was hummocky in appearance. The marine limit was occasionally difficult to define, in which case it was placed at the landward limit of obvious marine features such as beach ridges.

4.2.1 Western McMurdo Sound surveys

Figure 4.1 shows the survey profiles from Cape Bernacchi to Dunlop Island. All of the surveys have been corrected to mean sea level (MSL) and the elevations in the diagrams are in metres above MSL (m AMSL).

Differences in beach slope are evident both between sites and within individual profiles. Average profile slopes were calculated by drawing all of the surveys to scale and measuring the resulting angle (Table 4.1).

Western profiles		Eastern profiles	
Profile	**Slope (^{0})**	**Profile**	**Slope (^{0})**
Bernacchi 1	8^0	Bird 1	5^0
Bernacchi 2	8^0	Bird 2	1^0
Bernacchi 3	5^0	Bird 3	0.5^0
Bernacchi 4	4^0		
Marble 1	5^0		
Marble 2	4^0		
Marble 3	3^0		
Kolich 1	8^0		
Kolich 2	3^0		
Kolich 3	3^0		
Spike 1	5^0		
Spike 2	4^0		
Dunlop 1	3^0		
Dunlop 2	2^0		
Dunlop 3	5^0		

Table 4.1. Averge slope of profiles shown in Figure 4.1 and Figure 4.3.

Profiles located on northern-facing beaches tend to be steeper than those located on southern facing aspects. For example at Cape Bernacchi the average slope of the north eastern facing profiles Bernacchi 1 and Bernacchi 2 are about 8^0. In contrast, the south eastern facing Bernacchi 3 and Bernacchi 4 are 5^0 and 4^0 respectively. Average slopes of the profiles range from 2^0 on Dunlop 2 to 8^0 on Kolich 1 and Bernacchi 1 and 2.

Within the profiles, individual beaches have variable slopes. These variations are often consistent. For example, Bernacchi 2 has an average profile slope of 8^0 but the top beach ridge is 15^0, while Bernacchi 3 has an average profile slope of 5^0 but the top beach ridge is 9^0. (The two profiles are only 1.2km apart so it is not surprising that the top ridge is consistent between profiles). Profiles at Marble Point, Kolich Point, and Dunlop Island all seem to show a marked slope change between 8m and 13m AMSL (Marble 1 flattens out at 8.5m and Marble 2 flattens out at 12.5m. Kolich 1, which flattens out at 9.5m, and Dunlop 1, which flattens out at 11m, mirror this change).

Beach ridges at Spike Cape can be traced around the coast between profiles, however, the same beach ridges are 2m higher at Spike 2 than Spike 1. This pattern is also apparent at Kolich Point where the difference between the heights of the same beach ridges is between 2m and 3m. The highest ridges on Bernacchi 1 and 2 are about 2m higher than the same ridge on Bernacchi 3 and 4. The higher ridges at Kolich Point (Kolich 1) are to the north of Kolich Point, a pattern that is duplicated at Cape Bernacchi. However, the ridges become higher to the south of Spike Cape.

The Spike 1 and Kolich 1 profiles are distinctive as they have relict shore platforms at the bottom of the profiles. Both comprise a long flat section of bedrock of about 100m at Kolich Point and 300m at Spike Cape, which both have poorly sorted sediment on them. The shore platform on Spike 1 stretches 50m from the first ridge landward of the shore platform to the modern beach. On Kolich 1 the shore platform stretches 94m from the first ridge to the modern beach.

4.2.2 Cape Royds and Cape Barne surveys

Figure 4.2 shows survey profiles from Blacksand Beach at Cape Royds to Cape Barne. The surveys at Blacksand Beach at Cape Royds are narrower than the profiles on the western side of the sound or at Cape Bird. This is due to the absence of raised beaches in this area. The only raised beaches were found at Cape Barne (Barne 6, Barne 3 and

Barne 1). The profiles depict the wide range of active beaches between Cape Barne and Blacksand Beach.

The beach at Cape Barne with the greatest elevation above MSL was Barne 1, with an elevation of 9.7m AMSL. The beach cuts Sunk Lake off from the sea at its southern end and is approximately 400m north of the prominent rock cliff at Cape Barne. Figure 4.10 shows the beach at Cape Barne (view from south). The beach is a shore parallel feature approximately 22m long (from the exposed bedrock at the southern end to the exposed bedrock at the northern end).

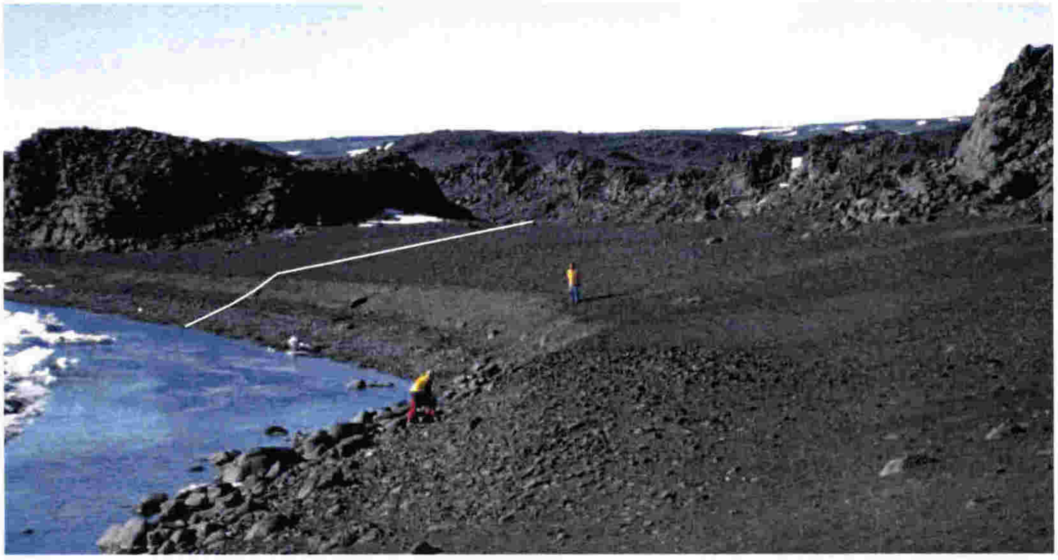

Figure 4.10. Beach ridge at Cape Barne. The white line in the background marks Barne 1 survey.

4.2.3 Cape Bird surveys

Figure 4.3 shows survey profiles at Cape Bird. The slopes of the Cape Bird surveys range from 3.5^0 for Bird 1 to 0.5^0 for Bird 3 (see Table 4.1). Although Bird 2 (Bird 2 faces north west) and Bird 3 (Bird 3 is closer to Priapulus Point than Bird 2 and faces north north west) are only 300m apart and the ridges can be traced from one profile to another, beach ridge heights differ by up to 1m. Bird 3 shows three distinct changes in slope down the profile. The top 350m of the profile has an average slope of 0.2^0, which corresponds well with the slope of 0.4^0 for the bottom 190m of the profile. In contrast, phase 2 has an average slope of 1^0. This is similar to the flattening out of the profiles at Dunlop Island and Marble Point noted earlier.

Although Bird 3 has a shallow slope compared with the surveys on the western side of McMurdo Sound, it has the greatest number of raised beaches and extends landward further than any other survey. Kirk (unpublished data) identified and mapped 25 beaches on Bird 3 (unpublished data) and an oblique photograph by Butler (1999) shows 16 clearly visible beaches on this survey line. In contrast, there are only 7 clearly identified raised beaches on Marble 2. The 25 beaches on Bird 3 extend 850m inland compared with less than 500m on Dunlop 2. Most of the surveys on the western side of the Sound extend considerably less than 300m.

4.2.4 Profile response to storms (Cape Royds)

The surveys at Cape Royds were undertaken on the 23rd January 1998 in fine conditions and then resurveyed after a storm on the 29th January 1998. Initial wind and wave direction was from the north but on the evening of the 29th January the wind direction changed to the south and began blowing at about 15m/s to 20m/s. This changed the wave direction to the south.

Figure 4.11. Sea ice frozen in place at Cape Royds. Where sea ice was frozen in place wave action at the shore was severely limited.

Significant wave height during the storm was about 0.5m with maximum wave heights of about 0.8m. Waves appeared to be steeper at the northern end of Blacksand Beach (profiles Royds 1, Royds 2 and Royds 3). Only a small amount of sea ice was offshore Cape Royds at the start of the storm. On the 29th January the southerly wind blew the remaining sea ice out of McMurdo Sound. Ice that remained on the beach was frozen in place (see Figure 4.11). The two surveys at each location are shown in Figures 4.12 and 4.13. At the time of the storm, the beach had a layer of ice on the base of the scarp. This layer increased in thickness as spray froze to the scarp (see Figure 4.11). In some places, the ice was removed by the wave action.

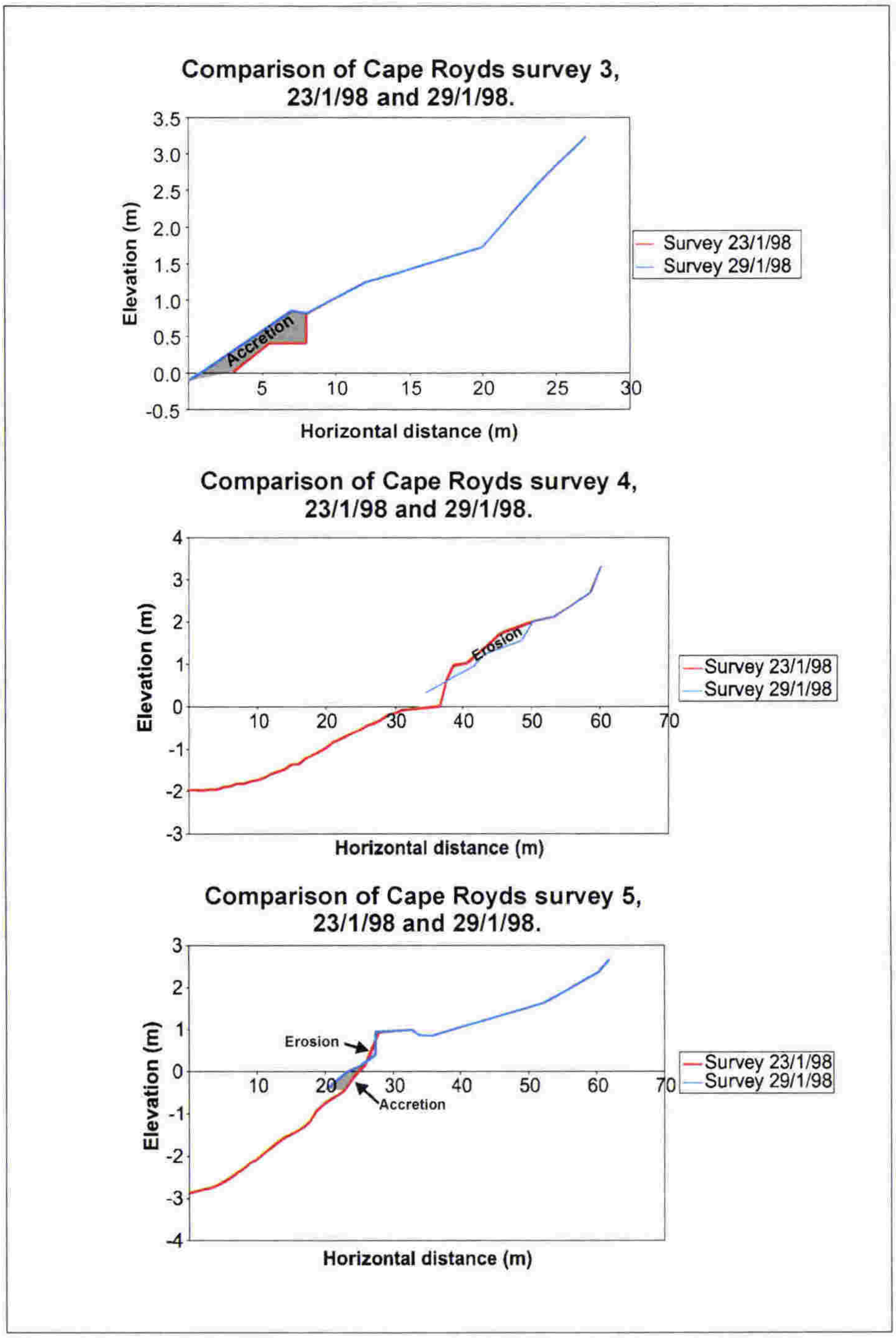

Figure4.12. Cape Royds surveys on 23 January 98 and 29 January 98. (Note: surveys are not all the same scale).

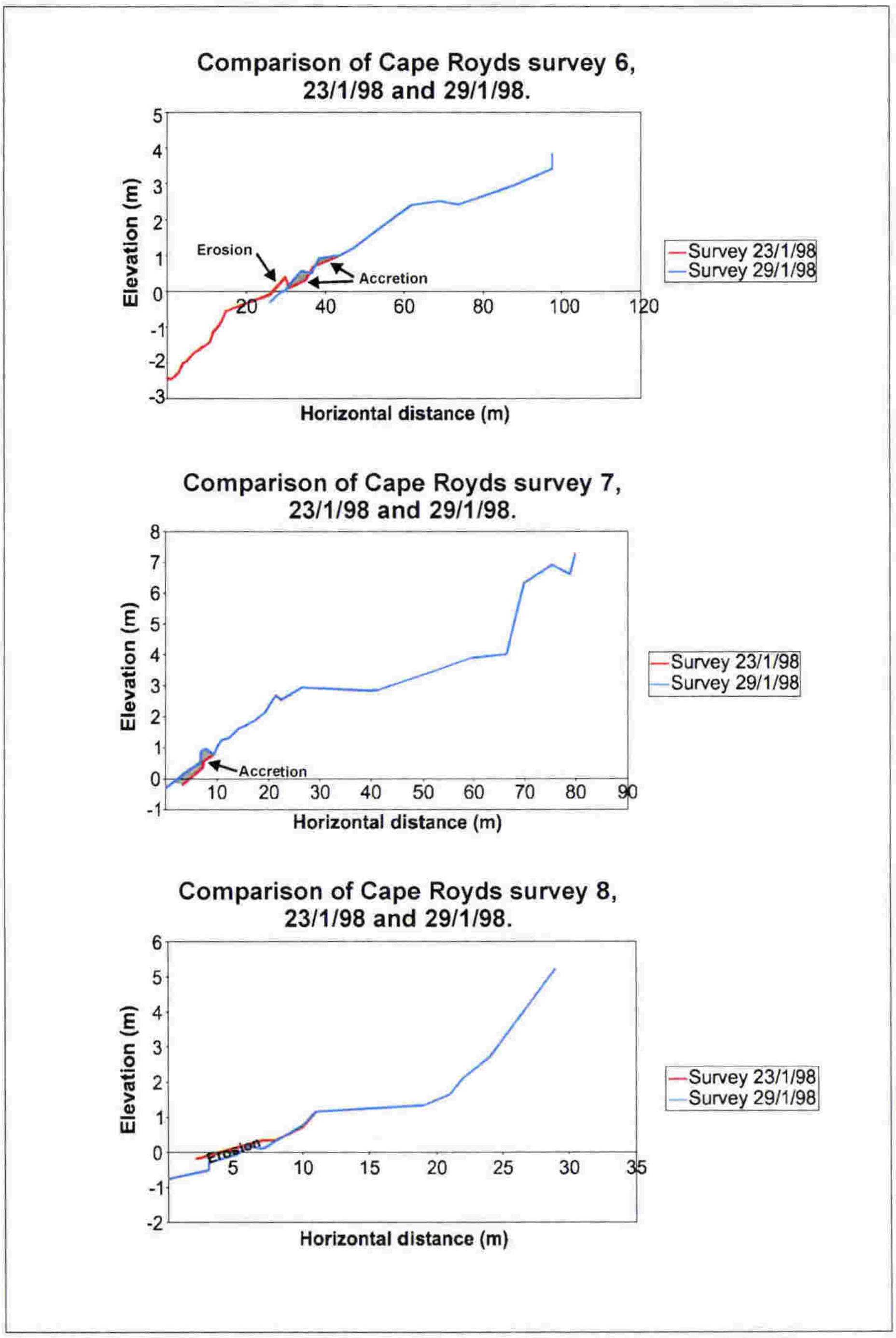

Figure4.13. Cape Royds surveys on 23 January 98 and 29 January 98. (Note: surveys are not all the same scale).

Figure 4.14. Sea spray frozen to the shore at Cape Royds. Boot is 40cm long.

All of the changes seen at Cape Royds are small in terms of volume of sediment moved during the storm. Sea spray freezing onto the beach (Figure 4.14) and the effect of small patches of sea ice (Figure 4.11) caused an irregular pattern of erosion and accretion. Therefore, the changes reflected in the profiles are not consistent. Profiles 6 and 8 show erosion at lower elevations. The changes in profiles 3, 4, 5 and 7 show accretion at lower elevations. Profiles 4 and 5 also show flattening of the profile at higher elevations. These changes have the effect of producing a dissipative beach profile consistent with what would be expected of a sandy beach during a storm in a temperate zone (Komar, 1998).

4.3 Sedimentology and stratigraphy of beaches in McMurdo Sound

4.3.1 Sedimentology of beaches in McMurdo Sound

Sediments from the modern and raised beaches in McMurdo Sound were measured to provide another tool for comparing beach ridges both between sites and within profiles. Sediments can also be useful for determining the processes that deposited them.

4.3.2. Overview of the sediment data

4.3.2.1 Size and sorting

There was a huge range of particle sizes present on the beaches in McMurdo Sound. Boulder counts were undertaken at both Kolich Point and Dunlop Island and boulders up to -10.5ϕ were measured. By contrast, there were silts in some pits that were 5.5ϕ. In general, the pits dug in the beaches comprised a poorly sorted mixed sand and gravel matrix with clast supported pebbles and cobbles. There were some pits that were well sorted and contained some bedding features at Marble Point, Kolich Point and Spike Cape. The sediment on the modern beaches at Cape Bird was better sorted than the sediment measured on the raised beaches. Samples ranged from very leptokurtic to very platykurtic. In general, most of the samples were platykurtic or mesokurtic. Similar to the kurtosis, the skewness values ranged from very fine-skewed to very negatively-skewed. However, most values were very negatively-skewed to negatively-skewed. Appendix 4 contains mean size, standard deviation, skewness and kurtosis values for all of the samples measured. In addition, a CD-Rom disk of all of the raw sediment data has been included.

4.3.2.2 Imbrication

There was strong imbrication of clasts at Marble Point, Spike Cape Dunlop Island and on the Cape Bird ice push feature. There was some weaker imbrication in some marine sediments at these sites as well. Most of the pit sediments had no or only very weak imbrication. (The strongest imbrication was on the Spike Cape barrier).

4.3.2.3 Shape

There was no clear pattern in the clast shape data. All of the Sneed and Folk shape diagrams showed clustering about the centre of the shape triangle, that is in the Platy, Bladed, Elongate, Compact Platy, Compact Bladed and Compact Elongate regions of the Sneed and Folk diagrams.

4.3.2.4 Roundness

The site with the most rounded clasts was Cape Bird followed by clasts on Dunlop survey 1 and Spike Cape barrier. The other sites had clasts that were generally sub-angular to sub-rounded. Mean rounding for each measured unit within pits is presented at the end of each description. Table 4.2 shows the terms used to describe the level of rounding.

	Very angular	Angular	Sub angular	Sub rounded	Rounded	Well rounded
Powers' rounding	1	2	3	4	5	6
Descriptive term	**Very poorly rounded**		**Poorly rounded**	**Well rounded**	**Very well rounded**	

Table 4.2. Terms used to describe rounding of clasts in pits.

There appeared to be greater rounding of clasts on the eastern side of McMurdo Sound and a multi-variate analysis of rounding was undertaken to determine whether a significant relationship existed and what the controls might be. Tukey's Honestly Significant Difference test with 95% significance level was undertaken using roundness as a variable and aspect (of the beach that the data were collected from) as the co-variable. The difference between two means is significant if:

$$\text{Mean(J)-Mean(I)}>=0.606*\text{range}*\sqrt{(1/n(I)+1/n(J))}$$

where range=3.65, J=variable roundness and I=variable aspect. The matrix in Table 4.3 shows that northern facing beaches have similarly rounded clasts to the southern beaches but significantly less rounded clasts compared with eastern and western facing beaches. Western facing beaches have significantly more rounded clasts on them compared with the other aspects.

Mean	Aspect	North	South	East	West
3.10	**North**				
3.30	**South**				
3.58	**East**	Sig. dif.	Sig. dif.		
4.23	**West**	Sig. dif.	Sig. dif.	Sig. dif.	

Table 4.3. Tukey's Honestly Significant Difference test of significance of rounding by aspect.

Tukey's Honestly Significant Difference test at a 95% significance level was also undertaken for roundness as a variable and sample site (Bernacchi, Marble, Kolich, Spike, Dunlop and Bird) as the co-variable. The difference between two means is significant if: $\text{Mean(J)-Mean(I)}>=0.579*\text{range}*\sqrt{(1/n(I)+1/n(J))}$ where range=3.04, J=variable roundness and I=variable site.

Mean	Site	Marble	Bernacchi	Dunlop	Spike	Kolich	Bird
3.08	**Marble**						
3.57	**Bernacchi**	Sig. dif.					
3.57	**Dunlop**	Sig. dif.					
3.83	**Spike**	Sig. dif.	Sig. dif.	Sig. dif.			
3.89	**Kolich**	Sig. dif.	Sig. dif.	Sig. dif.			
4.48	**Bird**	Sig. dif.	Sig. dif.	Sig. dif.	Sig. dif.	Sig. dif.	

Table 4.4. Tukey's Honestly Significant Difference test of significance of rounding by site.

The matrix in Table 4.3 shows that Marble Point has the most poorly rounded clasts of all the sites sampled and it is significantly different to all of the other sites. Cape Bernacchi and Dunlop Island have similar clast roundness but are significantly more angular than Spike Cape and Kolich Point. Cape Bird has the most well rounded clasts of all sites.

Analysis of Variance (anova) tests were undertaken on the roundness data using aspect as the independent variable. The first used all 1,692 data points and the other used mean values for rounding for individual sites (14 in all Bernacchi 2 and 3, Marble 1, 2 and 3, Kolich 1 and 2, Spike 1, 2 and 3, Dunlop 1, and 2, and Bird 2 and 3).

Source of variation	Sums of squares	Degrees of freedom	Mean squares	f	Significance of f
Within + residual	1237.91	1688	.73		
Aspect	158.28	3	52.76	71.94	0.000*
Model	188.51	4	47.13	64.26	0.000*
Total	1426.41	1692	0.84		

Table 4.5. Anova results for roundness verses aspect using 1,692 data points (clasts).

*i.e. significant at >99.999% confidence

R-squared = 0.132

Source of variation	Sums of squares	Degrees of freedom	Mean squares	f	Significance of f
Within + residual	2.02	10	.20		
Aspect	1.54	3	0.51	2.54	0.116
Model	1.54	3	0.51	2.54	0.116
Total	3.56	13	0.27		

Table 4.6. Anova results for roundness and aspect based on site means.

R-squared = 0.432

4.3.3 Detailed sedimentology of individual sites in McMurdo Sound

4.3.3.1 Cape Bernacchi sediment data

The sediments at Cape Bernacchi (Figures 4.15 and 4.16) display a range of sizes. Clasts in the pits on Bernacchi 3 ranged in size from -7ϕ to 4.5ϕ and with the exception of unit 1 in pits 1 and 4, were generally poorly sorted. Although ice-push features contained well-sorted clasts, there was a sandy matrix in all of the ice-push features that was not sampled. There appeared to be some weak shore normal (60^0) imbrication in Bernacchi 3 pit 4 and Bernacchi 3 Ice-push 1 and some weak imbrication in a 310° direction on Bernacchi 3 Ice-push 2. The shape data shows some clustering about the Platy, Bladed, Elongate, Compact Platy, Compact Bladed and Compact Elongate regions of the Sneed and Folk diagrams. The clasts were generally poorly rounded except Bern 2 ice-push, which showed the best Powers rounding of all the sites at an average of 4.1.

Bernacchi survey 3

Six beach ridges were identified on this profile and four sediment pits were examined. Pits 1, 3 and 4 were located at the crest of the active beach, and at the top of the third and fifth ridges respectively. Pits 2 and 5 were located in the swale at the base of the second and sixth ridges respectively.

Pit 1, top of 1st ridge (0.77m AMSL). This 700mm pit contained a massive well sorted sand matrix with matrix supported pebbles. The mean b axis of measured clasts in pit 1 was -5.40ϕ. The pebbles were not imbricated and were clustered around the Platy, Bladed, Elongate, Compact Platy, Compact Bladed and Compact Elongate regions of the Folk and Ward diagrams. The clasts were generally poorly rounded with an average rounding of 3.4.

Pit 2, base of 2nd ridge (0.68m AMSL). This 600mm pit contained a massive very poorly sorted sand matrix with a few matrix supported pebbles. The mean size of the sand fraction in the pit was -0.52ϕ. No clasts were measured in this pit.

Pit 3, top of 3rd ridge (5.53m AMSL). This 700mm pit contained a massive very poorly sorted sand matrix with a few matrix supported pebbles that was subdivided into 2 units at 0-550mm and 550-700mm. Unit 1 (550-700mm) comprised large cobbles and sandy gravel. No clasts from this unit were measured. Unit 2 (0-550mm) was a massive poorly sorted sand with a few matrix supported clasts present. A luminescence sample was collected from this unit. The mean size of the sand fraction in the pit was 0.50ϕ. No clasts were measured in this pit.

Pit 4, top of 5th ridge (5.53m AMSL). This 650mm pit contained a massive very poorly sorted sand matrix with a few matrix supported pebbles that was subdivided into 2 units at 0-250mm and 250-650mm. Unit 1 (250-650mm) comprised a massive poorly sorted sand with a few clasts present. The mean size of clasts in unit 1 was –1.20ϕ. Unit 2 (0-250mm) was a massive poorly sorted sand and gravel matrix with clast supported pebbles and small cobbles present. The mean b axis of measured clasts in unit 2 was -5.40ϕ. The pebbles were imbricated in a shore normal direction (60^0) and were clustered around the Platy, Bladed, Elongate, Compact Platy, Compact Bladed and Compact Elongate regions of the Sneed and Folk diagrams. The clasts were poorly rounded with an average rounding of 3.7.

Pit 5, base of 6th ridge (0.68m AMSL). This 700mm pit contained a massive poorly sorted sand and gravel matrix with a few matrix supported pebbles. The mean size of the sand fraction in the pit was 1.56ϕ. No clasts were measured in this pit.

Bernacchi ice push features

Figure 4.16 shows ice push features close to Bernacchi survey 3 and at the base of Bernacchi survey 2. Sea level was at or close to the base of the ice push features. Figure 4.17 shows a typical ice push feature at Cape Bernacchi.

The Bernacchi 2 ice push feature was 1.2m high, 4.45m long and 3.4m wide. It comprised a range of sizes from coarse sand and gravel to pebbles and cobbles. The

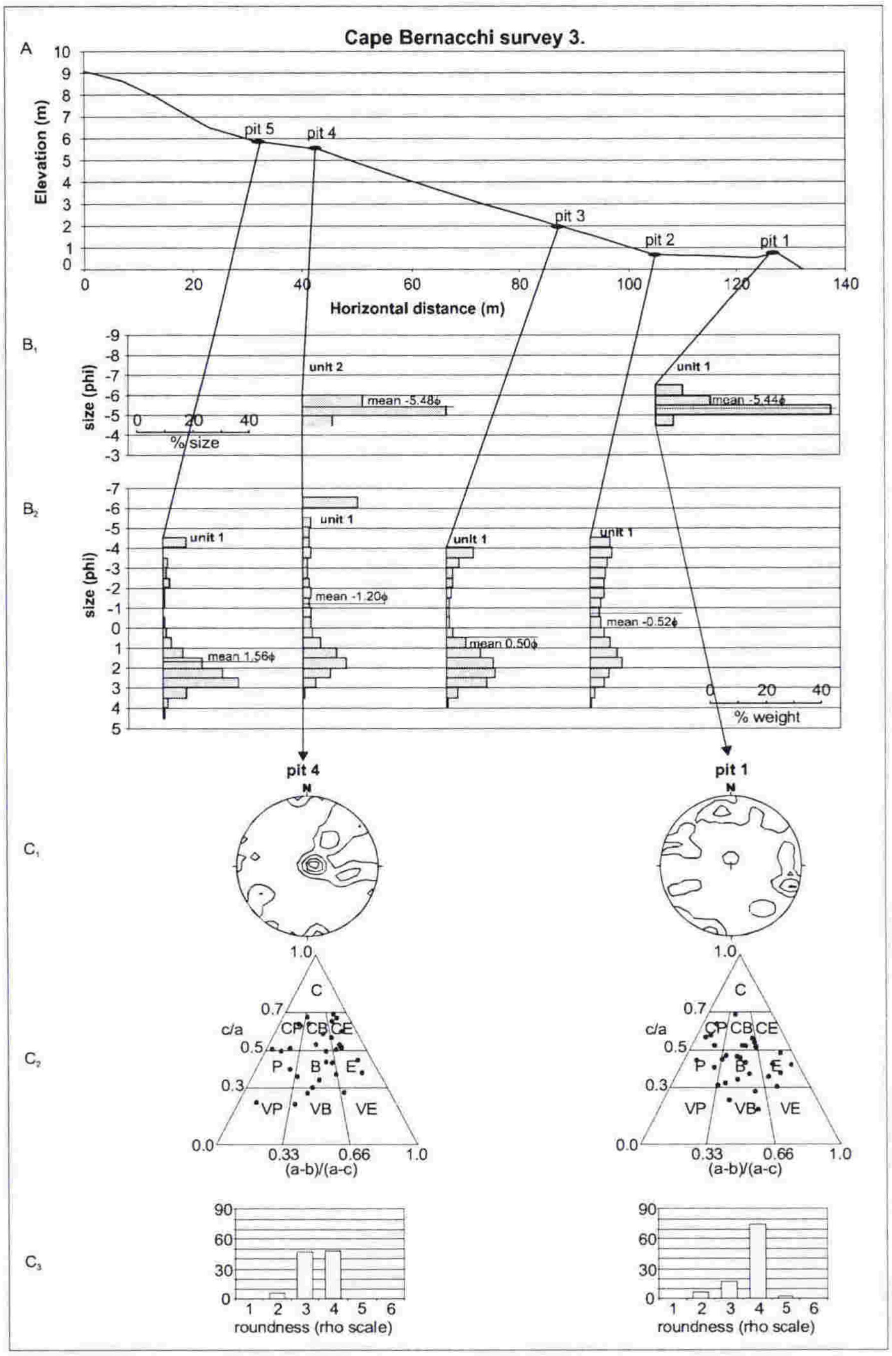

Figure 4.15. Summary profile and sedimentological information for Cape Bernacchi survey 3. Part A displays the profile and the locations of the sediment pits. Part B provides sediment size histograms; B_1 displays summary information for gravel beds while B_2 presents the same information for finer units. For the gravel units stereonet projections of gravel A axis dips (C_1), Sneed and Folk (1953) (C_2) shape triangles and Powers (1953) roundness (C_3) information are presented.

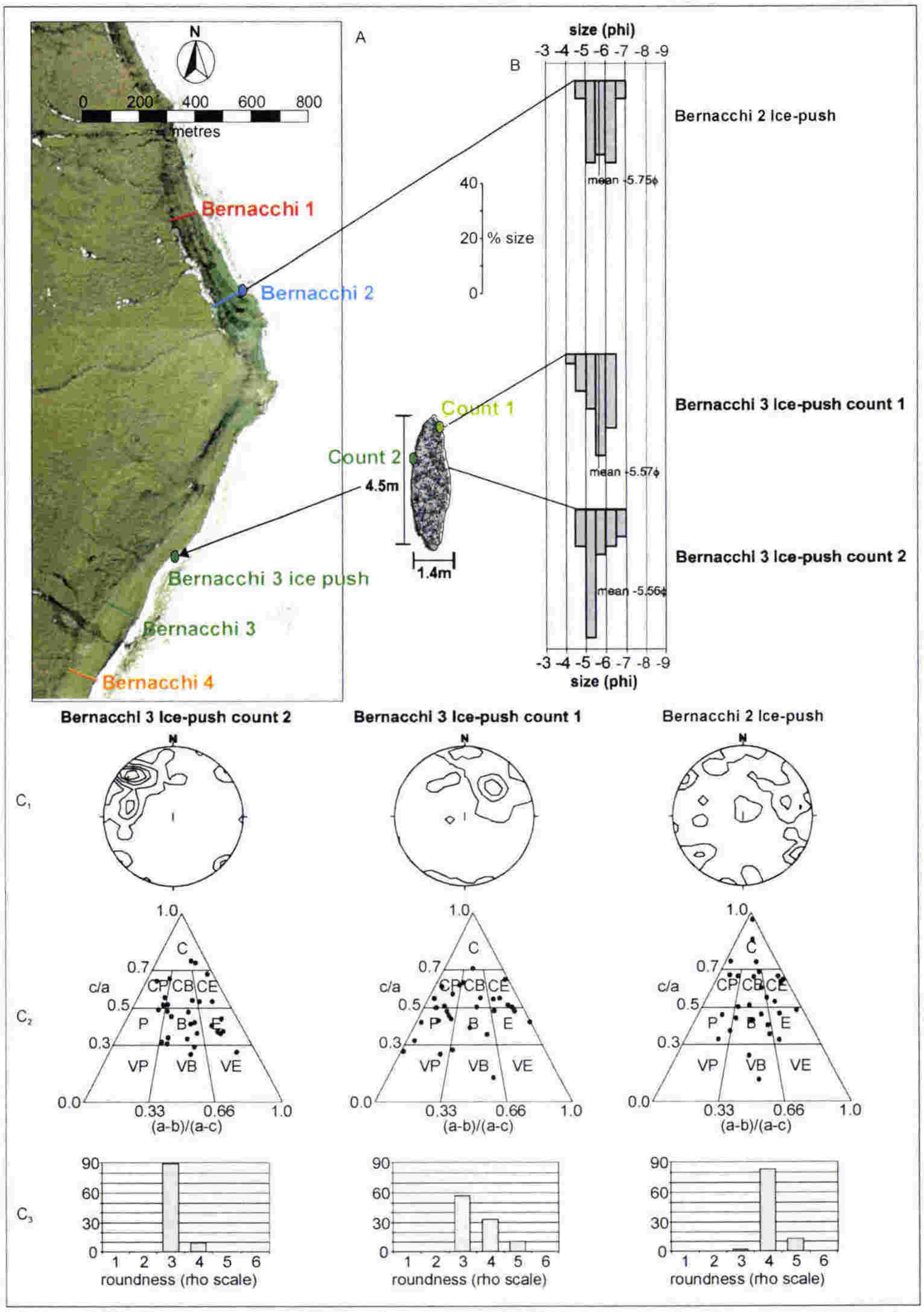

Figure 4.16. Summary location and sedimentological information for Cape Bernacchi ice push features. Part A displays the location of the pebble counts (note plan view of Bernacchi 3 ice push feature showing location of the counts on the ice push feature). Part B provides sediment size histograms. For all counts stereonet projections of gravel A axis dip (C_1), Sneed and Folk (1953) (C_2) shape triangles and Powers (1953) roundness (C_3) information are presented.

mean b axis of measured clasts on this feature was -5.75ϕ. There was no imbrication present. The pebbles were clustered around the Platy, Bladed, Elongate, Compact Platy, Compact Bladed and Compact Elongate regions of the Sneed and Folk diagram. The clasts were generally well rounded with an average rounding of 4.1.

The Bernacchi 3 ice push feature was 0.4m high, 4.5m long and 1.4m wide. Similar to the ice push feature at the base of Bernacchi survey 2, it comprised a range of sizes from coarse sand and gravel to pebbles and cobbles. The mean b axis of count 1 clasts on this feature was -5.57ϕ. The pebbles were weakly imbricated in a shore normal direction (60^0) and were clustered around the Platy, Bladed, Elongate, Compact Platy, Compact Bladed and Compact Elongate regions of the Sneed and Folk diagram. The clasts were generally poorly rounded with an average rounding of 3.1. The mean b axis of measured clasts on count 2 was -5.56ϕ. The pebbles were imbricated in a 320^0 direction and were clustered around the Platy, Bladed, Elongate, Compact Platy, Compact Bladed and Compact Elongate regions of the Sneed and Folk diagram. The clasts were generally poorly rounded with an average rounding of 3.5.

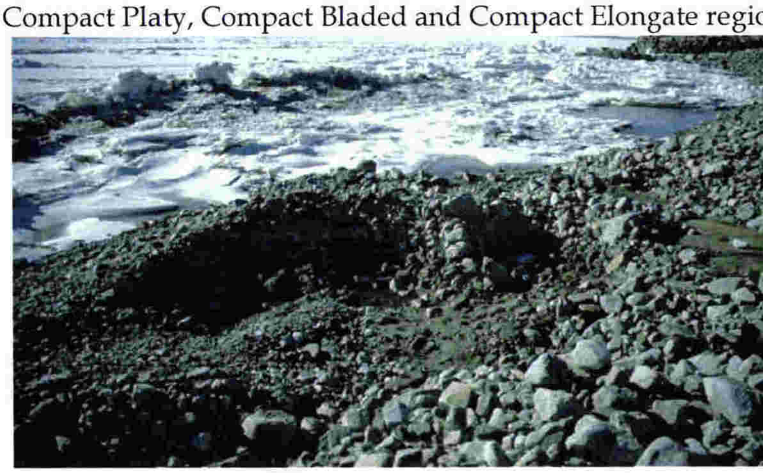

Figure 4.17. Typical ice push feature at Cape Bernacchi.

4.3.3.2 Marble Point sediment data

The sediments in the Marble Point Figures (Figures 4.19, 4.21 and 4.23) range in size from -8ϕ to 3ϕ and were generally poorly sorted with all of the pits on Marble 1 and Marble 3 containing cobbles and a mixed sand and gravel matrix. In contrast, pits 2, 5 and 6 on Marble 2 contained almost no clasts and were comparatively well sorted. Pits 2, 5 and 6 on Marble 2 contained clearly defined bedding structures. There appeared to be some weak shore normal 150^0 imbrication in Marble 3 pit 8. Apart from this example, there was no imbrication at Marble Point. The shape data shows some clustering about the Platy, Bladed, Elongate, Compact Platy, Compact Bladed and Compact Elongate regions of the Sneed and Folk diagrams. The clasts were generally poorly rounded.

Marble survey 1

Six beach ridges were identified on this profile and four sediment pits were examined. Pit 1 and 3 were located at the base of ridge 3 and 4 respectively and pit 2 and 4 were located at the top of these ridges.

Pit 1, base of the 3rd ridge (2.70m AMSL) (see Figure 4.18). This 760mm pit contained a massive poorly sorted sand and gravel matrix with matrix supported pebbles and cobbles. The mean size of the clasts in the pit was -5.65ϕ. The clasts were not imbricated and were clustered around the Platy, Bladed, Elongate, Compact Platy, Compact Bladed and Compact Elongate regions of the Sneed and Folk diagrams. The clasts were poorly rounded with an average rounding of 3.2.

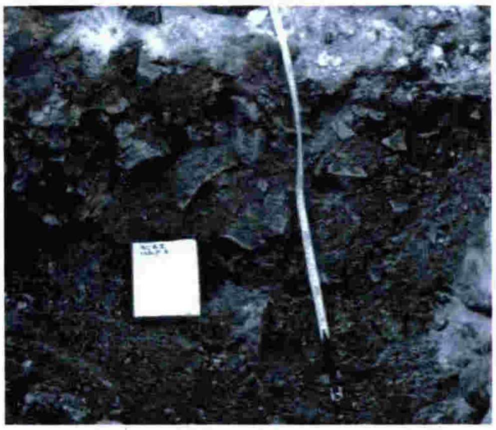

Figure 4.18. Pit 3 Marble survey 1. This pit was typical of all 4 of the pits on Marble survey 1. Note the extreme angularity of clasts in the face and absence of obvious sorting.

Pit 2, top of the 3rd ridge (5.00m AMSL). This 1000mm pit contained a massive poorly sorted sand and gravel matrix with matrix supported pebbles and cobbles. The mean size of measured clasts in pit 1 was -5.79ϕ. The clasts were not imbricated and were clustered around the Platy, Bladed, Elongate, Compact Platy, Compact

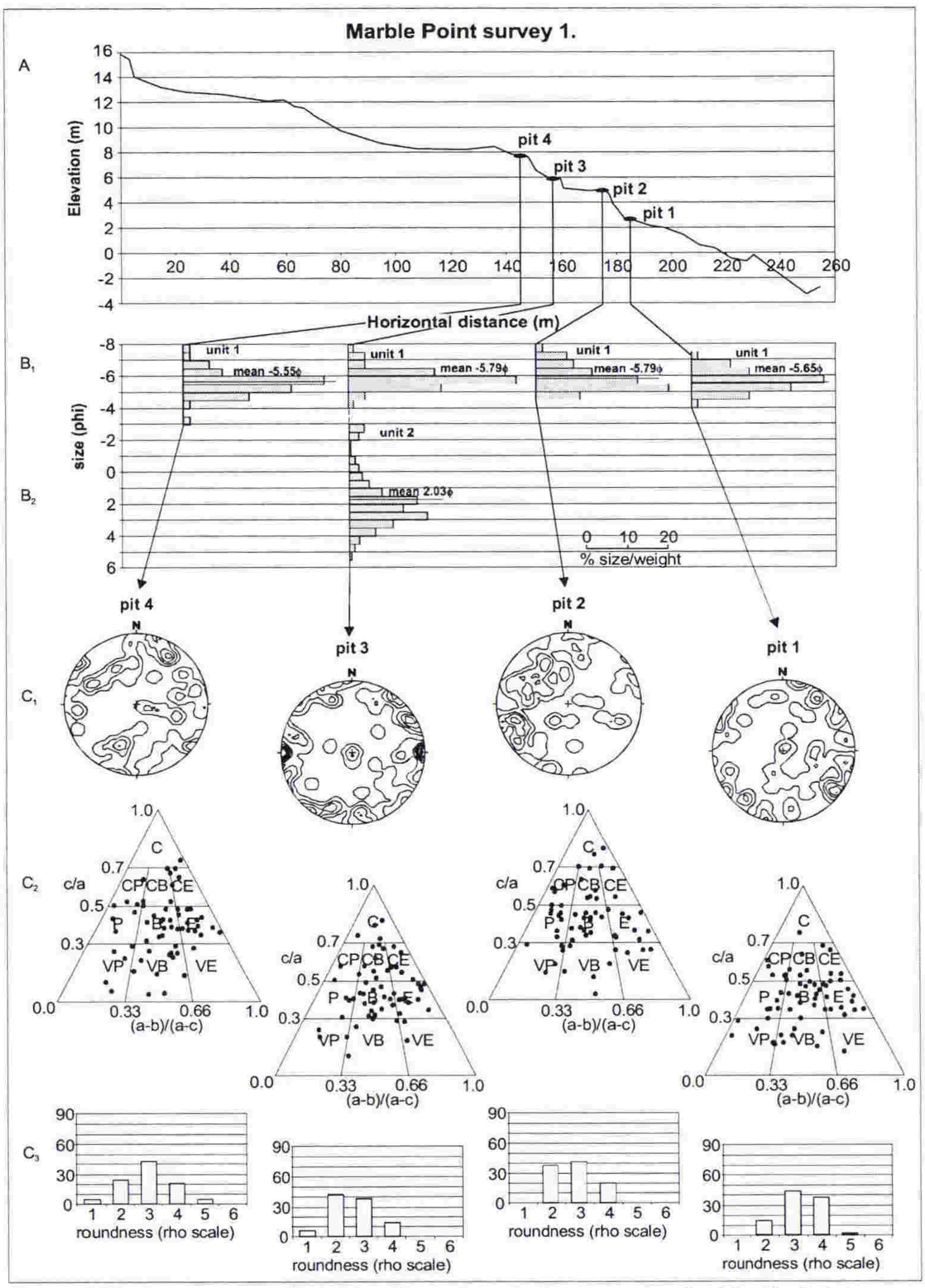

Figure 4.19. Summary profile and sedimentological information for Marble Point survey 1. Part A displays the profile and the locations of the sediment pits. Part B provides sediment size histograms; B_1 displays summary information for gravel beds while B_2 presents the same information for finer units. For the gravel units stereonet projections of gravel A axis dips (C_1), Sneed and Folk (1953) (C_2) shape triangles and Powers (1953) roundness (C_3) information are presented.

Bladed and Compact Elongate regions of the Sneed and Folk diagrams. The clasts were very poorly rounded with an average rounding of 2.8.

Pit 3, base of the 4th ridge (5.91m AMSL). This 780mm pit contained a poorly sorted mixed sand and gravel matrix with large pebbles and cobbles present at the base that fined upwards to a sandy unit at the top of the pit. The pit was subdivided into two units at 0-100mm and 100-780mm. Unit 1 (100-780mm) was a massive poorly sorted clast supported mixed sand and gravel with large pebbles and cobbles present. The mean size of the clasts in unit 1 was -5.79ϕ. The clasts were not imbricated and were clustered around the Platy, Bladed, Elongate, Compact Platy, Compact Bladed and Compact Elongate regions of the Sneed and Folk diagrams. The clasts were very poorly rounded with an average rounding of 2.6. Unit 3 (0-100mm) was a massive poorly sorted sand with some pebbles present. The mean size of the sand fraction in unit 1 was 2.03ϕ.

Pit 4, top of the 4th ridge (7.87m AMSL). This 800mm pit contained a massive poorly sorted sand and gravel matrix with matrix supported pebbles and cobbles. The mean size of clasts in this pit was -5.55ϕ. The clasts were not imbricated and were clustered around the Platy, Bladed, Elongate, Compact Platy, Compact Bladed and Compact Elongate regions of the Sneed and Folk diagrams. The clasts were very poorly rounded with an average rounding of 2.9.

Marble survey 2

Six beach ridges were identified on this profile and six sediment pits were examined. Pits 1, 3 and 5 were located at the top of ridges 4, 5 and 6 respectively and pits 2 and 4 were located at the base of ridges 5 and 6 respectively. Pit 6 was located about 20m to the east of Marble survey 2 at 19.02m AMSL.

Pit 1, top of the 4th ridge (5.04m AMSL). This 650mm pit contained a poorly sorted mixed sand and gravel with matrix supported pebbles and cobbles overlain by a poorly sorted sand. The pit was subdivided into two units at 0-50mm and 50-650mm. Unit 1 (50-650mm) was a massive poorly sorted mixed sand and gravel with matrix supported pebbles and cobbles. The mean b axis of measured clasts in unit 1 was -5.79ϕ. The pebbles had no imbrication and were clustered around the Platy, Bladed, Elongate, Compact Platy, Compact Bladed and Compact Elongate regions of the Sneed and Folk diagrams. The clasts were poorly rounded with an average rounding of 3.6. Unit 2 (0-50mm) was a massive poorly sorted sand. The mean grain size of the clasts in unit 2 was -2.71ϕ.

Pit 2 base of 5th ridge (5.63m AMSL). This 550mm pit contained massive poorly sorted sand with a few pebbles present. Mean grain size was -0.97ϕ.

Pit 3 top of the 5th ridge (8.24m AMSL). This 770mm pit contained a clast supported mixed sand and gravel with large pebbles and cobbles at the base of the pit that fined upwards. The matrix was collected from the pit and had a mean grain size of 0.03ϕ. The mean b axis of measured clasts was -5.55ϕ. The pebbles had no imbrication and were clustered around the Platy, Bladed, Elongate, Compact Platy, Compact Bladed and Compact Elongate regions of the Sneed and Folk diagrams. The clasts were poorly rounded with an average rounding of 3.3.

Pit 4, base of 6th ridge (8.96m AMSL). This 700mm pit contained a clast supported mixed sand and gravel with large pebbles and cobbles at the base of the pit that fined upwards. The mean b axis of measured clasts in units 1 and 2 was -5.45ϕ. The pebbles had no imbrication and were clustered around the Platy, Bladed, Elongate, Compact Platy, Compact Bladed and Compact Elongate regions of the Sneed and Folk diagrams. The clasts were very poorly rounded with an average rounding of 2.65.

Pit 5, top of the 6th ridge (10.50m AMSL). This 340mm pit contained a moderately sorted bedded sand which was subdivided into 2 units at 0-140mm and 140-340mm. Unit 1 (140-340mm) contained clearly defined 100mm long 18mm high, fine sand and coarse sand ripple cross lamination (Jopling and Walker, 1968) (see Figure 4.20). There were some small pebbles in both units. Unit 2 (0-140mm) was a massive moderately sorted sand. The mean grain size of the sediment in unit 1 was 0.45ϕ and 0.19ϕ in unit 2.

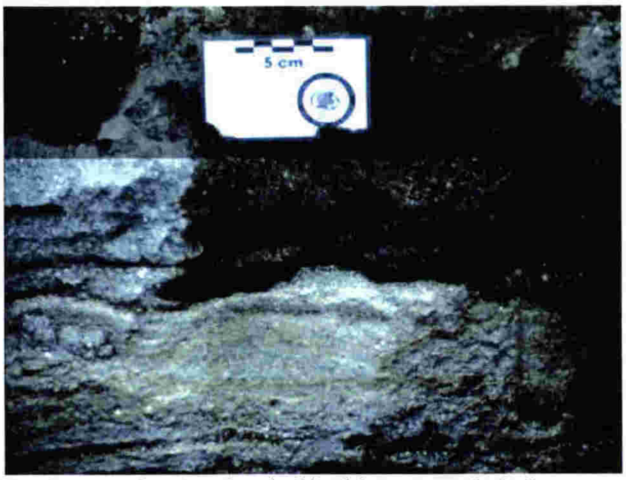

Figure 4.20. Ripple cross lamination in Marble survey 2 pit 5.

Pit 6, off to the east of Marble survey 2 (19.09m AMSL). This 370mm pit contained a poorly sorted bedded sand which was subdivided into 2 units at 0-170mm and 170-370mm. Unit 1 (170-370mm) contained clearly defined planar bedding and some dune bedding. The planar beds were 10mm high and dipped 8^0 in a shore normal (360^0) direction. The dunes were 1,000mm long and 85mm high and dipped between 8^0 to 17^0 in a 150^0 direction (Jopling and Walker, 1968). Unit 2 (0-170mm) was a massive poorly sorted sand with rare pebbles present. The mean grain size of sediment in unit 1 was 0.65ϕ and 0.87ϕ for unit 2.

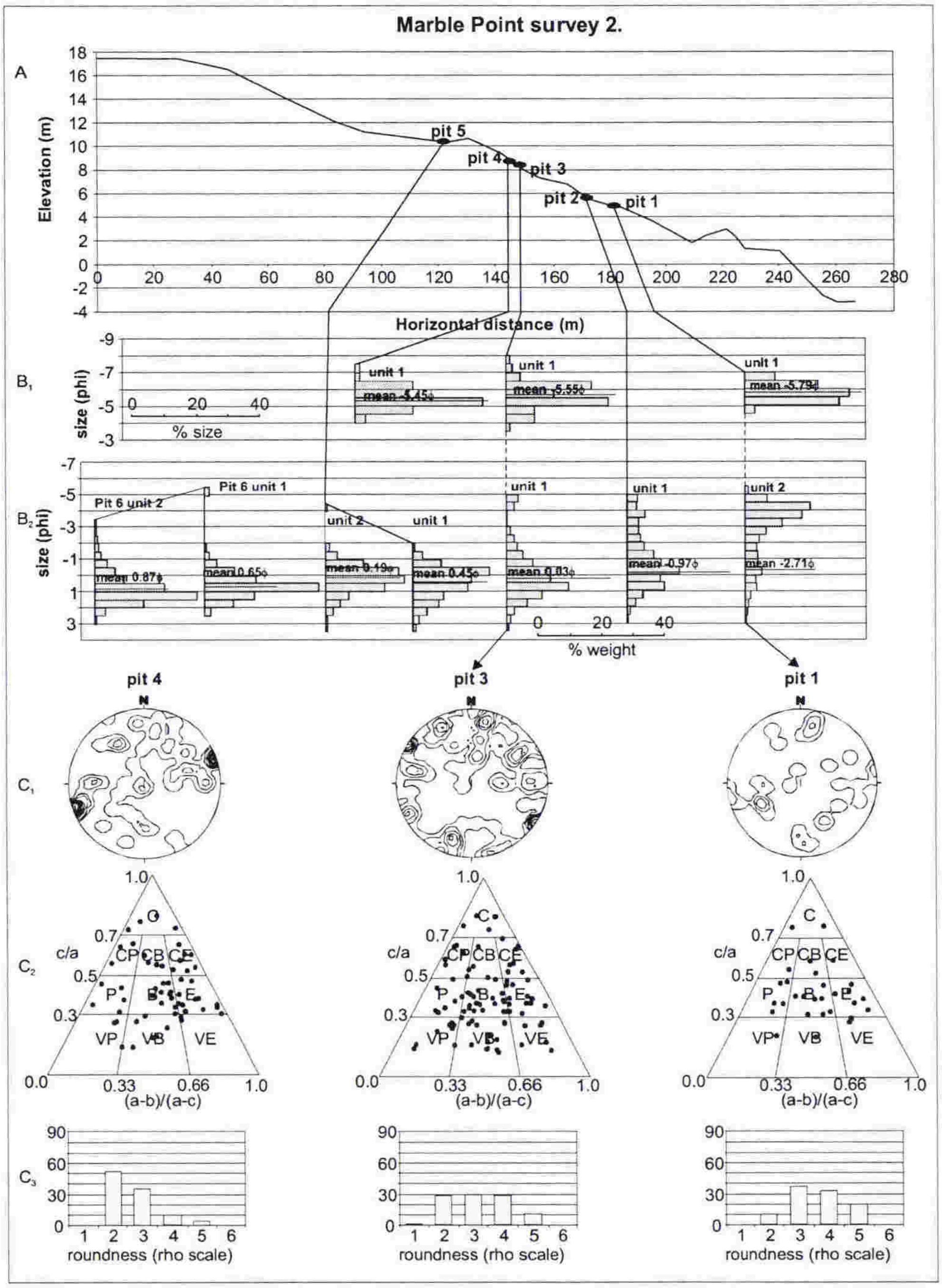

Figure 4.21. Summary profile and sedimentological information for Marble Point survey 2. Part A displays the profile and the locations of the sediment pits. Part B provides sediment size histograms; B_1 displays summary information for gravel beds while B_2 presents the same information for finer units. For the gravel units stereonet projections of gravel A axis dips (C_1), Sneed and Folk (1953) (C_2) shape triangles and Powers (1953) roundness (C_3) information are presented.

Marble survey 3

Four major beach ridges were identified on this profile and two sediment pits were examined. Pits 7 and 8 were located on the top and the base of the 3rd ridge respectively.

Pit 7, top of the 3rd ridge (11.65m AMSL). This 640mm pit contained a poorly sorted mixed sand and gravel with clast supported pebbles and cobbles. The mean b axis of measured clasts in this pit was -5.86ϕ. The pebbles had no imbrication and were clustered around the Platy, Bladed, Elongate, Compact Platy, Compact Bladed and Compact Elongate regions of the Folk and Ward diagrams. The clasts were poorly rounded with an average rounding of 3.7. The clasts in the pit were in an advanced state of weathering and some of the clasts were unable to be measured because they were frost shattered.

Pit 8, base of the 3rd ridge (10.95m AMSL). This 700mm pit contained a poorly sorted mixed sand and gravel with clast supported pebbles and cobbles that fined to the top of the pit (see Figure 4.22). The mean b axis of measured clasts in this pit was -5.57ϕ. The pebbles were strongly imbricated in a shore normal (190^0) direction and were clustered around the Platy, Bladed, Elongate, Compact Platy, Compact Bladed and Compact Elongate regions of the Folk and Ward diagrams. The clasts were poorly rounded with an average rounding of 3.2. The pit was in an advanced state of weathering and some of the clasts were unable to be measured because they were frost shattered.

Figure 4.22. Marble survey 3 pit 8.

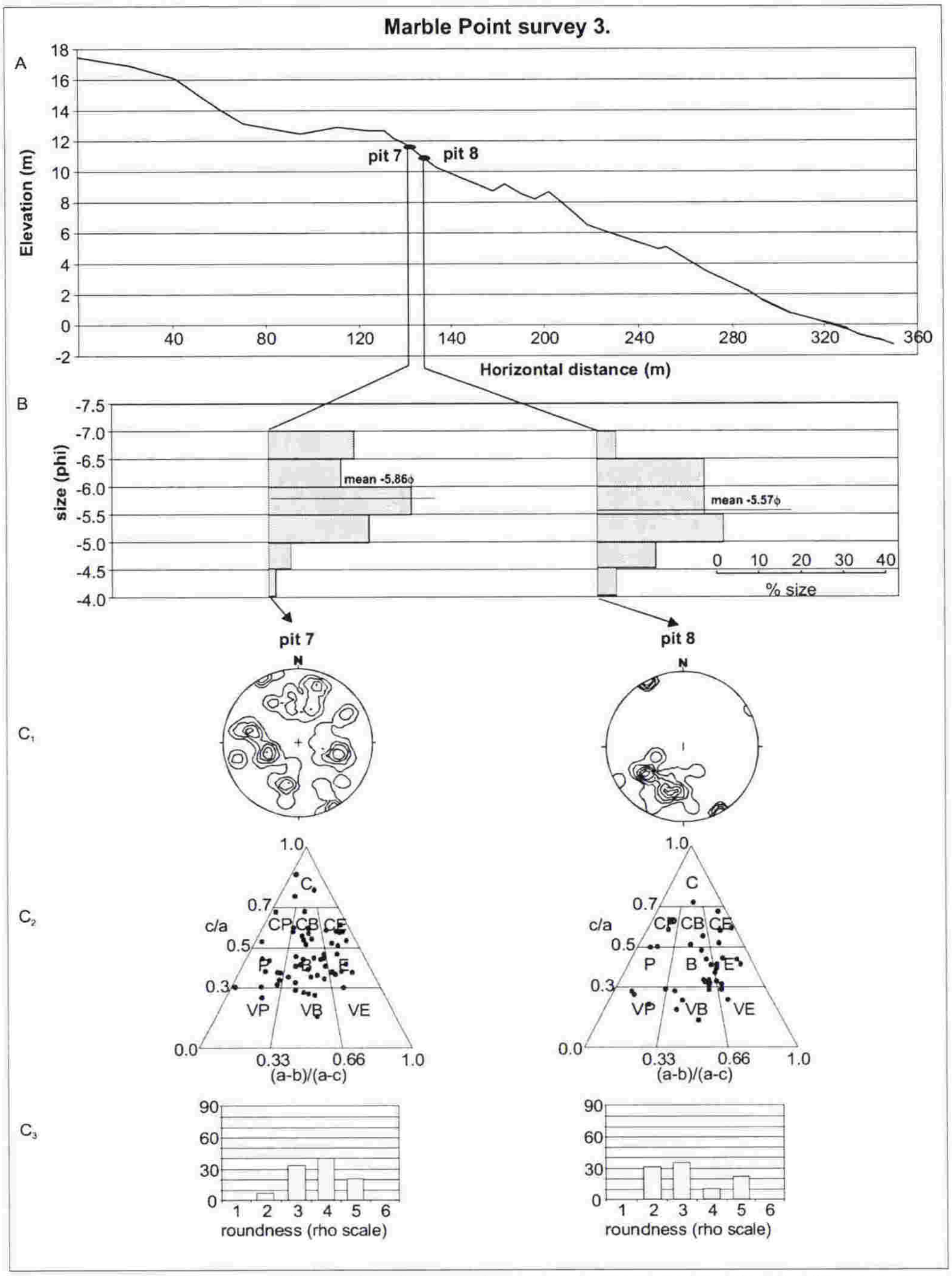

Figure 4.23. Summary profile and sedimentological information for Marble Point survey 3. Part A displays the profile and the locations of the sediment pits. Part B provides sediment size histograms for gravel beds. For all units stereonet projections of gravel A axis dips (C_1), Sneed and Folk (1953) (C_2) shape triangles and Powers (1953) roundness (C_3) information are presented.

4.3.3.3 Kolich Point size range

Kolich Point size range

The sediments at Kolich Point (Figure 4.24) ranged in size from boulders (-11ϕ) to sand (4.5ϕ). The clasts were well sorted (some clasts were present) at Kolich 3 but a range of sizes were present at Kolich 2 (sandy matrix in pit 2) and Kolich 1 (boulders to sand). The diagram shows a clear decrease in sediment size from the north to the south. The exposure at Kolich 3 shows a number of classic marine and polar features such as drop stones and overwash fans.

Size analysis was undertaken at three separate locations at Kolich Point. Boulder counts were done on each of the six major ridges on the Kolich 1 profile. Triaxial measurements were undertaken on clasts in pit 2 Kolich 2 and size analysis was done on a scarp face on Kolich 3. The stratigraphy of the scarp face is described below in Kolich 3. The boulders measured on the ridges of Kolich 1 were considerably larger than the clasts on the active beach. Three surface counts were undertaken on the active beach ridge. The counts were located at points on the active beach ridge where there was a slight change in slope. The three counts from the active beach show similar size clasts to pit 2 Kolich 2. Kolich 2 pit 2 was typical of pits found on Marble 1 with a poorly sorted sand and fine gravel matrix supporting pebbles and cobbles. It was located at 9.10m AMSL at the top of the second major beach ridge on Kolich 2. Kolich 2 pit 1 was located at 6.80m AMSL at the base of the second major beach ridge on Kolich 2. This 350mm pit was subdivided into three units at 0-100mm, 100-220mm and 220-350mm (see Figure 4.25). Unit 1 (A, see Figure 4.25) (220-350mm) was a massive poorly sorted sand with few clasts present. Unit 2 (B, see Figure 4.25) (100-220mm) contained mm scale ripple cross lamination dipping 8^0 in a 340^0 direction. Unit 3 (C, see Figure 4.25) (0-100mm) was a massive poorly

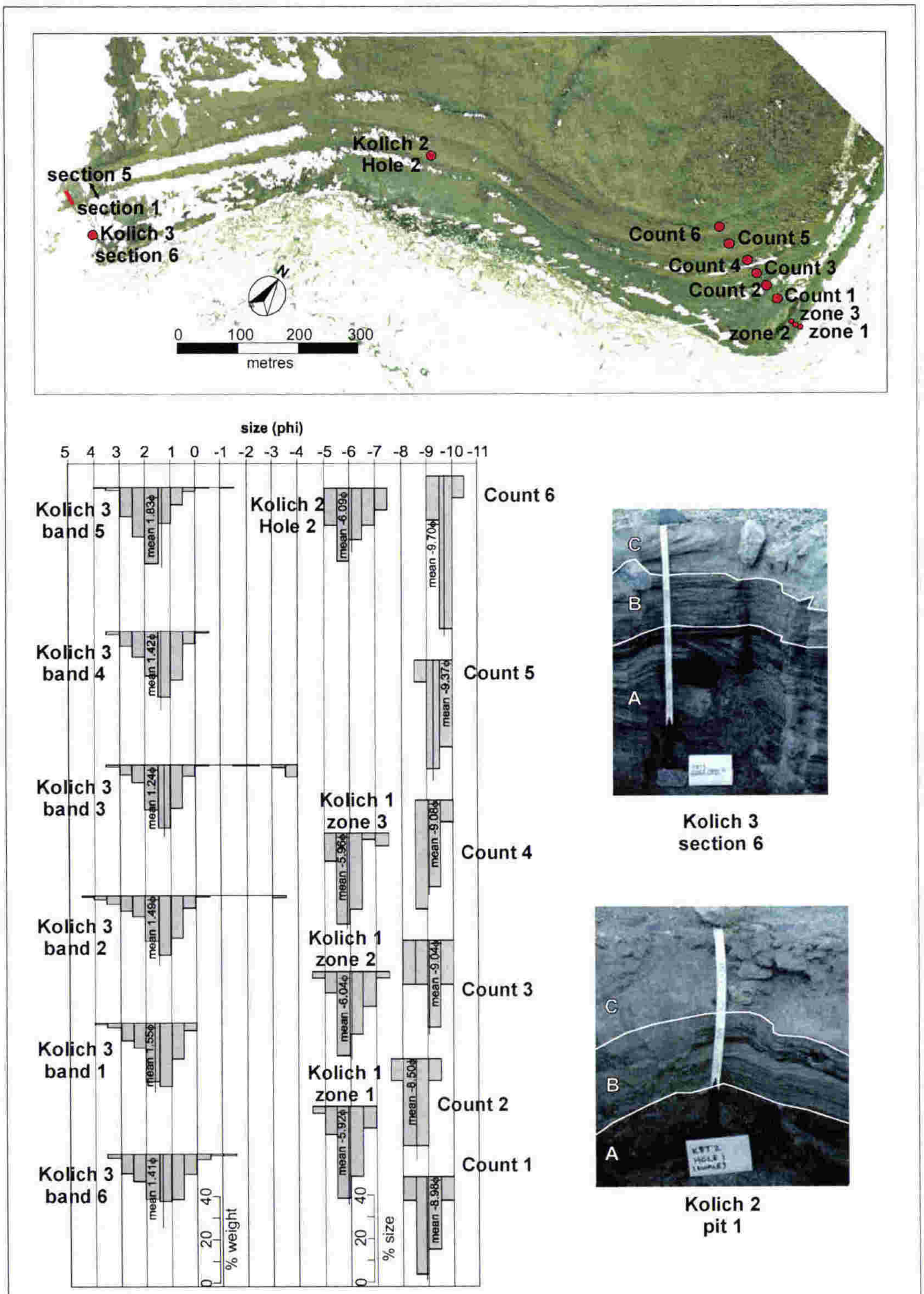

Figure 4.24. Size of material measured at Kolich Point. Kolich 3 section 6 and Kolich 2 pit 1, with bedding units marked are also shown.

sorted sand with few clasts present . The size of the sediment in pit 1 was closer to the size of the sediment on Kolich 3.

Kolich survey 3 stratigraphy

The most extensive area of continuous bedding on any of the beaches in McMurdo Sound was found at the top of Kolich survey 3. This exposure was 49m long and between 400mm and 600mm deep (see Figure 4.25). For ease of interpretation, the exposure was divided into 5 discrete sections. Section 1 shows a complex set of beds to the right of the section that were flaser bedding. Throughout the flaser bedding there are small pebbles and cobbles. To the left of the section there is a boulder and a number of small cobbles that dip 30^0 in a 90^0 direction that are part of an overwash fan. The bedding beneath the boulder is indistinct but the base of the overwash fan

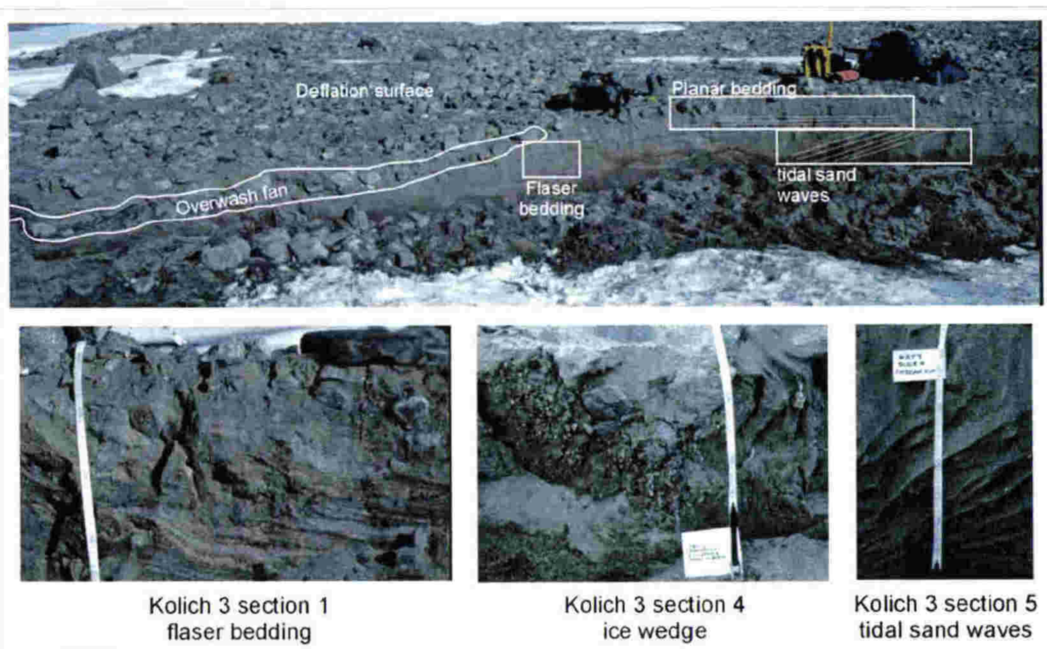

Figure 4.25. Sections 1, 4 and 5 on the scarp face on Kolich 3. The top photograph shows the scarp to the edge of section 3.

represents a truncation surface. Section 2 is a continuation of the flaser bedding seen in Section 1. Section 3 consisted of a fine to coarse moderately well to poorly sorted massive sand at the top and beds that dipped 19° in a 10° direction. These were probably tidal sand waves (Dalrymple, 1992) with a truncation surface at 200mm and at the very base of the section. These dunes had planar bedding overlying them. Section 4 showed a classic ice wedge polygon structure, which was identifiable from the frost crack at the surface. Section 5 contained moderately well sorted fine to coarse sand sigmoidal bedding that dipped 38° in a 252° direction. These were interpreted as longitudinal sections through tidal sand waves (Dalrymple, 1992).

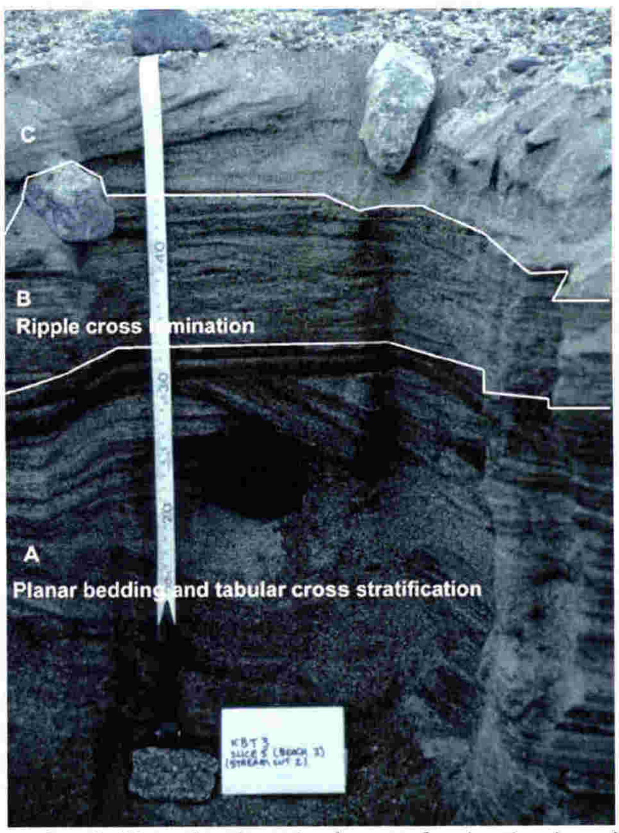

Figure 4.26. Kolich 3 section 6. Note the clear ripple cross lamination in unit 2 (B) and planar bedding and tabular cross stratification in unit 1 (A).

In addition to the exposure, half-way down and 10m to the south of Kolich 3 survey, another exposure was excavated (see Figure 4.26). This exposure contained three clear bedding structures. The top 220mm, contained mm scale to 150mm long, ripple cross lamination. Below this and to the base of the exposure the unit comprised dominantly planar bedding with some tabular cross stratification present. The beds ranged in thickness from about 1mm to 15mm. All units contained small cobbles which were interpreted as ice rafted dropstones.

4.3.3.4 Spike Cape sediment data

The sediments in the Spike Cape Figures (Figures 4.27, 4.28 and 4.29) range in size from -8ϕ to 3.5ϕ and were generally poorly sorted with all of the pits on Spike 1 and Spike 2 containing cobbles and a mixed sand and gravel matrix. Pit 2 on Spike 2 contained clearly defined bedding structures. There was some strong shore normal 330^0 imbrication in all surface counts on Spike Barrier. Apart from this example, there was no imbrication at Spike Cape. The shape data shows some clustering about the Platy, Bladed, Elongate, Compact Platy, Compact Bladed and Compact Elongate regions of the Folk and Ward diagrams. The clasts were generally poorly rounded on Spike 1 and 2 but well rounded on Spike Barrier.

Spike survey 1

Five major beach ridges were identified on this profile and three sediment pits were examined. Pits 1 and 3 were located at the crest of the 5^{th} and 3^{rd} ridges respectively. Pit 2 was located at the base of the 5^{th} ridge.

Pit 1, top of the 5^{th} ridge (15.36m AMSL). This 550mm pit contained a poorly sorted mixed sand and gravel with clast supported pebbles and cobbles. The mean b axis of measured clasts was -6.46ϕ. The pebbles had no imbrication and were clustered around the Platy, Bladed, Elongate, Compact Platy, Compact Bladed and Compact Elongate regions of the Sneed and Folk diagrams. The clasts were well rounded with an average rounding of 4.0.

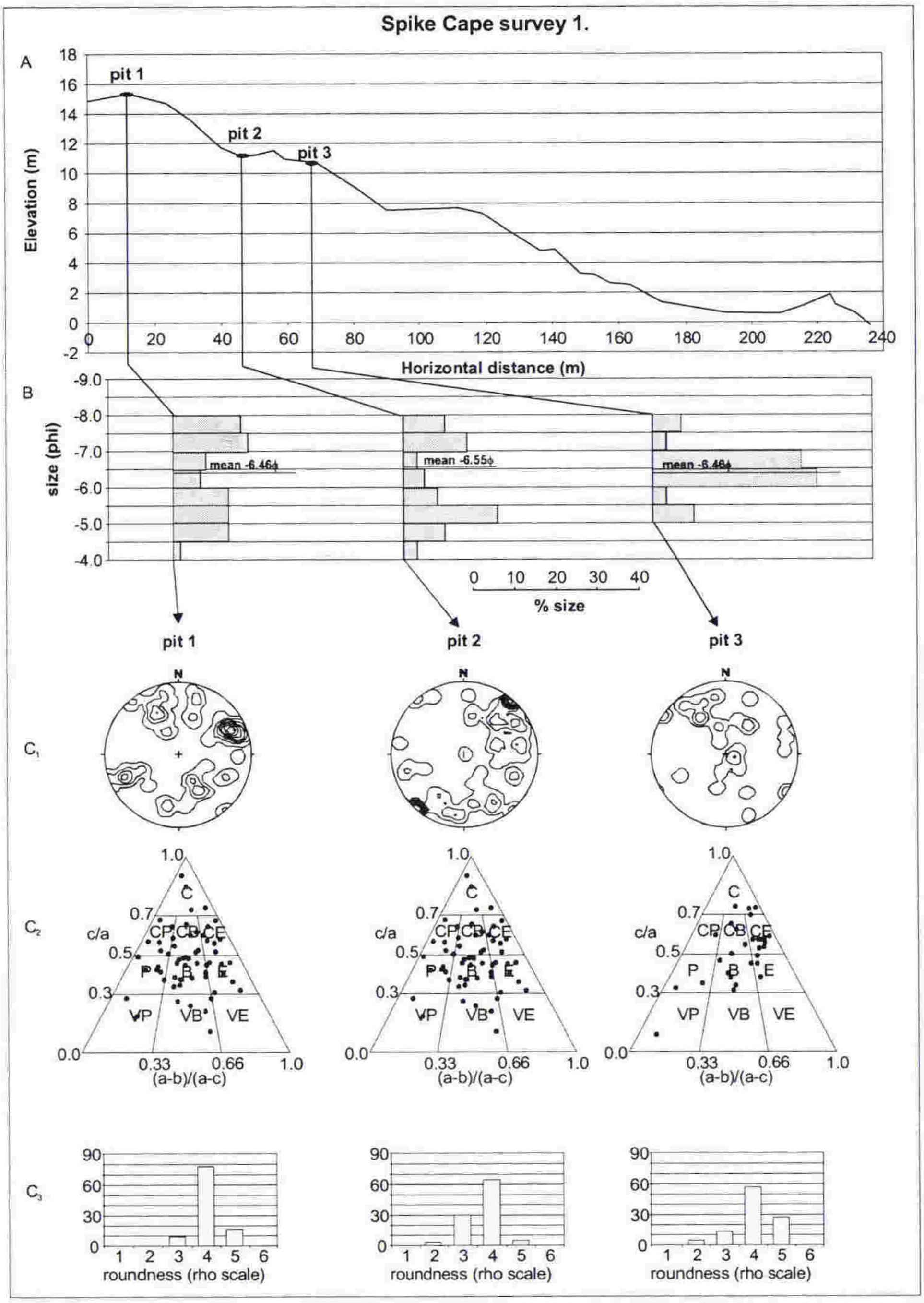

Figure 4.27. Summary profile and sedimentological information for Spike Cape survey 1. Part A displays the profile and the locations of the sediment pits. Part B provides sediment size histograms for gravel beds. For all pits stereonet projections of gravel A axis dips (C_1), Sneed and Folk (1953) (C_2) shape triangles and Powers (1953) roundness (C_3) information are presented.

Pit 2, base of the 5th ridge (11.14m AMSL). This 500mm pit contained a poorly sorted mixed sand and gravel with clast supported pebbles and cobbles that fined to the top of the pit. The mean b axis of measured clasts was -6.55ϕ. The pebbles had no imbrication and were clustered around the Platy, Bladed, Elongate, Compact Platy, Compact Bladed and Compact Elongate regions of the Sneed and Folk diagrams. The clasts were poorly rounded with an average rounding of 3.7.

Pit 3, top of the 3rd ridge (10.72m AMSL). This 550mm pit contained a poorly sorted mixed sand and gravel with clast supported pebbles and cobbles. The mean b axis of measured clasts in the pit was -6.46ϕ. The pebbles had no imbrication and were clustered around the Platy, Bladed, Elongate, Compact Platy, Compact Bladed and Compact Elongate regions of the Folk and Ward diagrams. The clasts were well rounded with an average rounding of 4.0.

Spike survey 2

Four major beach ridges were identified on this profile and two sediment pits were examined. Pits 2 and 1 were located at the crest and the base of the 5th ridge respectively.

Pit 1, base of the 4th ridge (13.93m AMSL). This 480mm pit contained a poorly sorted mixed sand and gravel with clast supported pebbles and cobbles. The mean b axis of measured clasts in the pit was -5.52ϕ. The pebbles had no imbrication and were clustered around the Platy, Bladed, Elongate, Compact Platy, Compact Bladed and Compact Elongate regions of the Sneed and Folk diagrams. The clasts were poorly rounded with an average rounding of 3.1.

Pit 2, crest of the 4th ridge (15.03m AMSL). This 660mm pit contained a poorly sorted mixed sand and gravel with some ripple cross lamination. The pit was subdivided into 5 units at 0-160mm, 160-250mm, 250-360mm, 360-570 and 570-

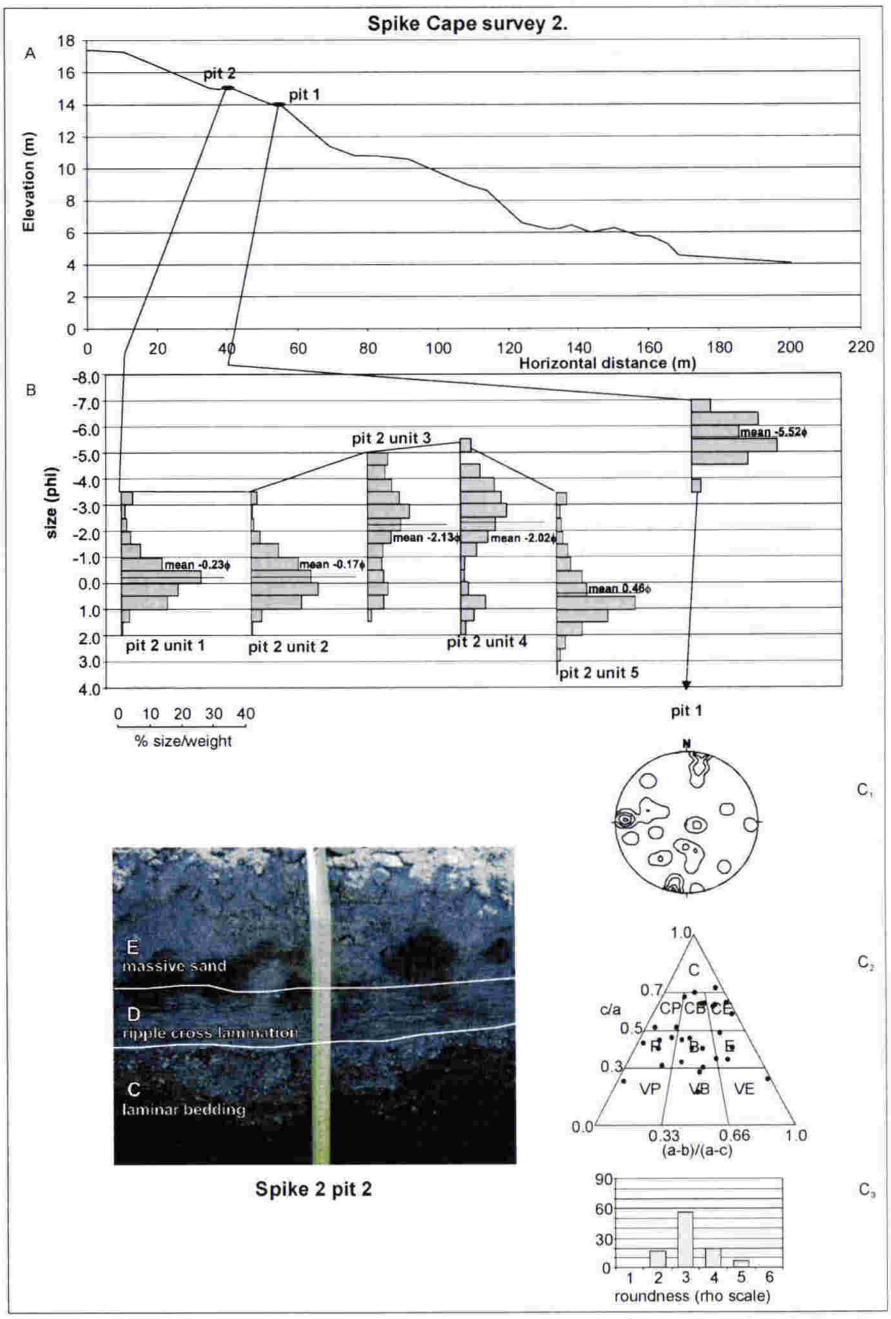

Figure 4.28. Summary profile and sedimentological information for Spike Cape survey 2. Part A displays the profile and the locations of the sediment pits. Part B provides sediment size histograms for gravel beds. For pit 1 stereonet projections of gravel A axis dips (C_1), Sneed and Folk (1953) (C_2) shape triangle and Powers (1953) roundness (C_3) information are presented. A photograph of Spike 2 pit 2 with the bedding units marked is also shown. Note the clear ripple cross lamination (marked D on photograph).

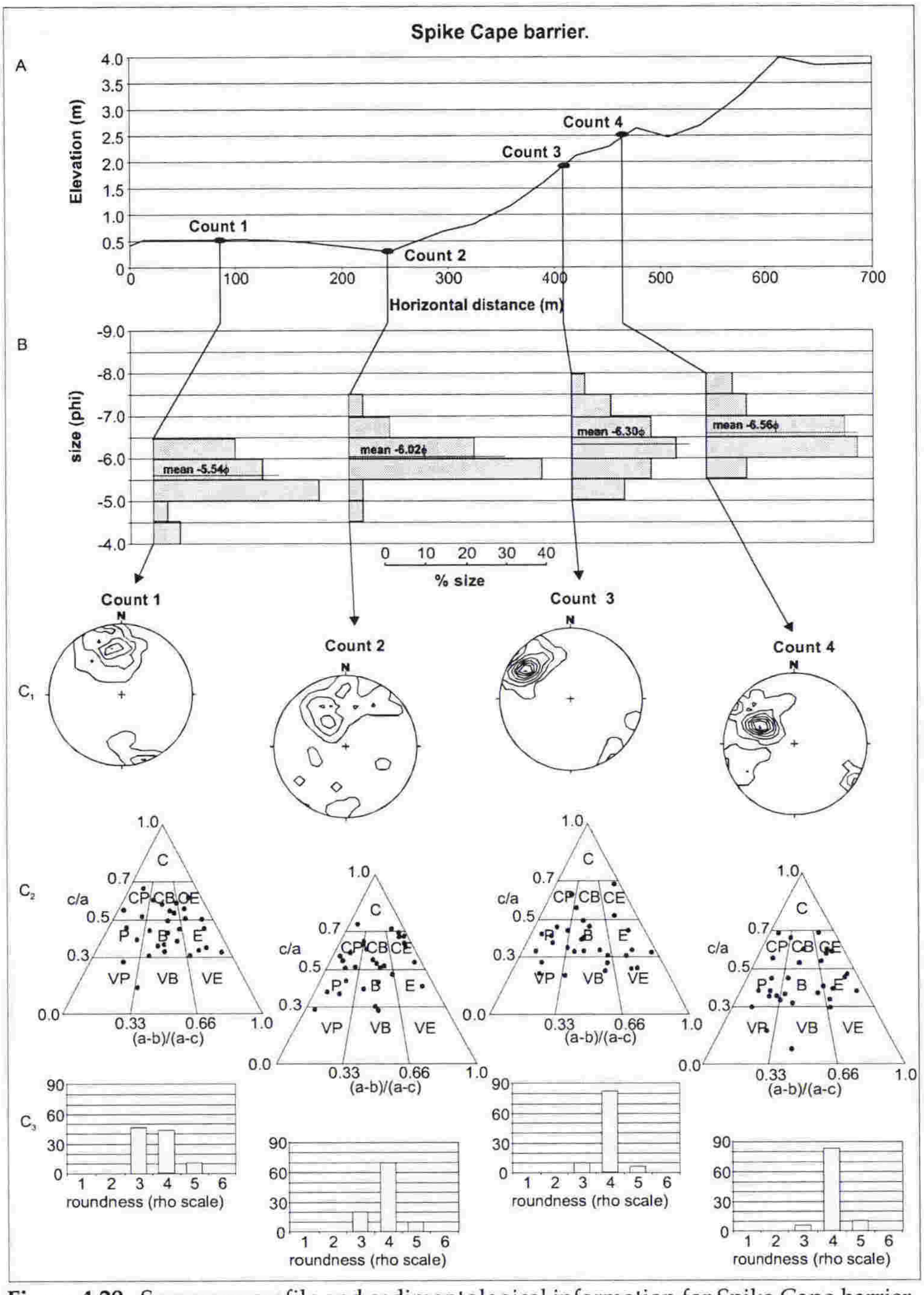

Figure 4.29. Summary profile and sedimentological information for Spike Cape barrier. Part A displays the profile and the locations of the surface counts. Part B provides sediment size histograms for gravel beds. For all counts stereonet projections of gravel A axis dips (C_1), Sneed and Folk (1953) (C_2) shape triangles and Powers (1953) roundness (C_3) information are presented.

660mm. Unit 1 (360-570mm) was a massive poorly sorted sand with a mean grainsize of 0.46ϕ. Unit 2 (360-570mm) was a massive poorly sorted mixed sand and gravel with a mean grainsize of -2.02ϕ. Unit 3 (marked C on Figure 4.29) (250-360mm) contained laminar bedded sand with a mean grainsize of -2.13ϕ. The beds were mm scale and dipped 8^0 in a 75^0 direction. Unit 4 (marked D on Figure 4.27) (160-250mm) was a sand unit with ripple cross lamination. The ripples were about 4mm high and were approximately 30-40mm long. The mean grainsize of sediment in this unit was -0.17ϕ. Unit 5 (marked E on Figure 4.29) (0-160mm) was a massive poorly sorted sand with a mean grainsize of -0.23ϕ.

Spike barrier

On the west-facing aspect of Spike Cape a migrating barrier was examined. The location of the barrier is shown in Figure 4.7. The barrier was 3.86m AMSL at the northern end and decreased in elevation to 0.42m AMSL at the southern end. Surface counts at points along the barrier were undertaken. Clasts on the barrier consisted of well-sorted pebbles with no matrix present. Size of clasts decreased from -6.56ϕ at the northern end to -5.54ϕ at the southern end. The clasts were generally clustered around the compact platy, bladed and elongate regions of the Sneed and Folk shape triangles. Of all of the sites visited, Spike barrier had the strongest imbrication with all sites along the barrier showing displaying very strong shore normal (330^0) imbrication. Clasts at all of the sites along the barrier were well rounded with an average rounding for count sites ranging from 3.6 to 4.0.

4.3.3.5 Dunlop Island sediment data

The sediments in the Dunlop Island Figures (Figures 4.30, 4.31 and 4.32) range in size from -10ϕ to -4ϕ. Surface counts of clasts were undertaken on Dunlop survey 1 and 2 and two pits were dug on Dunlop survey 2. Both pits were poorly sorted with cobbles and a mixed sand and gravel matrix. There appeared to be some weak shore normal (0-5^0) imbrication on ridge 1, 2 and 5 on Dunlop survey 1 and some weak shore normal imbrication (200^0) on Beach 1 and 5 and in pit 1 on Dunlop 2. The shape data shows some clustering about the Platy, Bladed, Elongate, Compact Platy, Compact Bladed and Compact Elongate regions of the Sneed and Folk diagrams. The clasts on Dunlop 1 were considerably better rounded than those on Dunlop 2.

Dunlop survey 1

Six beach ridges were identified on this profile and two sets of measurements were undertaken at various locations on Dunlop 1. The 10 largest boulders were measured and surface counts of clasts at these locations were undertaken. Boulder counts were undertaken on the crest of ridges 1, 2, 3, 5, and 6 and surface counts of clasts were undertaken on an ice push feature on the shore and on the crest of ridges 1, 2, 3 and 5. The elevation of the ridges was; 1.60m Dunlop 1 ice, 5.65m ridge 1, 7.68m ridge 2, 8.43m ridge 3, 10.43m ridge 5 and 15.92m ridge 6 (all AMSL). The boulder counts mean size ranged from -8.08ϕ to –9.44ϕ. The size of clasts on the surface counts was also close with mean clast size on the surface counts ranging from –5.35ϕ to -6.33ϕ. The surface counts showed weak shore normal (0-20^0) imbrication on ridges 1, 2 and 5. All of the surface count clasts were clustered around the Platy, Bladed, Elongate, Compact Platy, Compact Bladed and Compact Elongate regions of the Sneed and Folk diagrams. The clasts on the surface counts were well rounded with mean rounding ranging from 4.0 to 4.6.

Dunlop survey 2

Eleven beach ridges were identified on Dunlop survey 2. Surface counts of clasts were undertaken on an ice push feature at the shore and at the crest of ridges 1, 4, 5 and 6. Two pits were dug, one at the top of ridge 4 and the other at the top of ridge

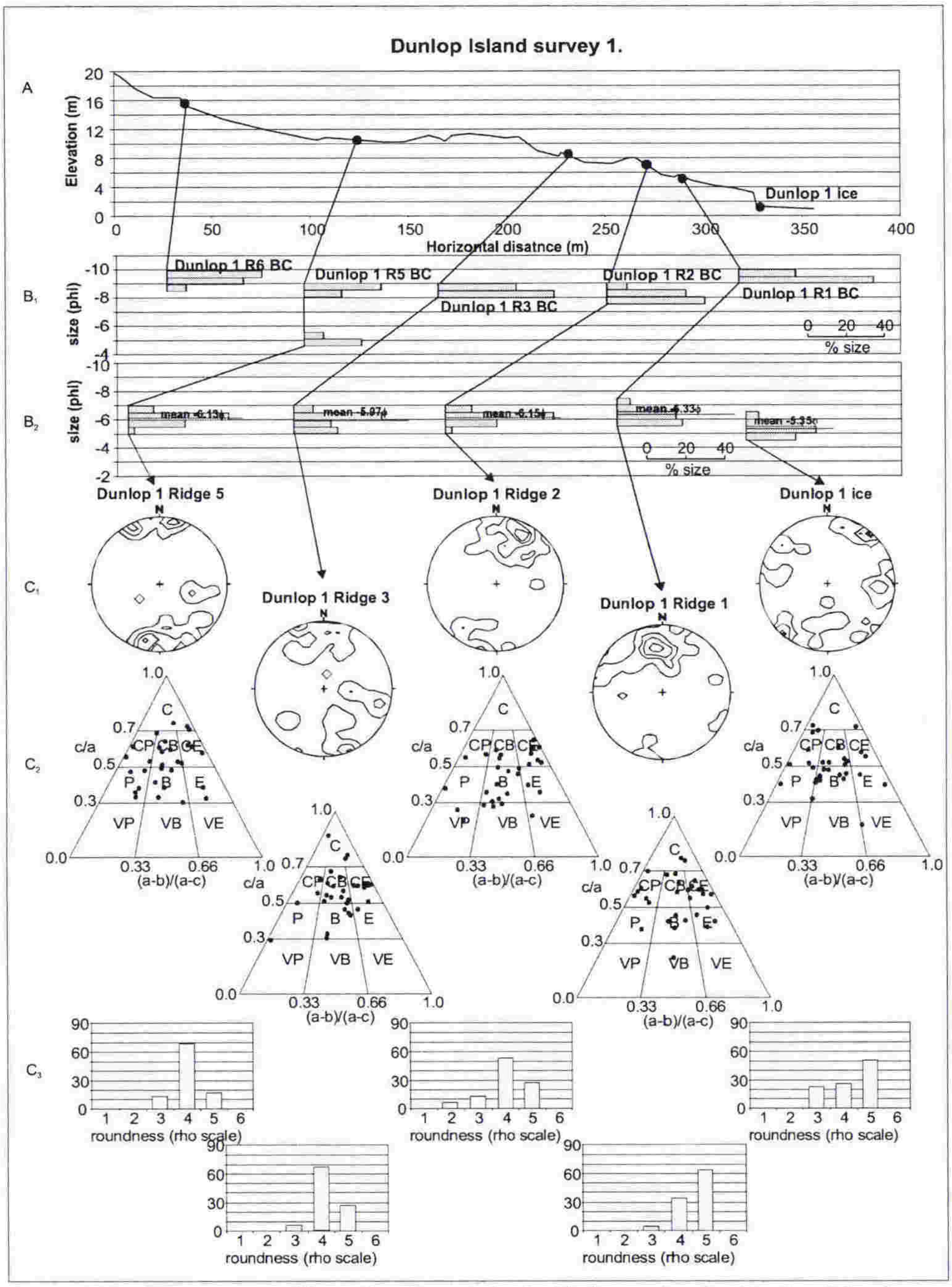

Figure 4.30. Summary profile and sedimentological information for Dunlop Island survey 1. Part A displays the profile and the locations of the sediment counts. Part B1 provides sediment size histograms for boulder counts and B2 provides sediment size histograms for surface pebble counts. For all surface counts stereonet projections of gravel A axis dips (C_1), Sneed and Folk (1953) (C_2) shape triangles and Powers (1953) roundness (C_3) information are presented.

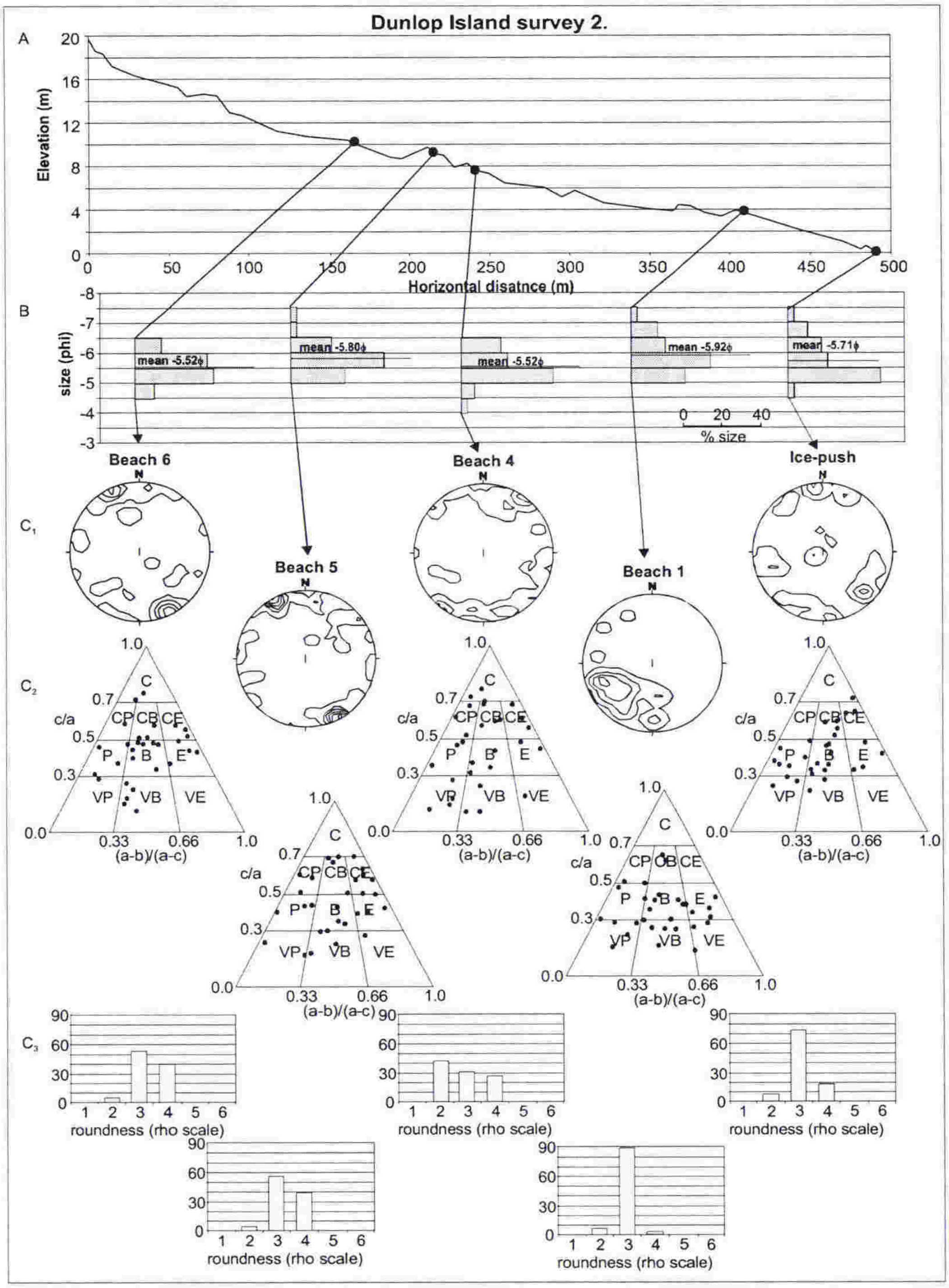

Figure 4.31. Summary profile and sedimentological information for Dunlop Island survey 2. Part A displays the profile and the locations of the counts. Part B provides sediment size histograms for surface pebble counts. For all surface counts stereonet projections of gravel A axis dips (C_1), Sneed and Folk (1953) (C_2) shape triangles and Powers (1953) roundness (C_3) information are presented.

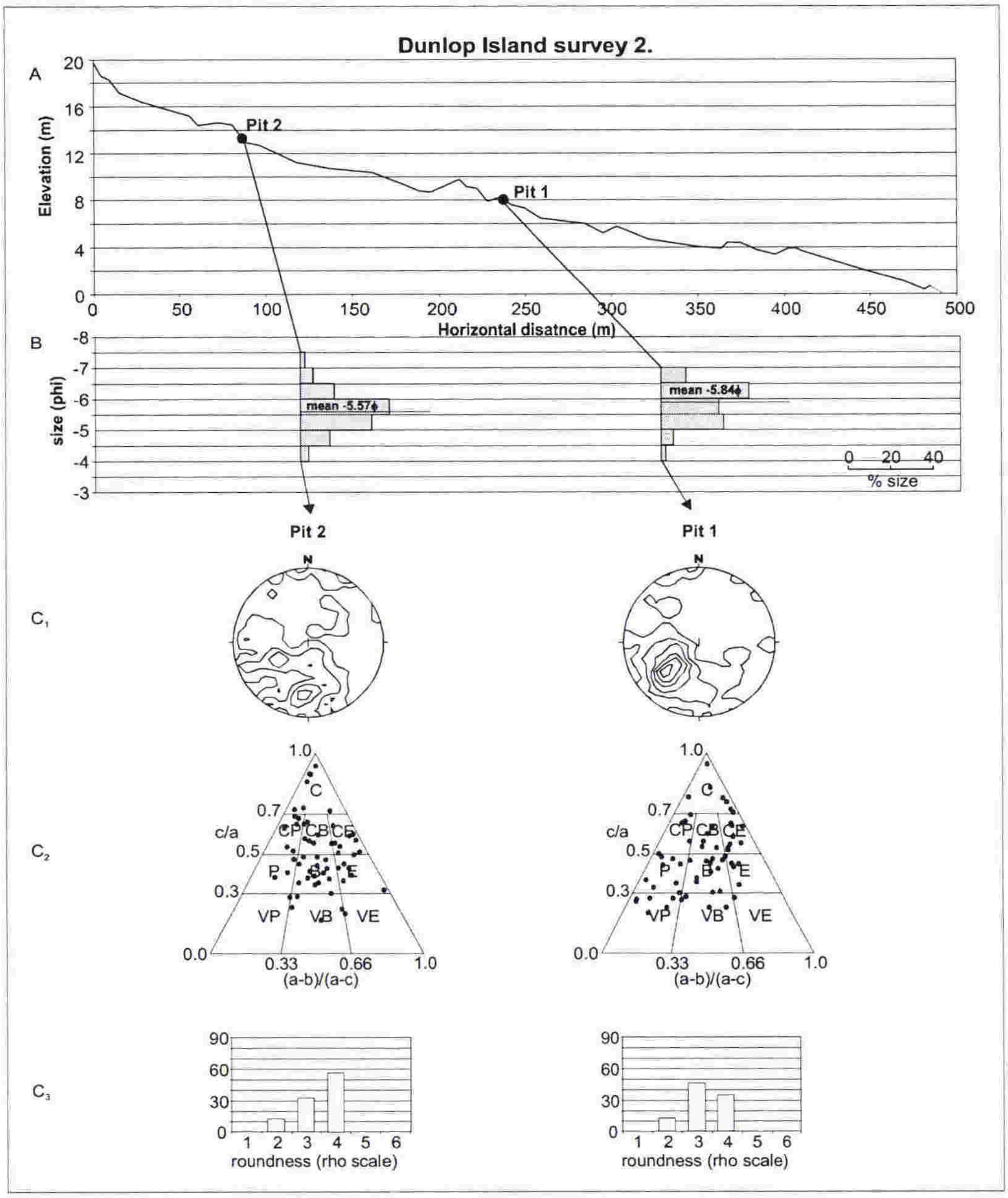

Figure 4.32. Summary profile and sedimentological information for Dunlop Island survey 2. Part A displays the profile and the locations of the pits. Part B provides sediment size histograms for gravel beds. For both pits stereonet projections of gravel A axis dips (C_1), Sneed and Folk (1953) (C_2) shape triangles and Powers (1953) roundness (C_3) information are presented.

7. The elevation of the counts was; 0.11m ice-push, 3.98m beach 1, 7.90m beach 4, 9.55m beach 5 and 10.18m beach 6 (all AMSL). The mean size of clasts on the surface counts ranged from -5.52ϕ to -5.92ϕ, with little variation between sites. There was weak shore normal (160^0) imbrication present on ridges 5 and 6 and stronger shore normal (220^0) imbrication on ridge 1. The clasts in the surface counts extended to all regions of the Sneed and Folk shape triangles. The clasts were very poorly rounded to poorly rounded with mean rounding values of 2.8 to 3.3.

Pit 1, crest of the 4^{th} ridge (8.05m AMSL). This 650mm pit contained a poorly sorted mixed sand and gravel with clast supported pebbles and cobbles that fined to the top of the pit. The mean b axis of measured clasts in the pit was -5.84ϕ. The pebbles were strongly imbricated in a shore normal (230^0) direction and were clustered around the Platy, Bladed, Elongate, Compact Platy, Compact Bladed and Compact Elongate regions of the Sneed and Folk diagrams. The clasts were poorly rounded with an average rounding of 3.2.

Pit 2, crest of the 7^{th} ridge (13.15m AMSL). This 300mm pit contained a poorly sorted mixed sand and gravel with clast supported pebbles and cobbles that fined to the top of the pit. The mean b axis of measured clasts in the pit was -5.57ϕ. The pebbles were not imbricated and were clustered around the Platy, Bladed, Elongate, Compact Platy, Compact Bladed and Compact Elongate regions of the Sneed and Folk diagrams. The clasts were poorly rounded with an average rounding of 3.4.

4.3.3.6 Cape Bird sediment data

The size of the sediments in the Cape Bird plots (Figures 4.33, 4.34 and 4.35) show a marked decrease in size to the north along the active beach but much larger sediments in the pits on Bird 2. The pits at Bird 2 contained a range of sediment sizes with most of the pits containing a sandy matrix in addition to the clasts. The ice-push feature had similar sized clasts to the pits on Bird 2. Clasts in the pits and on the active beach ranged in size from -7ϕ to 4.0ϕ. The active beach clasts were well sorted in contrast to that clasts in the pits which contained a range of sizes. There appeared to be some weak imbrication in Bird 2 pit 1 and pit 6 but the strongest imbrication is on the ice-push feature on the active beach to the south of Bird 1. Apart from these examples, there was no discernible imbrication at Cape Bird. The shape data shows some clustering about the middle of the Sneed and Folk diagrams Platy, Bladed, Elongate, Compact Platy, Compact Bladed and Compact Elongate indicating very average clast shapes. Cape Bird shows the most consistently rounded clasts of any site.

Bird survey 2

Six beach ridges were identified on this profile and eight sediment pits were examined. Pits 1, 3, 5 and 7 were located at the top of the 1st, 2nd, 3rd and 5th ridges respectively and pits 2, 4, 6 and 8 were located at the base of ridges 2, 3, 4 and 6 respectively.

Pit 1, top of the 1st ridge (5.04m AMSL). This 450mm pit contained a poorly sorted mixed sand and gravel with matrix supported pebbles and cobbles. The pit contained one unit. The mean b axis of measured clasts in unit 1 was -5.47ϕ. The pebbles were weakly imbricated in a 350^0 direction and were clustered around the Platy, Bladed, Elongate, Compact Platy, Compact Bladed and Compact Elongate regions of the Sneed and Folk diagrams. The clasts were well rounded with an average rounding of 4.3.

Pit 2 base of 2nd ridge (1.34m AMSL). This 500mm pit contained massive poorly sorted sand with a few pebbles present. The mean grain size of sediment in this pit was -1.47ϕ.

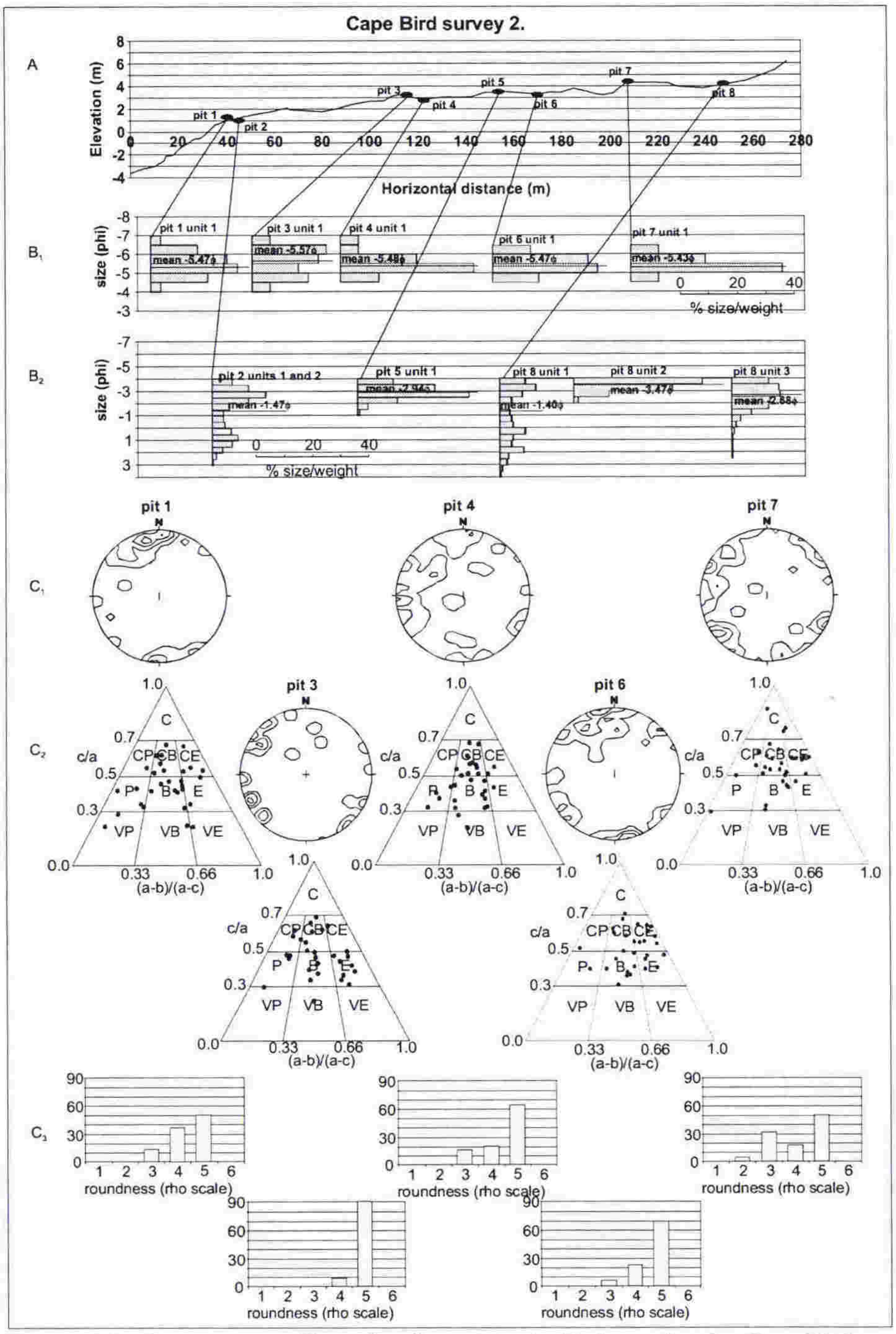

Figure 4.33. Summary profile and sedimentological information for Cape Bird survey 2. Part A displays the profile and the locations of the sediment pits. Part B provides sediment size histograms for gravel beds; B_1 displays summary information for gravel beds while B_2 presents the same information for finer units. For the gravel units stereonet projections of gravel A axis dips (C_1), Sneed and Folk (1953) (C_2) shape triangle and Powers (1953) roundness (C_3) information are presented.

Pit 3 top of the 2nd ridge (3.02m AMSL). This 600mm pit contained a clast supported mixed sand and gravel with pebbles and cobbles that fined towards the base of the pit. The pit contained only one unit (0-600mm). The mean b axis of measured clasts was -5.57ϕ. The pebbles had no imbrication and were clustered around the Platy, Bladed, Elongate, Compact Platy, Compact Bladed and Compact Elongate regions of the Sneed and Folk diagrams. The clasts were well rounded with an average rounding of 4.9.

Pit 4, base of 3rd ridge (2.45m AMSL). This 350mm pit contained a clast supported mixed sand and gravel with large pebbles and cobbles. The mean b axis of measured clasts was -5.48ϕ. The pebbles had no imbrication and were clustered around the Platy, Bladed, Elongate, Compact Platy, Compact Bladed and Compact Elongate regions of the Sneed and Folk diagrams. The clasts were well rounded with an average rounding of 4.4.

Pit 5, top of 3rd ridge (3.49m AMSL). This 450mm pit contained mixed sand and gravel with some large pebbles. The mean grainsize of clasts were -2.94ϕ.

Pit 6, base of 4th ridge (3.32m AMSL). This 550mm pit (see Figure 4.34) contained a clast supported mixed sand and gravel with large pebbles and cobbles. The mean b axis of measured clasts was -5.47ϕ. The pebbles had no imbrication and were clustered around the Platy, Bladed, Elongate, Compact Platy, Compact Bladed and Compact Elongate regions of the Sneed and Folk diagrams. The clasts were well rounded with an average rounding of 4.6.

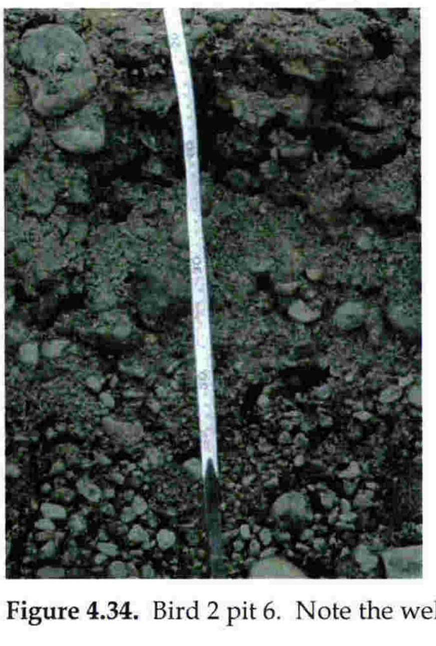

Figure 4.34. Bird 2 pit 6. Note the well rounded clasts and the absence of any sorting in the pit.

Pit 7, top of 5th ridge (4.10m AMSL). This 550mm pit contained a clast supported (some matrix support present) mixed sand and gravel with large pebbles and cobbles. The pit contained one unit (0-550mm). The mean b axis of measured clasts was -5.43ϕ. The pebbles had no imbrication and were clustered around the Platy, Bladed, Elongate, Compact Platy, Compact Bladed and Compact Elongate regions of the Sneed and Folk diagrams. The clasts were well rounded with an average rounding of 4.1. Some of the clasts in the pit were frost shattered.

Pit 8, base of 6th ridge (4.04m AMSL). This 400mm pit (see Figure 4.34) contained a poorly sorted mixed sand and gravel at the base coarsening to a small pebble into unit 2 and a mixed sand and gravel at the top of the pit. The pit was subdivided into three units at 0-100mm, 100-250mm and 250-400mm. Unit 3 (250-400mm) (marked on Figure 4.35 as C) contained a massive poorly sorted mixed sand and gravel. The mean grainsize of clasts in this unit were -2.68ϕ. Unit 2 (100-250mm) (marked on Figure 4.34 as B) contained moderately sorted clast supported small pebbles. The mean grainsize of the pebbles was -3.47ϕ. Unit 1 (0-100mm) (marked on Figure 4.34 as A) was a massive very poorly sorted mixed sand and gravel with a mean grainsize of -1.40ϕ.

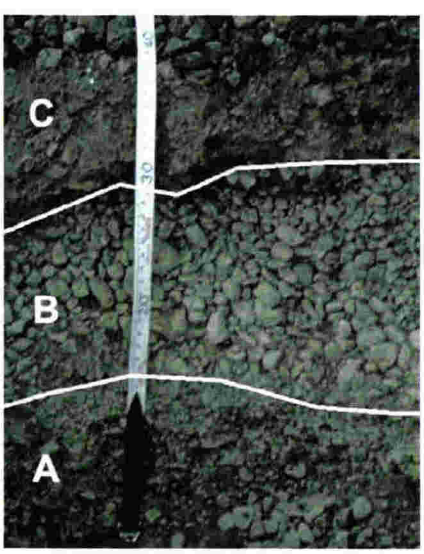

Figure 4.35. Bird 2 pit 8. Note rounding and sorting of sediment in unit 2 (marked B on photograph).

Bird modern beach sediments

Figure 4.36 shows composite samples collected at points along the shore between Bird surveys 2 and 3. All of the samples were moderately well-sorted except for

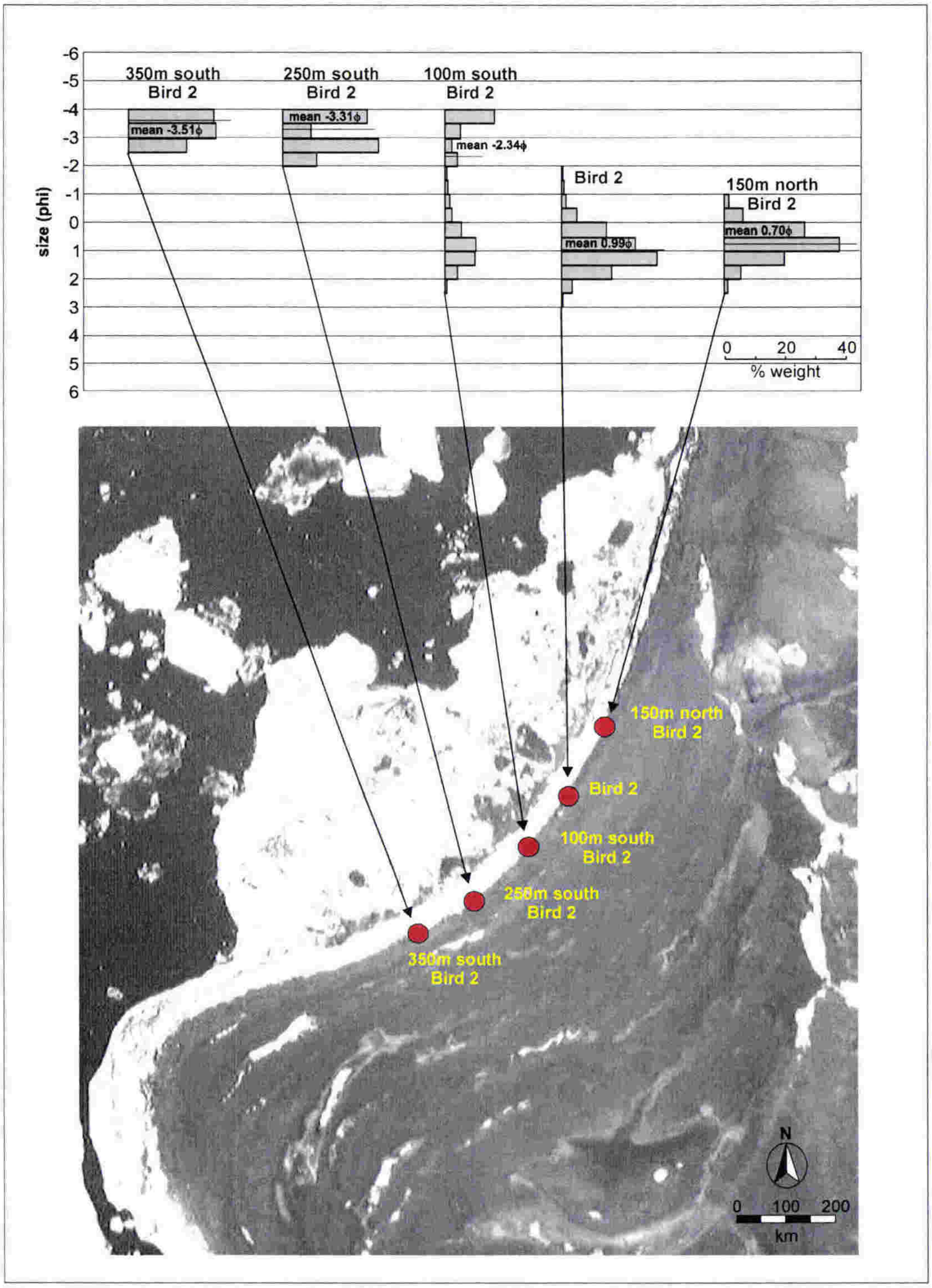

Figure 4.36. Size histograms of material measured on the modern beach between Cape Bird 2 and Cape Bird 3. Note strong fining to north.

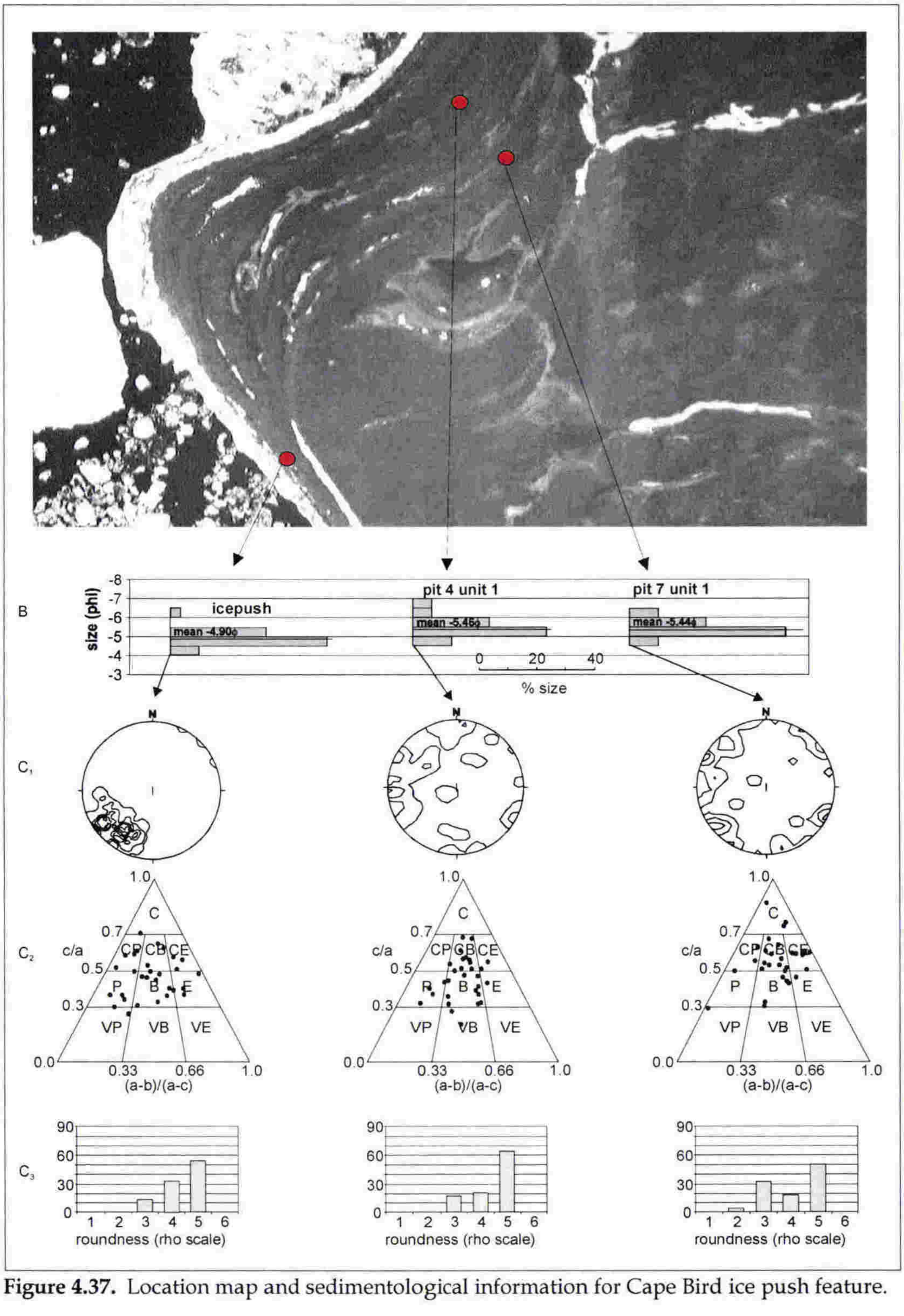

Figure 4.37. Location map and sedimentological information for Cape Bird ice push feature. Part B provides sediment size histograms for gravel beds. For all pebble counts stereonet projections of gravel A axis dips (C_1), Sneed and Folk (1953) (C_2) shape triangle and Powers (1953) roundness (C_3) information are presented.

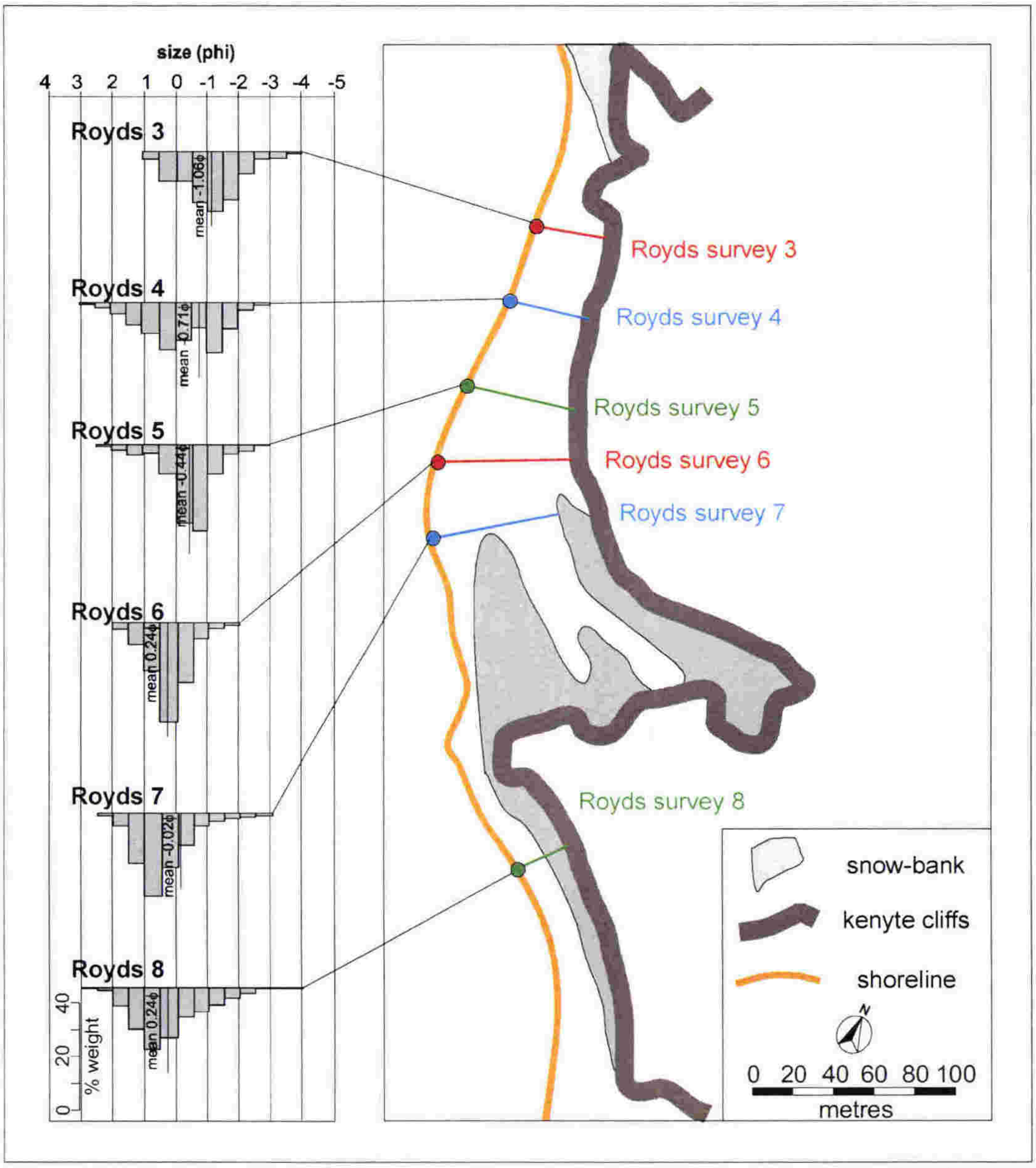

Figure 4.38. Size histograms of material measured on the modern beach at Cape Royds (air photograph unavailable for this area, sketch of Blacksand beach modified from Kirk, 1965).

100m south Bird 2 which was very poorly sorted. Mean grainsize for these samples shows sediment fining from the south (-3.51ϕ for 350m south Bird 2), to the north (0.70ϕ for 150m north Bird 2).

Bird ice push feature

Figure 4.37 shows clasts from Bird 2 pit 4 and pit 7 compared with clasts from an ice push feature. The size and roundness of the clasts on the ice push feature was comparable with the size of clasts from the two pits on Bird 2 but the imbrication on the icepush feature was strong in contrast with the lack of imbrication in the pits. The mean b axis of measured clasts was -4.90ϕ. The pebbles were very strongly imbricated in a shore normal (220^0) direction and were clustered around the Platy, Bladed, Elongate, Compact Platy, Compact Bladed and Compact Elongate regions of the Folk and Ward diagrams. The clasts were well rounded with an average rounding of 4.3.

4.3.3.7 Cape Royds sediement data

Composite samples were collected from the active beach at six of the survey points at Cape Royds. Figure 4.38 shows grainsize for samples collected at Cape Royds. The sediment ranged in size from 0.24ϕ to -1.06ϕ and fined from coarse at the northern end (-1.06ϕ) to finer at the southern end (0.24ϕ).

4.4 Luminescence ages of sites in McMurdo Sound

Five luminescence samples were dated using optically stimulated luminescence (OSL) at the Victoria University of Wellington luminescence laboratory. Table 4.7 gives information on the sample name, the source of the sample the estimated age and the elevation the sample was collected from for the five dated samples.

Sample Name	Source	Age (000's years B.P.)	Elevation (m AMSL)
Bernacchi 1	Bernacchi survey 3 pit 3 (top of 3rd beach ridge). Collected from unit 2 400mm from the surface.	2.9±0.2	2.00
Bernacchi 2	Bernacchi survey 3 pit 5 (base of 6th beach ridge). Collected 30cm from the surface.	6.0±0.4	5.91
Marble	Marble survey 2 pit 5 (top of 6th beach ridge). Collected from unit 2 160mm from the surface.	5.3±0.8	10.50
Kolich	Kolich survey 3 section 3 (top of Kolich 3 survey). Collected from unit 2 350mm from the surface.	3.9±0.3	9.40
Spike	Spike survey 2 pit 2 (top of 5th beach ridge). Collected from unit 2 250mm from surface.	7.2±0.7	15.03

Table 4.7. OSL sample information.

Figure 4.39 displays a typical shine-down curve. This example comes from the Cape Bernacchi sample 1 disks. These show the diminishing number of photons over time for a natural disk and natural disks with 10, 20, 40 and 80 Grays of β radiation.

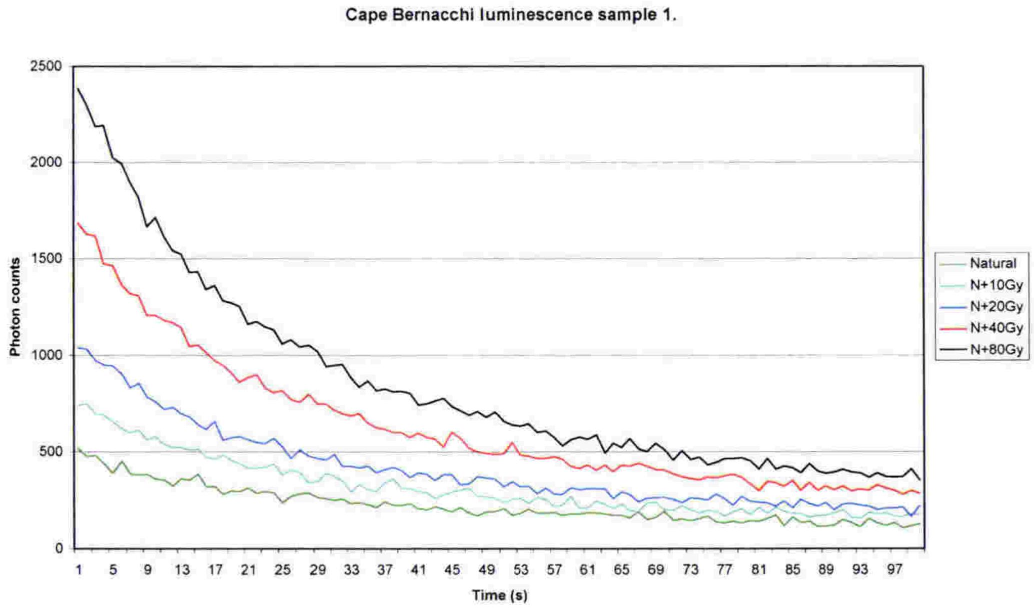

Figure 4.39. Cape Bernacchi shine-down curves for natural, natural + 10, 20, 40 and 80 grays of β radiation.

Figure 4.40 shows the additive dose and thermal correction data for Spike 1. This method was used by Dr Lian (Victoria University of Wellington, luminescence laboratory) to determine the equivalent dose for all of the samples. The blue curve shows the additive dose (the sample's natural radiation plus a laboratory dose). The red line shows the correction for thermal transfer (the samples are heated following irradiation which can cause an increase in the estimated age of the sample). The intersection point is the equivalent dose. Ages were then calculated by using the K, U, and Th concentrations (established by laboratory analyses shown in Table 4.8), the water contents of the collected samples (shown in Table 4.9), and the estimated cosmic ray effect to determine the dose/year in grays. The equivalent doses (Deq), b values, dose rates, and apparent optical ages are shown in Table 4.10.

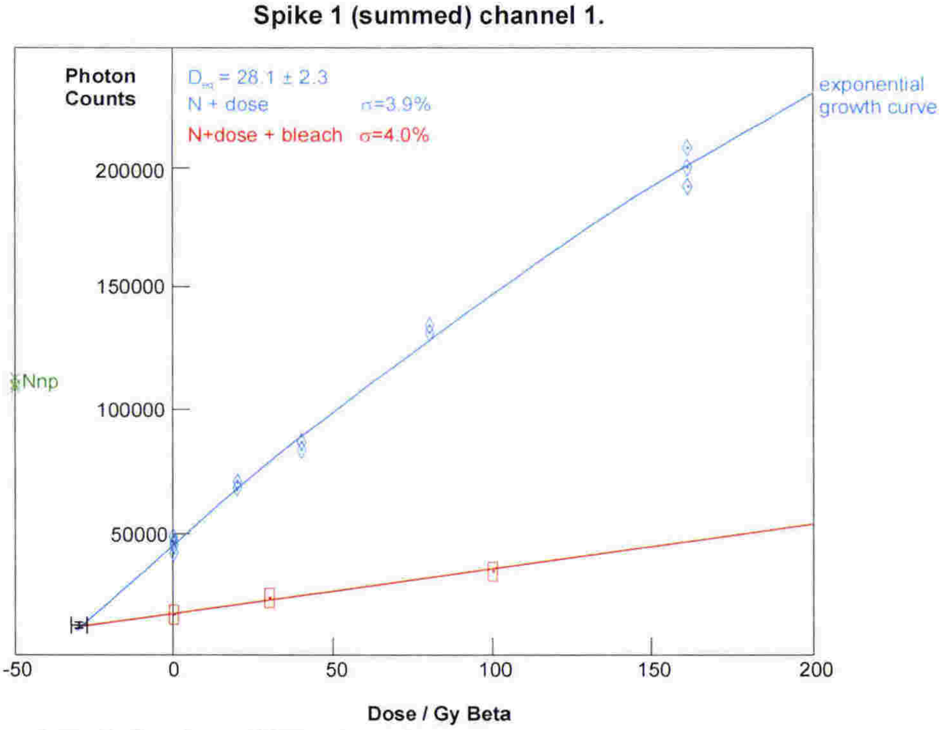

Figure 4.40. Spike Cape additive dose data.

Sample	K (%)*	Th (μg·g⁻¹)†	U (μg·g⁻¹)‡
Marb1	1.70 ± 0.08	7.6 ± 0.2	1.85 ± 0.08
Marb2	1.60 ± 0.08	5.80 ± 0.02	1.79 ± 0.08
Barne1	2.1 ± 0.1	11 ± 1	3.06 ± 0.09
Barne2	1.60 ± 0.08	11 ± 1	3.10 ± 0.09
Bern1	1.60 ± 0.08	7.0 ± 0.2	1.55 ± 0.07
Bern2	1.50 ± 0.07	5.90 ± 0.02	1.62 ± 0.07
Kolich1	1.10 ± 0.05	4.8 ± 0.2	0.64 ± 0.06
Spike1	3.2 ± 0.2	6.7 ± 0.2	1.12 ± 0.06

Table 4.8. K, U, and Th concentrations determined from laboratory analyses.

* From ICP-AES.

† From neutron activation analysis.

‡ From delayed neutron analysis.

	Water content †		
Sample	Δ^w_{ac}	Δ^w_{sat}	Δ^w
Marb1	0.030	0.288	0.16 ± 0.07
Bern1	0.345	0.593	0.47 ± 0.06
Bern2	0.056	0.271	0.16 ± 0.04
Kolich1	0.058	0.240	0.15 ± 0.04
Spike1	0.005	0.178	0.091 ± 0.043

Table 4.9. Water contents of samples.

† Δ^w_{ac} and Δ^w_{sat}, are the *as collected* and *saturated* water contents, respectively; Δ^w is the water content used for the dose rate calculation. Water contents are (water mass)/(mineral mass).

Note: The Δ^w chosen was that determined from the average of Δ^w_{ac} and Δ^w_{sat}, with an uncertainty to cover both extremes at two standard deviations.

	D_{eq} (Gy)				
Sample	**additive - dose**	**b value (Gy·μm²)***	$\dot{D}_c$ **(Gy·ka⁻¹)†**	$\dot{D}_T$ **(Gy·ka⁻¹) ‡**	**Optical age (ka)****
Marb1	16.6 ± 1.5	1.07 ± 0.05	0.20	3.15 ± 0.42	5.3 ± 0.8
Bern1	13.2 ± 0.7	1.0 ± 0.1	0.21	2.21 ± 0.12	6.0 ± 0.4
Bern2	7.68 ± 0.32	1.0 ± 0.1	0.20	2.68 ± 0.14	2.9 ± 0.2
Kolich	7.32 ± 0.33	1.0 ± 0.1	0.21	1.90 ± 0.10	3.9 ± 0.3
Spike1	31.2 ± 2.5	1.0 ± 0.1	0.22	4.36 ± 0.27	7.2 ± 0.7

Table 4.10. Equivalent doses (Deq), b values, dose rates, and apparent optical ages.

**b* value as defined by Huntley *et al.* (1988). Those for samples Bern1, 2, Kolich1, and Spike1 are estimates.

† $\dot{D}_c$: dose rate due to cosmic rays (Prescott and Hutton, 1994).

‡ $\dot{D}_T$: total dose rate (that due to cosmic rays plus that due to γ, β, and α radiation).

** In each case the D_{eq} from the additive-dose method was used for the age calculation.

Note: analytical uncertainties are all 1σ.

Figure 4.41 shows the locations of the samples and a chart with the ages and their locations plotted. The ages increase with increasing beach elevation and are all Holocene in stratigraphic order except for Bernacchi 2.

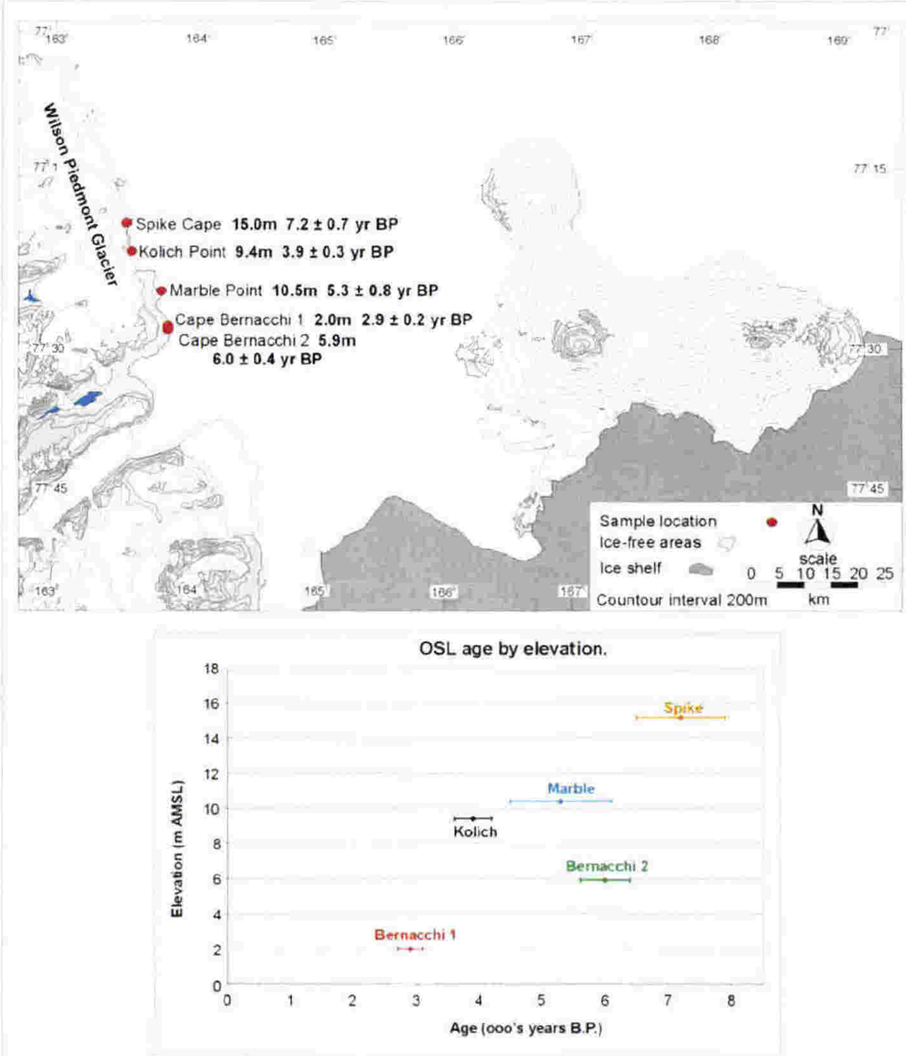

Figure 4.41. Location map of OSL samples and chart of OSL ages with errors and their relative elevations AMSL.

Chapter 5

Beach development and coastal evolution in McMurdo Sound

5.1 Introduction

This chapter describes the formation and the related processes of the beaches in McMurdo Sound. It also outlines the history of the Ross Ice shelf in McMurdo Sound since the Last Glacial Maximum.

5.2 Modern process regimes in McMurdo Sound

5.2.1 Influence of ice on the modern beaches

As noted in Chapter 1 the presence of sea ice in McMurdo Sound differs considerably from the western to the eastern side of the Sound. The western side of the Sound (from Dunlop Island south to the McMurdo Ice Shelf) is free of sea ice only 1.6% of the time compared with the eastern side (from Cape Bird to Cape Royds), which is sea ice free 51.1% of the time. It is not surprising that this sea ice pattern is reflected in the characteristics of the beaches along these coasts.

Forbes and Taylor (1994) presented a list of polar coastal products and their associated processes (see Table 2.1). The process information on Forbes and Taylor's (1994) list is absent from Nichols' (1961) 13 characteristics of polar beaches. However as Nichols based these 13 characteristics on the beaches in McMurdo Sound his work was used in preference to Forbes and Taylor's. If we examine some of Nichols (1961) characteristic features of polar beaches there are systematic variations in which features are recorded on either side of McMurdo Sound. Nichols, who worked on the western side of the Sound, concentrated on cryogenically formed features. These can be divided into those related to active marine processes and those that are primarily non marine in origin. Not all of Nichols features were used in this analysis because some of the characteristics are not specifically diagnostic to marine or cryogenic processes. For example, one of Nichols (1961) characteristic features is; *they contain cold water fossils*. These could be incorporated into a beach by ice push as well as marine processes.

Feature	Origin	Occurrence
1. They rest on ice	sea ice pushed under beach sediments deposition onto frozen bed by marine processes	eastern McMurdo Sound
2. They are pitted	melt out in beach from stranded sea ice or ice rafted fragments	western and eastern McMurdo Sound
3. There are ice push mounds on them	sea ice pushed up the beach	western and eastern McMurdo Sound
4. Ice rafted fragments are found on them	wave action	eastern McMurdo Sound
5. They have poorly rounded beach stones	lack of marine action and frost action	western McMurdo Sound
6. Frost cracks are found on them	periglacial processes	western and eastern McMurdo Sound
7. There are erosional gaps on them	fluvio-glacial	western and eastern McMurdo Sound

Table 5.1. Origin and occurrence of seven out of thirteen of Nichols (1961) characteristic features of polar beaches on the beaches in McMurdo Sound.

5.2.1.1 Melt pits

Table 5.1 demonstrates that although both sides of the Sound contain examples of ice-type and marine-type features more extensive areas of ice push features and melt pits are produced along the western side of the Sound. For example, at Marble Point and Spike Cape there were extensive areas of pitted beaches. These are shown in Figure 5.1. Cape Royds also had areas of pitted beaches but these were small in comparison with those found on the western side of the Sound. Air photos of Marble Point (photograph A in Figure 5.1) show relict beaches that have numerous pits but was the only site where pits are preserved on relict beaches.

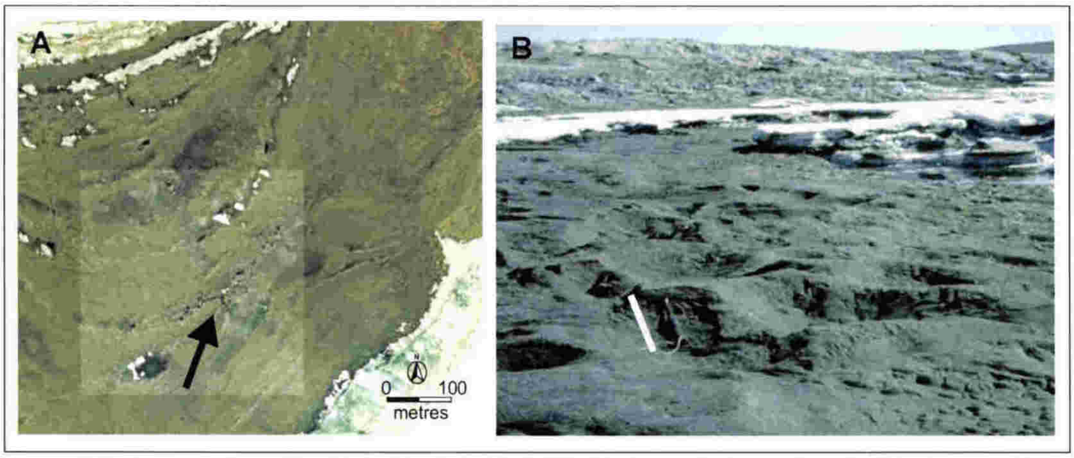

Figure 5.1. Areas of ice pits at Marble Point (highlighted on photograph A by black arrow) and at Spike Cape (photograph B) (white bar next to hammer on photograph B is 33cm).

Pitted beaches can be formed either by sea ice pushed onto the beach by ice push action or by ice blocks being thrown onto the beach during high wave energy events in open water settings. Preservation of the pits is much less likely with ice blocks being thrown onto the beach as there is a strong probability of reworking of the open coast beaches by subsequent storms. The sites where the melt pits are located at Marble Point and Spike Cape contain dominantly sandy sediments and the site at Spike Cape is also a cusp between mainland Spike Cape and the seaward end of the point. This location at Spike Cape provides a natural area for sea ice to accumulate on the low energy sandy flats and create melt pits. At higher relative sea level similar conditions would have prevailed at Marble Point. At Marble Point the sheltered nature of this area has allowed these pits to remain undisturbed.

5.2.1.2 Ice push features

Ice push features were found on every site examined except Cape Royds but were once again concentrated on the western side of the Sound, with large areas present at both Spike Cape and Kolich Point (on the modern beaches). At Cape Bird, ice push ridges were present early in the season (see Figure 5.2) but these were reworked later in the season after the ice had broken up.

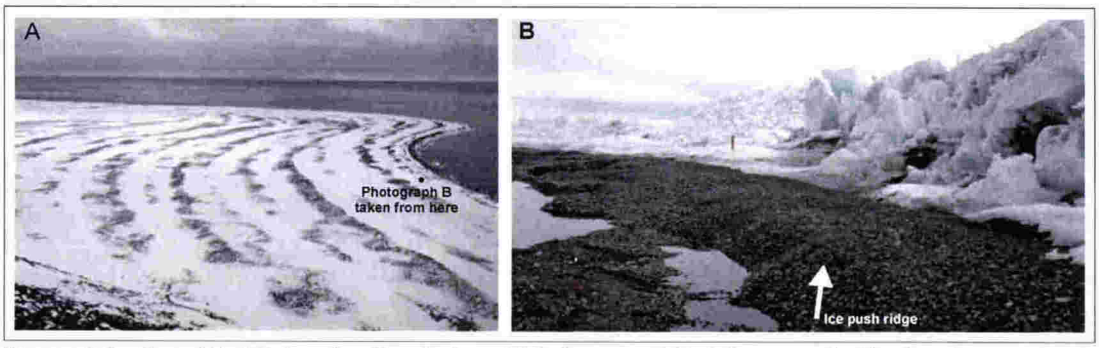

Figure 5.2. Cape Bird Priapulus Beach; in mid-February 1998 (photograph A) after the sea ice had broken up; and in early January 1999 (photograph B) when the sea ice was still piled against the shore (stake with red flag on top in photograph B is 1.3m high). Both photographs look south with photograph B taken from the point indicated on photograph A.

Although Cape Bird is ice free more often than any other site in the Sound it had a number of features that showed the presence of ice on the beaches. Returning to Nichols (1961) 13 characteristic features of polar coastlines at the beginning of the chapter, we can identify at least three of the features occurring at Cape Bird early in the season. These are they rest on ice, have ice push mounds and ice rafted fragments on the beaches.

5.2.1.3 Ice piles

The yearly progression of large ice piles on Priapulus Beach and their absence later in the season is shown in Figure 5.2.. This shows ice piles at Cape Bird rising to about 3m above the top of the modern beach. These ice piles are similar to those reported by Reimnitz et al. (1990) on the Beaufort Sea coastline. The ice piles in Figure 5.2 were documented early in January 1999 when the sea ice was just beginning to break out. No ice piles were present at this location during a visit at the end of February 1998 when there was open water from the northern to the southern rookeries at Cape Bird. In addition to the absence of ice piles later in the season, the modern beach had no ice push features or melt pits as marine processes had reworked these. In contrast, a 150m long ice cored ridge shoreward of the icefoot was measured in January 1999 (see Figure 5.2).

The presence of ice piles and ice cored ridges early in the season at Cape Bird and absent later in the season highlights the importance of marine processes on the beaches. After the sea ice breaks out and the ice foot is destroyed, marine processes rapidly re-order the beach, sorting the material and reshaping the ice cored and ice push ridges into marine-type features. The absence of ice-push features on the older higher beaches suggests that such a process has been occurring for at least as long as the beaches have been forming in this area.

The prominence of marine processes on the eastern side of the Sound explains the relative lack of ice push features here. On the western side of the sound the infrequency of open water conditions makes it unlikely that marine action will significantly alter these features from one season to the next. These findings are consistent with the observations of Nichols (1961; 1966; 1968), who suggested that ice processes were dominant on the western shores of McMurdo Sound, and those of Kirk (1966; 1972), who showed that marine processes dominated the beaches in the Cape Royds area in the summer months. The key factor is not the absence of ice effects from the eastern side of the Sound but the low preservation potential of ice derived features if there is even a short period of open water conditions during the year.

5.2.1.4 The icefoot

The level of marine action at any site in the sound will depend almost entirely on the presence or absence of the icefoot. At Cape Bird the icefoot along Priapulus Beach breaks up earlier than at any other site in the Sound. This allows marine processes to act on the beaches earlier than any other site and explains the well rounded and well sorted clasts here (see Figure 5.5A).

Figure 5.3 shows the icefoot north of Priapulus Beach. The icefoot at Priapulus Beach had broken up before 5 January 1998 and on 12 January 1998, the icefoot to the north and south of the beach was still breaking up. On the western side of the Sound the icefoot at Dunlop Island was still in place at the end of January 1997. If the icefoot persists at a location towards the end of February it is likely that it will not break up during that season at all. This is because the Sound begins to freeze over towards the end of February following the summer thaw.

Figure 5.3. Icefoot at Cape Bird. The spade in the foreground is 1.5m high. Note the incorporation of gravel in the icefoot. This type of icefoot is probably a storm icefoot following Wright and Priestly's (1922) descriptions.

5.2.2 Differences between northern and southern facing profiles on the western side of McMurdo Sound

Differences between north and south-facing profiles on the western side of the Sound are evident in both rounding and beach steepness. Beach slope is controlled by a number of factors, including sediment supply, wave energy (Komar, 1998; Bascom, 1951; Weigel, 1964), substrate gradient (Roy et al., 1994) and sediment size (Komar, 1998; Shephard, 1963), and less importantly, wave steepness (Rector, 1954; Harrison, 1969), and sediment sorting (Krumbein and Graybill, 1965; McClean and Kirk, 1969). In general, steeper gravel/cobble beaches are the result of; greater wave energy, larger beach material, shallower waves, better-sorted beach material and/or a decrease in sediment supply. In the case of comparisons of overall profile steepness between sites (for example Cape Bernacchi and Dunlop Island), sediment supply is the first order control in beach steepness (without a supply of sediment the beach can not form).

However, when comparing profiles at the same sites (for example Marble 1 and Marble 2) it is unlikely that sediment supply would be the dominant control. It appears that the dominant control between profiles at the same locations is the angle of wave approach which controls the wave energy.

The differences between the northern and southern profiles most likely reflect changes in energy conditions. The dominant wave direction in McMurdo Sound is from the south, which follows the dominant wind direction. However, the presence of waves on the southern-facing beaches on the western side of the Sound is dependent on the absence of sea ice. Both the rarity of the western shores of the sound being ice-free and the dominant wind blowing ice into south-facing bays conspires to make this situation uncommon. In the unlikely event that the shores are ice free, the fetch is severely limited so wave heights and therefore wave energy will be curbed compared with the fetch unlimited north eastern waves. The northern-facing beaches will be cleared of ice naturally by the dominant southerly wind, adding to the likelihood of these beaches being acted on by marine processes. These energy differences are expressed clearly in the profiles at several locations.

For example, Dunlop 2 on the south of Dunlop Island has an average beach slope over the profile of about 2^0 whereas Dunlop 1 (on the northern side) has a slope of about 4.5^0. Similarly, the northern profiles at Marble Point (Marble 1 and Marble 2, about 4^0) are steeper than the southern profile (Marble 3, 3^0). The southern profiles tend to have more ridges preserved than the northern profiles, probably due to the limited fetch to the south resulting in lower storm energies at the beach compared with the northern facing profiles that receive waves from the northeast. This situation is further enhanced by ice being pushed into the southern embayments, as it obstructs beach reworking under storm conditions. Even large magnitude storm events will produce small beach ridges close to sea level. As the land rebounds these smaller ridges will be elevated beyond the range of normal marine processes and will be preserved. On the northern profiles, low frequency large magnitude storm events can reorganise several smaller beaches into one large storm ridge, which will be elevated beyond the range of normal marine processes.

In addition to recognising a difference in energy conditions between north and south facing beaches on the western side of the Sound, differences in energy conditions can also be identified at separate sites between profiles. Cape Bernacchi surveys Bernacchi 1 and Bernacchi 2 have average slopes of 7^0 in contrast to Bernacchi 3 and Bernacchi 4, which have average slopes of 4.7^0 and 3.5^0 respectively. This difference is reflected in the sediment size also, as the two north eastern facing profiles (Bernacchi 1 and 2) comprise coarse poorly sorted cobbles and pebbles in a sand and gravel matrix in contrast to the two south eastern facing profiles, which comprise coarse sandy beaches.

The differences in energy can best be seen by the beach heights at Kolich Point. Figure 4.6 shows the surveys at Kolich Point. Three large ridges visible on the air photo at Kolich Point can be traced around the coast between Kolich 1 to Kolich 3. These ridges are indicated on the survey (Figure 4.6) with red and blue and green arrows. The elevations of the ridges for Kolich 1 and Kolich 2 surveys are shown in Table 5.2. The ridges on the higher energy north eastern facing Kolich 1 survey are considerably higher than those on the lower energy south south eastern facing profile.

Survey	Ridge 1 (elevation in m AMSL)	Diff. 1 to 2	Ridge 2 (elevation in m AMSL)	Diff. 2 to 3	Ridge 3 (elevation in m AMSL)
Kolich 1	7.6	3.9	11.5	7	18.5
Difference	0.7		2.4		3.7
Kolich 2	6.9	2.2	9.1	5.7	14.8

Table 5.2. Elevation of beach ridges at Kolich Point in m AMSL. Differences between the ridges and the surveys are also shown.

Table 5.2 shows a systematic increase in both the height and the height differences between the individual ridges on Kolich survey 1 and 2. The difference in height between the ridges on Kolich survey 1 and 2 is due to a decrease in wave energy at these different sites. (The fetch limited southerly waves are clearly too small to produce the large ridges at Kolich Point so waves from the north east must have created them). As the waves refract into the bay from Kolich Point (see Figure 5.4) they would lose energy and the height of the ridges would decrease proportionately. The differences of elevation between the ridges, is discussed later in section 5.3.2.

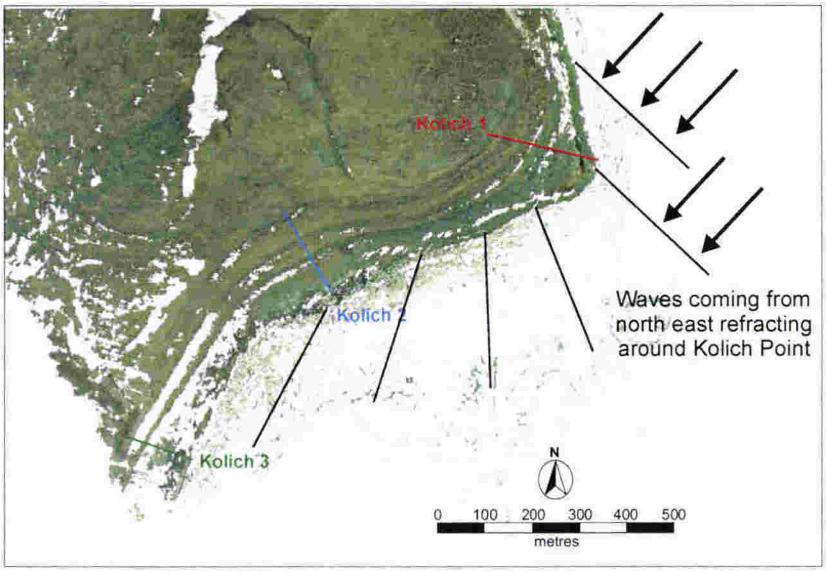

Figure 5.4. Waves refracting around Kolich Point.

5.2.3 Rounding of beach clasts

Of the features identified by Nichols (1961), perhaps the most useful indicator of the duration and efficiency of marine action on the beaches is the roundness of the clasts. Rounding is a function of the level of abrasion a clast has undergone (Lewis and McConchie, 1994). In pure sea ice systems, clasts are likely to be angular as the physical action of ice shatters clasts and subsequent transport is of short duration and associated with non fluid flows. In contrast, because waves provide consistently high energy conditions in a fluid environment that promotes clast to clast friction, beaches are considered to be the most effective subaqueous setting for physical rounding of clasts (Lewis and McConchie, 1994).

On both the western and eastern sides of the Sound clasts on the beaches are most likely sourced from the local glaciers. In all cases the clasts would have travelled no more than a couple of kilometres in meltwater streams before being deposited in the coastal zone. The short distances of fluvial transport are important because fluvial systems will round clasts much faster than cold based glaciers.

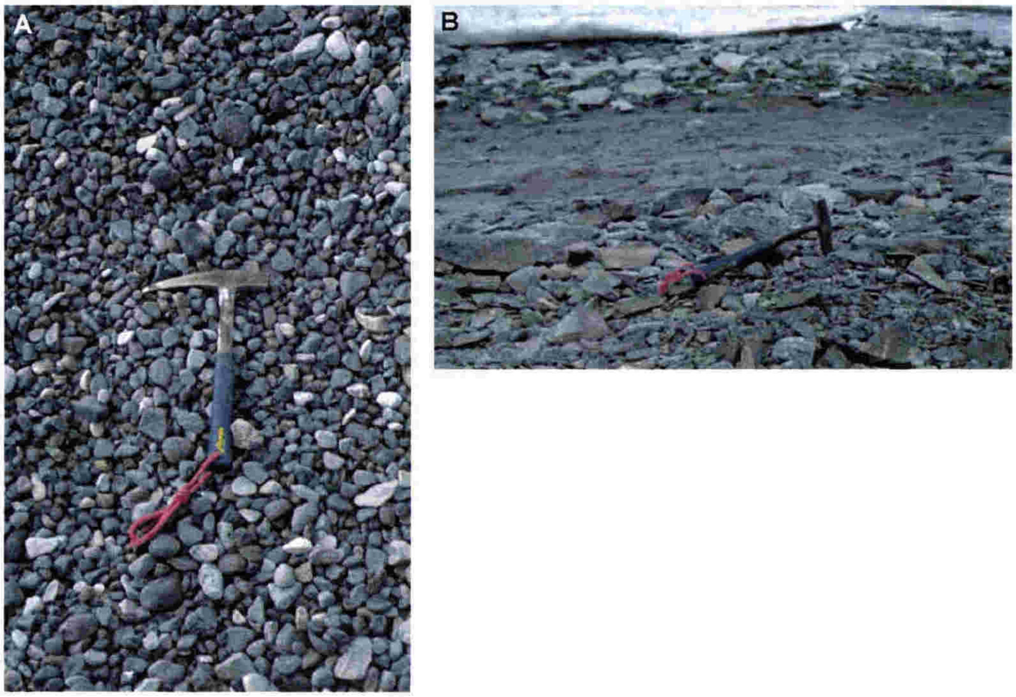

Figure 5.5. Relative roundness of clasts on the active beach at Cape Bird (photograph A) and Spike Cape (photograph B). The rock hammer in the photographs is 33cm long. Note the obvious lack of sorting at Spike Cape and the well sorted clasts at Cape Bird.

Studies by van Andel et al. (1954) and Sneed and Folk (1958) demonstrated that as clasts travel further from the source area and undergo greater levels of abrasion, the more rounded they become. Dobkins and Folk (1970) measured pebble roundness on nine rivers and fourteen high energy and low energy coasts on Tahiti-Nui. They showed that the greatest levels of abrasion and the most rounded pebbles were found on the high energy coasts. King and Buckley (1968) showed that roundness could be used to differentiate sedimentary environments on Baffin Island. They measured clasts from ice contact deposits, eskers, kames, moraines, solifluction deposits and beaches. Their results showed that the beach clasts had the greatest level of rounding.

The roundness of clasts at Cape Bird (a site with well rounded clasts) and Spike Cape (a site that had some very poorly rounded clasts) is graphically illustrated in Figure 5.4 and supports these well established studies.

Large variations in mean beach clast roundness were observed from site to site (see Figure 5.5). Tables 5.3 and 5.4 demonstrate that there were both significant roundness differences based on beach aspect (Table 5.3) and between individual sites (Table 5.4). What these demonstrate is; 1. the strongest rounding occurs on coasts with open water, and 2. on the ice bound western side of the Sound, coasts that face east (into the prevailing wave direction) have sediments that are more rounded than north/south facing beaches. This latter observation can be made from both tables 5.3 and 5.4.

Mean roundness	**Aspect**	**North**	**South**	**East**	**West**	**Comments**
3.10	**North**					mainly on western side of Sound and sheltered from waves
3.30	**South**					
3.58	**East**	Sig. dif.	Sig. dif.			wave direction for western side of Sound
4.23	**West**	Sig. dif.	Sig. dif.	Sig. dif.		open water on eastern side of Sound

Table 5.3. Tukey's Honestly Significant Difference test of significance of rounding by aspect. Northern facing beaches have similarly rounded clasts to the southern beaches but significantly less rounded clasts compared with eastern and western facing beaches. Western facing beaches have significantly more rounded clasts on them compared with the other aspects.

Mean roun-dness	Site	Marb	Bern	Dun	Spk	Kol	Bird	Overall aspect	Beach faces
3.08	**Marble**							West	N/S
3.57	**Bernacchi**	Sig. dif.						West	NE/SE
3.57	**Dunlop**	Sig. dif.						West	N/S/ W
3.83	**Spike**	Sig. dif.	Sig. dif.	Sig. dif.				West	E mainly
3.89	**Kolich**	Sig. dif.	Sig. dif.	Sig. dif.				West	S/E
4.48	**Bird**	Sig. dif.	Sig. dif.	Sig. dif.	Sig. dif.	Sig. dif.		East	(open water)

Table 5.4. Tukey's Honestly Significant Difference test of significance of rounding by site. Marble Point has the least well rounded clasts of all the sites sampled and it is significantly different to all of the other sites. Cape Bernacchi and Dunlop Island have sediments with similar clast roundness but are significantly different to Spike Cape, Kolich Point and Cape Bird. Kolich Point and Spike Cape have similar clast roundness and Cape Bird has the most well rounded clasts of all sites. The last two columns provide the overall beach aspect and the direction the beaches at that location face. Note that for eastern facing beaches on the western side of the Sound (Kolich Point and Spike Cape) the mean rounding is significantly higher than for other sites on the western side of the Sound.

The result of anova tests shows that aspect is highly significant in determining clast roundness though it explains only about 13% (r^2=0.132) of the observed roundness variability. In order to test whether this relatively low r^2 indicates that over 80% of roundness can be explained by a systematic factor other than aspect, the test was re-run on the sample means of all of the transects. This reduced the data set from > 1600 individual clasts to 14 sites and removes intra-site variability (noise) as a factor. The result of the re-run anova was an r^2 of 0.432, which suggests that aspect is the primary inter-transect control (via wave energy received) on clast roundness. It is unsurprising with the low sample numbers in the second run that this r^2 is not significant at a 95% confidence level.

One confounding factor in the roundness analysis is rock type, as there is a systematic difference across the Sound with granites/granodiorites on the western side and basalt on the eastern side. This rock type effect does not affect the internal comparisons of transects on the western side of the Sound and is inferred to be insignificant for east/west contrasts. This is because the microcrystalline basalts should be harder to abrade that the granites. This should cause higher roundness values on the western side of the Sound. The opposite is observed.

Consequently, simple measures of roundness are powerful tools for distinguishing the relative importance of marine action on high latitude coasts and could be used diagnostically. The key point, however, is the relative changes in roundness between similar sites. The absolute numbers contain confounding information.

5.2.4 Imbrication

The strength of imbrication is a good indicator of unimodal transport regimes and can often be a reliable measure of wave action in the formation of the beaches. Waves will imbricate clasts as they will naturally present the smallest surface area to the direction of force. Bluck (1967) and Postma and Nemec (1990) described gravelly beach structures and showed that seaward imbrication of disc shaped clasts on the upper shoreface was a classic feature of gravel beaches.

However, waves are not the only mechanism of producing imbrication. Flow in rivers and glacier ice also imbricate clasts and observations in this study show that clasts can imbricate as they fall down the avalanche face of an ice push ridge during its formation. This can be seen in the imbrication plots for modern ice-push features around the Sound at Cape Bernacchi and Cape Bird where the features can be identified as ice push on other criteria (see Figures 4.15 and 4.38). Clearly these ridges would be much more difficult to identify in ancient settings and roundness data should be used in association with imbrication, as a matter of course.

In an Antarctic environment any imbrication may be confounded by frost heave. Washburn (1973) showed that frost heave can sort, reorient and imbricate clasts. However, the preferred orientation of these clasts is vertical so they can easily be distinguished from other imbricated deposits. Figure 5.6 shows a frost wedge at Kolich Point, which displays the sorting, and orientation of clasts under these processes. Tricart (1970) and Washburn (1973) note that frost wedges are stable features that grow very slowly in size so it is unlikely that these processes would be found on an active beach. They also demonstrate that ice wedges require finer material to form. The finer material fills the crack left by freezing water within the sand. This process repeats and the crack widens. The clasts on the gravel barriers at Spike Cape and Kolich Point lack the fine sediments and frost wedges would not be expected to form at these locations.

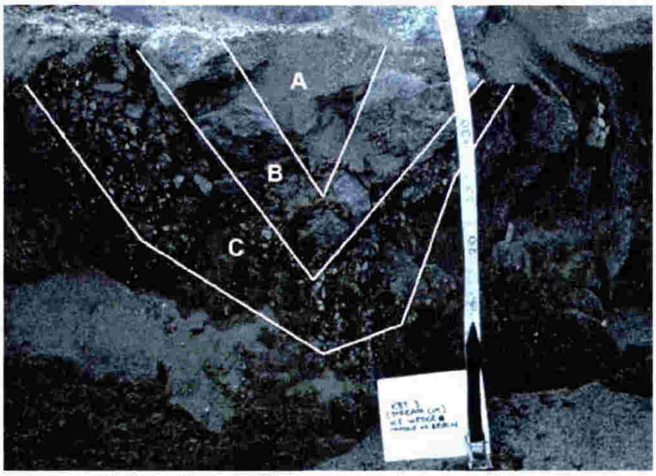

Figure 5.6. Ice wedge at Kolich Point. The area at the top of the photograph (marked A) is the fine sand material that falls into the gap as the ice expands and contracts creating the ice wedge. The area below this, (marked B on the photograph), shows cobbles that have migrated as more cycles of freezing and thawing have taken place. Area C is the pebble and gravel band that has migrated with frost heave.

5.2.5 'Marine' barrier beach at Spike Cape

Although the relative prevalence of marine processes on the eastern side of the Sound is true as a general statement, marine processes can play a significant role on beaches on the western side of the Sound as well. Clasts along a gravel barrier at Spike Cape (Figure 5.7) show very strong imbrication and comprise well sorted and well rounded sediments that fine toward the centre of the bay. The barrier at Spike Cape is oriented to the south west and is protected from the short period southerly waves but open to the longer period north easterly waves. The aspect of the barrier also allows the dominant southerly wind to blow the sea ice abutting the barrier offshore so incoming northerly waves can act on it. As the waves travel around the north of Spike Cape and are refracted into the bay, their energy will decrease (see Figure 5.7). Field observations noted that waves appeared to be higher along the barrier than in the bay, probably due to the steep offshore slope close to the barrier and the shallow slope in the middle of the bay reducing wave energy on the western shore. Bascom (1951) showed clear changes in wave energy, clast size and the resultant beach steepness at Halfmoon Bay, California. He showed that as wave energy increased in the less sheltered part of the bay the size of the beach material and the steepness of the beaches also increased.

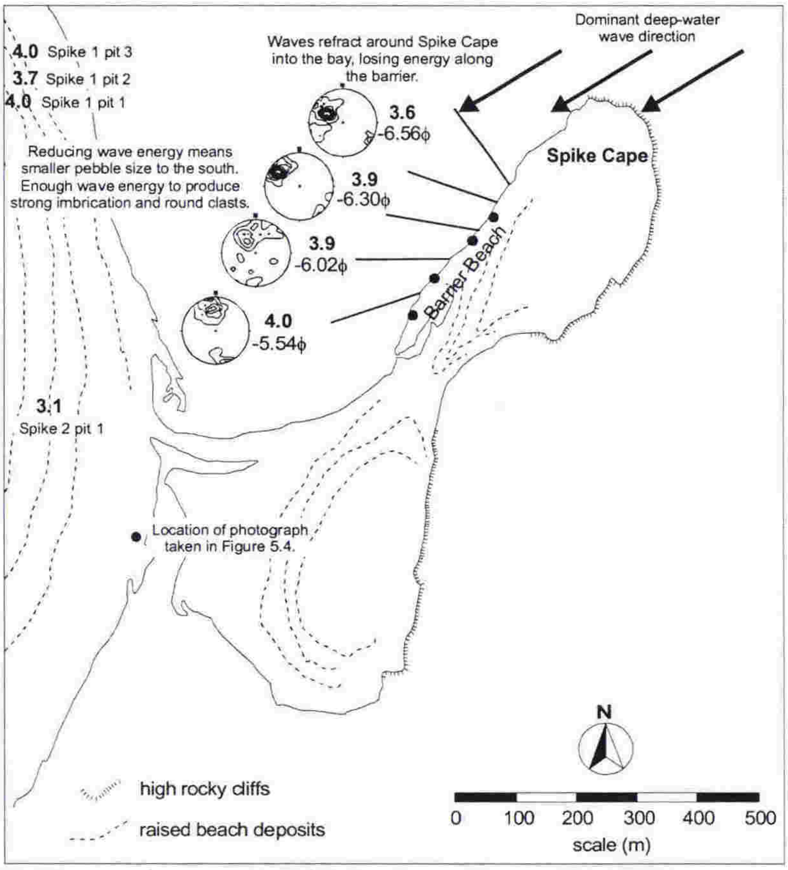

Figure 5.7. Waves refracting around Spike Cape. The stereo net plots, mean roundness (numbers in bold type next to the stereo net plots) and mean pebble size are data collected from points indicated by black dots on the barrier. The prevalence of marine processes is clear from the strong imbrication and well rounded clasts. The reduction in pebble size to the south indicates a decrease in wave energy along the barrier. Mean roundness values for all other sites at Spike Cape are also displayed. The location of the photograph in Figure 5.5B is indicated by the black dot on mainland Spike Cape.

The mean roundness values shown on Figure 5.7 show classic downdrift rounding. Folk and Ward (1957) showed that in a fluvial environment, the further clasts travel from the source area the more rounded they become. The clasts for the barrier were most likely sourced from the cliffs at the north end of Spike Cape. As the distance from the source area increases the clasts become more rounded. On mainland Spike Cape the clasts are more consistently rounded than those on the barrier which shows the effects of being more exposed to the north easterly waves than on the barrier. At Spike 2 pit 2 the clasts are the most poorly rounded of any site measured at Spike Cape which suggests that this location was more sheltered from the north easterly waves than the Spike survey 1. In addition, Figure 5.5 shows the angular clasts on the sheltered southern extent of the tombolo (indicated on Figure 5.7). This location probably does not receive any marine action at all.

In addition to the roundness and imbrication, other evidence suggests a prevalence of marine processes at the Spike Cape barrier. The barrier is 3.9m AMSL and has a mean pebble size of -6.56ϕ at the northern and is 0.4m AMSL and has a mean pebble size of -5.54ϕ at the southern end (see Figure 5.7). The clasts are becoming more abraded and smaller the further they travel from the gravel source. The elevation changes on the barrier can be attributed to both the wave energy differences along the barrier and the clast size. As the wave energy decreases to the south, the ability of the waves to move larger clasts will also decrease so clasts will fine towards the centre of the bay. The larger waves in the north will transport the clasts higher up the beach so the elevation of the barrier will be greater at the northern end.

5.2.6 Identification of nearshore environments from bedding features

5.2.6.1 Bedding features

On uplifted coastlines nearshore marine beds may be preserved. This is useful because they are often diagnostic of a marine origin and they allow refined estimates of paleo sea levels. There are several examples in this study. Pit 2 unit 2 at Spike Cape (marked D on Figure 4.27) (160-250mm) was a sand unit with ripple cross lamination. The ripples were 4mm high and were 30-40mm long. Jopling and Walker (1968) and Walker and Plint (1992) describe these features as either fluvial or marine in origin. The location of Spike 2 pit 2 (see Figure 4.7) on a continuous shore parallel feature that is not intersected by any stream cuts makes it unlikely that the bedding is of fluvial origin.

Marine bedding was also found at Marble Point survey 2 and Kolich Point survey 3. On Marble 2 there were two pits that contained well sorted sand and clear bedding features. Pit 5 on Marble 2 survey contained shore parallel ripple cross lamination (Jopling and Walker, 1968). Pit 6 on Marble 2 contained mega ripples, some planar bedding and some ripple cross lamination in the first and second units (Jopling and Walker, 1968). In both pits small cobbles were present in most of the units. The ripples are interpreted as Type B ripple drift cross lamination (Jopling and Walker, 1968). This type of bedding is compatible with both fluvial and shallow marine settings (Jopling and Walker, 1968; Walker and Plint, 1992). The source of the ripples here is almost certainly shallow marine and wave generated. Marble Point pit 5 is located on a tombolo that connects a former offshore island to Marble Point. Figure 5.8 shows a modern example of ripples forming. Clearly defined ripples have formed offshore probably as the result of currents, and the effects of small ice bergs on the sediment offshore are visible.

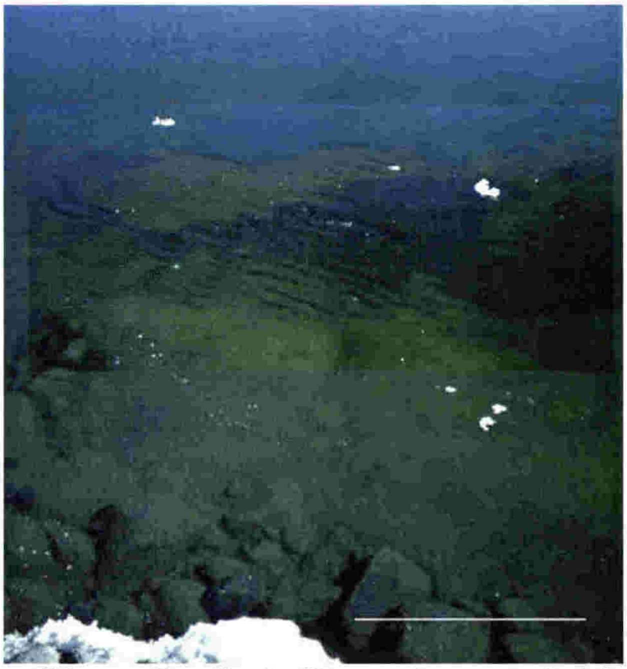

Figure 5.8. Ripples offshore at Cape Royds. The grey furrows to the left of the ripples and the depressions at the top of the ripples were most likely created by small pieces of ice being ground into the sea floor. The white bar at the base of the photograph is 1m long at the shore.

The most extensive area of continuous bedding on any of the beaches in McMurdo Sound was found at the landward end of Kolich survey 3. For ease of interpretation the exposure was divided into 5 discrete sections. Section 1 shows a complex set of beds to the right of the band that was interpreted as flaser bedding (type A), which consists of a series of flood and ebb tidal deposits (Dalrymple, 1992). Throughout the flaser bedded sands there are small pebbles and cobbles of inferred drop stone origin. To the left of the section there is a boulder and a number of small cobbles that dip 30^0 in a 90^0 direction. These clasts occupy a tongue like bed draped over the underlying units and it is interpreted as part of an overwash fan. Section 2 is a continuation of the flaser bedding seen in section 1. Section 3 consisted of a fine to coarse moderately well to poorly sorted massive sand at the top and beds that dipped 19⁰ in a 10⁰ direction. These appeared to be tidal sand waves (Dalrymple, 1992). Section 4 showed a classic ice wedge polygon structure, which was identifiable from the frost crack at the surface. Section 5 contained moderately well sorted fine to coarse sand tidal sand waves that dipped 38⁰ in a 252⁰ direction.

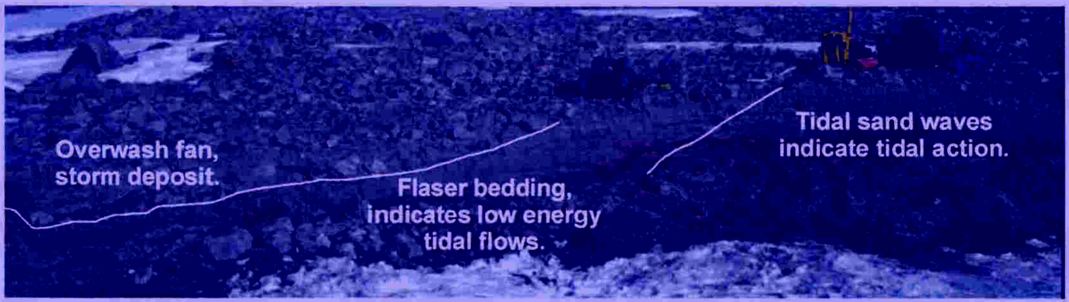

Figure 5.9. Kolich 3 exposure showing major features. Yellow pack in background is 45cm high.

Figure 5.9 shows this exposure which shows the progression of a relatively low energy rebounding beach. The highest section was interpreted as tidal sand waves, which indicates sub tidal conditions at the time of deposition. Tidal sand waves form in shallow sub tidal areas with tidal current speeds of between 0.5-1.5m/s (Dalrymple, 1992). The presence of dropstones in most of the sections signifies that the beach was in fact a nearshore marine unit rather than an true beach. As the rebound continued the flaser bedding was created as the water depth shallowed and tidal flows dominated. The overwash fan shows that the beach had rebounded beyond the range of most marine action and a high magnitude storm (probably a single wave) washed the tongue of material over these lower energy features.

The second section at Kolich Point was much closer to modern sea level. This exposure contained three clear units (see Figure 4.25). The base of the exposure had planar bedding and some tabular cross stratification which are indicative of storm or spring tidal berm deposits (Reinson and Rosen, 1982). The second unit consisted of ripple cross lamination which indicates a shallow marine wave generated environment (Jopling and Walker, 1968). The beds above the overwash fan are characteristic of shallow low energy marine conditions. The presence of sets of beds characteristic of similar conditions below the overwash fan indicates a return to lower energy conditions following the storm that deposited the overwash fan.

Bedding type	**Interpretation**	**Estimated water depth**	**Location of bedding**
Flaser bedding[1]	tidal	inter tidal 0m to -0.5m AMSL	Kolich survey 3 section 1 Kolich survey 3 section 2
Tidal sand waves[1]	tidal	inter tidal 0 to -0.5m AMSL	Kolich survey 3 section 3 Kolich survey 3 section 5
Ripple cross lamination[2]	wave generated	shallow water 0.5m to -0.5m AMSL	Marble survey 2 pit 5 Marble survey 2 pit 6 Spike survey 2 pit 2 Kolich survey 2 pit 2
Planar bedding between beds of poorly sorted and gravel[3,4]	storm/spring tidal berm deposit	shallow water 0 to 0.5m AMSL	Marble survey 2 pit 6 Spike survey 2 pit 2

Table 5.5. Summary of bedding types, their interpretation, estimated water depth at time of deposition and the location of these types of bedding.

[1]Dalrymple, 1992.

[2]Jopling and Walker, 1968, Walker and Plint, 1992.

[3]Reinson and Rosen, 1982.

[4]Require contextual information to confirm marine origin.

Table 5.5 summarises the types of bedding described in Chapter 4. It interprets the bedding and provides an estimated water depth at the time of deposition. The identification of deposits that constrain sea level is important for reconstructing sea level curves. These are discussed later in Chapter 5.

Some of the features Reinson and Rosen (1982) presented on the beaches near the Michael River, Labrador are also apparent in the stratigraphic units in the Sound (see Table 5.5). Reinson and Rosen (1982) described a 4 stage process of beach formation. The units represent the seasonal changes in the processes that act on the beaches from a well sorted fine to medium grain sand that represent summer and autumn conditions, to a mixed sand and gravel that represents ice-rafted and ice push deposits in winter and spring (see Figure 2.14).

The summer deposits described by Reinson and Rosen (1982) were fine to medium grained planar bedded sands. This description matches unit 1 on Kolich survey 3 section 6. Following Reinson and Rosen's (1982) description, this unit was most likely deposited during the open water period in the summer season. Spike survey 2 pit 2 also shows some of these seasonal features. Units 2 and 3 in pit 2 Spike survey 2, resemble the summer accretionary berm deposits with sand and gravel at the base of the unit (unit 2) grading upwards into planar bedding. Unit 4 contained ripple cross laminated sands which most closely resemble the summer beach face deposits.

The likelihood of preservation of all units, showing a seasonal progression, will depend largely on whether the beach is accretionary. A rapidly prograding shoreline will be more likely to preserve these structures than a beach that is eroding. During the summer months, the beaches at Cape Bird are dominated by marine action, which rework the deposits characteristic of ice action left during the winter. At both Kolich Point (Kolich 3 section 6) and Spike Cape (Spike 2 pit 2) the upper most unit (unit 3 at Kolich Point and unit 5 at Spike Cape) was most likely deposited in a storm in the summer months during a period of open water. These open water events in the summer probably reworked the winter deposits of the type described by Reinson and Rosen (1982).

In contrast with Reinson and Rosen (1982) none of the features that Dionne (1969; 1981, 1998) describes were present in any of the stratigraphic units. Dionne (1969; 1981, 1998) described a series of features such as ice-push ridges, circular depressions and gouges or furrows in intertidal areas associated with the transport of boulders. Although none of these features were found in any of the stratigraphic units, there were examples of these processes occurring today. Figure 5.7 shows ripples (probably formed by currents) offshore at Cape Royds. The photograph also shows a deep furrow to the left of the ripples and some circular depressions at the top of the ripples that are consistent with those features found by Dionne.

The preservation potential of these features in the St. Lawrence estuary is high because of the relatively low energy conditions in estuarine environments. Although there were boulder pavements at Spike Cape and Dunlop Island, which show that boulders were being transported, these were very localised as their formation is constrained by the supply of boulders (Hansom, 1983a) (see section Chapter 2, 2.2.2 Sea ice). In contrast with the environments Dionne describes, all of the deposits in McMurdo Sound were found along comparatively open stretches of coast and these types of features are unlikely to be preserved.

5.2.6.2 Dropstones

In addition to the morphological evidence of a marine origin, dropstones can also be diagnostic of marine settings (they also occur in lakes). The small clasts present in the Marble Point pits are identified as dropstones. Dropstones can occur due to a number of different processes. Leeder (1983) describes dropstones in ice shelf environments where generally fine sediment is interspersed with larger clasts which have dropped from melting icebergs. Eyles and Eyles (1992) also mention ice-rafted dropstones in glaciomarine environments. Bennett et al. (1996) presented four processes (biological rafting, ice rafting, flotation and projectile) that can result in dropstones. In this situation the dropstones represent ice rafted deposition in a marine environment.

Figure 5.10. Ice rafted pebbles at Marble Point (length of ice floe is 45cm).

Figure 5.10 shows ice rafting of gravel at Marble Point. This process is widespread on open coasts during the summer.

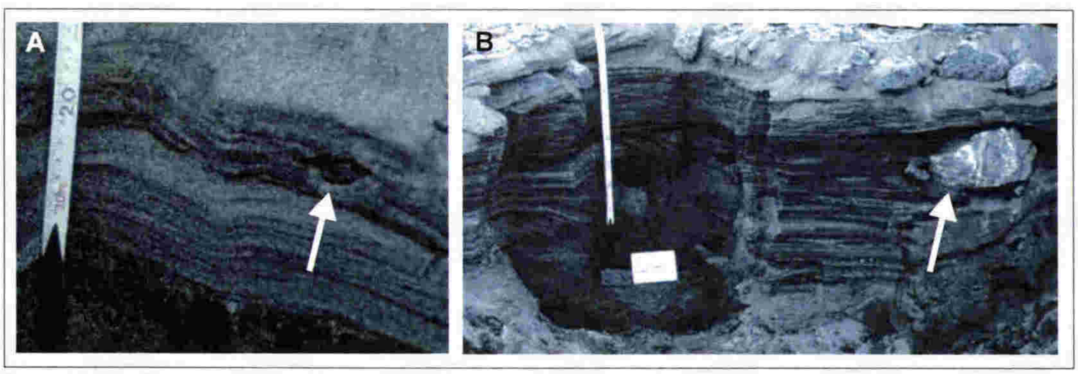

Figure 5.11. Dropstones at Kolich 2 pit 1 unit 2 (photograph A) and Kolich 3 section 6 unit 3 (photograph B).

Figure 5.11 shows dropstones at Kolich Point on survey 2 pit 1 and Kolich 3 section 6. The dropstones (indicated in the photographs by arrows) in the bedded units display a number of features associated with dropstones in sedimentary beds. Impact marks in the bedding at the base of the dropstone consistent with the clast falling into the unit may occur and there may be teardrop shaped bedding around the dropstone. The scale of the bedding around the dropstones and the sorting of the clasts suggest a low velocity flow, incapable of moving either of the dropstones in the photographs. Not all of the dropstones identified in bedding units around the Sound displayed all of these traits. Most of the dropstones were identified on the basis of unusually large clasts sitting in a matrix of smaller material in a clearly marine bed.

5.3 Ancient beach formation in McMurdo Sound

5.3.1 Mode of formation of Ancient beaches

In contrast to the modern beaches, the raised beaches on both sides of the Sound share a number of similar characteristics. The majority of the samples on raised beaches around the Sound were poorly sorted and the imbrication was generally very weak. The clasts on the raised beaches at Cape Bird are sub-angular, compared with the rounded and sub-rounded clasts observed on the modern beach. Although ice processes generally produce small discontinuous features, they can produce much larger beach-ridge-like features (e.g. Owens and McCann, 1970). The shore parallel nature of the ridges and their continuity over several hundred metres, however, indicates marine action.

The weak imbrication within the ridges and especially the poor sorting suggests that the ridges were built by short-lived large magnitude storm events. The modern beach at Cape Bird comprises mixed sand and gravel in contrast to the raised beaches, which contain considerably larger clasts. Gravel beaches typically have a number of characteristic features such as clast shape zones (Bluck, 1967; Postma and Nemec, 1990) which are typical of long exposure to 'normal' coastal conditions. In contrast, Forbes et al. (1995) showed that barriers on paraglacial coasts could undergo rapid changes in response to large magnitude storm events. This causes barrier structures and facies patterns to be broken down, and sediments become less well sorted.

The infrequency of open water conditions on the western side of McMurdo Sound will reduce the duration that storms can act on this shoreline. Even if the beaches start with open water, the length of time that the beaches remain open to wave action is severely limited due to sea ice being transported onto the beaches during storms by the waves. This has the effect of interrupting wave action on the beaches, preventing the storm from resorting the beach as the energy levels wane.

The number of ridges is primarily a function of maximum incident wave energy. Protected sites are likely to receive lower critical wave heights during storms and bathymetry may even create a maximum storm wave at a site. Beach ridges that can be traced between sites at Kolich Point and Spike Cape in areas sheltered from north east waves, demonstrate that open water storms are critical to beach ridge formation, height and numbers. This is clearly seen in Table 5.2, which shows the reduction in beach ridge elevation from a site open to north east waves to a more sheltered site (from Kolich survey 1 to Kolich survey 2).

As the coastline in McMurdo Sound rebounded following deglaciation, low frequency high magnitude storm events would create ridges that were formed above the elevation of normal marine or ice processes. As the coast continued to rise these ridges were elevated beyond the range of subsequent storms. In due course, another larger magnitude event would occur, depositing a ridge below the first and incorporating the smaller ridges that formed in the interim, into this large ridge. These large storm ridges are visible on the air photos at Spike Cape, Kolich Point, Marble Point and Cape Bernacchi. For example, on the profiles Spike 1 and Kolich 1 there are three easily identifiable ridges present. Although there were often more than just two or three ridges present on the profiles, these were the ones that were identifiable on air photos and could be traced continuously for 500m or more. The major ridges at Spike Cape represent the high magnitude storm events that have been preserved.

It is notable that ridge numbers are highest in low energy settings, for example on Cape Bird survey 2 there are 9 identifiable ridges (see Figure 5.10) that extend to 6.1m AMSL. On Kolich Point survey 1 there are only 3 major beach ridges that extend up to 19.9m AMSL. The western side of McMurdo Sound receives significantly larger waves because it is open to the north east. Storm events at Cape Bird that are large enough magnitude to create ridges out of range of normal marine or ice processes would be far smaller than the storms that produced similar ridges on the western side of the Sound. In addition, due to the regularity of ice-free conditions at Cape Bird, the frequency of these storms would also be greater.

The lower energy environment at Cape Bird is also reflected in the slope of the surveys. Average slopes for the western beaches that have major ridges identified on them (Spike 1, Kolich 1, Marble 1, Bernacchi 2) are between 4.1^0 and 7^0. This contrasts with Cape Bird survey Bird 3, where the average slope is 0.6^0. Figure 5.12 shows Kolich 1 survey and Bird 2 survey which graphically illustrate the difference between the steep western profiles and the comparatively shallow eastern profiles. The ridges at Cape

Bird are also considerably smaller than their western counterparts. Individual beach ridges at Cape Bird are up to 1m high (measured from base to top of ridge) compared with up to 5m high at Kolich Point (Butler, 1999).

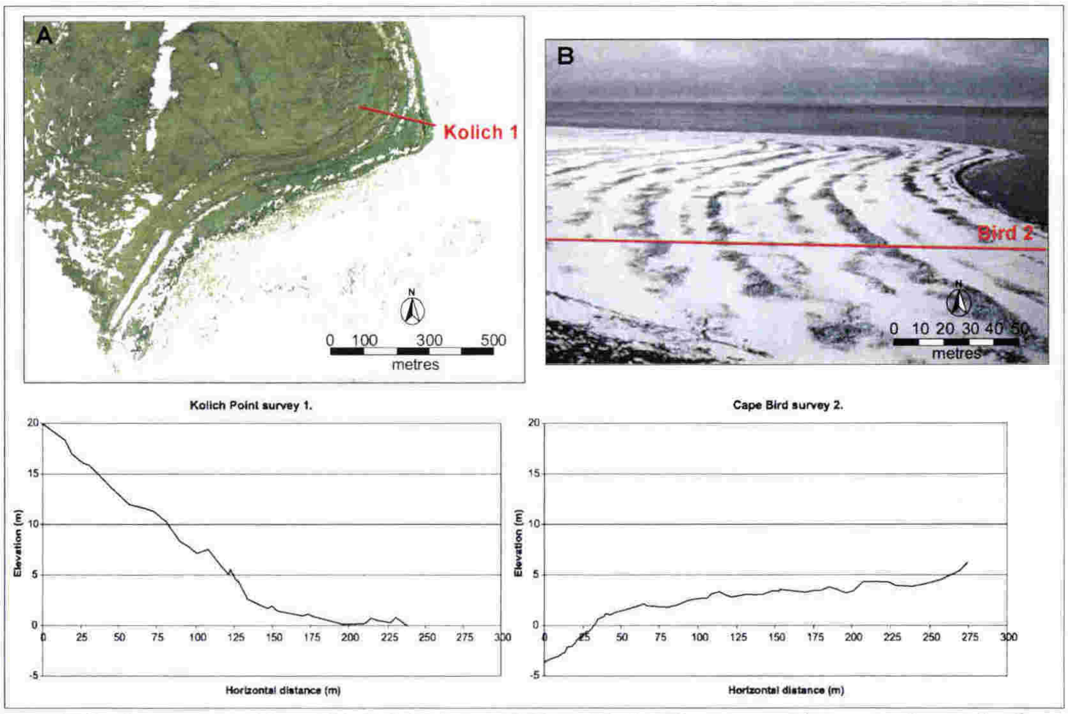

Figure 5.12. Survey profiles at Kolich Point and Cape Bird. The survey lines are shown in the photographs of the respective areas.

Abrupt changes of overall gradient of the beach ridges within profiles may provide insights into changes of former energy conditions at some locations. On survey Bird 3 at Cape Bird, there appears to be three distinct phases of beach development, which could be linked to energy conditions. The top 350m of the survey (phase 1) and the lower 190m (phase 3) both have relatively shallow slopes (0.2^0 and 0.4^0 respectively), in contrast to the middle 250m (phase 2), which is considerably steeper (1^0). The changes identified at Cape Bird could be due to changes in any of the factors that control beach slope including rate of uplift and sediment supply. However, as sediment size remains almost constant over the profile and uplift rates are unlikely to oscillate in this manner a volume change in sediment supply or wave energy is the most likely cause for the changes in the slope. The relationship between phase 1 and phase 3 suggests that sometime in the past, energy conditions and sediment supply at Cape Bird were similar to those experienced today. The difference in slope of phase 2 indicates a sediment deficit or a period of increased energy conditions. If the differences in slope were the result of an increase in wave energy at Cape Bird this should be repeated around the Sound.

This pattern of differing slope reaches or segments on the beaches in the Sound is also apparent at Cape Bernacchi, Marble Point and Dunlop Island. Figure 4.4 shows steepening of the Cape Bernacchi surveys 1 and 2 at about 8m AMSL and of Bernacchi 3 at about 6m AMSL. Figure 4.5 shows a flattening of the profile on Marble surveys 1 and 3 at about 8.5m AMSL and about 13m AMSL respectively and Figure 4.8 shows the Dunlop survey 1 profile flattening at about 11m AMSL. The Cape Bernacchi profiles show a steepening of the profile at the top of the profile rather than in the middle as with the Cape Bird profile. The Marble Point and Dunlop Island changes show a flattening of the middle of the profile rather than a steepening as seen at Cape Bird. However, as these changes are not reflected at Kolich Point or Spike Cape the changes must be a localised phenomenon.

Clearly the lack of synchroneity or even uniformity of slope changes mitigates against a regional change in wave climate and supports complex local sediment histories (Butler, 1999). For example, the dominant control of sediment supply at Priapulus Beach at Cape Bird is the condition of the Shell Glacier. The dominant wave direction at Cape Bird is from the south. The waves transport clasts from the south and deposit them at Priapulus Beach. The recurved beaches are clearly evident from the air photo in Figures 4.35 and 4.36. The Shell Glacier feeds Fitzgerald Stream, which terminates at the coast about 4km south of Priapulus Beach. When the glacier is advancing, material is frozen to the glacier and only small amounts of material will be transported down the outwash stream to the coast. In contrast, when the Glacier is retreating, large quantities of material are transported down the outwash stream to the coast. The changes in slope on the Bird survey 1 profile may indicate a time when the Shell Glacier was retreating.

5.3.2 Isostatic rebound and the Ancient beaches

Table 5.2 also shows as ridges at Kolich Point approach current mean sea level the difference between the elevation of the ridge crests above MSL decreases. This is shown diagrammatically in Figure 5.13. The decrease in height between ridges is apparent on both Kolich survey 1 and 2. Because the difference is evident on both Kolich survey 1 and 2 it is unlikely that the difference is due to a localised effect. The difference could be due to changes in the rate of rebound, changes in storm intensity over time or changes in storm return period.

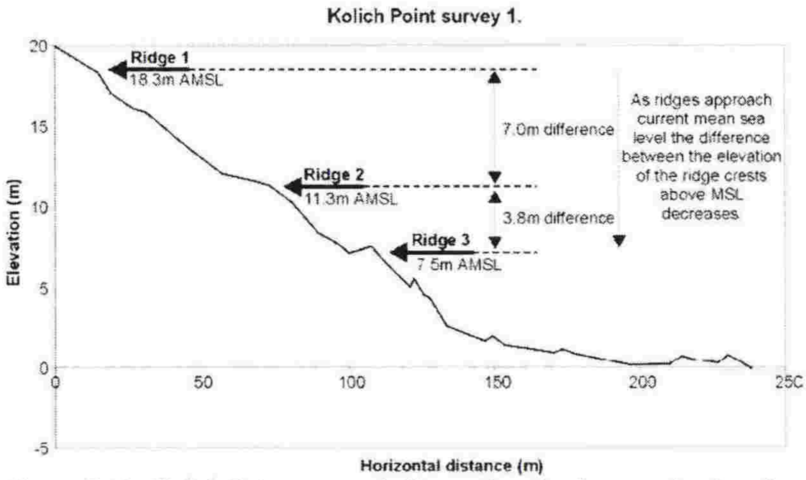

Figure 5.13. Kolich Point survey 1, illustrating the decrease in elevation difference AMSL of major ridges as they approach current sea level.

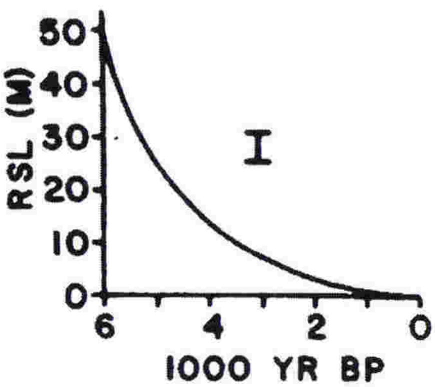

Figure 5.14. Zone I of the six predicted sea level zones resulting from retreat of the Northern Hemisphere ice sheets (Clark et al., 1978). Type I was chosen as the closest match for the situation in McMurdo Sound compared with Northern Hemisphere sites.

Figure 5.14 shows zone I of the six relative sea level response zones to deglaciation predicted by Clark et al. (1978). Zone I which is analogous to the McMurdo Sound record is a curve typical of an area glaciated during the Last Glacial Maxmum. The curve shows rapid rebound after the weight of local ice has been removed with a geometric decline in rebound rates over time. If a relative sea level curve like this is applied to the coast, and storm ridge formation rates remained constant the elevation between ridges will decrease as the rebound rate slows.

Alternatively elevation changes between ridges could also be a function of changes in either storm intensity or return period. A higher magnitude storm event will produce a larger beach ridge. If the highest ridge at Kolich Point was produced by a very high magnitude event and the subsequent ridges were produced by successively smaller events, then the difference in elevation between ridges would also reduce. Alternatively, if the return period of these storms decreased over time the longer return period from the creation of ridge 1 to 2 would produce a smaller difference between ridge elevation. A decline in isostatically driven sea level fall is characteristic of this type of glacial setting and can explain the ridge pattern without additional pleading. Consequently the rebound driven model is preferred.

An important point is that the differences between the raised ridges and the modern beaches suggest they were not formed under the same conditions. For example, at Cape Bernacchi there are numerous ice push features along the modern beach (see Figure 4.16) yet the raised beaches at Cape Bernacchi have no ice push features on them. This pattern is reflected at all sites on the western side of the Sound. This helps confirm the hypothesis that these ridges are not high magnitude storm beach ridges. Consequently, modern beach ridges are unlikely to attain similar heights above mean sea level as the relict ridges.

5.4 Determining marine limits

The difference in beach elevations between northern and southern facing profiles is important for rebound reconstructions as over and underestimation of sea levels could result from using incorrect marine limits. For example, on Kolich survey 1 the marine limit is 19.9m AMSL and on Kolich survey 2 the marine limit decreases to 15.7m AMSL. If Kolich survey 1 was chosen as a marine limit to represent a past sea level a correction for energy condition would have to be applied. This would require an estimation of the storm intensity, so that the height the ridge was deposited above sea level could be established.

However, correcting for energy conditions can lead to incorrect estimations of paleo sea level. For example, the highest ridge at Spike Cape can be traced between Spike survey 1 and 2 (ridge 3 see Figure 4.7). The elevation of the ridge on Spike 1 is 15.36m AMSL and the elevation on Spike 2 is 15.03m AMSL. They were probably deposited in the same storm event. However, Spike 1 pit 1 (on the crest of ridge 3) comprised a poorly sorted mixed sand and gravel with clast supported pebbles and cobbles, which is consistent with a high energy event. In contrast, Pit 2 unit 2 on Spike 2 comprised a sand unit with ripple cross lamination which is consistent with low energy conditions. The ripple cross lamination in Spike 2 pit 2 was most likely deposited well before the storm that created the ridge at the top of Spike 1, under average coastal conditions. Any record of lower energy conditions on Spike survey 1 was destroyed as the ridge was reorganised by the storm but preserved on Spike survey 2 because of it's relatively sheltered nature.

Ideally paleo sea levels could be determined for an individual raised beach ridge by subtracting the elevation above modern mean sea level of the modern beach ridge from the raised beach. However, even though the beaches in McMurdo Sound represent storm events, this still assumes that both the modern beach and the raised beach were deposited in a similar magnitude event. This has already been shown to be a false assumption. If such a correction is employed overestimation of the marine limit will occur. Sites sheltered from the dominant fetch direction and susceptible to smaller storm waves are likely to be deposited closer to mean sea level. These beaches are better analogues for paleo sea level studies. Even on these ridges, however, sea level estimates will be somewhat inaccurate, because they are storm ridges not beaches. Sea level reconstructions would be much improved if features with stronger associations with true sea levels were used.

There are three features that are particularly useful in this respect for estimating paleo sea levels. Boulder pavements and low energy marine bedding features such as tidal bedding (eg. flaser bedding) and shallow water wave ripples. Figure 5.15 shows a boulder pavement at Kolich Point. Boulder pavements were found on the south facing shores at Spike Cape and the western and southern facing shores on Dunlop Island. Boulder pavements form in intertidal zones as boulders are transported by sea ice in low energy tidal environments (Dionne 1981; Drake and McCann, 1982). The possibility of dateable material being found under boulder pavements is high. Tidal environments will most likely have sand or silt beneath the boulders that would be suitable for luminescence dating.

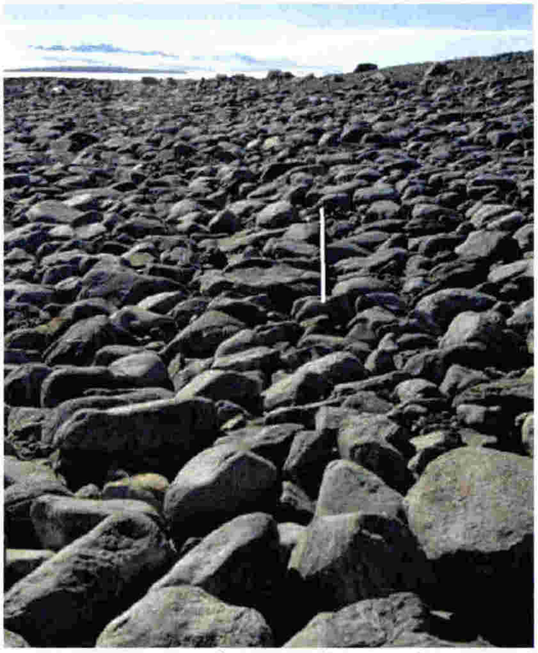

Figure 5.15. Boulder pavement at Dunlop Island (white bar is 1m long).

Low energy bedding units are a useful indicator of paleo sea levels when used in conjunction with dropstones. The bedding units on their own can be used to infer a tidal environment but the dropstones give further certainty that the bedding units (such as those found at Kolich Point, see Figure 5.11) are tidal in origin. Therefore, when used in conjunction with dropstones, the best analogues for paleo sea levels in McMurdo Sound are those bedding features indicated in Table 5.5 (shallow marine bedding and tidal bedding features).

5.4.1 Dating sea levels

The majority of the dates of sea levels in McMurdo Sound have been ^{14}C dates (Nichols, 1968; Stuiver et al., 1981; Hall and Denton, 1999) and have been used to infer past ice sheet history in the Sound. This reflects the wide use of the technique, however, luminescence dating has a number of advantages over carbon dating in this setting. Sediment suitable for luminescence dating, including quartz and feldspar sands and silts, are more common than carbonaceous material on the beaches in McMurdo Sound. In addition, rather than establishing when an organism died, as in ^{14}C dating, luminescence dating determines when sediment was last exposed to light. Material suitable for ^{14}C dating can be incorporated into a beach long after the organism that yielded the material has died. The waters surrounding Antarctica contain 'old' carbon from the melting of ancient ice sheets. This will return an unusually old age for marine organisms and is called the marine reservoir effect (see Berkman and Forman, 1996). While marine reservoir effects are well documented around the world and easily corrected for, in Antarctica the corrections are larger and more variable. Luminescence suitable for luminescence dating will invariably be exposed to light because the beaches in Antarctica are only active in the summer months when there is 24 hours of light. In an isostatically rebounding coastal environment this will indicate when a beach was last active or at least when it was forming. It is particularly applicable to an Antarctic coastal environment.

Figure 5.16 shows the luminescence ages from this study (the luminescence ages have been converted to radiocarbon years) and 54 ^{14}C dates of marine shells, seal skin, and elephant seal remains (Hall and Denton, 1999). Because some of the samples were collected from storm ridges, Hall and Denton (1999) increased the y intercept of the sea level curve to 4m (the inferred storm ridge maximum in the Sound). Although such a correction might be applicable to some of the sites in the Sound, most corrections for energy conditions would be considerably less than 4m. In addition, material suitable for ^{14}C dating could be deposited on a smaller ridge many hundreds of years before a large magnitude storm event incorporated it into the larger storm ridges. As a crude estimate, there are three major storm ridges at Spike Cape and a luminescence age for the top ridge of 7,200 years. Thus, the average interval of time between these large intensity storms is about 2,400 years. This means that the average age of carbonaceous material in any ridge was likely to 1,200 years old at the time of formation of the ridge.

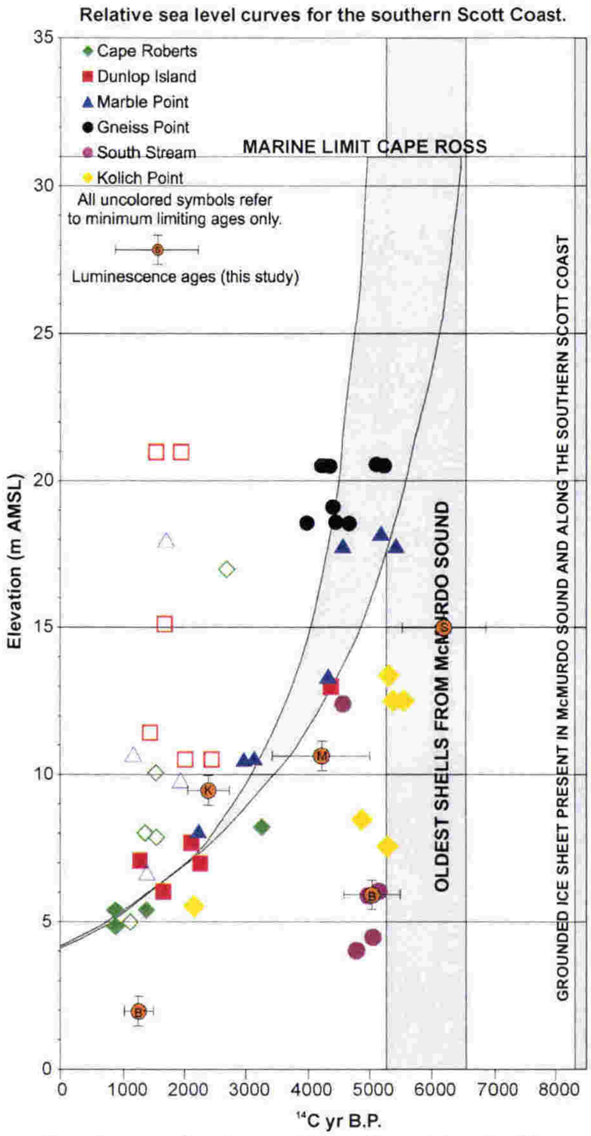

Figure 5.16. Relative sea level curve for the southern Scott Coast. Diagram represents 54 ^{14}C dates from Marble Point to Cape Roberts (Hall and Denton, 1999). Note all of the dates have been corrected for δ^{13} and the marine reservoir effect. The coloured symbols indicate the age of the beaches. The open symbols indicate only minimum ages for sea level change. The shaded curve represents the sea level curve. The y intercept of the sea level curve is at 4m because all of the raised beaches are inferred to be storm beaches. The yellow diamonds are from deltas at Kolich Point and the purple circles from South Stream represent maximum ages at these elevations. The luminescence ages from this study are shown in orange circles and have both

age and sea level error bars on them (the letters in the circles are the first letter of the sample name). The luminescence ages have been converted to radiocarbon years (Stuiver and Reimer, 1993) so that they can be compared with Hall and Denton's (1999) data. Note the luminescence ages generally show much older dates for the beaches.

The luminescence ages infer that the beaches are on average older than the dates presented by Hall and Denton (1999). Even though this study has only 5 isolated luminescence ages, the treatment of Hall and Denton's (1999) samples with respect to the elevation they were collected from raises serious doubts about the validity of the inferred sea level curve. Of Hall and Denton's (1999) dates, the sites that best represent sea level are Kolich Point (represented by the yellow diamonds) and South Stream (shown by the purple circles). At these sites material was collected from deltas rather than storm beaches. The settings for these deltas make them much better sea level markers than the ridges. These dates correspond remarkably well with the luminescence ages and suggest that Hall and Denton (1999) may have rejected the wrong ages. The increased age of the beaches will cause substantial reductions in rebound rates and impact on local ice histories.

5.4.1 Breakup of the Ross Ice Shelf from raised beaches

The reconstructions of the Ross Ice Sheet at the LGM (about 22,000 years before present (BP)) put the grounding line somewhere south of Coulman Island (Licht et al., 1996) or as far as the edge of the continental shelf (Kellogg et al., 1996) (see Figure 5.16) and almost anywhere between these two points (Denton et al., 1970; Kellogg et al., 1979; Drewry, 1979; Clark and Lingle, 1979; Lingle and Clark, 1979; Stuiver et al., 1981; Mabin, 1986; Denton et al., 1989; Colhoun et al., 1992; Anderson et al., 1992; Hall and Denton, 1994) (see Figure 5.17). Sea-level rise after 17,000 years BP caused the initial break-up of the ice sheet, which has subsequently retreated to its present position to the west of Ross Island (Kellogg et al., 1996). As the areas became ice free, beaches formed above sea level.

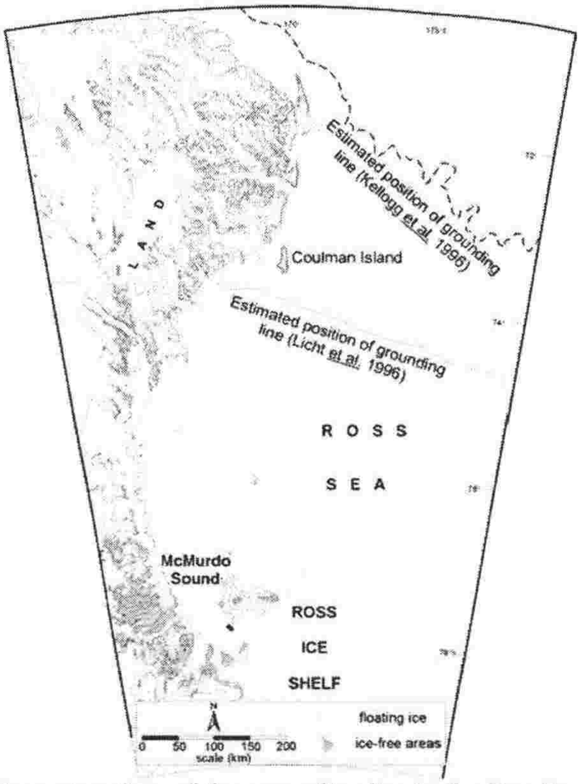

Figure 5.17. Reconstructions of the grounding line in the Ross Sea at the Last Glacial Maximum Licht et al. (1996), and Kellogg et al. (1996).

The timing of the first beach at any site in McMurdo Sound signifies the retreat of ice from that location. This retreat has been mapped by Stuiver et al. (1981) and Kellogg et al. (1996) to determine when an area became ice-free. In both of these cases the elevation of the marine limit (the highest elevation of marine action) was not corrected for energy conditions, a concept first presented for this setting by Colhoun et al. (1992). This study suggests that even in the most recent work (Hall and Denton,1999) the problem of true sea level identification has not been thought through. Nevertheless, the patterns are indicative.

Marine limits around McMurdo Sound are shown in Table 5.6 and Figure 5.18. The 'Location' column describes where the marine limit was observed and the 'Type of marine limit' column describes the landform that was used to identify the marine limit at that location. 'Observed marine limit (AMSL)' and 'Previous estimates' columns refer to the observed elevation of the marine limit (i.e. the crest of a storm ridge) and previous reported estimates of marine limits respectively. The last column refers to the elevation where a past sea level was identified in this study. For example at Cape Bernacchi the maximum elevation of marine action is found at 11.9m AMSL in the form of a storm beach. In the literature, Stuiver (1981) reports the marine limit at Cape Bernacchi at 5.0m. In this study, the storm beach reflects a sea level at the time of deposition of 8.4m AMSL.

Location	Type of marine limit	Observed marine limit (AMSL)	Previous estimates	Corrected marine limit (this study unless cited AMSL)
Cape Bernacchi	Storm beach	11.9m	5.0m [1]	8.4m
Marble Point	Fine marine sands	20.5m	9.5m [2] to 20m [1]	20.5m
Kolich Point	Storm beach	17.5m	17.0m [1]	14.5m
Spike Cape	Storm beach	15.03m	14.6m [2,3] to 17.0m [1]	15.03m
Dunlop Island	Storm beach	19.4m	15.5m [2,3] to 20.0m [1]	15.4m
Cape Roberts	Storm beach	no data	17.3m [3]	14.6m [3]/21.0m[4]
Cape Ross	Storm beach	no data	36.5m [3]	32.0m [3]
Cape Bird	Storm beach	8.4m	4m[2,3] to 9.5m[1]	7.2m
Cape Barne	Fine marine sands	9.7m	No level	8.2m

Table 5.6. Previous estimates of marine limits with corrections for energy conditions at locations along the McMurdo Sound coast.

[1] Stuiver et al., 1981.

[2] Colhoun et al., 1992.[3] Kirk, 1991.

[4] Hall and Denton (1999).

If all sites in McMurdo Sound became ice free at the same time and the marine limits around the Sound are assumed to be synchronous following past practices (Colhoun et al., 1992), this would lead to a complex pattern of rebound. In some areas, the elevation of the marine limit varies by many metres over short distances. For example, between Cape Bernacchi and Marble Point, the marine limit varies 12.1m in elevation over a distance of 6km.

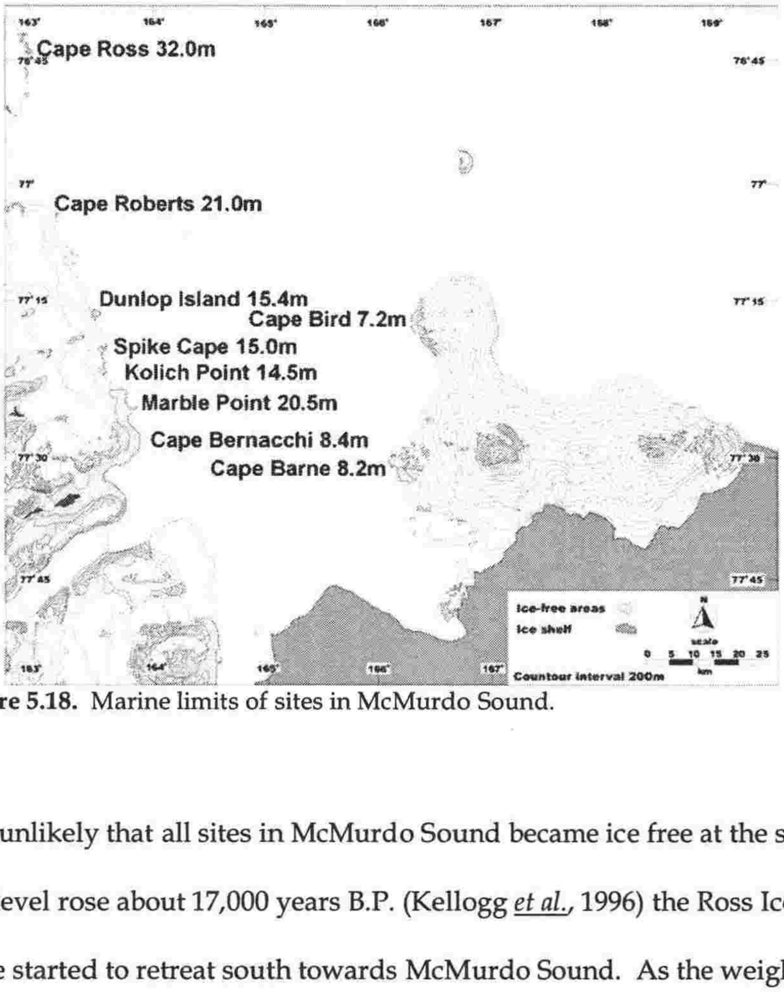

Figure 5.18. Marine limits of sites in McMurdo Sound.

It is unlikely that all sites in McMurdo Sound became ice free at the same time. When sea level rose about 17,000 years B.P. (Kellogg *et al.*, 1996) the Ross Ice Shelf would have started to retreat south towards McMurdo Sound. As the weight of the ice lifted, the McMurdo Sound coastline would have started to rebound. If all sites in McMurdo Sound rebounded at the same rate the seemingly complex pattern of rebound can be explained by a series of ice breakouts from McMurdo Sound and advances of local glaciers.

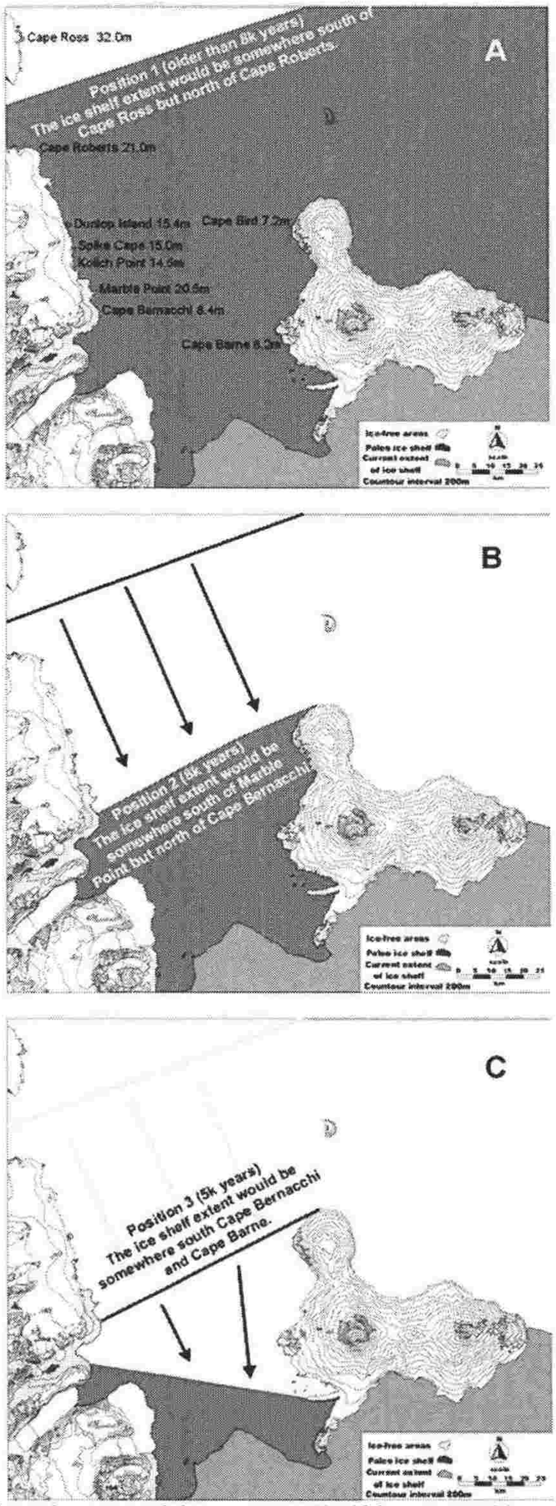

Figure 5.18. Inferred retreat of the Ross Ice Shelf from raised beaches. Map A shows the inferred position 1 of the Ice Shelf (the locations of the extent of the Ross Ice Shelf are estimates only). Map B shows inferred position 2 and Map C shows inferred position 3 of the Ice Shelf.

When the Ice Shelf retreated south of Cape Ross beaches would have started to form at Cape Ross but not towards the south where the Ice Shelf still occupied McMurdo Sound. As the land continued to rebound the beaches at Cape Ross would have been elevated. Further retreat of the Ice Shelf would have exposed sites further to the south and beaches would have started to develop at these locations as well. Thus, the sites with higher marine limits are merely those that have been ice free for the longest.

Figure 5.19 shows the three stages of the ice shelf indicated by marine limits in McMurdo Sound.

1. The first position of the ice shelf must be somewhere north of Cape Roberts and Cape Bird but south of Cape Ross to produce a 32m marine limit at Cape Ross and significantly lower marine limits to the south. There are no dates available for Cape Ross but the oldest shells in McMurdo Sound are about 8,000 years B.P. (Hall and Denton, 1999) so the ice shelf was at position 1 (see Figure 5.18) before 8,000 years B.P.
2. Position two indicates the Ross Ice Shelf was north of Cape Bernacchi and Cape Bird but south of Marble Point. The luminescence ages show that Spike Cape has been ice free for about 7,200 years. The marine limit at Spike Cape is 15.03m AMSL so at this time 5.47m of uplift had already occurred (the marine limit at Marble Point is 20.5). The oldest shells in McMurdo Sound are 8,000 years B.P. (Hall and Denton, 1999), which puts the date for the retreat of the Ice Shelf to position 2 at about 8,000 years B.P.
3. The final position is somewhere south of Cape Bernacchi, Cape Bird and Cape Barne (see Figure 5.19). Cape Bernacchi 2 luminescence age shows Cape Bernacchi ice free at 6,000 years. This was the only luminescence age that was not in stratigraphic order with the rest of the ages and may not have been completely

zeroed, returning an older age for that elevation. Bernacchi 1 luminescence age was collected from 2m AMSL and indicates that the beaches at this elevation are at least 2,900 years B.P. At this time 6.4m of uplift had already occurred, which puts the date of the marine limit considerably older than this. The oldest ^{14}C dated beach at Cape Bird is 4,885 years B.P. (Kellogg et al., 1996). There are no dates for the beach at Cape Barne. The luminescence age from Cape Bernacchi and the date from Cape Bird indicate that position 3 was probably reached by about 5,000 years.

Local glacier advances confuse the general pattern of marine limits in McMurdo Sound (northern sites having higher marine limits than those to the south), by producing low marine limits between sites with higher marine limits. For example, the marine limit at Marble Point and Cape Roberts is 20.5m AMSL and 21m AMSL respectively. This indicates that both sites became ice free simultaneously (position 2 in Figure 5.18). However, marine limits at Kolich Point and Dunlop Island are 14.5m AMSL and 15.4m AMSL respectively. These differences could be due to the presence of local Wilson Piedmont ice covering these sites after the Ross Ice Shelf retreated. Kolich Point Spike Cape and Dunlop Island would have been covered by local glacier ice at position 2 when Marble Point was ice free. Table 5.6 shows similar elevations for marine limits for Dunlop Island, Spike Cape and Kolich Point. Therefore, these sites would have become ice free at about the same time, which based on the luminescence age at Spike Cape was about 7,000 years B.P.

This reconstruction of the retreat of the Ross Ice Shelf into McMurdo Sound over the past 8,000 years agrees with the general southward pattern of retreat presented by Hall and Denton (1999), Kellogg et al. (1996) and Stuiver et al. (1981) but disagrees with all these studies on timing. Kellogg et al. (1996) suggest that at 8,000 years B.P. the Ice

Shelf edge was north of McMurdo Sound (somewhere north of Cape Ross) and at 4,000 years B.P. the Ice Shelf edge had retreated to Marble Point and south of Cape Bird. In contrast, Stuiver et al. (1981) show a more complex pattern of retreat. They suggest that the Ice Shelf edge was at or north of Marble Point between 6,430 years B.P. and 5,650 years B.P. and then retreated on the western side of the Sound to the south of Cape Bernacchi sometime around 5,650 years B.P. At this time, they place the edge of the Ice Shelf north of Cape Bird until a retreat to the south of the Shell Glacier sometime after 5,650 years B.P.. Denton and Hall (1999) date the retreat of the Ross Ice Shelf from McMurdo Sound at about 6,500 year B.P.

In contrast with other studies that have mapped the retreat of the Ross Ice Shelf from McMurdo Sound using raised beaches (Denton and Hall, 1999; Kellogg et al., 1996; Stuiver et al., 1981) this study has accurately identified and mapped marine limits in McMurdo Sound based on energy conditions at the time of deposition on a site by site basis and used higher precision markers where available. Combined with the identification of a previously unreported marine limit (Cape Barne), a more accurate picture of retreat of the Ross Ice Shelf has been constructed.

Marine limits have previously been overestimated in McMurdo Sound and ages of the sea levels are too young. If the data presented by Hall and Denton (1999) are considered in light of the work presented here, they would infer reduced levels of uplift along the coast. A crude interpretation of these data, suggest less ice in McMurdo Sound during the Last Glacial Maximum than previously thought.

Chapter 6

Conclusions

6.1 Introduction

This thesis has presented baseline data on the beaches in McMurdo Sound. The specific aims of this work were to determine how Antarctic beaches responded to the interaction between the marine and cryogenic processes acting on them, and to determine what raised beaches in McMurdo Sound can tell us about the Holocene environmental history of the Sound. The data presented here has allowed the processes that dominate beaches in different locations around the Sound to be determined and allowed a history of beach formation to be established. It has provided the tools for other workers to determine sea levels on the raised beach ridges with more accuracy and shown that previous sea level histories of McMurdo Sound are questionable.

6.2 History of beach development in McMurdo Sound

Examination of satellite images of McMurdo Sound showed that the western side of the Sound was ice free only 1.6% of the time compared with 51.1% of the time ice free on the eastern side of the Sound. This trend is reflected in the processes that act on the beaches and the features that are produced as a consequence. The beaches on the western side of McMurdo Sound are characterised by ice push ridges, poorly rounded clasts, poorly sorted sediments and ice pits. In contrast, the eastern side of the Sound is characterised by well rounded clasts, well sorted sediments and an absence of features associated with ice processes. The most effective tool used to determine the relative importance of marine verses ice processes was the rounding of material on the beaches.

Despite the prominence of ice processes on the western side of the Sound some marine features were preserved on the western raised beaches. At Marble Point, Kolich Point and Spike Cape there were well preserved marine bedding features. These were used to redefine the marine limits at these locations. The most useful features for determining the marine limit were low energy bedding features and boulder pavements. In addition to redefining some of the former estimates of marine limits in McMurdo Sound, a marine limit at Cape Barne that has not previously been identified aided in the reconstruction of the retreat of the Ross Ice Shelf from McMurdo Sound.

There are also significant differences in morphology on the western side of the Sound between the northern and southern facing beaches. These are again due to the relative prominence of ice and marine processes at these locations. Ice processes are prominent on the beaches on the southern facing profiles as the dominant southerly wind drives sea ice onto the beaches suppressing marine processes. In contrast, the wind forces sea ice off the beaches in the northern facing bays allowing marine processes to act on them.

The dominant wave direction in the Sound is from the fetch restricted south but large storm waves come from the north east. Therefore, the beaches and storm ridges facing north and east are much larger than the beaches facing the south or west. This is reflected in the number of ridges preserved with a small number of large ridges (x=3) on east facing aspects and many more (x>10) smaller ridges on southerly and westerly aspects.

As the coastline in McMurdo Sound rebounded following deglaciation low frequency high magnitude storm events created ridges that formed above the elevation of normal marine or ice processes. As the coast continued to rise these storm ridges were elevated beyond the range of subsequent large magnitude storms. In due course, another larger magnitude event would occur, depositing a ridge below the first and incorporating the smaller ridges that formed in the interim into this larger one. Decreasing elevation between the highest and lowest beach ridge at Kolich Point could indicate changes in either storm intensity or return period but the change in spacing can be explained by changes in isostatic rebound rates and requires no changes in marine conditions in the Holocene.

The preservation of ice push features on the modern beaches and their absence on the raised beaches indicates that the magnitude of storm required to create the flights of raised storm ridges has not yet acted on the modern beach. Previous sea level curves have used corrections based on the assumption that the modern and raised beaches are the product of similar magnitude storm events. The validity of the sea level curves based on this assumption is questionable, with the relict flights occurring at higher elevations and landward of the modern beaches and modern sea level.

6.3 History of the Ross Ice Shelf in McMurdo Sound

The elevation and ages of corrected marine limits were used to reconstruct the retreat of the Ross Ice Shelf into McMurdo Sound. If the coastline around McMurdo Sound rebounded the same amount, the elevations of marine limits will represent when the beaches were free of the Ross Ice Shelf. The corrected marine limits show a three stage southward retreat of the Ross Ice Shelf. A breakout from somewhere north of Cape Roberts and south of Cape Ross back to Marble Point (on the western side of the Sound) but remaining north of Cape Bird (on the eastern side of the Sound) occurred sometime around 8,000 years ago. Another breakout cleared ice from Cape Bird south of Cape Barne and south of Cape Bernacchi around 4,500 years ago. Local glaciers covering sites between Ice Shelf free locations confound this simple pattern of Ross Ice Shelf retreat. For example Kolich Point, Spike Cape and Dunlop Island have lower marine limits than Marble Point and Cape Roberts which are along the same stretch of coast. Local Wilson Piedmont ice retreated from Kolich Point, Spike Cape and Dunlop Island about 7,200 years ago, whereas the Ross Ice Shelf had evacuated Marble Point and Cape Roberts earlier.

The redefinition of marine limits and the refinement of paleo sea levels in McMurdo Sound have shown that the Ross Ice Shelf retreated from the Sound earlier than previously believed. This automatically reduces the isostatic rebound rate along the coast and suggests that the ice thickness in McMurdo Sound during the Last Glacial Maximum was less than previously thought. This may be of interest to ice sheet modellers.

6.4 Recommendations for further and future work

This thesis has raised some issues with the accuracy of past estimates of paleo-sea level data and has suggested some ways in which the beaches could be re-examined in order to increase the accuracy of paleo-sea level studies. This raises some opportunities for further work on the beaches in McMurdo Sound. The following list makes some suggestions for further work on the beaches in McMurdo Sound.

1. Ice modellers need to recalculate ice thicknesses in McMurdo Sound during the Holocene using the refined paleo-sea level data presented in this study. Further modelling of ice thicknesses from paleo-sea levels from raised beaches in McMurdo Sound should establish how these sea levels were obtained. If the sea levels were estimated using high energy beaches with no corrections for energy conditions they should be discarded.
2. Future studies should note the best analogues for paleo-sea levels on Antarctic beaches (boulder pavements, low energy marine bedding features such as tidal bedding, and shallow water wave ripples), and use these to determine more accurate datum.
3. More data needs to be collected on the internal structure of the beaches in McMurdo Sound. This will allow more sites to be identified for further luminescence dating and help to establish the primary controls on beach steepness at various locations.

References

Aitken, M.J., 1994. Optical dating: A non-specialist review. *Quaternary science reviews,* 13, 503-508.

Anderson, J.B., Shipp, S.S., Bartek, L.R., Reid, D.E., 1992. Evidence for a grounded ice sheet on the Ross Sea continental shelf during the late Pleistocene and preliminary paleodrainage reconstruction. *Antarctic Research Series,* 57, 39-62.

Antarctic Field Book, 144, 5. Land Information New Zealand.

Araya-Vergara, J.F., 1982. Antarctica, coastal morphology. In: *The Encylopedia of Beaches and Coastal Environments,* (Schwarts, M.L., ed.), Encyclopedia of Earth Science Series, 15, 43-47. Hutchinson Ross, Pennsylvania.

Armstrong, T., Roberts, B., Swithinbank, C., 1973. *Illustrated glossary of snow and ice,* (2nd ed). The Scott Polar Research Institute, Cambridge.

Bannister, A. Raymond, S. Baker, R., 1992. Surveying. Longman Scientific and Technical, Essex.

Barnes, P.W., Kempema, E.W., Reimnitz, E., McCormick, M., 1994. The influence of ice on Southern Lake Michigan coastal erosion. *Journal of Great Lakes Research,* 20, 1, 179-195.

Barnes, P.W., Kempema, E.W., Reimnitz,E., McCormick,M., Weber, W.S., Hayden, E.C., 1993. Beach profile modification and sediment transport by ice: an overlooked process on Lake Michigan. *Journal of Coastal Research*, 9, 65-86.

Barrett, P.J., 1980. The shape of rock particles, a critical review. *Sedimentology*, 27, 291-303.

Bascom, W.H., 1951. The relationship between sand size and beach face slope. *Transactions American Geophysical Union*, 32, 866-874.

Bennett, M.R., Doyle, P. Mather, A.E., 1996. Dropstones - their origin and significance. *Paleogeography Paleoclimatology Paleoecology*, 121, (3-4), 331-339.

Berkman, P.A., Forman, S.L., 1996. Pre-bomb radiocarbon and the reservoir correction for calcareous marine species in the Southern Ocean. *Geophysical Research Letters*, 23, 363-366.

Bluck, B.J., 1967. Sedimentation of beach gravels: Examples from South Wales. *Journal of Sedimentary Petrology*, 37, 1, 128-156.

Boyd, G.L., 1981. The March 1978 ice piling event on Lake St. Clair, Ontario. *Workshop on Ice Action on Shores*, 1-13.

Butler, E.R.T., 1999. Process environments on modern and raised beaches in McMurdo Sound, Antarctica. *Marine Geology*, 162, 105-120.

Clark, J.A., Farrell, W.E., Peltier, W.R., 1978. Global changes in postglacial sea level: A numerical calculation. *Quaternary Research*, 9, 265-287.

Clark, J.A., Lingle, C.S., 1979. Predicted relative sea-level changes (18,000 years B.P. to present) caused by late-glacial retreat of the Antarctic ice sheet. *Quaternary Research*, 11, 279-298.

Colhoun, E.A., Mabin, M.C.G., Adamson, D.A., Kirk, R.M., 1992. Antarctic ice volume and contribution to sea-level fall at 20,000 yr BP from raised beaches. *Nature*, 358, 316-318.

Dalrymple, R.W., 1992. Tidal depositional systems. In: *Facies models response to sea level change*, (Walker, R.G., James, N.P. eds.), 195-218. Geological Association of Canada, Ontario.

David, T.W.E., Priestly, R.E., 1909. Appendix 2. Geological Observations in Antarctica by the British Antarctic Expedition 1907-1909. In: *The Heart of the Antarctic*, (Shackleton, E.H. ed.), 2, 268-314. Willian Heinemann, London.

de la Mare W.K., 1997. Abrupt mid-twentieth-century decline in Antarctic sea-ice extent from whaling records. *Nature*, 389, 57-60.

Denton, G.H., Armstrong, R.L., Stuiver, M., 1970. Late Cenozoic glaciation in Antarctica: the record in the McMurdo Sound region. *Antarctic Journal of the United States*, 5, 15-22.

Denton, G.H., Bockheim, J.G., Wilson, S.C., Stuiver, M., 1989. Late Wisconsin and early Holocene Glacial history, inner Ross embayment, Antarctica. *Quaternary Research*, 31, 151-182.

Dionne, J., 1968. Schorre morphology on the south shore of the St. Lawrence estuary. *American Journal of Science*, 266, 380-388.

Dionne, J., 1969. Tidal flat erosion by ice at La Pocatiere St. Lawrence estuary. *Journal of Sedimentary Petrology*, 39, 3, 1174-1181.

Dionne, J., 1981. Ice action in muddy tidal flats, middle St. Lawrence estuary. *Workshop on Ice Action on Shores*, 81-87.

Dionne, J., 1998. Sedimentary structures made by shore ice in muddy tidal-flat deposits, St. Lawrence estuary, Quebec. *Sedimentary Geology*, 116, 261-274.

Dobkins, J.E., Folk, R.L., 1970. Shape development on Tahiti-Nui. *Journal of Sedimentary Petrology*, 40, 4, 1167-1203.

Drake, J.J., McCann, S.B., 1982. The movement of isolated boulders on tidal flats by ice floes. *Canadian Journal of Earth Science*, 19, 748-754.

Dredge, L.A., 1982. Relict ice scour marks and late phases of Lake Agassiz in northernmost Manitoba. *Canadian Journal of Earth Science*, 19, 1079-1087.

Drewry, D.J., 1979. Late Wisconsin reconstruction for the Ross Sea region, Antarctic. *Journal of Glaciology*, 24, 90, 231-244.

Dubrovin, L.I., 1979. Major types of Antarctic ice shores. *Byulleten' Sovetskoy Antarkticheskoy expeditsii*, 93, 5-12.

Evenson, E.B., 1973. The ice-foot complex: Its morphology, classification, mode of formation, and importance as a sediment transporting agent. *Michigan Academician*, 6, 43-57.

Eyles, N., Eyles, C.H. Glacial depositional systems. In: 1992. *Facies models response to sea level change*,(Walk er, R.G., James, N.P. eds.), 73-100. Geological Association of Canada, Ontario.

Folk, R.L., Ward, W.C., 1957. Brazos River Bar: A study in the significance of grain-size parameters. *Journal of Sedimentary Petrology*, 27, 3-26.

Forbes, D.L., Taylor, R.B., 1994. Ice in the shore zone and the geomorphology of cold coasts. *Progress in Physical Geography*, 18, 1, 59-89.

Forbes, D.L., Orford, J.D., Carter, R.W.G., Shaw, J., Jennings, S.C., 1995. Morphodynamic evolution, self-organisation, and instability of coarse clastic barriers on paraglacial coasts. *Marine Geology*, 126, 63-85.

Gale, S.J., Hoare, P.G., 1992. Bulk sampling of coarse clastic sediments for particle-size analysis. *Earth Surface Processes and Landforms*. 17, 729-733.

Gilbert, R., 1990. A distinction between ice-push and ice-lifted landforms on Lacustrine and marine coasts. *Earth Surface Processes and Landforms*, 15, 15-24.

Gordon, D.C., Desplanque, C., 1981. Ice dynamics in the Chignecto Bay region of the Bay of Fundy. *Workshop on Ice Action on Shores*, 35-52.

Greene, H.G., 1970. Microrelief of an Arctic beach. *Journal of Sedimentary Petrology*, 40, 419-427.

Gregory, M.R., Kirk, R.M., Mabin M.C.G., 1984. Shore types of Victoria Land, Ross Dependency, Antarctica. *New Zealand Antarctic Record*, 5, 3, 23-40.

Gregory, M.R., Kirk, R.M., 1990. The shores of the Ross Sea. In: *Antarctica the Ross Sea Region*, (Hatherton, T. ed.), 85-95. DSIR Publishing, Wellington.

Griffith, D.A., Amrhein, C.G., 1991. *Statistical Analysis for Geographers*. Prentice Hall, New Jersey.

Gunn, B.M., Warren, G., 1962. Geology of Victoria Land between the Mawson and Mulock glaciers, Antarcitca. *New Zealand Geological Survey Bulletin*, 71.

Hall, B., Denton, G.H., 1994. Late Wisconsin / Holoceme history of the Wilson Piedmont glacier. *Antarctic Journal Review*, 20-22.

Hall, B. L., Denton, G.H ., 1999. New relative sea-level curves for the Southern Scott Coast, Antarctica: Evidence for Holocene deglaciation of the western Ross Sea. *Journal of Quaternary Science*, 14, 7, 641-650.

Hansom, J.D., 1983a. Ice-formed intertidal boulder pavements in the sub-Antarctic. *Journal of Sedimentary Petrology*, 53, 1, 135-145.

Hansom, J.D., 1983b. Shore platform development in the South Shetland islands, Antarctica. *Marine Geology*, 53, 211-229.

Hansom, J.D., Kirk, R.M., 1989. Ice in the intertidal zone: examples from Antarctica. *Essener Geografisce Arbeiten*, 18, 211-236.

Harper, J.R., 1990. Morphology of the Canadian Beaufort Sea Coast. *Marine Geology*, 91, 75-91.

Harrison, W., 1969. Empirical equations for foreshore changes over a tidal cycle. *Marine Geology*, 7, 529-551.

Hequette, A., Barnes, P.W., 1990. Coastal retreat and shoreface profile variations in the Canadian Beaufort Sea. *Marine Geology*, 91, 113-132.

Hume, J.D., Schalk, M., 1964. The effects of ice push on Arctic beaches. *American Journal of Science*, 262, 267-273.

Hume, J.D., Schalk, M., 1967. Shoreline processes near Point Barrow, Alaska: a comparison of the normal and the catastrophic. *Journal of the Arctic Institute of North America*, 20, 2, 86-103.

Huntley, D.J., Berger, G.W., Bowman S.G.E., 1988. Thermoluminescence responses to alpha and beta irradiations, and age determination when the high dose response is non-linear. *Radiation Effects*, 105, 279-284.

Huntley, D.J., Lian, O.B. 1999. Using optical dating to determine when a sediment was last exposed to sunlight. In: *Holocene climate and environmental changes in the Palliser Triangle: A geoscientific context for evaluating the impacts of climate change on the southern Canadian prairies*, (Lemmen D.S., Vance, R.E. eds.), 534. Geological Survey of Canada Bulletin in press.

Jopling, A.V., Walker, R.G., 1968. Morpholohy and origin of ripple-drift cross-lamination, with examples from the Pleistocene of Massachusetts. *Journal of Sedimentary Petrology*, 38, 4, 971-984.

Joyce, J. R. F., 1950. Notes on ice-foot development, Neny Fjord, Graham Land, Antarctica. *Journal of Geology*, 58, 646-649.

Kellogg, T.B., Truesdale, R.S., Osterman, L.E., 1979. Late Quaternary extent of the West Antarctic ice sheet: New evidence from Ross Sea cores. *Geology*, 7, 249-253.

Kellogg, T. Hughes, T. Kellogg, D., 1996. Late Pleistocene interactions of East and West Antarctic ice-flow regimes: evidence from the McMurdo Ice Shelf. *Journal of Glaciology*, 42, 142, 486-500.

Kempema, E.W., Reimnitz, E., Barnes, P.W., 1989. Sea-ice sediment entrainment and rafting in the Arctic. *Journal of Sedimentary Petrology*, 59, 2, 308-317.

King, C.A.M., Buckley, J. T., 1968. The analysis of stone size and shape in Arctic environments. *Journal of Sedimentary Petrology*, 38, 1, 200-214.

Kirk, R. M., 1966; Beach observations at Cape Royds, Ross Island, McMurdo Sound, Antarctica 1965-66. Unpublished Report, *Geography Department, University of Canterbury.*

Kirk, R.M., 1972. Antarctic beaches as natural hydraulic models. *Proceedings of the 7th New Zealand Geographical Conference, Hamilton*, 227-234.

Kirk, R.M., 1991. Raised beaches, late Quaternary sea-levels and deglacial sequences on the Victoria Land coast, Ross Sea, Antarctica. In: *Quaternary Research in Australian Antarctica: Future Directions*, (Gillieson, D.S. and Fitzsimons, S. eds.), Special Publication 3, 85-105. Department of Geography and Oceanography, Canberra.

Komar, P.D., 1998. *Beach processes and sedimentation.* 2nd Edition. Prentice Hall, New Jersey.

Krumbein, W.C., Graybill, F.A., 1965. *An introduction to statistical models in Geology.* McGraw-Hill, New York.

Kyle, P.K., 1976. Geology, mineralogy and geochemistry of the late Cenozoic McMurdo volcanic group, Victoria Land, Antarctica. Unpublished PhD thesis, Victoria University of Wellington.

Laing, A.K., Gorman, R.M., 2000. The ocean wave climate around New Zealand from satellites and modelling. *Water and Atmosphere,* 8, 1, 20-23.

Leeder, M.R., 1983. *Sedimentology.* George Allen and Unwin, London.

Licht, K.J., Jennings, A.E., Andrews, J.T., Williams, K.M., 1996. Chronology of late Wisconsin ice retreat from the western Ross Sea, Antarctica. *Geology,* 24, 3, 223-226.

Lien, R., Solheim, A., Elverhoi, A., Rokongen, K., 1989. Iceberg scouring and sea bed morphology on the eastern Weddell Sea shelf, Antarctica. *Polar Research,* 7, 4, 43-57.

Lingle, C.S., Clark, J.A., 1979. Antarctic ice-sheet volume at 18000 years B.P. and Holocene sea-level changes at the west Antarctic margin. *Journal of Glaciology,* 24, 90, 213-230.

Mabin, M.C.G., 1986. Glacial Geology of Spike Cape, McMurdo Sound. *Antarctic Journal of the United States,* 21, 88-89.

MacCarthy, G.R., 1953. Recent changes in the shoreline near Point Barrow, Alaska. *Journal of the Arctic Institute of North America*, 6, 1, 44-51.

Marsh, WM., Marsh, B.D., Dozier, J., 1973. Formation, structure, and geomorphic influence of Lake Superior icefoots. *American Journal of Science*, 273, 48-64.

McCann, S.B. Dale, J.E. Hale, P.B., 1981. Ice conditions and effects in a macrotidal subarctic environment, southeast Baffin Island. *Workshop on Ice Action on Shores*, 105-115.

McCann, S.B. Owens, I.H., 1969. The size and shape of sediments in three arctic beaches, Southwest Devon Island, N.W.T., Canada. *Arctic and Alpine Research*, 1, 4, 267-278.

McCann, S.B. Owens, E.H., 1970. Plan and profile characteristics of beaches in the Canadian Arctic Archipelago. *Shore and Beach*, 38, 2, 26-30.

McCann, S.B., Taylor, R.B., 1975. Beach freezeup at Radstock Bay, Devon Island, Arctic Canada. *Arctic and Alpine Research*, 7, 4, 379-386.

McLaren, P., 1980. The Coastal Morphology and Sedimentology of Labrador: A Study of Shoreline Sensitivity to a Potential Oil Spill. *Geological Survey of Canada*, 79-28.

McLean, R.F., Kirk, R.M., 1969. Relationships between grain size, size-sorting, and foreshore slope on mixed sand-shingle beaches. *New Zealand Journal of Geology and Geophysics*, 12, 1, 138-155.

Meylan, M.H., Squire, V.A., 1994. Response of a circular ice floe to ocean waves. *Journal of Geophysical Research,* 101, 4, 8869-8884.

Miner, J.J., Powell, R.D, 1991. An evaluation of ice-rafted erosion caused by an icefoot complex, Southwestern Lake Michigan, U.S.A. *Arctic and Alpine Research,* 23, 3, 320-327.

Moore, G.W., 1966. Arctic Beach Sedimentation. In: *Environment of the Cape Thompson region Alaska,* (Wilimovsky, N.J., ed.), 587-608. United States Committee on Environmental Studies for Project Chariot, United States Atomic Energy Commission.

Mosley, M.P., Tindale, D.S., 1985. Sediment variability and bed material sampling in gravel-bed rivers. *Earth Surface Processes and Landforms.* 10, 465-482.

Naval Oceanography Command Detatchment (NOCD), 1985. *Sea-ice climatic atlas: Volume 1 Antarctic,* Naval Oceanography Command Detatchment, Ashville.

Nichols, R.L., 1953. Marine and lacustrine ice-pushed ridges. *Journal of Glaciology,* 2, 172-174.

Nichols, R.L., 1961. Characteristics of beaches formed in polar climates. *American Journal of Science,* 259, 694-708.

Nichols R.L., 1966. Geomorphology of Antarctica. In: *Antartctic soils and soil forming processes*, (Tedrow, J.C.F., ed.), 1-46, Antarctic Research Series 8, American Geophysical Union.

Nichols, R.L., 1968. Coastal geomorphology, McMurdo Sound, Antarctica. *Journal of Glaciology*, 7, 51, 449-478.

Owens, E.H., McCann, S.B., 1970. The role of ice in the arctic beach environment with special reference to Cape Ricketts, Southwest Devon Island, Northwest Territories, Canada. *American Journal of Science*, 268, 397-414.

Philip, A.L., 1990. Ice pushed boulders on the shores of Gotland Sweeden. *Journal of Coastal Research*, 6, 3, 661-676.

Postma, G., Nemec, W., 1990. Regressive and transgressive sequences in a raised Holocene gravelly beach, southwestern Crete. *Sedimentology*, 37, 907-920.

Powers, M.C., 1953. A new roundness scale for sedimentary particles. *Journal of Sedimentary Petrology*, 23, 2, 117-119.

Priestly, R.E., 1909. Appendix 3. Scientific Results of the Western Journey. IN: *The Heart of the Antarctic*, (Shackleton, E.H. ed.) 2, 268-314. Willian Heinemann, London.

Prestcott, J.R., Hutton, J.T., 1994. Cosmic ray contributions to dose rates for luminescence and ESR dating: large depths and long-term variations. *Radiation Measurements*, 23, 2/3, 497-500.

Rector, R.L., 1954. Laboratory studies of the equilibrium profile of beaches. U.S. Army Corps of Engineers, Beach Erosion Board, Technical Memo 41.

Reimnitz, E., Barnes, P., Forgatsch, T., Rodieck, C., 1972. Influence of grounding ice on the Arctic shelf of Alaska. *Marine Geology*, 13, 323-334.

Reimnitz, E., Barnes, P.W., Toimil, L.J., Melchior, J., 1977. Ice gouge recurrence and rates of sediment reworking, Beaufort Sea, Alaska. *Geology*, 5, 405-408.

Reimnitz, E., Barnes, P.W., Harper, J.R., 1990. A review of beach nourishment from ice transport of shoreface materials, Beaufort Sea, Alaska. *Journal of Coastal Research*, 6, 2, 439-470.

Reimnitz, E., Kempema, E., 1982. Dynamic ice-wallow relief of Northern Alaska's nearshore. *Journal of Sedimentary Petrology*, 52, 2, 451-461.

Reimnitz, E., Kempema, E.W., Barnes, P.W., 1987. Anchor ice, seabed freezing, and sediment dynamics in shallow arctic seas. *Journal of Geophysical Research*, 92, 14,671-14,678.

Reimnitz, E., Toimil, L., Barnes, P., 1978. Arctic continental shelf morphology related to sea-ice zonation, Beaufort Sea, Alaska. *Marine Geology*, 28, 179-210.

Reinson, G. E., Rosen, P. S., 1982. Preservation of ice-formed features in a subarctic sandy beach sequence: Geologic implications. *Journal of Sedimentary Petrology*, 52, 2, 463-471.

Rex, R. W., 1964. Arctic beaches, Barrow, Alaska. In: *Papers in Marine Geology*, (Miller, R. L., ed.), 384-400. The McMillian Co.

Rosen, P.S., 1978. Degradation of ice-formed beach deposits. *Maritime Sediments*, 14, 2, 63-68.

Rowe, G.H., 1990. *Sea level measurements in McMurdo Sound Antarctica*. The Department of Survey and Land Information, Wellington.

Roy, P.S., Powell, P.J., Ferland, M.A., Thom, B.G., 1994. Wave dominated coasts. In: *Coastal evolution, Late Quaternary shoreline morphodynamics*. (Carter, R.W.G., Woodroffe, C.D. eds). Cambridge University Press Cambridge.

Shaw, J., Taylor, R.B., Forbes, D.L., 1990. Coarse clastic barriers in Eastern Canada: Patterns of Glaciogenic Sediment dispersal with rising sea levels. *Journal of Coastal Research*, 9, 160-200.

Shephard, F.P., 1963. *Submarine Geology*. Harper and Row, New York.

Shih, S., Komar, P.D., 1994. Sediments, beach morphology and sea cliff erosion within an Oregon Coast littoral cell. *Journal of Coastal Research*, 10, 1, 144-157.

Short, A.D., Wiseman, W.J., 1974. Freezeup processes on Arctic beaches. *Arctic*, 27, 3, 215-224.

Sneed, E.D., Folk, R.L., 1958. Pebbles in the lower Colorado River, Texas. A study in particle morphogenesis. *Journal of Geology*, 66, 114-150.

Squire, V.A., Moore, S.C., 1980. Direct measurement of the attenuation of ocean waves by pack ice. *Nature*, 283, 365-368.

Stuiver, M., and Reimer, P.J., 1993. Extended 14C database and revised CALIB radiocarbon calibration program. *Radiocarbon*, 35, 215-230.

Stuiver, M., Denton, G.H., Hughes, T.J., Fastook, J.L., 1981. History of the Marine ice sheet in West Antarctica during the last glaciation: A working hypothesis. In: *The Last Great Ice Sheets*, (Stuiver, M., Denton, G.H., Hughes, T.J., eds.), 319-416, New York, Wiley Interscience.

Taylor, G., 1922. British (Terra Nova) Antarctic expedition 1910-1913. *The Physiography of the McMurdo Sound and Granite Harbour region*. Harrison and Sons, London.

Taylor, R.B., McCann, B., 1976. The effect of sea and nearshore ice on coastal processes in Canadian Arctic archipelago. *Rev. Geogr. Montreal*, 30, 1-2, 123-132.

Taylor, R.B., 1978. The occurrence of grounded ice ridges and shore ice piling along the Northern coast of Somerset Island, N.W.T. *Arctic*, 31, 2, 133-149.

Taylor, R.B., 1980. Coastal environments along the Northern shore of Somerset Island, district of Franklin. *Geological Survey of Canada*, 80-10, 239-250.

Tricart, J., 1970. *Geomorphology of cold environments.* MacMillan and CO, Limited, London.

van Andel, T.J.H., Wiggers, A.J., Maarleveld, G., 1954. Roundness and shape of marine gravels from Urk (Netherlands), a comparison of several methods of investigation. *Journal of Sedimentary Petrology*, 24, 2, 100-116.

Walker, R.G., Plint, A.G., 1992. Wave and storm dominated shallow marine systems. IN: *Facies models response to sea level change.* (Walker, R. G., James, N. P. eds.), 219-238, Geological Association of Canada, Ontario.

Washburn, A.L., 1973. *Periglacial processes and environments.* Edward Arnold, London.

Weigel, R.L., 1964. *Oceanographical Engineering.* Englewood Cliffs New Jersey, Prentice Hall.

Wright, C.S. Priestley, R.E., 1922. *British (Terra Nova) Antarctic Expedition 1910-1913. Glaciology.* Harrison and Sons, London.

Glossary of terms

Circular depressions shallow depressions left behind when a boulder is removed by ice

Ice pile-up *"similar to ice ride up but accompanied by buckling and crumbling of an advancing sheet of ice"* (Reimnitz et al., 1990).

Ice ride-up *"a process in which a sheet of ice slides smoothly landward across a low relief beach and steeper relief areas beyond for distances as great as 800m, but generally much shorter"* (Reimnitz et al., 1990).

Icefoot that part of the sea-ice that is frozen to the shore

Ice-lifted landforms *"occur during the rise and fall of tides or the thermal expansion of floating ice"* (Gilbert, 1990).

Ice-push ridgea semi-continuous ridge that has been bulldozed into place by sea-ice or ice-pushed boulders (see ice-pushed landforms).

Ice-pushed landforms a landform that has been pushed by sea-ice that has been moved by winds and currents (see ice-push ridge).

Kaimoo *"the name given by the Eskimo to an ice and gravel rampart formed in winter on the surface of Arctic beaches"* (Moore, 1966).

Melt pit a concave feature produced by the melting of ice beneath beach sediments or the melting of ice thrown or pushed onto the beach.

A SHORE-BASED KITE-DEPLOYMENT SYSTEM FOR MEASURING OFFSHORE PROFILES.

Edward R. T. Butler

Antarctic Research Centre, School of Earth Science

Victoria University of Wellington

PO Box 600

Wellington

New Zealand

Abstract

A shore-based kite-deployment system for measuring nearshore profiles in remote field areas is described. The Supa Kite™ system was used successfully on beaches in McMurdo Sound, Antarctica where it was impractical to use a boat or swim equipment offshore. A Unidata model 6508 D water depth probe was deployed 35 m offshore using the Supa Kite™. The transducer was pulled ashore at 1 m intervals marked off on a cable so depths at a given distance from shore could be measured. These depths were then corrected for the slope of the sea floor and an offshore profile was constructed.

Index words; profiles, instrumentation.

Introduction

The measurement of nearshore profiles in many field locations can present a problem either because it is too dangerous to enter the water or getting a boat to the area is impractical. In the 1997/1998 austral summer field season in McMurdo Sound Antarctica, six offshore profiles were measured using a Unidata model 6508 D water depth probe connected to a Campbell CR10 datalogger and a Supa Kite™ shore-based fishing kite. During the field season, 6 separate offshore profiles were measured by deploying the pressure transducer to a distance of up to 35m offshore. Distances from the pressure transducer marked on the cable allowed an offshore profile to be constructed, which could then be corrected for the offshore slope.

The kite deployment system

The Supa Kite™ used in this study was developed and manufactured by Pauls Fishing Kites® in Auckland New Zealand. It is constructed from lightweight ripstop nylon fabric and carbon fibre tubes. Figure shows the dimensions of the Supa Kite™. The cross member is constructed from 10mm wooden dowel so that if winds exceed a certain threshold, the dowel will break and the kite will remain undamaged.

The rig for deploying sensors to measure offshore profiles and the rig developed by Pauls Fishing Kites in Auckland New Zealand® for shore-based fishing are essentially the same. As shown in Figure , two lines are attached to the kite, a "control line" and a "float line". The lines used were 55kg (120 pound) breaking strain monofilament fishing line attached to the kite with stainless steel snaplinks. The kite is released and initially flown using the "control line" allowing the "float line" to be released. When the "float line" becomes tight, a floating weight (a 2 litre bottle ½ filled with sand weighing approximately 2.5kg was used in this study) is attached to the end of the "float line" and the sensor is attached to the floating weight with a soluble candy release (a Lifesaver™ or Polo Mint™ was used, see Figure). The "control line" is then allowed to go slack while the "float line" flies the kite and pulls the transducer offshore.

The floating weight attached to the float line allows the kite to pull weights offshore but prevents the kite from lifting the entire rig from the water. The floating weight is connected to the sensor by a candy, which dissolves and eventually releases the sensor, which sinks to the sea floor. (During the field trials a Lifesaver™ or Polo Mint™ was found to last about 5 minutes before dissolving and releasing the sensor). Once the kite has been recovered using the "control line" the sensor can be pulled ashore at predetermined intervals marked on the cable and depth readings can be taken with respect to distance from the shore, which can subsequently be corrected for the slope of the sea floor.

The kite can fly in windspeeds from 10 to 50 knots. Although the kite requires an offshore wind to deploy the transducer rig, it can be tacked by attaching weights to the spars. The maximum reported tack achieved was 80° in a 10 knot wind (Pauls Fishing Kites, 1998), thereby allowing the kite to be used under a range of offshore wind directions. Transducer cables up to 60m were tested but the windspeed required to deploy these longer rigs (30 knots) was seldom attained. Alternatively a water depth probe complete with data logger could be deployed and recovered using a weighted line allowing considerably longer offshore profiles to be constructed.

Typical results, collected on February 8th 1998 as an extension of a shore-based survey undertaken at Cape Bird, McMurdo Sound, Antarctica, are shown in Figure. The Unidata model 6508 D water depth probe was deployed 33.5 m offshore and pulled ashore at 1 m intervals that were marked at a distance from the pressure transducer. Distance from shore was then corrected for the slope of the sea floor by calculating individual angles at 1 m intervals. (This assumes that the cable was lying on the sea floor, and that the slope between each 1m point was constant).

Conclusions

A shore-based kite deployment system has been described that can be used to obtain data on the physical nature of offshore profiles in field areas where the use of more conventional techniques is impractical. The deployment system may be used under a wide range of offshore wind directions and windspeeds which during field trials, allowed pressure transducers to be deployed 60m offshore. Data collected in the field allowed offshore profiles to be to a distance of 40m offshore.

Acknowledgements

This work would not have been possible without the financial assistance of a Victoria University of Wellington graduate grant. Thanks to Alex Pyne and Eric Broughton who helped with the selection of suitable pressure transducers, dataloggers and the kite. Thanks also to Anita Foy for help testing and refining flying of the kite and Pauls Fishing Kites for help with designing a suitable rig. Staff of Antarctica New Zealand at Scott Base and Christchurch helped throughout the field seasons in Antarctica.

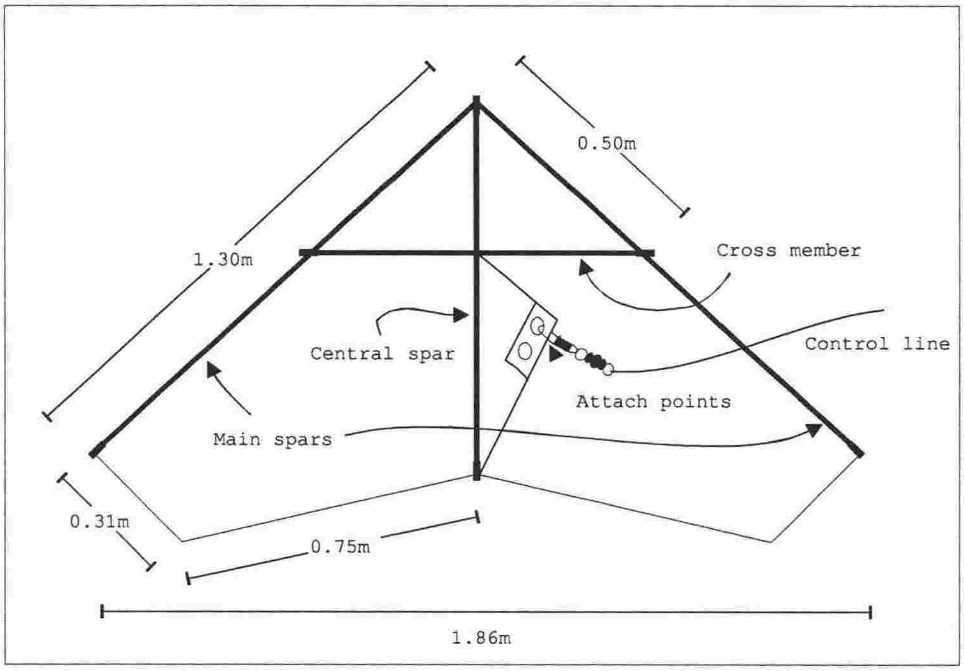

Figure 1. Schematic diagram of the Supa Kite™. The main kite spars are made of 0.5mm carbon fibre tubing. The central spar is made of 0.65mm carbon fibre tubing and the cross member is made of 10mm wooden dowel.

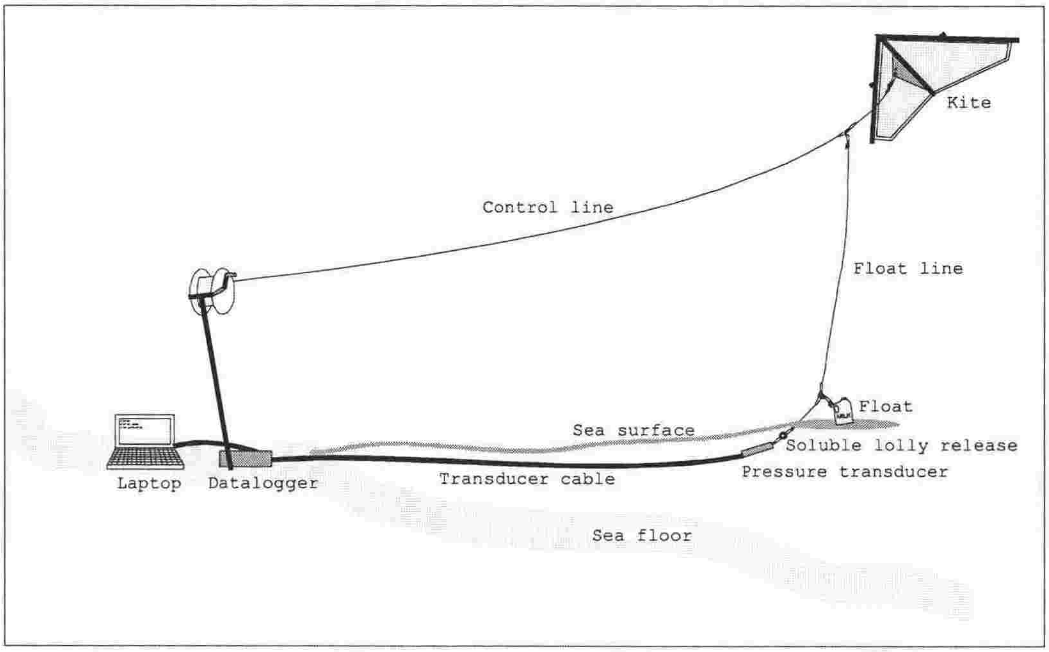

Figure 2. The transducer deploying rig.

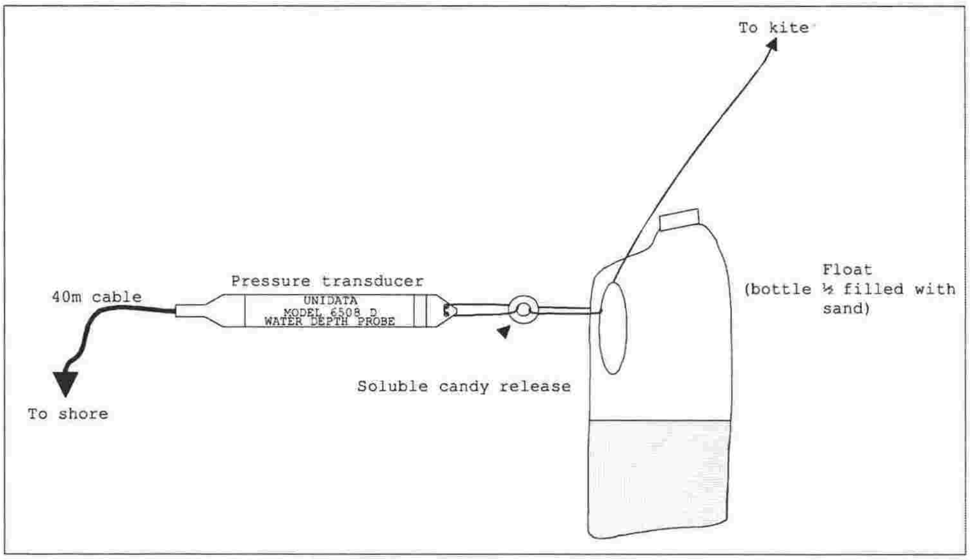

Figure 3. Expanded view of the mechanism used to release the transducer. When the soluble candy release dissolves the transducer and transducer cable sink to the sea floor where they can be retrieved at predetermined intervals.

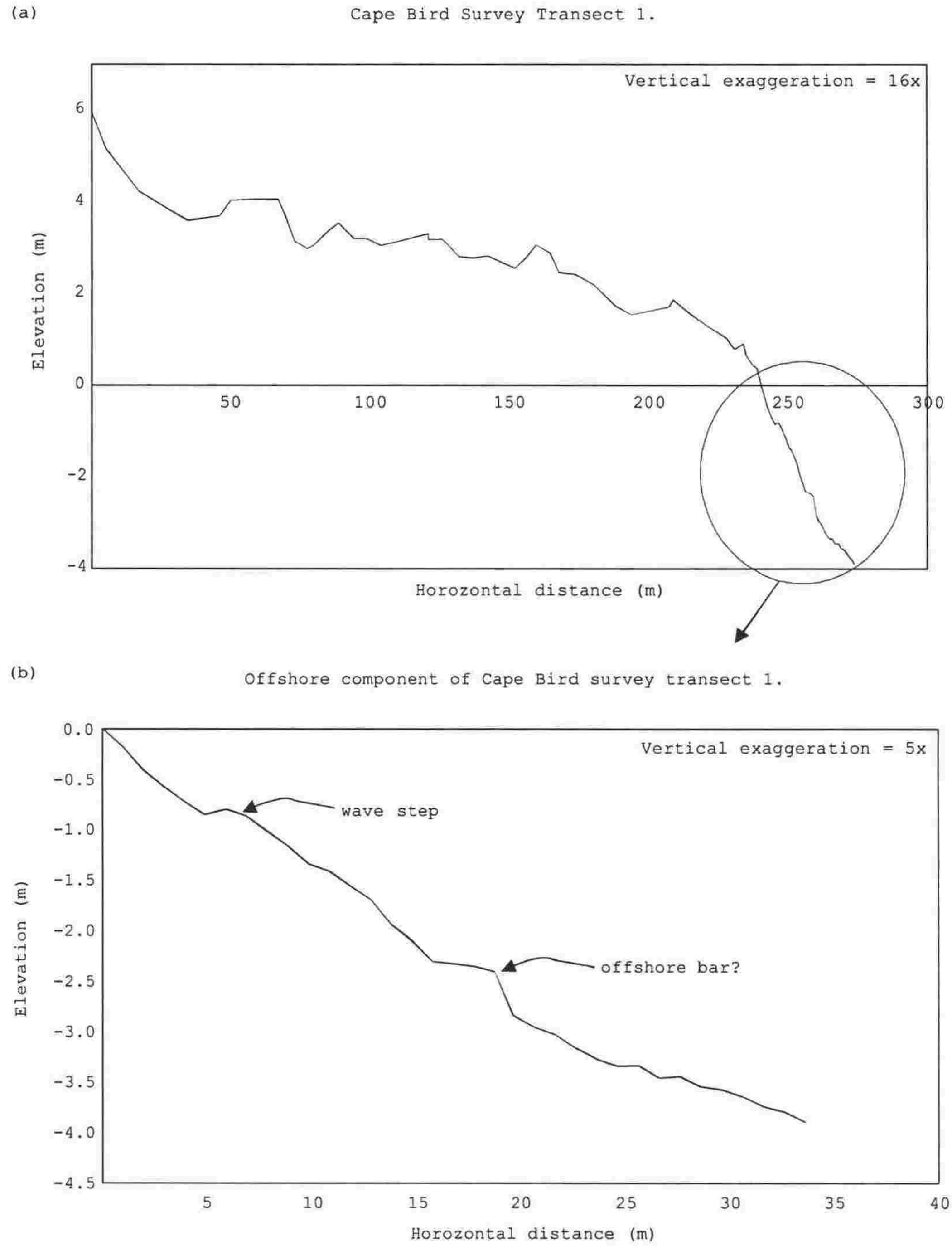

Figure 4. Profile of Cape Bird beach with offshore profile (a). Expanded view of offshore profile showing some offshore features (b).

Luminescence sample preparation.

Sample preparation was started on May 20 1999 and was finished for all 8 samples on June 15 1999. Sample preparation is undertaken so that only the feldspar or quartz grains between 4μ and 11μ are dated. Sample preparation involved adding hydrochloric acid to the sample (to remove the carbonates), adding hydrogen peroxide (to remove the organics), adding a solution of sodium citrate, sodium bicarbonate and sodium dithionate (sodium citrate 71g, sodium bicarbonate 8.5g, sodium dithionate 2g to 1 litre of water) (to etch any iron coating the grains may have, an iron coating may inhibit the release of light from the grains) and finally a settling regime is employed to separate the size fraction between 4μ and 11μ. Once the 4μ to 11μ grains have been separated, they are placed in a solution of acetone. Aluminium disks 10mm in diameter and 0.5mm thick are etched with hydrofluoric acid and placed in a small amount of acetone in a 3ml vial. Following this, 1ml of a set concentration of acetone and sample is added to the vial. As the acetone evaporates off, the sample in the solution settles onto the aluminium disk at the bottom of the vial. Due to the lack of fine material an ideal number of disks (60) was not produced for all samples. Table 3.3 shows the number of disks made for each sample.

Sample name	Number of disks
Bernacchi 1	46
Bernacchi 2	10
Marble 1	60
Marble 2	60
Kolich 1	18
Spike 1	30
Barne 1	60
Barne 2	60

Table 1. Number of disks made for each sample. Ideally 60 disks would have been made for each sample but a lack of fine material in some samples made this impossible.

Bernacchi 1	
6 disks	natural
3 disks	natural + 10 Gy β
3 disks	natural + 20 Gy β
3 disks	natural + 40 Gy β
3 disks	natural + 80 Gy β
4 disks	natural + 10 Gy β + bleach
2 disks	natural + 20 Gy β + bleach
2 disks	natural + 40 Gy β + bleach
2 disks	natural + bleach
2 disks	natural + no preheat
Bernacchi 2	
3 disks	natural
2 disks	natural + 20 Gy β
2 disks	natural + 40 Gy β
2 disks	natural + bleach
Marble 1	
6 disks	natural
3 disks	natural + 10 Gy β
3 disks	natural + 20 Gy β
3 disks	natural + 40 Gy β
3 disks	natural + 80 Gy β
3 disks	natural + 160 Gy β
4 disks	natural + bleach
2 disks	natural + 20 Gy β + bleach
2 disks	natural + 40 Gy β + bleach
2 disks	natural + 80 Gy β + bleach
2 disks	natural + no preheat
2 disks	natural + bleach + no preheat
3 disks	natural + 105 min. α
3 disks	natural + 210 min. α
3 disks	natural + 420 min. α
Kolich 1	
5 disks	natural

3 disks	natural + 10 Gy β
3 disks	natural + 50 Gy β
2 disks	natural + bleach
2 disks	natural + 30 Gy β + bleach
2 disks	natural + no preheat
Spike 1	
6 disks	natural
3 disks	natural + 20 Gy β
3 disks	natural + 40 Gy β
3 disks	natural + 80 Gy β
3 disks	natural + 160 Gy β
4 disks	natural + bleach
2 disks	natural + 30 Gy β + bleach
2 disks	natural + 100 Gy β + bleach
2 disks	natural + no preheat
1 disk	natural

Table 2. Luminescence experiments performed on dated samples.

Sample	***Mean***	***Std. Deviation***	***Skewness***	***Kurtosis***
Bernacchi 2 Ice	-5.75	0.50	0.00	0.81
Bernacchi 3 Ice 1	-5.57	0.50	0.33	0.82
Bernacchi 3 Ice 2	-5.56	0.55	-0.39	0.88
Bernacchi 3 H1 U1	-5.44	0.34	-0.28	1.15
Bernacchi 3 H5	1.56	1.91	-0.65	2.16
Bernacchi 3 H4 U2 and 3	-1.20	3.32	-0.57	0.58
Bernacchi 3 H3 U1 and 2	0.50	2.31	-0.61	1.23
Bernacchi 3 H2 U1 to 4	-0.52	2.36	-0.23	0.64
Marble 1 H1	-5.65	0.64	-0.06	1.00
Marble 1 H2	-5.79	0.72	-0.33	0.95
Marble 1 H3 U2 and 3	-5.79	0.57	-0.14	1.30
Marble 1 H3 U1	2.03	1.58	-0.31	1.61
Marble 1 H4	-5.55	0.64	-0.06	1.16
Marble 2 H1 U1	-2.71	1.79	0.55	0.89
Marble 2 H1 U2	-5.79	0.49	-0.11	0.85
Marble 2 H2 U1	-0.97	1.80	-0.33	0.99
Marble 2 H3 U1 to 3	-5.55	0.73	-0.09	0.98
Marble 2 H3 U1	0.03	1.58	-0.31	1.61
Marble 2 H4	-5.45	0.58	-0.19	0.89
Marble 2 H5 AU	0.31	0.91	0.15	1.13
Marble 2 H6 AU	0.65	1.39	-0.38	1.81
Marble 3 H7	-5.86	0.58	-0.05	0.79
Marble 3 H8	-5.57	0.60	0.02	0.88

Kolich 1 BC1	-8.98	0.38	-0.09	0.88
Kolich 1 BC2	-8.50	0.37	0.00	0.89
Kolich 1 BC3	-9.04	0.46	0.20	0.67
Kolich 1 BC4	-9.08	0.25	-0.47	0.92
Kolich 1 BC5	-9.37	0.25	0.27	0.88
Kolich 1 BC6	-9.70	0.22	-0.04	0.92
Kolich 2 H2	-6.09	0.58	-0.24	0.78
Kolich 3 U1	1.55	0.69	0.13	1.07
Kolich 3 U2	1.49	0.85	0.19	1.17
Kolich 3 U3	1.24	1.28	-0.29	2.61
Kolich 3 U4	1.42	0.69	0.16	1.00
Kolich 3 U5	1.83	0.63	-0.04	1.05
Kolich 3 H1	1.41	0.82	0.06	0.95
Spike Barrier C1	-5.54	0.49	0.02	1.01
Spike Barrier C2	-6.02	0.45	-0.18	1.25
Spike Barrier C3	-6.30	0.72	-0.14	0.97
Spike Barrier C4	-6.56	0.48	-0.19	1.06
Spike 1 H1	-6.46	1.19	0.12	0.67
Spike 1 H2	-6.55	1.47	-0.17	0.76
Spike 1 H3	-6.46	0.53	-0.01	1.53
Spike 2 H1	-5.52	0.64	-0.14	0.76
Spike 2 H2 U1	-0.23	0.96	-0.24	1.37
Spike 2 H2 U2	-0.17	0.83	-0.18	0.98
Spike 2 H2 U3	-2.13	1.71	0.22	0.88
Spike 2 H2 U4	-2.02	1.82	0.39	1.16
Spike 2 H2 U5	0.46	1.24	-0.37	1.39

Dunlop 2 H1 AU	-5.84	0.54	0.17	0.83
Dunlop 2 H2 AU	-5.57	0.58	-0.02	1.14
Dunlop 2 C1	-5.92	0.50	-0.37	0.87
Dunlop 2 C4	-5.52	0.45	-0.11	0.90
Dunlop 2 C5	-5.80	0.40	-0.30	1.05
Dunlop 2 C6	-5.52	0.39	-0.05	0.85
Dunlop 2 Ice-push	-5.71	0.57	-0.52	0.92
Dunlop 1 Ice-push	-5.35	0.39	-0.14	0.75
Dunlop R1 BC	-9.44	0.13	-0.09	1.07
Dunlop R2 BC	-8.08	0.25	-0.47	0.92
Dunlop R3 BC	-8.47	0.13	-0.05	1.01
Dunlop R5 BC	-7.26	1.51	0.79	0.44
Dunlop R6 BC	-9.42	0.25	0.47	0.92
Dunlop R1	-6.33	0.40	-0.20	0.73
Dunlop R2	-6.15	0.32	0.10	1.00
Dunlop R3	-5.97	0.42	0.22	0.68
Dunlop R5	-6.13	0.32	0.07	0.95
350m south Bird 2	-3.51	0.57	-0.10	0.89
250m south Bird 2	-3.31	0.69	-0.05	0.79
100m south Bird 2	-2.34	2.45	0.50	0.58
Bird 2	0.99	0.64	-0.14	1.01
150m north Bird 2	0.70	0.52	0.03	1.07
Bird 2 H1	-5.47	0.58	-0.05	0.87
Bird 2 H2 U1 and 2	-1.50	1.80	0.44	0.70
Bird 2 H3	-5.56	0.68	0.15	0.74
Bird 2 H4	-5.46	0.47	-0.28	1.14
Bird 2 H5	-2.95	0.55	-0.06	1.11

Bird 2 H6	-5.47	0.42	-0.03	0.77
Bird 2 H7	-5.44	0.36	-0.19	0.96
Bird 2 H8	-2.25	1.93	0.60	1.07
Bird ice-push	-4.90	0.31	-0.05	0.98
Royds 1	0.13	1.01	0.52	1.21
Royds 2	-0.60	1.69	0.36	0.89
Royds 3	-1.06	0.95	0.02	1.07
Royds 4	-0.71	1.15	0.01	0.86
Royds 5	-0.44	0.76	0.15	1.52
Royds 6	0.24	0.65	0.00	1.26
Royds 7	-0.02	0.82	-0.28	1.27
Royds 8	0.24	1.06	-0.28	1.04
Royds ice-base	-0.91	1.44	-0.35	0.66

Table 1 (Appendix 4). 'Graphic' statistics of sediment samples.

Reprinted from

MARINE GEOLOGY

INTERNATIONAL JOURNAL OF MARINE GEOLOGY, GEOCHEMISTRY AND GEOPHYSICS

Marine Geology 162 (1999) 105–120

Process environments on modern and raised beaches in McMurdo Sound, Antarctica

Edward R.T. Butler *

Antarctic Research Centre, Victoria University of Wellington, PO Box 600, Wellington, New Zealand

Received 14 October 1998; accepted 19 May 1999

ELSEVIER

MARINE GEOLOGY

Scope of the journal

Marine Geology is an international medium for the publication of original studies and comprehensive reviews in the field of Marine Geology, Geochemistry and Geophysics. The editors endeavour to maintain a high scientific level and it is hoped that with its international coverage the journal will contribute to the sound development of this field.

A *letter section* is provided as a publication outlet for short papers which require *rapid* publication.

Publication information

Marine Geology (ISSN 0025-3227). For 1999, volumes 153—161 are scheduled for publication. Subscription prices are available upon request from the Publisher or from the Regional Sales Office nearest you or from this journal's website (http://www.elsevier.nl/locate/margeo). Further information is available on this journal and other Elsevier Science products through Elevier's website: (http://www.elsevier.nl). Subscriptions are accepted on a prepaid basis only and are entered on a calendar year basis. Issues are sent by standard mail (surface within Europe, air delivery outside Europe). Priority rates are available upon request. Claims for missing issues should be made within six months of the date of dispatch.

Orders, claims, and product enquiries: please contact the Customer Support Department at the Regional Sales Office nearest to you:

New York: Elsevier Science, P.O. Box 945, New York, NY 10159-0945, USA; phone: (+1) (212) 633 3730 [toll free number for North American customers: 1-888-4ES-INFO (437-4636)]; fax (+1) (212) 633 3680; e-mail: usinfo-f@elsevier.com

Amsterdam: Elsevier Science, PO Box 211, 1000 AE Amsterdam, The Netherlands; phone: (+31) 20 4853757; fax: (+31) 20 4853432; e-mail: nlinfo-f@elsevier.nl

Tokyo: Elsevier Science K.K., 9-15 Higashi-Azabu 1-chome, Minato-ku, Tokyo 106-0044, Japan; phone: (+81) (3) 5561 5033; fax: (+81) (3) 5561 5047; e-mail: info@elsevier.co.jp

Singapore: Elsevier Science, No. 1 Temasek Avenue, #17-01 Millenia Tower, Singapore 039192; phone: (+65) 434 3727; fax: (+65) 337 2230; e-mail: asiainfo@elsevier.com.sg

Rio de Janeiro: Elsevier Science, Rua Sete de Setembro 111/16 Andar, 29959-002 Centro, Rio de Janeiro - RJ, Brazil; phone: (+55) (21) 509 1991; e-mail: elsevier@campus.com.br [Note (Latin America): for orders, claims and desk information, please contact the Regional Sales Office in New York as listed above]

∞ The paper used in this publication meets the requirements of ANSI/NISO Z39.48-1992 (Permanence of Paper).

PRINTED IN THE NETHERLANDS

ELSEVIER

Marine Geology 162 (1999) 105–120

MARINE GEOLOGY
INTERNATIONAL JOURNAL OF MARINE GEOLOGY, GEOCHEMISTRY AND GEOPHYSICS

www.elsevier.nl/locate/margeo

Process environments on modern and raised beaches in McMurdo Sound, Antarctica

Edward R.T. Butler *

Antarctic Research Centre, Victoria University of Wellington, PO Box 600, Wellington, New Zealand

Received 14 October 1998; accepted 19 May 1999

Abstract

Modern beaches in McMurdo Sound can be divided into three process regimes. Beaches on Ross Island (eastern McMurdo Sound) are characterised by normal marine processes with little ice modification. On ice-bound western McMurdo Sound, coastal orientation is of paramount importance. Ice thrust features are prominent on south facing beaches, which are open to the predominant wind direction, while more marine dominated beaches occur on north facing coasts where sea ice is blown offshore. In contrast to the modern beaches, raised beaches are similar all around McMurdo Sound. These are inferred to be storm ridges. The size and frequency of the ridges is a product of the local wave climate. The number of raised beaches at any site is a useful indicator of the paleo-wave climate. More ridges occur in sheltered south facing locations, because they are more protected from open marine conditions, than on beaches in ice-free or north facing locations. This is important for rebound reconstructions in the Sound as marine limits have been incorrectly identified in the past. © 1999 Elsevier Science B.V. All rights reserved.

Keywords: McMurdo Sound Antarctica; raised beaches; paleo-wave climate; storm deposits

1. Introduction

There have been very few investigations of Antarctica beaches as geomorphological features (Nichols, 1961, 1966, 1968; Kirk, 1966, 1972, 1991; Gregory and Kirk, 1990; Gregory et al., 1984). Nichols (1961; 1966; 1968) stressed the dominance of ice processes on the beaches while Kirk (1966; 1972) showed that marine processes produced some of the beaches. Despite Kirks' work, the concept that Antarctic beaches are the product of ice processes has become established in the literature (Owens, 1982; Gregory et al., 1984; Hansom and Kirk, 1989). Although there is an extensive literature on Arctic beaches (Hequette and Barnes, 1990; Reimnitz et al., 1990; Forbes and Taylor, 1994; Dionne, 1998) it appears that despite the similar processes that these areas share, beach morphologies are site specific.

There is widespread interest in determining Holocene sea levels around Antarctica as they are used as proxies for rebound in reconstructions of past ice sheets (Korotkevich, 1971; Simeoni et al., 1989; Baroni and Orombelli, 1991; Kirk, 1991; Colhoun et al., 1992; Igarashi et al., 1995; Hjort et al., 1997; Zwartz et al., 1997, 1998). Most of these studies are simplistic in their application of raised beaches, making assumptions about the formation, heights and genesis of the features that are, at best,

* Fax: +64-4-495-5186; E-mail: edward.butler@vuw.ac.nz

PII: S0025-3227(99)00061-4

poorly supported. There is an obvious need for work in this area, both to understand the dynamics of coastal evolution on polar coastlines and as a test of the reliability of the data inputs for ice sheet reconstructions. This paper addresses these issues.

2. Coastal setting

2.1. Physiography

Very little (3–5%) of the Antarctic shoreline is ice-free (Dubrovin, 1979). McMurdo Sound, is unusual with 36.5% of the coast from Cape Bird to Gregory Island ice-free, however only 1.5% of this section of coastline comprises beaches (Taylor, 1922). This paper focuses on the sedimentary beaches in McMurdo Sound (Fig. 1). These beaches consist of reworked glacial deposits. The glacial deposits on the western side of the sound consist of coarsely crystalline marble, gneiss, and granodiorite rocks that are intruded by finer microgranodiorite and basaltic dykes (Gunn and Warren, 1962). The deposits on the eastern side of the Sound consist of Ross Island volcanics which are mainly basanite and phonolite. The glacial deposits are very angular, very poorly sorted and chaotic in appearance. The size of

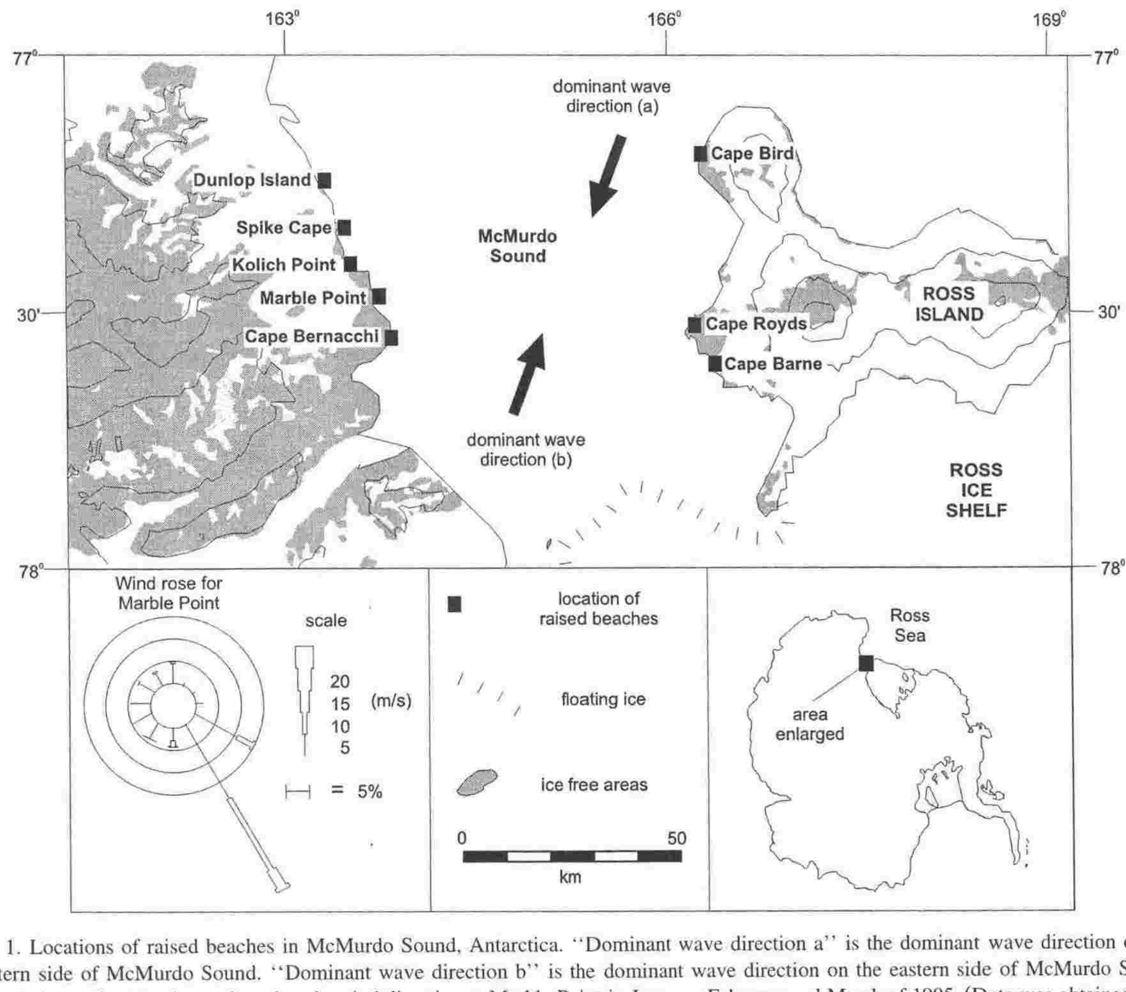

Fig. 1. Locations of raised beaches in McMurdo Sound, Antarctica. ''Dominant wave direction a'' is the dominant wave direction on the western side of McMurdo Sound. ''Dominant wave direction b'' is the dominant wave direction on the eastern side of McMurdo Sound. The windrose diagram shows three-hourly wind direction at Marble Point in January, February and March of 1995. (Data was obtained from University of Wisconsin).

the undisturbed glacial deposits ranges from large boulders (up to 2-m diameter) to fine sand.

Large areas on many of the modern beaches display evidence of ice action on the shores. Poorly rounded and sorted sediments with only weak imbrication are common. In other areas the beaches have well-sorted, well-rounded and well-imbricated sediments which contrast with the glacial deposits that can often be found directly above the beaches. The maximum level of marine action (often the highest beach ridge in an area) at any site is termed the marine limit. Fig. 2 shows flights of beach ridges at Cape Bird. In general, the ridges that are above the level of current day marine action are made up of cobble-sized material that appears to be poorly sorted.

2.2. Polar shoreline processes

The major difference between beaches in polar and temperate regions is the role of ice in beach formation and modification. Early work on Antarctic beaches, carried out by Nichols (1961; 1966; 1968) suggested 13 features that are characteristic of polar coastlines. The most common forms of ice features observed in McMurdo Sound are ice-push ridges, pitted beaches, beach ridges that terminate abruptly and ice rafted fragments on the beaches. The presence of any of these features on the beaches depends on the presence of sea ice in McMurdo Sound and the presence of an icefoot on the beaches.

The icefoot is a narrow fringe of ice attached to the coast which may remain long after the fast ice has broken free (Armstrong et al., 1973). There are several different types of icefoot, which reflect the mode of formation. The most common type in McMurdo Sound is the tidal platform icefoot (Taylor, 1922). This type of icefoot forms as seawater freezes onto the shore as the tide rises and falls. Therefore, the tidal platform icefoot reflects the tidal range of an area, which in McMurdo Sound is 1.1 m. The horizontal extent of the icefoot can be constrained to the foreshore or continue offshore for several tens of metres.

The initial effect of the icefoot is to prevent wave activity between its seaward edge and the shore and provide a protective barrier for the beach from sea ice. Later in the season during its destruction the icefoot may also lead to the formation of melt-pits as parts of the icefoot covered in sediment melt on the beach leaving a pit behind (Taylor and McCann, 1976). Ice wedges can also form, as small sections of the icefoot may remain long after the icefoot has

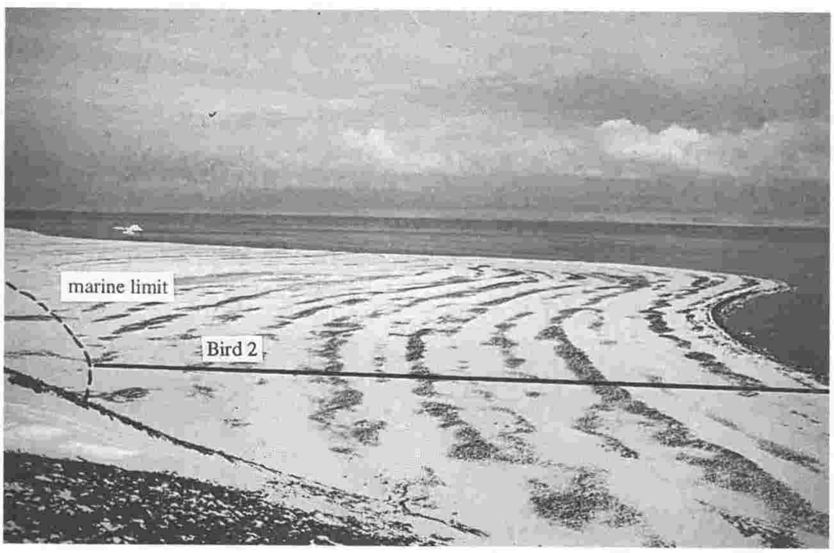

Fig. 2. Raised beaches at Priapulus Beach, Cape Bird (view southwest). Bird 2 (white line in foreground) marks a survey line (240 m long). The highest beaches (to the left of the photo) on Bird 2 are about 6 m above MSL. White dashed line represents the marine limit.

been removed. As the icefoot is destroyed during the summer months, sediment can adhere to the icefoot as it is removed from the shore and be carried offshore and deposited in deeper water. No-one has investigated sediment concentrations of the icefoot in the Antarctic but studies on Lake Michigan show sediment concentrations of shore-based ice can range from 0.28 tons per metre of shore for anchor ice (Barnes et al., 1993) to 5.9 tons per metre of shore for the icefoot (Miner and Powell, 1991) depending on availability of sediment during time of icefoot formation.

Another active agent in polar beach morphology is sea ice. Sea ice will affect polar beaches indirectly by limiting wave fetch and reducing wave energy as the waves travel through the pack ice, and directly by advancing onto or into beaches creating ice push ridges. Squire and Moore (1980) showed that the amount of energy sea ice attenuates depends on the wave period with shorter period waves undergoing greater attenuation than longer period waves.

In extreme circumstances sea ice can bulldoze sediment up the beach face into ridges of sediment 80 m long and 7 m high (Owens and McCann, 1970) or build piles of sea ice up to 12 m high (Boyd, 1981). Stranded ice on the beach can form melt pits over 3 m in diameter and 0.5 m deep (Taylor and McCann, 1976). In intertidal areas ice can cut grooves into tidal flat sediment. These grooves range up to 0.8 m wide 0.35 m deep and 2000 m long (Dionne, 1969). The relative importance of ice features on the profile of a beach is dependent on the length of time sea ice is present in an area, the tidal range in the area and whether an icefoot is present. If sea ice in an area persists long into the summer season it is more likely to be driven onto the beaches by waves winds or tides. The tidal range will determine to what altitude above mean sea level that ice may become stranded on the beach. The presence of an icefoot will prevent sea ice from acting on the shore. Sea ice in McMurdo Sound persists longer on the western side than the eastern side. Analysis of 10 years of satellite images from McMurdo Sound shows the western side of the sound rarely ice-free. Of 307 images of sea ice conditions in McMurdo Sound from 1987 to 1998, 62.1% of the images showed Cape Bird ice-free and only 3.4% showed western McMurdo Sound ice-free.

2.3. Wave climate

The wave climate in McMurdo Sound reflects the aspect of the coastline and the presence of sea-ice. During the winter, wave fetch in McMurdo Sound is severely limited by sea ice both to the north and the south but winter breakouts, although not common, may provide enough fetch for waves to act on the shore. The eastern side of the sound is protected from the dominant north-east wave direction while receiving locally generated southerly waves. In contrast, the western side of the sound receives the north-east waves but is relatively sheltered from the southerly waves. Observed wave heights at Spike Cape during a storm in the southern Ross Sea on 23rd January 1997 were between 0.2 m and 0.4 m. These waves propagated through an estimated 5 km of sea ice. Observed wave periods and heights for Cape Royds are between 0.8 s and 6 s for wave period and 0.08 m and 0.7 m for wave height (Kirk, 1966; this study). Estimated wave heights at Cape Bird during a southerly storm on the 7th February 1998 were between 1.2 m and 1.5 m.

3. Methods

Surveys of the beaches were undertaken using a survey level and graduated staff. Surveys extended from the icefoot to the marine limit except at Marble Point, Cape Royds and Cape Bird where nearshore profiles were obtained using a kite deployment or a plumb line system. The surveys on the western side of McMurdo Sound except for those conducted at Cape Bernacchi were tied back to GPS benchmarks so their elevations represent height above mean sea level in metres. The transects on the eastern side of McMurdo Sound and Cape Bernacchi were surveyed to mid tide mark.

Pits were dug to examine the stratigraphy on most transects. Sedimentary units were distinguished on gross lithological characteristics including; size, shape and imbrication. Clast size was measured using vernier callipers. A minimum number of 30 clasts was measured from each unit in each pit. Clast size is presented in class histogram form using a program generated by Single (unpublished data). Clast imbrication from within units in pits and the surface of some beaches was measured using an inclinometer and a compass. Imbrication data was plotted on a contour plot using the StereoNet package to display mean vectors and overall fabric slope (dip and strike of material).

4. Results

4.1. Surveys

Figs. 3 and 4 show survey transects at sites in McMurdo Sound and their relative locations. The top of the surveys represents the marine limit. Above the marine limit the material became more poorly sorted and rounded and was hummocky and chaotic in appearance. Where the difference between marine and non-marine sediments was difficult to identify, the marine limit was determined on gross geomorphological features such as shore normal ridges.

Larger individual beach ridges are identified on the profiles in Fig. 3 and have been marked on these surveys as ridge 1, ridge 2 and ridge 3. Although several other smaller ridges are present in these surveys these are the more significant ridges that can be traced from site to site on air photos. Differences in beach slope are evident both between sites and within individual profiles. For example at Cape Bernacchi the average slope of profiles Bernacchi 1 and Bernacchi 2 are about 7°. In contrast, Bernacchi 3 and Bernacchi 4 are 4.7° and 3.5°, respectively. The beaches on the western side of the Sound (Fig. 3) are generally about 4° but in some cases the individual ridge faces are as steep as 12°. There is a sharp contrast between the beach slopes on the western side of the Sound and those from Cape Bird (Fig. 4). Average slopes at Cape Bird are relatively shallow (0.5–3.3°) compared with the other beaches.

Differences in average slope within some profiles are also evident. Cape Bird profile Bird 3 shows three distinct "phases" of slope evolution down the profile. The top 350 m of the profile has an average slope of 0.2°, which corresponds closely with the slope of 0.4° for the bottom 190 m of the profile. In contrast, phase 2 has an average slope of 1°. Dunlop Island survey Dunlop 1 also shows three "phases" of development through the profile. The slope of these individual phases is the opposite of the Cape Bird profile with the steepest sections of the profile at the top and the shallowest in the middle. The top 105 m has a slope of 5°, the middle 100 m has a slope of 0.2° and the lower 150 m has a slope of 4°.

4.2. Sediment fabric and size

The fabric data for selected sites is presented on stereo plots so that broad imbrication can be shown. Points at the edge of the circle represent material lying flat on the beach, in contrast to points in the middle of the circle, which represent material with a 90° dip on the A–B plane. Size data is presented in histograms. Figs. 5–7 show plots of the fabric and size of material on beaches and from within pits at Marble Point Cape Bird and Spike Cape.

The Spike Cape plots (Fig. 7) show very strong northwesterly imbrication and a distinct change in clast size from the northern end of the barrier toward the southern end. The Marble Point and Cape Bird plots (Figs. 5 and 6) represent clasts measured from within pits dug into the beaches. 60 clasts were measured within the Marble Point pits compared with the 30 measured at Cape Bird. The pits at Marble Point varied in depth from 0.6 m to 1.0 m, the depth of the pit usually corresponded with the depth of permafrost or ice (700–1000 mm). They all had a deflationary lag surface present at the top. The top 100 mm in all pits was dominantly matrix supported and became clast supported down the unit. The matrix was a poorly sorted mixed sand and gravel. The mean clast size generally coarsened down the unit.

Pits at Cape Bird were similar but lacked the surface matrix supported unit. The imbrication at Cape Bird is generally weak with northerly and westerly imbrication present in the plots. Marble Point displays almost no imbrication at all except Marble 1 Hole 2, which exhibits westerly dipping clasts. The size plots indicate that beaches on the western side of the sound comprise larger material that the beaches on the eastern side. Cape Bird has a mean *b*-axis value of about 46 mm whereas the mean value at Marble Point, Dunlop Island and

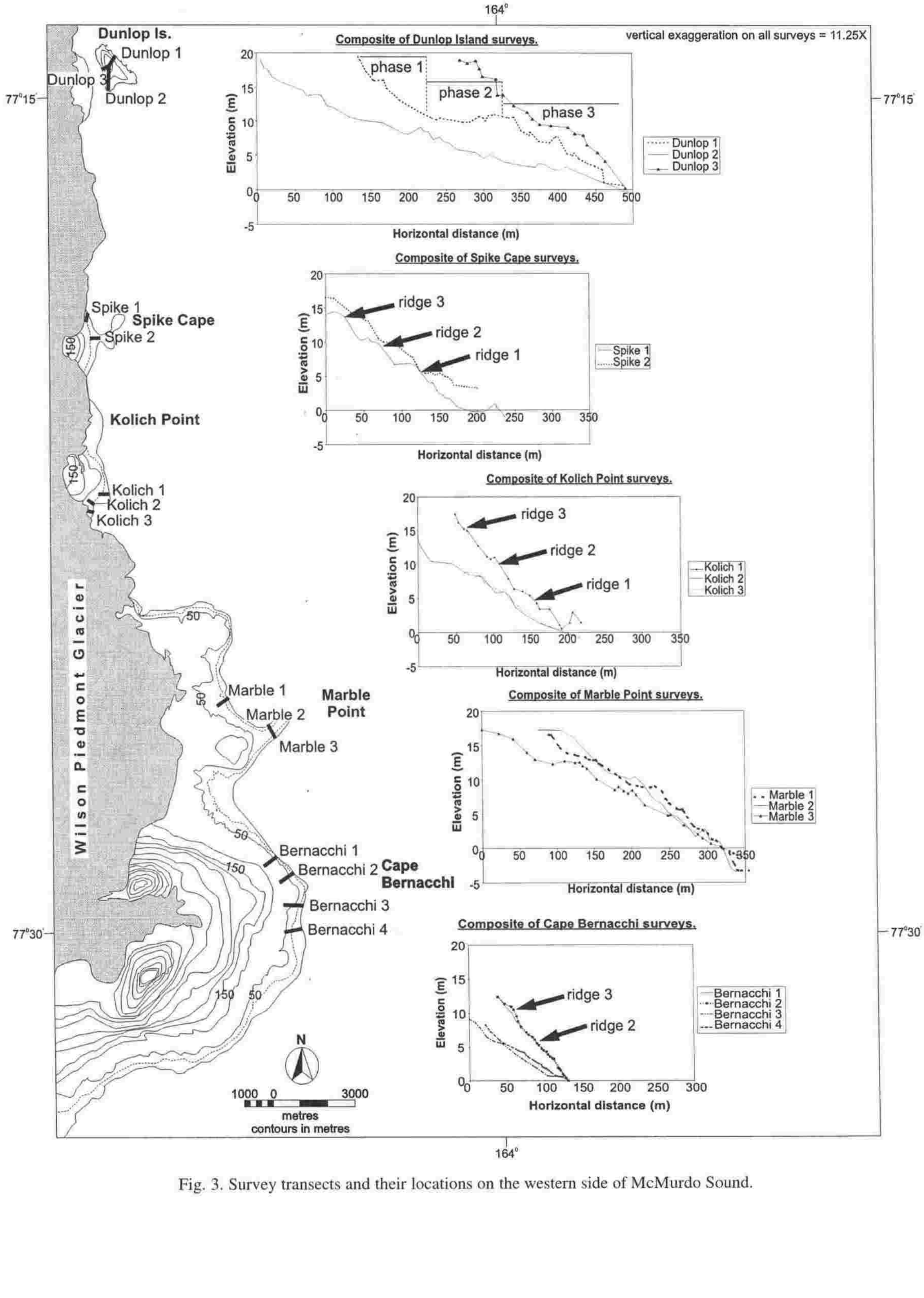

Fig. 3. Survey transects and their locations on the western side of McMurdo Sound.

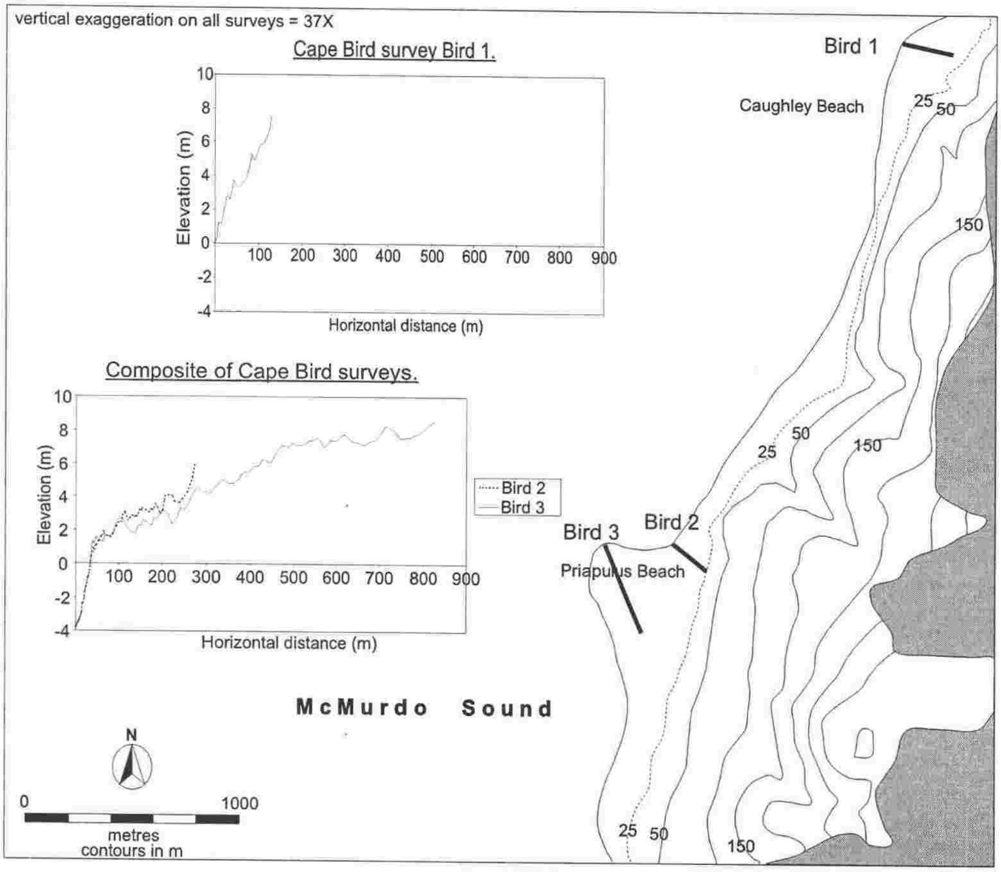

Fig. 4. Survey transects and their locations at Cape Bird (eastern side of McMurdo Sound).

Spike Cape varies from about 55 mm up to 101.5 mm.

5. Discussion

5.1. Differences between eastern and western beaches in McMurdo Sound

Differences between beaches in McMurdo Sound are apparent both from the survey, clast size and imbrication data. Fig. 8 graphically illustrates the differences in material on the modern beaches on the western and eastern aspects of the Sound. These differences are not surprising considering the western side of the Sound is ice free only 3.4% of the time compared with the eastern side which is ice free 62.1% of the time. Consequently, more ice push features and melt pits are produced along the western side of the Sound. On the eastern side of the Sound marine processes rework these features which develop in the winter months. Nichols (1961; 1966; 1968), suggested that ice processes were dominant on the western shores of McMurdo Sound reflects these views in his early work, as does Kirk (1966; 1972), who showed that marine processes dominated the beaches in the Cape Royds area in the summer months.

Although this is true as a general statement, marine processes can play a major role on beaches on the western side of the Sound. Material along a gravel barrier at Spike Cape shows very strong imbrication and has well sorted and well rounded clasts that fine toward the centre of the bay (Fig. 7). This suggests a strong marine influence rather than the prominent ice processes that can be found elsewhere

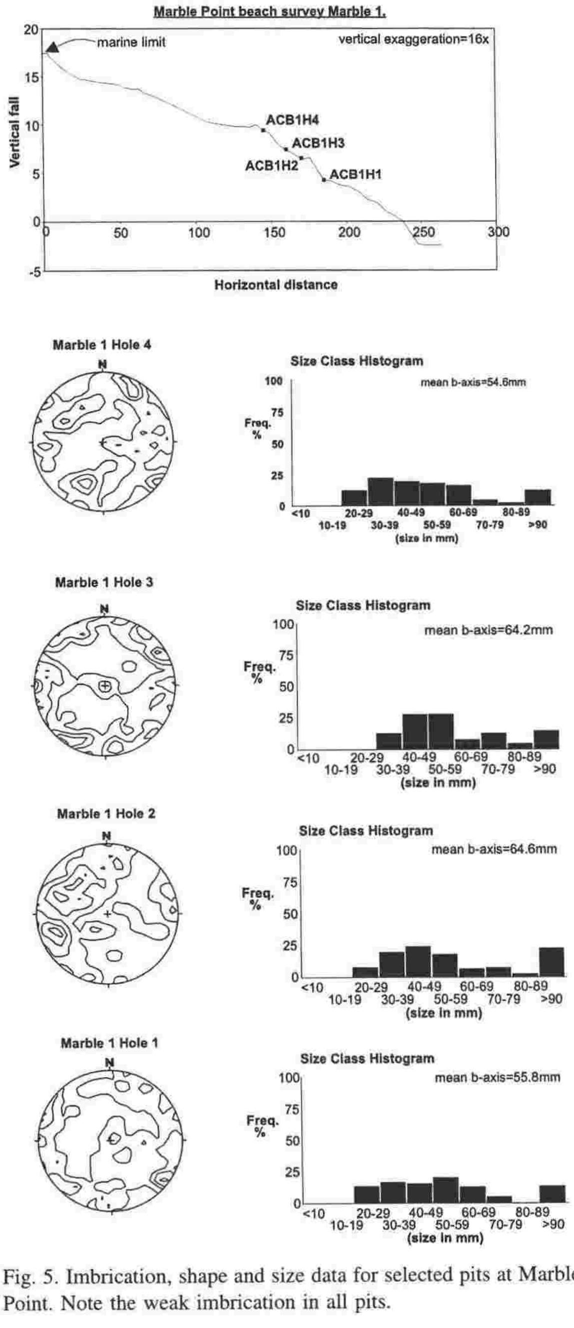

Fig. 5. Imbrication, shape and size data for selected pits at Marble Point. Note the weak imbrication in all pits.

on the western side of the Sound. The dominant wave direction at Spike Cape is from the northeast so the north end of the Cape protects the western shore of the embayment from most of the wave energy. Field observations noted that waves appeared to be higher along the barrier than in the bay, probably due to the steep offshore slope at this point and the shallow slope in the middle of the bay reducing wave energy on the western shore. This is further enhanced by the dominant southerly wind

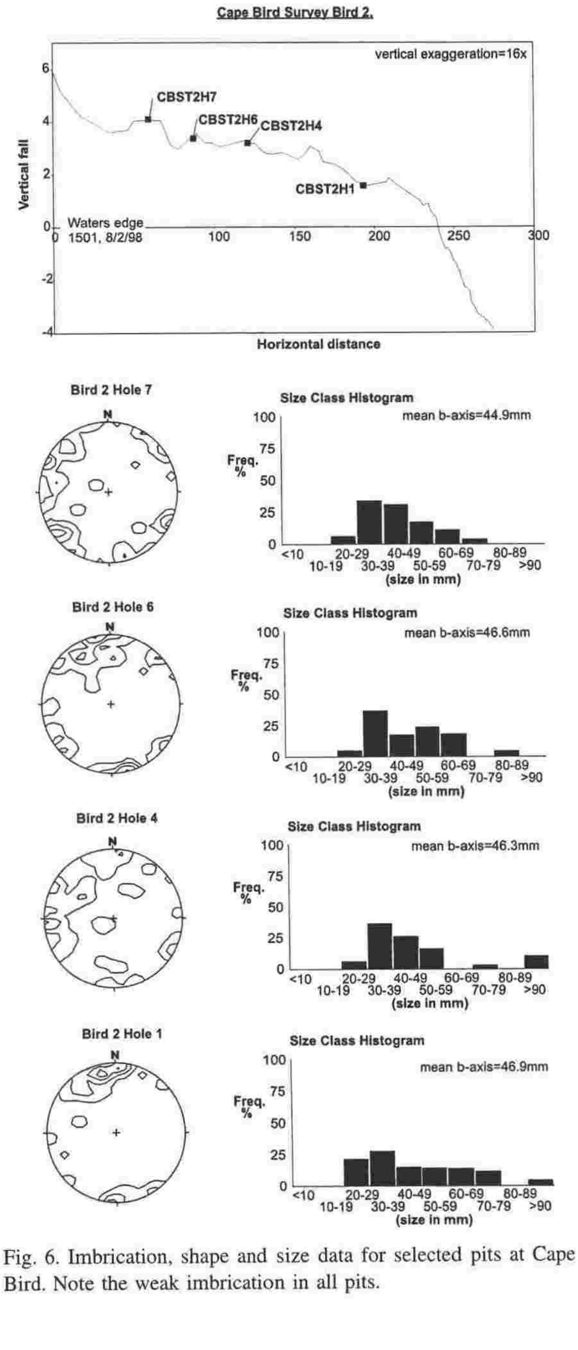

Fig. 6. Imbrication, shape and size data for selected pits at Cape Bird. Note the weak imbrication in all pits.

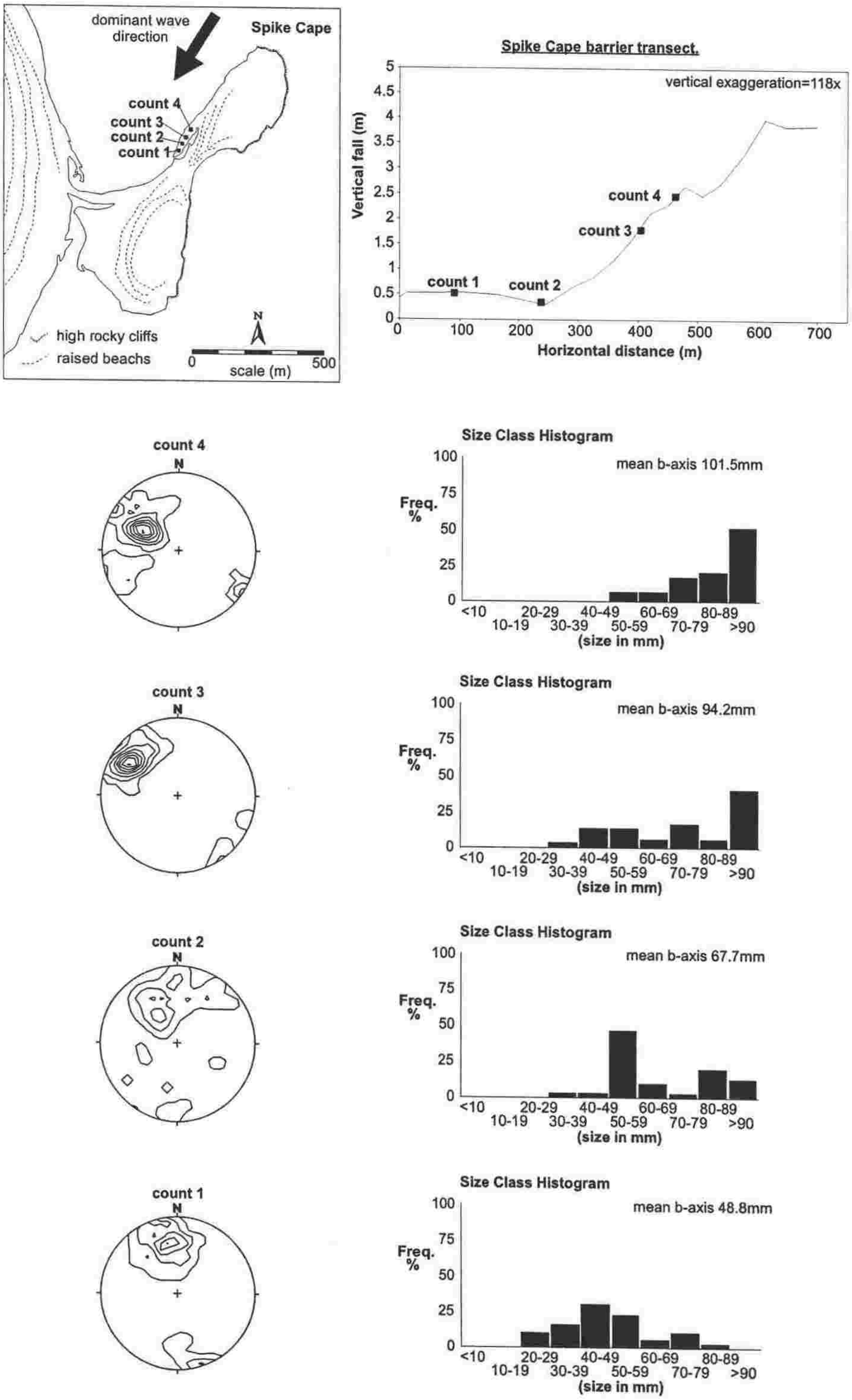

Fig. 7. Imbrication, shape and size data for selected surface counts at Spike Cape. Note the strong imbrication to the northwest.

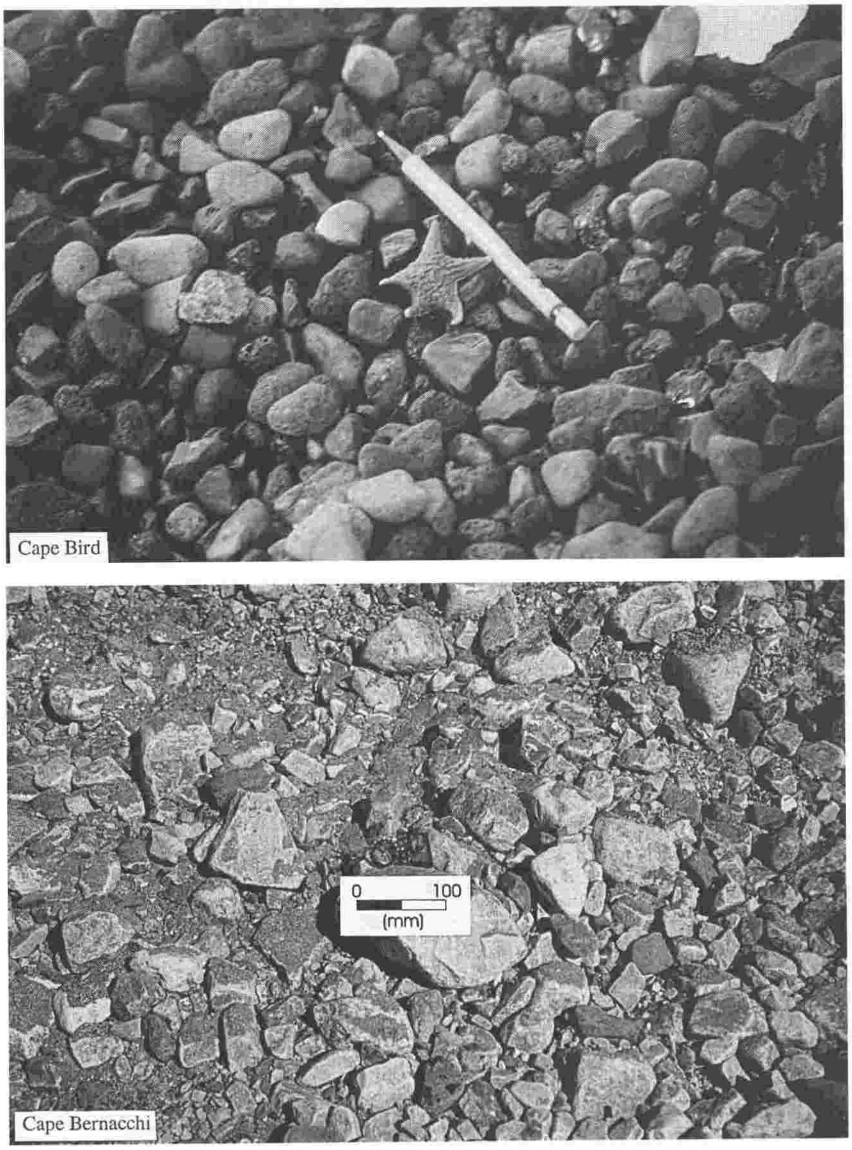

Fig. 8. Modern beach at Cape Bird (top photo, pencil is 150 mm long) and Cape Bernacchi (lower photo). Note the sand on top of the poorly rounded and sorted clasts at Cape Bernacchi compared with the relatively well rounded and sorted material at Cape Bird. The rounding, sorting and imbrication at Cape Bernacchi is representative of a typical ice push feature.

forcing ice offshore on the northern shore of Spike Cape (see Fig. 1).

In contrast with the modern beaches, the raised beaches on both sides of the Sound share a number of similar characteristics. All of the samples on raised beaches were poorly sorted and the imbrication at Cape Bird and Marble point was very weak. The material on the raised beaches at Cape Bird is sub-angular, compared with the rounded and sub-rounded clasts observed on the modern beach. Initial examination of these characteristics may indicate an ice-dominated environment. Although ice processes generally produce small discontinuous features, they can produce larger features, which are discussed by (Owens and McCann, 1970). The poorly rounded, poorly sorted and weakly imbricated clasts on a modern beach at Cape Bernacchi (Fig. 8) reflect what is often observed on ice push features on the modern beaches in other locations around McMurdo Sound. This contrasts with material on the modern beach at Cape Bird (Fig. 8).

The shore normal nature of the ridges and their continuity over several hundred metres (Fig. 2), however, indicates marine action. The weak imbrication, poorly rounded beach stones within the beaches and the presence of a wide range of sizes of material suggests that the ridges were built by short-lived large magnitude storm events. The modern beach at Cape Bird comprises mixed sand and gravel in contrast to the raised beaches, which contain considerably larger material. Although gravel beaches typically have a number of characteristic features such as clast shape zones (Bluck, 1967; Postma and Nemec, 1990), Forbes et al. (1995) showed that barriers on paraglacial coasts could undergo rapid changes in response to large magnitude storm events. They suggested that the stable barrier structures and facies patterns could be broken down, and remixing of sediment could occur. The frequency and duration of open water conditions on the western side of McMurdo Sound will reduce the interval that storms can act on this shoreline. Therefore, storms would not always have time to sort the material into well-organised, "typical" gravel beaches. In addition, Shulmeister and Kirk (1997) showed that modern beaches often contained finer material than relict beaches in an area. Such a difference between material on the modern beaches and the raised beaches is evident at Cape Bird. The modern beach at Cape Bird comprises mixed sand and gravel in contrast with the raised beaches that comprise pebbles and cobbles.

As the coastline in McMurdo Sound rebounded following deglaciation low frequency high magnitude storm events would create ridges that were above the elevation of normal marine or ice processes. As the coast continued to rise these ridges were elevated beyond the range of storms. In due course, another large magnitude event would occur depositing a ridge below the first. Fig. 3 shows storm ridges identified on Spike Cape, Kolich Point, Marble Point and Cape Bernacchi surveys. Although there were often more than just two or three ridges present on the profiles, these were the ones that were identifiable on air photos and could be traced continuously for 500 m or more. Fig. 9 shows an air photo of the northern tip of Spike Cape with the three major ridges identified. These major ridges represent the high magnitude storm events that have been preserved.

Cape Bird has considerably more than the 3 major relict ridges on the western side of the Sound (BIRD2 (shown in Figs. 2 and 4) has six major ridges present). I argue that this is due to the lower wave energy that occurs at Cape Bird as compared with the western side of the sound. Fig. 1 shows dominant wave directions in McMurdo Sound. Cape Bird receives waves from the south, which has a limited fetch (90 km maximum, dominant wave direction a, Fig. 1). In contrast, the western side of McMurdo Sound receives waves from the northeast, which has a fetch of many thousands of kilometres (dominant wave direction b, Fig. 1). Storm events at Cape Bird that are large enough magnitude to create ridges out of range of normal marine or ice processes would be far smaller than the storms that produced similar ridges on the western side of the Sound. In addition, due to the regularity of ice-free conditions at Cape Bird, the frequency of these storms would also be greater. (As no suitable dates from the beaches at Cape Bird are available an estimated return period for these storms is not offered). The lower energy environment at Cape Bird is reflected both in the surveys and the beach material. Beach slope is controlled by a number of factors, including sediment supply, wave energy (Bascom, 1951; Weigel, 1964) and sediment size (Shephard, 1963), and less importantly, wave steepness (Rector, 1954; Harrison, 1969), and sediment sorting (Krumbein and Graybill, 1965; McLean and Kirk, 1969). In general, steeper gravel/cobble beaches are the result of; a sediment deficit, greater wave energy, larger beach material, shallower waves, or better-sorted beach material. Average slopes for the western beaches that have major ridges identified on them (Spike 1, Kolich 1, Marble 1, Bernacchi 2) are between 4.1° and 7°. This contrasts with Cape Bird survey Bird 3, where the average slope is 0.6°. Marble 2 survey and Bird 2 survey (Fig. 10) graphically illustrate the difference between the steep western profiles and the comparatively shallow eastern profiles. The ridges at Cape Bird are also considerably smaller than their western

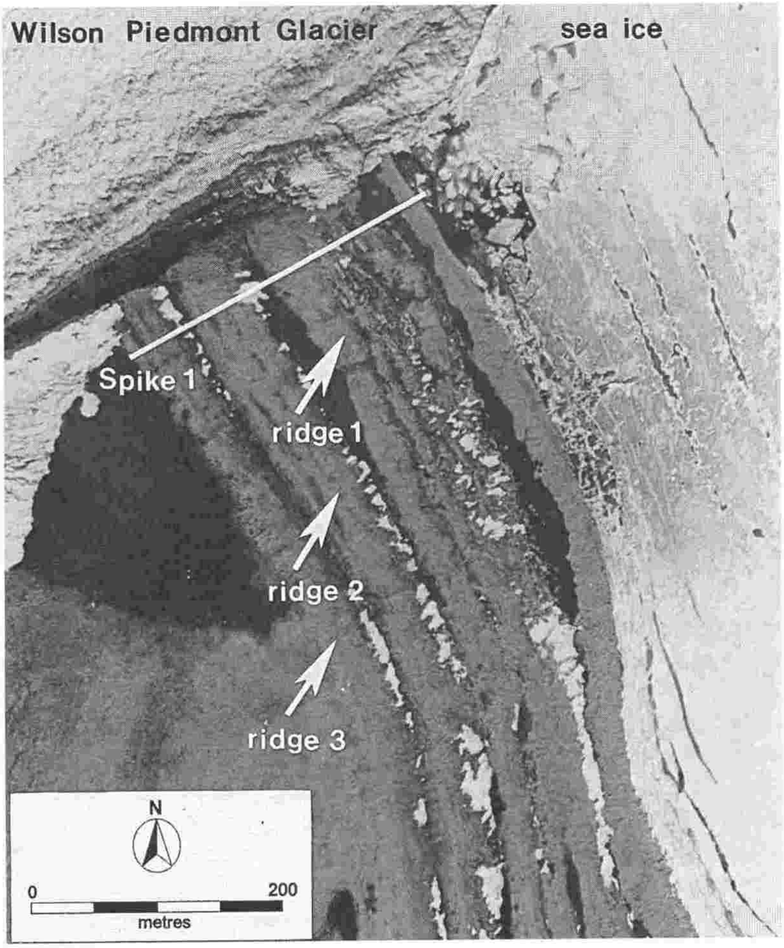

Fig. 9. Air photo of the beach ridges at the northern end of Spike Cape. These are the three major ridges identified on the survey transect in Fig. 3. Spike 1 marks a survey line (white line).

counterparts. Individual beaches at Cape Bird are up to 1 m high (measured from top of ridge to top of next ridge) compared with up to 5 m high at Kolich Point. The mean *b*-axis for clasts at Marble Point is 60 mm compared with a mean *b*-axis of 46 mm at Cape Bird, which also indicates greater wave energy at Marble Point.

5.2. Difference between northern and southern facing profiles in McMurdo Sound

The prominence of ice processes over marine processes between north and south-facing profiles on the western side of the Sound is also evident. This is reflected in the profiles as lower energy beaches. Dunlop 2 on the south of Dunlop Island has an average beach slope over the profile of about 2° whereas Dunlop 1 (on the northern side) has a slope of about 4.5°. Similarly, the northern profiles at Marble Point (Marble 1 and Marble 2, about 4°) are steeper than the southern profile (Marble 3, 3°). The southern profiles tend to have more ridges preserved than the northern profiles, probably due to the limited fetch to the south resulting in less energy at the beach compared with the northern facing profiles that receive waves from the northeast. This is further enhanced by ice being pushed into the southern embayments by the dominant southerly wind and out of the northern bays where marine processes can act on the shores (see Fig. 1).

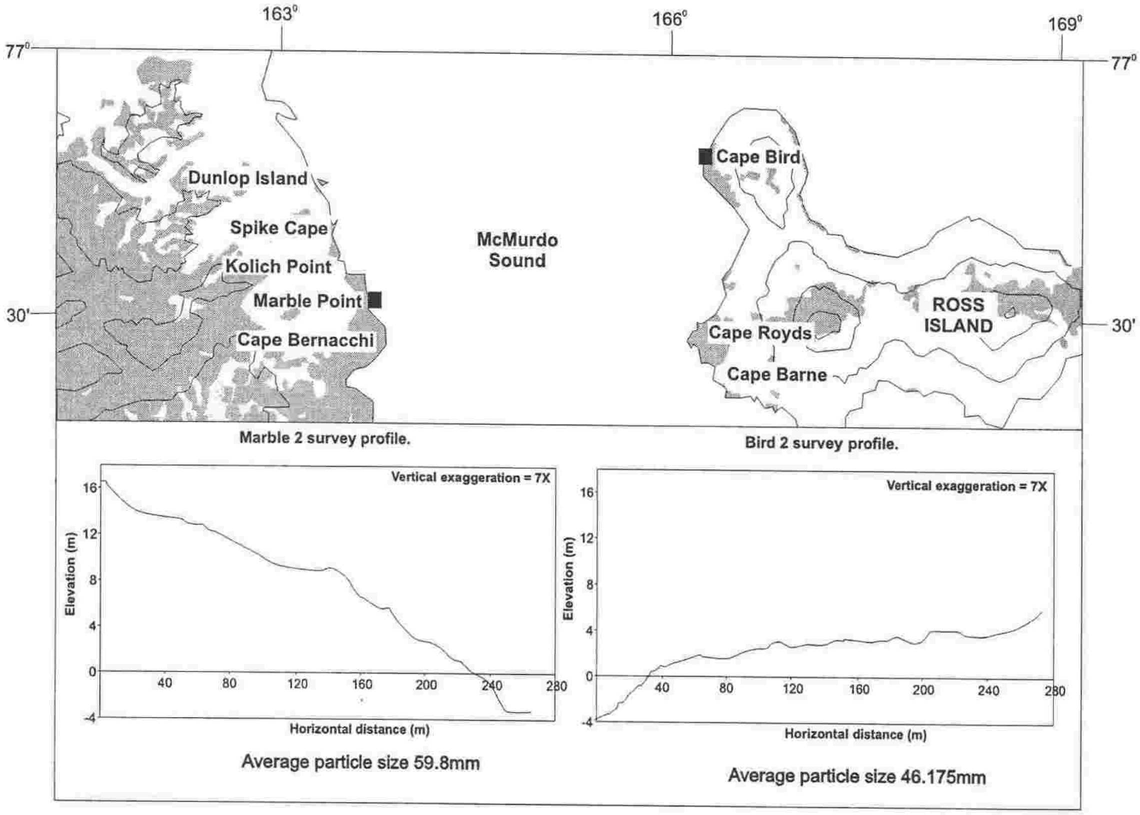

Fig. 10. Summary diagram of a beach profile from western McMurdo Sound (Marble 2) and a profile from eastern McMurdo Sound (Bird 2). Both profiles have the same vertical exaggeration so the differences in slope are graphically illustrated.

In addition to recognising a difference in energy conditions between north and south facing beaches on the western side of the Sound, differences in energy conditions can also be identified at separate sites between profiles. Cape Bernacchi surveys Bernacchi 1 and Bernacchi 2 have average slopes of 7° in contrast to Bernacchi 3 and Bernacchi 4, which have average slopes of 4.7° and 3.5°, respectively. This difference is reflected in the sediment size also, as the two northern profiles comprise similar sediments as those found at Marble Point on the raised beaches in contrast to the two southern profiles, which comprise coarse sandy beaches. These differences can also be seen at Kolich Point (between Kolich 1, which slopes 6.8° and Kolich 3, which slopes 4°) and Dunlop Island (between Dunlop 1, which slopes 4.5° and Dunlop 2, which slopes 2.2°). These changes in energy conform to dominant waves approaching the western shores of the Sound from the northeast. In this case, the exposed northern profiles are receiving considerably more energy than the relatively sheltered southern profiles.

5.3. Paleo-wave conditions in McMurdo Sound

Using the overall gradient of the beach ridges as an indicator of paleo-energy conditions may provide insights into changes of former energy conditions at some locations. On survey Bird 3 at Cape Bird, there appears to be three distinct phases of beach development, which could be linked to energy conditions. The top 350 m of the survey (phase 1) and the lower 190 m (phase 3) both have relatively shallow slopes (0.2° and 0.4°, respectively), in contrast to the middle 250 m (phase 2), which is considerably steeper (1°). The changes identified at Cape Bird (Fig. 4) could be due to changes in any of the factors that control beach slope including rate of uplift and sediment supply. However, as sediment size remains almost constant over the profile and uplift rates will only change marginally, a change in sediment supply or wave energy most likely caused the changes in the slope. The relationship between phase 1 and phase 3 suggests that sometime in the past, energy conditions and sediment supply at Cape Bird were similar to those experienced today. The difference in slope of phase 2 indicates a sediment deficit or a period of increased energy conditions. If the differences in slope were the result of an increase in energy at Cape Bird the size of the beach ridges would be expected increase proportionally. The size of the beach ridges does not appear change between the different phases identified on Bird 3, so it is suggested that this difference is the result of a change in sediment supply.

5.4. Relationship between raised beaches and sea level in the Holocene

The difference in beach elevations between northern and southern profiles is important for rebound reconstructions as overestimation of marine limits could result from using a marine limit located on a northern aspect on the western side of McMurdo Sound. For example, the difference in marine limits between the south (8.2 m marine limit) and the north side of Cape Bernacchi (12.3 m marine limit) is 4.1 m even though these beaches are contiguous. If the Marble Point datum of 5650 ± 150 years BP at 13.4 m (Nichols, 1968; Stuiver et al., 1981) is applied to the northern profile at Cape Bernacchi (Bernacchi 1) a rebound rate of 2.37 mm/year would be calculated. Using this same datum a rebound rate of 1.62 mm/year would be calculated for the Bernacchi 4 profile, which is only 2 km to the south. This does not reflect variations in isostatic rebound but shows the importance of variable energy conditions along a coastline.

Ideally paleo sea levels could be determined for an individual raised beach ridge by subtracting the elevation above modern mean sea level of the modern beach ridge from the raised beach. However, even though polar beaches, unlike their mid-latitude counterparts, represent storm events, this still assumes that both the modern beach and the raised beach were deposited in a similar magnitude event. Sites sheltered from the dominant fetch direction and susceptible to smaller storm waves are likely to be deposited closer to mean sea level. These beaches should be the best analogues for paleo sea level studies. Even on these beaches however, sea level estimates may be somewhat inaccurate as the effects of ice push may result in anomalously high marine limits.

6. Conclusion

The modern beaches in McMurdo Sound are the result of a combination of ice processes and marine processes. The relative importance of each process is dependent on the amount of time the coast is ice-free. For example Cape Bird is ice-free about 62% of the time and the material is rounded and sorted. In contrast, Marble Point is ice free only 3% of the time and the material is poorly rounded and sorted.

Although previous workers have highlighted the role of ice processes in the formation of the raised beaches in McMurdo Sound (Nichols, 1961, 1966, 1968) the continuous nature of the raised ridges and their general morphology suggests a marine origin. It is suggested here that the raised beaches in this area are storm beaches, deposited and stranded as the land was slowly rebounding during the Holocene. The first order control on the number of raised beaches at any site is incident wave energy. Subsidiary factors that also influence the number of ridges include the aspect of the beach, rate of rebound, sediment budget and storm magnitude. The lower energy beaches on the southern aspect of western McMurdo Sound provide better analogues of past sea levels compared with the higher energy storm deposits on the northern aspects.

Acknowledgements

This study was funded in part by a New Zealand Post Ross Dependency Research Committee Scholarship and Victoria University of Wellington internal grants. Antarctica New Zealand, especially Paul Fitzgerald, provided support, which was much appreciated. Thanks to Jamie Shulmeister, Julie Quinn, Peter Webb, Jon Allen and Alexis Lambeck for help in the field and Peter Barrett for help throughout the project. I am indebted to Jamie Shulmeister for guidance and spending time and energy on drafts of this paper.

References

Armstrong, T., Roberts, B., Swithinbank, C., 1973. Illustrated Glossary of Snow and Ice, 2nd edn. The Scott Polar Research Institute, Cambridge.

Barnes, P.W., Kempema, E.W., Reimnitz, E., McCormick, M., Weber, W.S., Hayden, E.C., 1993. Beach profile modification and sediment transport by ice: an overlooked process on Lake Michigan. Journal of Coastal Research 9, 65–86.

Baroni, C., Orombelli, G., 1991. Holocene raised beaches at Terra Nova Bay, Victoria Land, Antarctica. Quaternary Research 36, 157–177.

Bascom, W.H., 1951. The relationship between sand size and beach face slope. Transactions of the American Geophysical Union 32, 866–874.

Bluck, B.J., 1967. Sedimentation of beach gravels: examples from South Wales. Journal of Sedimentary Petrology 37 (1), 128–156.

Boyd, G.L., 1981. The March 1978 ice piling event on Lake St. Clair, Ontario. Workshop on Ice Action on Shores, pp. 1-13.

Colhoun, E.A., Mabin, M.C.G., Adamson, D.A., Kirk, R.M., 1992. Antarctic ice volume and contribution to sea-level fall at 20,000 yr BP from raised beaches. Nature 358, 316–318.

Dionne, J., 1969. Tidal flat erosion by ice at La Pocatiere St. Lawrence estuary. Journal of Sedimentary Petrology 39 (3), 1174–1181.

Dionne, J., 1998. Sedimentary structures made by shore ice in muddy tidal-flat deposits, St. Lawrence estuary, Quebec. Sedimentary Geology 116, 261–274.

Dubrovin, L.I., 1979. Major types of Antarctic ice shores. Byulleten Sovetskoy Antarkticheskoy Expeditsii 93, 5–12.

Forbes, D.L., Taylor, R.B., 1994. Ice in the shore zone and the geomorphology of cold coasts. Progress in Physical Geography 18 (1), 59–89.

Forbes, D.L., Orford, J.D., Carter, R.W.G., Shaw, J., Jennings, S.C., 1995. Morphodynamic evolution, self-organisation, and instability of coarse clastic barriers on paraglacial coasts. Marine Geology 126, 63–85.

Gregory, M.R., Kirk, R.M., 1990. The shores of the Ross Sea. In: Hatherton, T. (Ed.), Antarctica the Ross Sea Region. DSIR Publishing, Wellington, pp. 85–95.

Gregory, M.R., Kirk, R.M., Mabin, M.C.G., 1984. Shore types of Victoria Land, Ross Dependency, Antarctica. New Zealand Antarctic Record 5 (3), 23–40.

Gunn, B.M., Warren, G., 1962. Geology of Victoria Land between the Mawson and Mulock Glacier, Antarctica. New Zealand Geological Survey Bulletin 71.

Hansom, J.D., Kirk, R.M., 1989. Ice in the intertidal zone: examples from Antarctica. Essener Geografisce Arbeiten 18, 211–236.

Harrison, W., 1969. Empirical equations for foreshore changes over a tidal cycle. Marine Geology 7, 529–551.

Hequette, A., Barnes, P.W., 1990. Coastal retreat and shoreface profile variations in the Canadian Beaufort Sea. Marine Geology 91, 113–132.

Hjort, C., Ingolfsson, O., Moller, P., Lirio, J.M., 1997. Holocene glacial history and sea-level changes on James Ross Island, Antarctic Peninsula. Journal of Quaternary Science 12 (4), 259–273.

Igarashi, A., Harada, N., Moriwaki, K., 1995. Marine fossils of 30–40 ka in raised beach deposits, and late pleistocene glacial history around Lutzow–Holm Bay, East Antarctica. Proceedings of the National Institute of Polar Research Symposium on Antarctic Geoscience, Vol. 8, pp. 213–218.

Kirk, R.M., 1966. Beach observations at Cape Royds, Ross Island, McMurdo Sound, Antarctica 1965–1966. Unpublished Report, Geography Department, University of Canterbury.

Kirk, R.M., 1972. Antarctic beaches as natural hydraulic models. Proceedings of the 7th New Zealand Geographical Conference, Hamilton, pp. 227–234.

Kirk, R.M., 1991. Raised beaches, late Quaternary sea levels and deglacial sequences on the Victoria Land coast, Ross Sea, Antarctica. In: Gillieson, D.S., Fitzsimons, S. (Eds.), Quaternary Research in Australian Antarctica: Future Directions. Special Publication 3. Department of Geography and Oceanography, Canberra, pp. 85–105.

Korotkevich, Y.S., 1971. Quaternary marine deposits and terraces in Antarctica. Soviet Antarctic Expedition Bulletin 82, 4, 185–190.

Krumbein, W.C., Graybill, F.A., 1965. An Introduction to Statistical Models in Geology. McGraw-Hill, New York.

McLean, R.F., Kirk, R.M., 1969. Relationships between grain size, size-sorting, and foreshore slope on mixed sand-shingle beaches. New Zealand Journal of Geology and Geophysics 12 (1), 138–155.

Miner, J.J., Powell, R.D., 1991. An evaluation of ice-rafted erosion caused by an icefoot complex, Southwestern Lake Michigan, USA. Arctic and Alpine Research 23 (3), 320–327.

Nichols, R.L., 1961. Characteristics of beaches formed in polar climates. American Journal of Science 259, 694–708.

Nichols, R.L., 1966. Geomorphology of Antarctica. In: Tedrow, J.C.F. (Ed.) Antartctic soils and soil forming processes. Antarctic Research Series 8, American Geophysical Union, pp. 1–46.

Nichols, R.L., 1968. Coastal geomorphology, McMurdo Sound, Antarctica. Journal of Glaciology 7 (51), 449–478.

Owens, E.H., 1982. Ice along the shore. In: Schwartz, M.L. (Ed.), The Encyclopedia of Beaches and Coastal Environments, Encyclopedia of Earth Science Series, Vol. 15. Hutchinson Ross, PA, pp. 475–479.

Owens, E.H., McCann, S.B., 1970. The role of ice in the arctic beach environment with special reference to Cape Ricketts, Southwest Devon Island, Northwest Territories, Canada. American Journal of Science 268, 397–414.

Postma, G., Nemec, W., 1990. Regressive and transgressive sequences in a raised Holocene gravelly beach, southwestern Crete. Sedimentology 37, 907–920.

Rector, R.L., 1954. Laboratory studies of the equilibrium profile of beaches. US Army Corps of Engineers, Beach Erosion Board, Technical Memo 41.

Reimnitz, E., Barnes, P.W., Harper, J.R., 1990. A review of beach nourishment from ice transport of shoreface materials, Beaufort Sea, Alaska. Journal of Coastal Research 6 (2), 439–470.

Shephard, F.P., 1963. Submarine Geology. Harper and Row, New York.

Shulmeister, J., Kirk, R.M., 1997. Holocene fluvial–coastal interactions on a mixed sand and sand and gravel beach system, North Canterbury, New Zealand. Catena 30, 337–355.

Simeoni, U., Baroni, C., Meccheri, M., Taviani, M., Zanon, G., 1989. Coastal studies in Northern Victoria Land (Antarctica): Holocene beaches of Inexpressible Island, Thetys Bay and Edmonson Point. Bollettino di Oceanologia Teorica ed Applicata 7 (1–2), 5–17.

Squire, V.A., Moore, S.C., 1980. Direct measurement of the attenuation of ocean waves by pack ice. Nature 283, 365–368.

Stuiver, M., Denton, G.H., Hughes, T.J., Fastook, J.L., 1981. History of the Marine ice sheet in West Antarctica during the last glaciation: a working hypothesis. In: Stuiver, M., Denton, G.H., Hughes, T.J. (Eds.), The Last Great Ice Sheets. Wiley Interscience, New York, pp. 319–416.

Taylor, G., 1922. British (Terra Nova) Antarctic expedition 1910–1913. The Physiography of the McMurdo Sound and Granite Harbour region. Harrison and Sons, London.

Taylor, R.B., McCann, B., 1976. The effect of sea and nearshore ice on coastal processes in Canadian Arctic archipelago. Rev. Geogr. Montreal 30 (1–2), 123–132.

Weigel, R.L., 1964. Oceanographical Engineering. Englewood Cliffs, NJ, Prentice Hall.

Zwartz, D., Lambeck, K., Bird, M., Stone, J., 1997. Constraints on the former Antarctic ice sheet from sea-level observations and geodynamic modelling. In: Ricci, C.A. (Ed.), The Antarctic Region: Geologic Evolution and Processes. Terra Antarctica, Siena, pp. 821–828.

Zwartz, D., Bird, M., Stone, J., Lambeck, K., 1998. Holocene sea-level changes and ice sheet history in the Vestfold Hills, East Antarctica. Earth and Planetary Science Letters 155, 131–145.

US mailing notice — *Marine Geology* (ISSN 0025-3227) is published monthly by Elsevier Science B.V. (P.O. Box 211, 1000 AE Amsterdam, The Netherlands). Annual subscription price in the USA US$2593 (valid in North, Central and South America), including air speed delivery. Periodical postage paid at Jamaica, NY 11431. **USA POSTMASTER:** Send address changes to *Marine Geology*, Publications Expediting Inc., 200 Meacham Avenue, Elmont, NY 11003. **AIRFREIGHT AND MAILING:** in the USA by Publications Expediting Inc., 200 Meacham Avenue, Elmont, NY 11003.

NOTE TO CONTRIBUTORS

A detailed Guide for Authors is available upon request. Please pay attention to the following notes:

Language
The official language of the journal is English.

Preparation of the text
a) The manuscript should preferably be prepared on a word processor and printed with double spacing and wide margins and include an abstract of not more than 500 words.
b) Authors should use IUGS terminology. The use of S.I. units is also recommended.
c) The title page should include the name(s) of the author(s), their affiliations, fax and e-mail numbers. In case of more than one author, please indicate to whom the correspondence should be addressed.

References
a) References in the text consist of the surname of the author(s), followed by the year of publication in parentheses. All references cited in the text should be given in the reference list and vice versa.
b) The reference list should be in alphabetical order.

Tables
Tables should be compiled on separate sheets and should be numbered according to their sequence in the text. Tables can also be sent as glossy prints to avoid errors in typesetting.

Illustrations
a) All illustrations should be numbered consecutively and referred to in the text.
b) Figure captions should be supplied on a separate sheet.
c) If contributors wish to have their original figures returned this should be requested in proof stage at the latest.
d) Colour figures can be accepted providing the reproduction costs are met by the author. Please consult the publisher for further information.

Page proofs
One set of page proofs will be sent to the corresponding author, to be checked for typesetting/editing. Proofs should be returned within 3 days.

Reprints
Fifty reprints of each article are supplied free of charge. Additional reprints can be ordered on a reprint order form which will be sent to the corresponding author upon receipt of the accepted article by the publisher.

Submission of manuscripts
a) All manuscripts should be submitted in triplicate to the Editorial Office *Marine Geology*, P.O. Box 1930, 1000 BX Amsterdam, The Netherlands.
b) Illustrations should also be submitted in triplicate. One set should be in a form ready for reproduction: the other two may be of lower quality.
c) Authors are requested to submit the names, addresses and telephone, facsimile and e-mail numbers of four potential referees with their manuscripts.
d) Letter-type contributions should not exceed 8 printed pages and should be complete in themselves. No foldout illustrations can be accepted. The manuscripts received will be published ca. three *months after* acceptance.
e) **The indication of a FAX and e-mail number on submission of the manuscript could assist in speeding communications. The FAX number for the Amsterdam office is: +31-20-4852319.**
f) Submission of an article is understood to imply that the article is original and unpublished and is not being considered for publication elsewhere.

Submission of electronic text
Authors are requested to submit the final text on a 3.5″or 5.25″ diskette. It is essential that the name and version of the word processing program, the type of computer on which the text was prepared, and the format of the text files are clearly indicated. Authors are requested to ensure that the contents of the diskette correspond exactly to the contents of the hard copy manuscript. Discrepancies can lead to proofs of the wrong version being made. The word processed text should be in single column format. If available, electronic files of the figures should also be included on a separate floppy disk.
Authors in Japan please note: **Upon request, Elsevier Science K.K. will provide authors with a list of people who can check and improve the English of their paper *(before submission)*. Please contact our Tokyo office: Elsevier Science K.K., 9-15 Higashi Azabu, Minato-ku, Tokyo 106-0044, tel. (+81) (3) 5561 5033, fax (+81) (3) 5561 5047.**